Total Synthesis of Diterpene (±)-Aspewentin A via a Michael/Aldol Cascade

By

Nicolas Alfredo Diaz

A dissertation submitted in partial fulfillment
of the requirements for the degree of
Doctor of Philosophy
(Chemistry)
in the University of Michigan
2022

Doctoral Committee:

Professor Pavel Nagorny, Chair
Assistant Professor Timothy Cernak
Professor John Montgomery
Professor David Sherman

Nicolas A. Diaz

nicdiaz@umich.edu

ORCID iD: 0000-0002-5422-9287

Dedication

I dedicate this thesis to my family, loved ones, and any reader who appreciates the perspective on natural products presented herein.

Acknowledgements

I would like to express special appreciation to Pavel Nagorny, for his intellectual guidance and resource throughout these doctoral studies. Similarly, I would like to thank my undergraduate research advisor, George Negrete, for his close guidance during my time as an undergraduate researcher. My parents have both worked as educators of young students during my upbringing and contributed to my appreciation for comprehension and discovery in nature. My significant other, Maria Luisa, has also been a vital support for perseverance against the challenges that undoubtably arise during graduate school. I must also thank the other researchers, past and present, who have contributed intellectually and in discovery to the fields of chemistry and biology. Without the work of my predecessors, the perspectives and inspiration that outline the studies presented herein would not have been prompted.

Table of Contents

Dedication ii

Acknowledgements iii

List of Tables viii

List of Figures ix

List of Abbreviations xiv

Abstract xxii

CHAPTER I Introduction 1

I.1 Introduction to Relevance of the Isopimarane Diterpene Scaffold 1

I.2 Selected Examples of Natural Isopimarane-related Diterpenes 3

I.3 Proposed Biosynthetic Pathway to Isopimaranes 5

I.4 Selected Examples of Synthetic Biomimetic Tricyclization 8

I.4.1 The van Tamelen Biomimetic Approach to the Diterpene Scaffold 10

I.4.2 The Corey Biomimetic Approach to the Diterpene Scaffold 10

I.4.3 Alternative Corey Biomimetic Approach to the Diterpene Scaffold 11

I.4.4 The Pattenden Biomimetic Radical Approach to the Diterpene Scaffold 12

I.4.5 The MacMillan Biomimetic Radical Approach to the Diterpene Scaffold 13

I.5 Selected Examples of Ionic Tricyclization 13

I.5.1 The Meyer Approach to the Diterpene Scaffold 14

I.5.2 The Cai Approach to Diterpene Scaffold 15

I.5.3 The Overman Approach to the Diterpene Scaffold 16

I.5.4 The Pan Approach to the Diterpene Scaffold 19

I.5.5 The Tu Approach to the Diterpene Scaffold 20

I.5.6 The Qin Approach to Diterpene Scaffold 21

I.5.7 The Koert Approach to Diterpene Scaffold 23

I.5.8 The Herzon Approach to Diterpene Scaffold 26

I.5.9 The Carter Approach to the Diterpene Scaffold 29

I.6 Selected Examples of Redox-Initiated Tricyclization 30

I.6.1 The Maimone Approach to the Diterpene Scaffold 30

I.6.2 The Xu Approach to the Diterpene Scaffold 32

I.6.3 The Luo Approach to the Diterpene Scaffold 34

I.6.4 The Liang Approach to the Diterpene Scaffold 37

I.7 Selected Examples of Sigmatropic Tricyclization 41

I.7.1 The Zaragozá Approach to the Diterpene Scaffold 41

I.7.2 The Deslongchamps Approach to the Diterpene Scaffold 42

I.7.3 The Toyota Approach to the Diterpene Scaffold 47

I.7.4 Alternative Deslongchamps Approach to the Diterpene Scaffold 50

I.7.5 The Fukuyama Approach to the Diterpene Scaffold 53

I.7.6 The Li Approach to the Diterpene Scaffold 56

I.7.7 Alternate Herzon Approach to the Diterpene Scaffold 57

I.8 Summary 58

CHAPTER II Studies Towards the Synthesis of a Strategic Tricarbocyclic Motif via a Copper-Catalyzed Tandem Michael/Aldol Approach 60

II.1 Introduction 60

II.2 Overview of Aspewentin Biosynthesis 60

II.3 The Stoltz Approach to Aspewentins A–C 64

II.4 Proposed Synthetic Route to the Strategic Intermediate and Isopimaranes 66

II.5 Decarboxylation Overview 73

II.6 Model Studies of the Michael/Aldol Cascades 83

II.7 Conclusion/Summary 106

II.8 Graphical Summary 108

II.9 Experimental 109

CHAPTER III Total Synthesis of (±)-Aspewentin A 130

III.1 Introduction 130

III.2 Model Studies of *gem*-Dimethyl Michael Donors 135

III.3 Total Synthesis of (±)-Aspewentin A ((±)-1-16) 146

III.4 Conclusion/Summary 151

III.5 Graphical Summary 153

III.6 Experimental 154

III.7 NMR Spectra 174

References 194

List of Tables

Table II.1 Effect of donor 2-30 stoichiometry in Cu(II)-Michael process. 86

Table II.2 Aldol condensation screening of adduct 2-31. 88

Table II.3 Rhodium-mediated oxidation studies of 2-181. 104

Table III.1 Reactivity study of donor 3-14 in the Cu(II)-Michael process. 138

Table III.2 Base-mediated aldol approach. 148

Table III.3 ^{1}H NMR comparison of synthetic and natural aspewentin A. 172

Table III.4 ^{13}C NMR comparison of synthetic and natural aspewentin A. 173

List of Figures

Figure I.1 Selected natural products with a significant impact on human activity. 1

Figure I.2 Representative biotransformation of GGPP 1-5 to the isopimarane scaffold 1-6. 2

Figure I.3 Selected plant, fungal, and algal derived diterpenes. 4

Figure I.4 Accepted major biosynthetic pathway leading to DMAPP and IPP. 6

Figure I.5 Accepted major biosynthetic pathway leading to GGPP. 7

Figure I.6 Proposed biosynthetic pathway leading to scaffold 1-31. 8

Figure I.7 Biomimetic van Tamelen key cyclization step. 10

Figure I.8 Biomimetic Corey key cyclization step. 10

Figure I.9 Alternative biomimetic Corey key cyclization step. 11

Figure I.10 The Biomimetic Pattenden key radical cyclization step. 12

Figure I.11 The Biomimetic MacMillan key radical cyclization step. 13

Figure I.12 The Meyer tricyclic scaffold synthesis. 14

Figure I.13 The Cai tricyclic scaffold synthesis. 15

Figure I.14 The Overman synthesis of a precursor of scopadulcic acid B. 16

Figure I.15 The Overman synthesis of scopadulcic acid B. 18

Figure I.16 The Pan synthesis of (±)-celaphanol A. 19

Figure I.17 The Tu tricyclic synthesis of pisiferic acid core scaffold. 20

Figure I.18 The Qin synthesis of 1-oxomiltirone 21

Figure I.19 The Koert synthesis of intermediate to (+)-elevenol. 23

Figure I.20 The Koert synthesis of (+)-elevenol. 25

Figure I.21 The Herzon synthesis of intermediate to core of myrocin G. 26

Figure I.22 The Herzon synthesis of myrocin G. 28

Figure I.23 The Carter synthesis of an aromatic abietane. 29

Figure I.24 The Maimone synthesis of precursor to (+)-chatancin. 30

Figure I.25 The Maimone synthesis of (+)-chatancin. 31

Figure I.26 The Xu synthesis of atropurpuran. 32

Figure I.27 The Luo synthesis of precursor to (−)-oridonin. 34

Figure I.28 The completion of (−)-oridonin by Luo et al. 36

Figure I.29 The Liang synthesis of intermediate to isorosthin L. 37

Figure I.30 The Liang radical cyclization of intermediate 1-170. 38

Figure I.31 The Liang synthesis of isorosthin L. 40

Figure I.32 The Zaragozá synthesis of steroidal core 1-185. 41

Figure I.33 The Deslongchamps synthesis of first intermediate for (+)-anhydrochatancin. 42

Figure I.34 Continued Deslongchamps synthesis of first intermediate for (+)-anhydrochatancin. 43

Figure I.35 The Deslongchamps synthesis of second intermediate for (+)-anhydrochatancin. 44

Figure I.36 The Deslongchamps synthesis of (+)-anhydrochatancin. 46

Figure I.37 The Toyota synthesis of intermediate to serofendic acids A and B. 47

Figure I.38 The Toyota synthesis of serofendic acids A and B. 49

Figure I.39 Deslongchamps synthesis of intermediate to (+)-cassaine. 50

Figure I.40 Deslongchamps synthesis of (+)-cassaine. 52

Figure I.41 The Fukuyama synthesis of intermediate to (−)-lepenine. 53

Figure I.42 The Fukuyama synthesis of (−)-lepenine. 55

Figure I.43 The Li synthesis of arcutinidine. 56

Figure I.44 Explored synthetic route during Herzon synthesis of myrocin G. 57

Figure II.1 Currently described members of the aspewentin family (A–M). 63

Figure II.2 The Stoltz total synthesis of (−)-aspewentins A–C. 64

Figure II.3 The Stoltz total synthesis of (−)-aspewentins A–C. 66

Figure II.4 Sequential Cu(II)-catalyzed Michael/aldol approach to isopimaranes. 67

Figure II.5 Precedent Cu(II)-Michael addition results. 68

Figure II.6 Precedent tandem Cu(II)-Michael/aldol results. 69

Figure II.7 Precedent total synthesis enabled by a Cu(II)-Michael/aldol condensation strategy. 70

Figure II.8 Precedent total synthesis enabled by a Cu(II)-Michael/aldol condensation strategy. 71

Figure II.9 Total synthesis of cannogenol (2-46) via a Cu(II)-Michael/aldol strategy. 72

Figure II.10 Select examples of Krapcho Decarboxylation. 73

Figure II.11 Transition state of thermal decarboxylation and precedent γ-decarboxylation. 75

Figure II.12 Mechanism of pyruvate (2-66) decarboxylation mediated by either PDC or PDH. . 76

Figure II.13 General aromatic L-amino acid and neurotransmitter decarboxylation. 78

Figure II.14 Oxidation of testosterone 2-90 and select CYP active-site species. 79

Figure II.15 Accepted biosynthetic mechanism of oxidation for testosterone 2-90. 81

Figure II.16 Biosynthetic elaboration of 1-32 to (+)-aspewentin A (1-16). 82

Figure II.17 First-generation retrosynthetic analysis of (±)-aspewentin A ((±)-1-16). 83

Figure II.18 Proposed Michael-aldol-aldol process leading to key scaffold 2-112. 84

Figure II.19 Synthesis of donor 2-30. 85

Figure II.20 Screening of Michael acceptor 2-116. 86

Figure II.21 Hypothesized mechanism for loss of diastereoenrichment in 2-118. 89

Figure II.22 Synthesis of Michael acceptor 2-130. 91
Figure II.23 Screening of Michael-aldol reaction implementing donor 2-30 acceptor 2-130. 91
Figure II.24 Proposed stepwise synthesis leading to key scaffold 2-133. 92
Figure II.25 Synthesis and reactivity of acceptor 2-142. 93
Figure II.26 Synthesis and reactivity of acceptor 2-147. 94
Figure II.27 Pathway leading to the formation of 2-151. 95
Figure II.28 Synthesis of Michael acceptor 2-153. 96
Figure II.29 Screening of Michael reaction implementing acceptor 2-153. 96
Figure II.30 Deprotection approaches of adduct 2-155. 97
Figure II.31 Reductive transposition of adduct 2-155. 98
Figure II.32 Synthesis and attempted modification of adduct 2-164. 99
Figure II.33 Continued chemical modification of adduct 2-164. 100
Figure II.34 Observed reactivity of donor 2-174. 101
Figure II.35 Second-generation retrosynthetic analysis of (±)-aspewentin A ((±)-1-16). 102
Figure II.36 Synthesis of model tricycle 2-181. 103
Figure II.37 Decarboxylative aromatization to phenol 2-189. 105
Figure III.1 Proposed synthetic pathway leading to (±)-aspewentin A ((±)-1-16). 131
Figure III.2 First-generation synthesis of Michael acceptor 2-21. 132
Figure III.3 Second-generation synthesis of Michael acceptor 2-21. 133
Figure III.4 Synthesis and attempted oxidation of tricycle 2-25. 135
Figure III.5 Third-generation retrosynthetic analysis of (±)-aspewentin A ((±)-1-16). 136
Figure III.6 Synthesis of *gem*-dimethyl keto-ester donor 3-14. 136
Figure III.7 Decarboxylative Michael approach towards a tricyclic scaffold. 139

Figure III.8 Synthesis of *gem*-dimethyl keto-acid donor 3-18. 139

Figure III.9 Attempted decarboxylative cascade to construct aspewentin. 140

Figure III.10 Decarboxylative Cu(II)-catalyzed coupling of ynones and keto-acids. 141

Figure III.11 Mukaiyama-Michael approach to (±)-aspewentin A ((±)-1-16). 142

Figure III.12 Synthesis of acceptor 3-36. 143

Figure III.13 Reactivity of silyl ether donor 3-32. 144

Figure III.14 Third-generation retrosynthetic analysis of (±)-aspewentin A ((±)-1-16). 145

Figure III.15 High-pressure synthetic approach. 146

Figure III.16 Synthesis of model intermediate 3-42. 147

Figure III.17 Decarboxylative aromatization leading to phenol 3-47. 149

Figure III.18 Key cyclization generating (±)-aspewentin A ((±)-1-16). 150

Figure III.19 Precedent synthesis of enantioenriched Michael acceptor (*R*)-2-21. 151

List of Abbreviations

α: alpha

AADC: aromatic L-amino acid decarboxylase

acac: acetylacetone

AIBN: azobisisobutyronitrile

Alloc: allyloxycarbonyl

Ar: aryl

Ac: acyl

Ac-CoA: acyl coenzyme A

β: beta

9-BBN: 9-borabicyclo[3.3.1]nonane

BOX: bisoxazoline

Bu: butyl

Bz: benzoyl

c: cyclo

C: Celsius

CAN: ceric ammonium nitrate

cap: caprolactam

CoA: coenzyme A

CNS: central nervous system

CPME: *cyclo*-pentyl methyl ether

CSAD: cysteine-sulfinate decarboxylase

Cu: copper

CYP: cytochrome P450

dba: dibenzylideneacetone

DCE: 1,2-dichloroethane

DCM: dichloromethane

DDQ: 2,3-dichloro-5,6,-dicyano-1,4-benzoquinone

DEC: diethylcarbonate

DIBALH: diisobutylaluminium hydride

DIEA: *N*,*N*-diisopropylethylamine

DLD: dihydrolipoamide dehydrogenase

DMAP: 4-dimethylaminopyridine

DMAPP: dimethylallyl pyrophosphate

DMC: dimethylcarbonate

DME: dimethoxyethane

DMF: dimethylformamide

DMSO: dimethyl sulfoxide

DPEphos: bis[(2-diphenylphosphino)phenyl] ether

dppf: 1,1′-bis(diphenylphosphino)ferrocene

dppp: 1,3-bis(diphenylphosphino)propane

dr: diastereomeric ratio

ee: enantiomeric excess

EPR: electron paramagnetic resonance

Et: ethyl

EtOAc: ethyl acetate

Et_2O: diethyl ether

Equiv.: equivalent

EVK: ethyl vinyl ketone

FPP: farnesyl diphosphate

γ: gamma

GC-FID: gas chromatography-flame ionization detector

GCMS: gas chromatography-mass spectrometry

gem: geminal

GGPP: geranylgeranyl diphosphate

GPP: geranyl diphosphate

h: hour

HAT: hydrogen atom transfer

HDC: histidine decarboxylase

HFIP: 1,1,1,3,3,3-hexafluoroisopropanol

HMG-CoA: 3-hydroxy-3-methylglutaryl coenzyme A

HMPA: hexamethylphosphoramide

HRMS: high resolution mass spectroscopy

hv: ultraviolet light

i: iso

i-Bu: isobutyl

i-Pr: isopropyl

IBX: 2-iodoxybenzoic acid

IDI: isopentenyl-diphosphate delta isomerase

ImH: imidazole

IPP: isopentyl diphosphate

LAH: lithium aluminum hydride

LDA: lithium diisopropylamide

µ: micro

m-CPBA: *meta*-chloroperoxybenzoic acid

M: molarity

MAc: methoxyacetyl

Me: methyl

$MeNO_2$: nitromethane

mg: milligram

MOM: methoxymethyl

MTBE: methyl *tert*-butyl ether

n-Bu: butyl

n-Hex: hexyl

n-Pent: pentyl

n-Pr: propyl

$NADP^+$: nicotinamide adenine dinucleotide phosphate

NADPH: reduced form of $NADP^+$

nbd: bicyclo[2.2.1]hepta-2,5-diene

NBS: *N*-bromosuccinimide

NMO: *N*-methylmorpholine N-oxide

NMP: *N*-methyl-2-pyrrolidone

NMR: nuclear magnetic resonance

$O(MAc)_2$: methoxyacetic anhydride

p-TSA: *para*-toluene sulfonic acid

PDC: pyruvate decarboxylase

PDH: pyruvate dehydrogenase

PG: protecting group

PLP: pyridoxal phosphate

PPTS: pyridinium *para*-toluene sulfonate

Ph: phenyl

PhH: benzene

PhMe: toluene

Piv: pivalate

Pr: propyl

psi: pounds per square inch

R: variable molecular group unless specified

r.t.: room temperature

(*S*)-CBS: (*S*)-(−)-2-methyl-oxazaborolidine

(*S*)-*t*-BuPHOX: (*S*)-4-*tert*-butyl-2-[2-(diphenylphosphino)phenyl]-2-oxazoline

SAR: structure-activity relationship

sat.: saturated

SIPr: 1,3-bis(2,6-diisopropylphenyl)-4,5-dihydroimidazole-2-ylidene

t: tertiary

t-Bu: *tert*-butyl

T-HYDRO: 70% aqueous *tert*-butyl hydroperoxide

TBAF: tetrabutylammonium fluoride

TBS: *tert*-butyldimethyl silyl

TBD: 1,5,7-triazabicyclo[4.4.0]dec-5-ene

TBDMS: *tert*-butyldimethylsilyl

TBDPS: *tert*-butyldiphenylsilyl

TCDI: 1,1′-thiocarbonyldiimidazole

TEA: triethylamine

TEMPO: (2,2,6,6-tetramethylpiperidin-1-yl)oxyl

TES: triethylsilyl

Tf: triflate

THF: tetrahydrofuran

TMS: trimethylsilyl

TMS-EBX: 1-[(trimethylsilyl)ethynyl]-1,2-benziodoxol-3(1H)-one

TPAP: tetrapropylammonium perruthenate

TPP: tetraphenylporphyrin

TPSH: 2,4,6-triisopropylbenzenesulfonyl hydrazide

TTBP: 2,4,6-tri-*t*-butylphenol

Xantphos: 4,5-bis(diphenylphosphino)-9,9-dimethylxanthene

Abstract

Diverse natural product carbocycles and heterocycles are continuously of interest to the biochemical, synthetic, and medicinal communities. The biosynthetic pathways that lead to structurally diverse diterpenes, and other natural products, involve genes that are both highly conserved and mutable in their characteristic. These properties help ensure that healthy ecosystems continue generating novel complex molecules with diverse biological activity. Many synthetic approaches towards these natural products have been described, however, as known structural diversity in nature increases so does the need for novel methods to access the relevant structural analogues. The total synthesis of (±)-aspewentin A via a tandem Michael-aldol reaction approach has been developed and described herein. The key Michael reaction can be accomplished using copper (II)-catalysis of a ketoester and enone to provide an aldol substrate needed for a key carbocyclization to yield a desired complex intermediate. The first chapter will introduce the broad relevance of natural products to medicine and society. Then, tricyclic diterpene natural products that have been described and feature the fused bicyclic scaffold related to isopimaranes will be highlighted. Numerous syntheses that together encapsulate the breadth of synthetic approaches to access the isopimarane-like bioactive scaffolds have been organized and presented herein. Synthetic approaches may mimic natural biosynthesis or be derived from *de novo* approaches in synthetic connectivity. In the second chapter, the accepted biosynthetic pathway leading to (±)-aspewentin A is presented beginning from common metabolites. A precedent total synthesis will be introduced before the introduction of the novel, concise synthetic approach developed herein. The failed synthetic strategies that provided unexpected, but often in synthetically interesting,

carbocycles have also been presented. In the third chapter, the synthetic developments for the Cu(II)-Michael process implementing *gem*-dimethyl donors, that rapidly enable the formation of a highly congested intermediate are described. Synthetic access to these hindered intermediates enable the concise total synthesis of (±)-aspewentin A.

CHAPTER I

Introduction

I.1 Introduction to Relevance of the Isopimarane Diterpene Scaffold

Natural product discovery incessantly generates novel small molecule scaffolds that may become lead compounds for the treatment of a wide variety of illness and disease states.[1,2] Notably, the diversity of naturally available chemical space, and therefore bioactivity, is directly related to the delicate dynamics of available biodiversity within various regional ecosystems.[3-5] The resulting chemical diversity in these natural products help ensure that there exists a consistent interest in the characterization of novel structures and/or biotechnologies that facilitate their discovery. Furthermore, an argument can be made that certain natural products such as caffeine (**1-1**) from coffee (Figure I.1), morphine (**1-2**) from poppy, Δ^9-tetrahydrocannabinol (**1-3**) from cannabis,

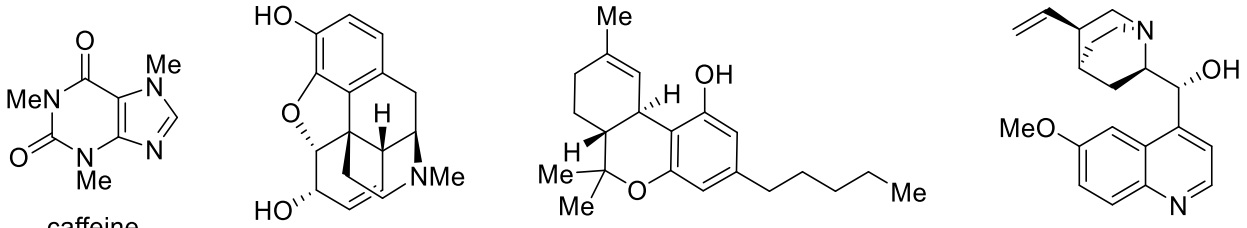

Figure I.1 Selected natural products with a significant impact on human activity.

quinine (**1-4**) from cinchona, and the many more that constitute desirable fragrances, dyes, or edible spices have themselves influenced politics, diplomacy, and conquest throughout human history.[6] In the modern age, many known natural products with less desirable addictive or

psychotropic properties remain the subject of intense medicinal and social investigation.[7,8] As effective as small molecules have been at affecting disease states as do we continue to seek novel structures.

Structural diversity, such as in isopimarane **1-6**, is achieved by complex molecular templating and cationic cyclization of linear polyene diphosphate biosynthetic precursors, like GGPP **1-5**, that are derived from the mevalonate pathway (Figure I.2).[9] The complex molecular architecture of terpenes are often synthetically challenging to produce in-flask, but can be carefully reconstructed via synthetic organic chemistry to facilitate access to complex natural products and their

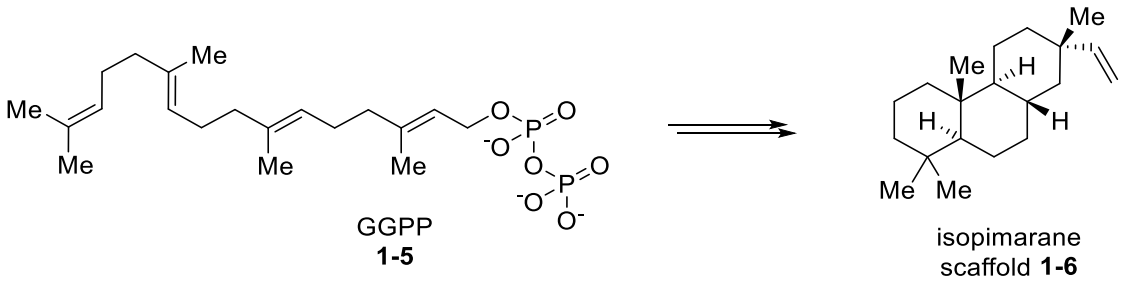

Figure I.2 Representative biotransformation of GGPP **1-5** to the isopimarane scaffold **1-6**.

bioisosteric analogues. The synthetic chemist finds an application within natural product drug discovery by building these diverse, structurally complex scaffolds from simple starting materials using the ever-evolving space of known chemical reactivity to develop unique strategies for precise chemical reconstruction.[10-15] Natural product total synthesis has an additional impact on the greater field of chemical synthesis as these syntheses may result in novel strategies for synthetic methodology, just as developments in synthetic methodology can enable novel disconnection strategies in total synthesis. In addition, chemical synthesis of natural products provides an opportunity for structural diversification and medicinal SAR studies through the synthesis of

functionally distinct product analogues. Thus, by synthetic means an investigator can optimize the bioavailability and bioactivity of natural products for therapeutic use.[16]

I.2 Selected Examples of Natural Isopimarane-related Diterpenes

The natural biosynthesis of large pools of distinct natural products is better enabled by enzymatic substrate promiscuity within a species.[17,18] These rationalizations help explain how changes in even slight alterations in gene expression may contribute to large phenotypic changes within single species.[19] Within the domain of natural product classes, terpenes are a large and diverse group of secondary metabolites originating from the biologically conserved mevalonate pathway found in organisms of every form.[20,21] Terpenoid molecules are found to feature varied structural motifs in nature, which provides them with an equally broad set of pharmacodynamics. Although terpene structural diversity allows for its functional use in nature ranging from toxins, repellants, or attractants,[22] their molecular polyene precursors are also vital as a primary metabolite for cholesterol biosynthesis and therefore for all subsequently derived sterol hormones that facilitate the regulation of bodily development or certain aspects of the physiological stress response.[23] Various cyclase enzymes create distinct carbon scaffolds and occasionally enable iterative biosynthetic transformations to provide a large scope of structural diversity.[24,25] One common skeletal motif for diterpenes is the presence of a fused tricarbocyclic core which often bears enantioenriched, and functionally elaborated, quaternary stereocenters (Figure I.3). For instance, the rhizome stem and root of some *Acanthopanax*,[26] *Illicium*,[27] *Kaempferia*,[28] and *Vellozia*[29] genera have revealed structurally diverse oxygenated diterpene isomers (**1-7** – **1-10**). The fungal genera of *Diaporthe*,[30] *Diplodia*,[31] *Epicoccum*,[32] and *Smardaea*[33] have generated

isopimaranes with notable diversity in structure and activity (**1-11** – **1-14)**. Red algae, *Laurencia perforata*, has produced a brominated analogue (**1-15**) of the tricarbocycle of interest.[34] A deep

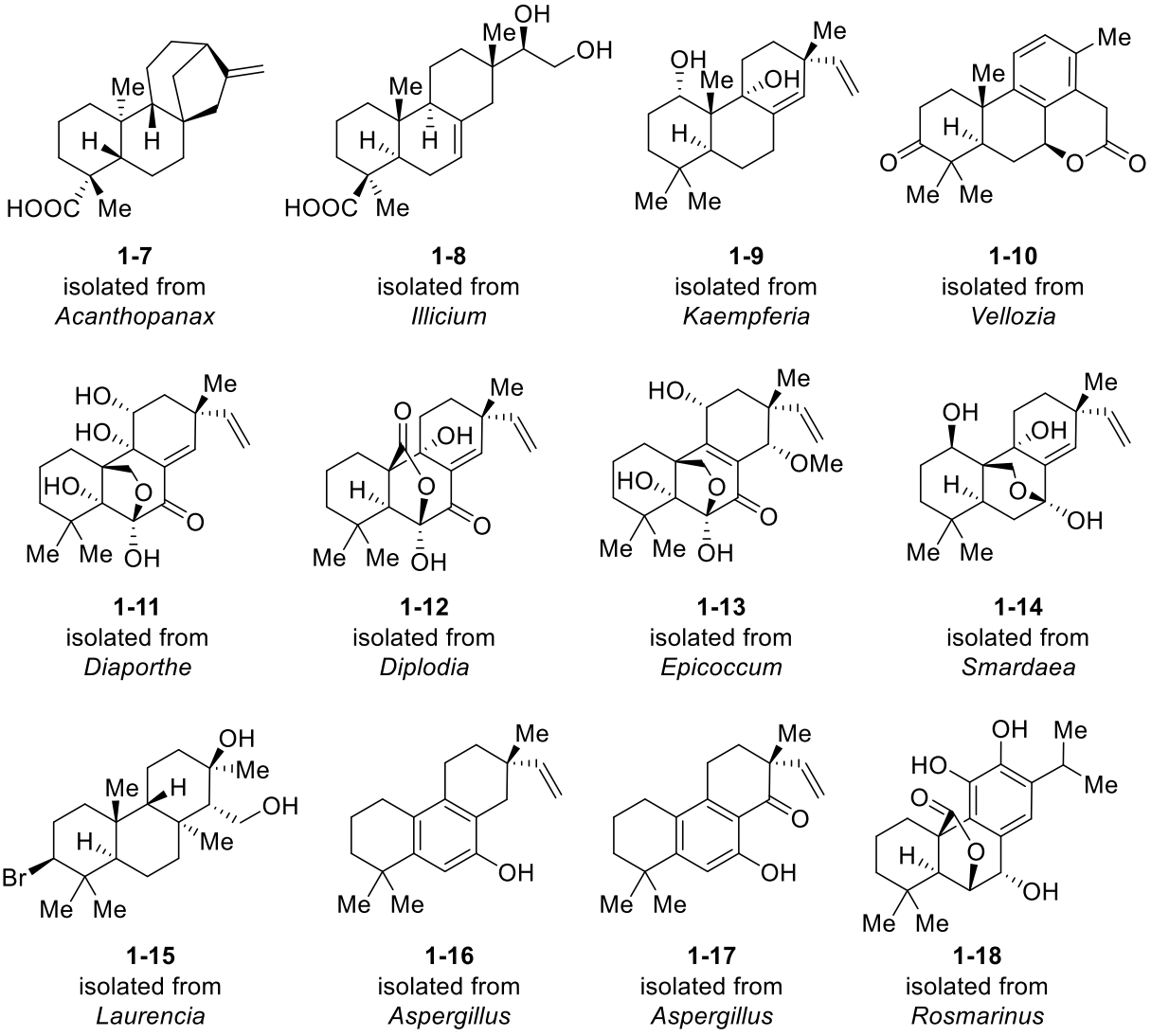

Figure I.3 Selected plant, fungal, and algal derived diterpenes.

sea sediment soil sample produced an initial report of the aspewentins, such as in (+)-aspewentin A (**1-16**) and (+)-aspewentin B (**1-17**), following the activation of a cryptic natural product pathway in an algicolous sample of *Aspergillus wentii*.[35] Notably, structurally analogous tricyclic phenolic diterpenes are one of the major electron-rich plant secondary metabolites associated with

antioxidant activity in certain plants[36,37] and remain of interest to the greater health community. Particularly, phenolic diterpenes associated with isomers of compound **1-18** are often associated with the desirable antioxidant activity of plants like rosemary (*Rosmarinus*).[38] However, it is unknown how the biological effects of standout diterpene compounds like (+)-aspewentin A (**1-16**) or B (**1-17**) are affected by the presence of its aromatic moiety.

I.3 Proposed Biosynthetic Pathway to Isopimaranes

Although a non-mevalonate pathway to the necessary biogenic compounds for terpene biosynthesis is well studied and utilizes starting materials available from glycolysis,[39] a more commonly described precursor is Ac-CoA (**1-19**), which is frequently derived biologically from fatty acid catabolism. Ac-CoA (**1-19**) is elongated to acetoacetyl CoA (**1-20**) by Ac-CoA thiolase (Figure I.4). Chiral alcohol, HMG-CoA (**1-21**), is produced by HMG-CoA synthase from acetoacetyl CoA (**1-20**) and subsequently reduced to mevalonic acid (**1-22**) by HMG-CoA reductase activity. Phosphorylation of **1-22** is achieved by mevalonate kinase whose phosphate product **1-23** is transformed to the diphosphate (pyrophosphate) product **1-24** by

phosphomevalonate kinase. Decarboxylation and dehydration of diphosphate **1-24** is performed by pyrophosphomevalonate decarboxylase to yield IPP (**1-25**) which may then be isomerized

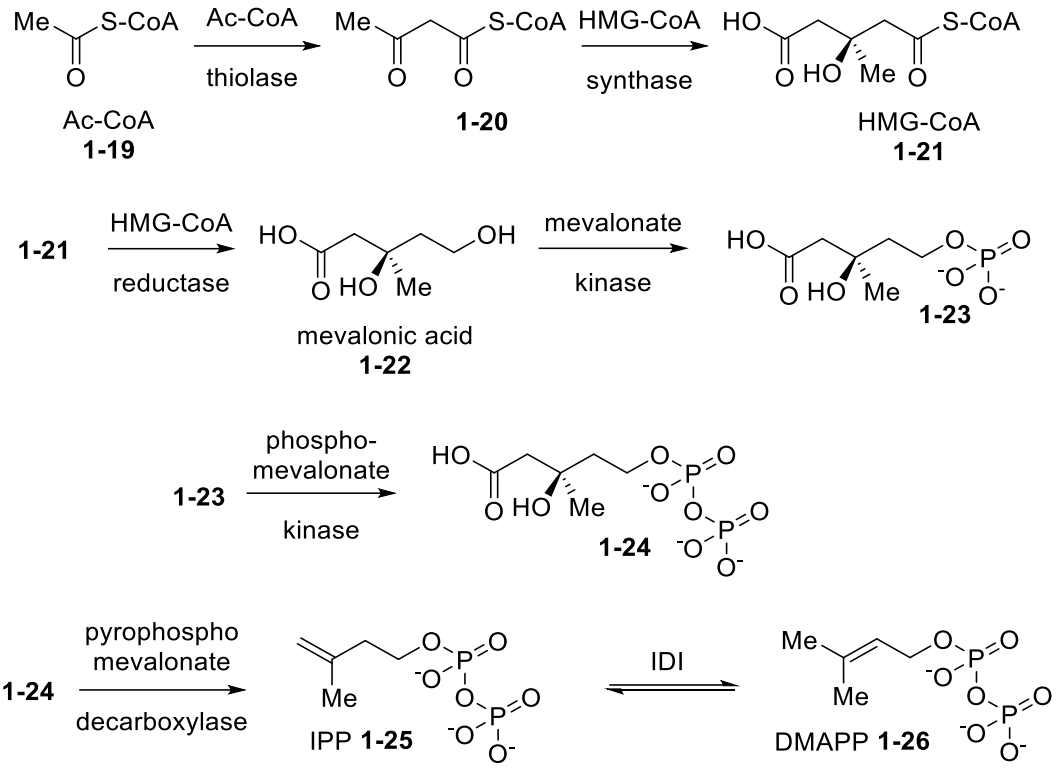

Figure I.4 Accepted major biosynthetic pathway leading to DMAPP and IPP.

by IDI to provide DMAPP (**1-26**). These two materials, DMAPP and IPP are two highly conserved biosynthetic building blocks which are requisite for polyene elongation and thus enable the biosynthesis of terpenes with highly variable molecular masses, structural isomerization, chiral character, and heteroatomic functionalization. Firstly, IPP (**1-25**) and DMAPP (**1-26**) are coupled by GPP synthase to synthesize GPP (**1-27**) (Figure I.5). FPP synthase then couples GPP (**1-27**) with IPP to yield FPP (**1-28**). FPP (**1-28**) is elongated to GGPP (**1-5**) by GGPP synthase using IPP. Now that GGPP is accessible to the organism, its cyclization by various cyclase enzymes may produce varied structural isomers,[9,24,25] but will also enable access to the familiar tricarbocyclic scaffold associated with the isopimarane diterpenes (Figure I.6). “Head-to-tail” activation (class II

cyclase activity) of GGPP (**1-5**) via protonation leads to rapid cyclization and formation of cationic species **1-29** that may form a stable exocyclic alkene **1-30** upon deprotonation. This ionic

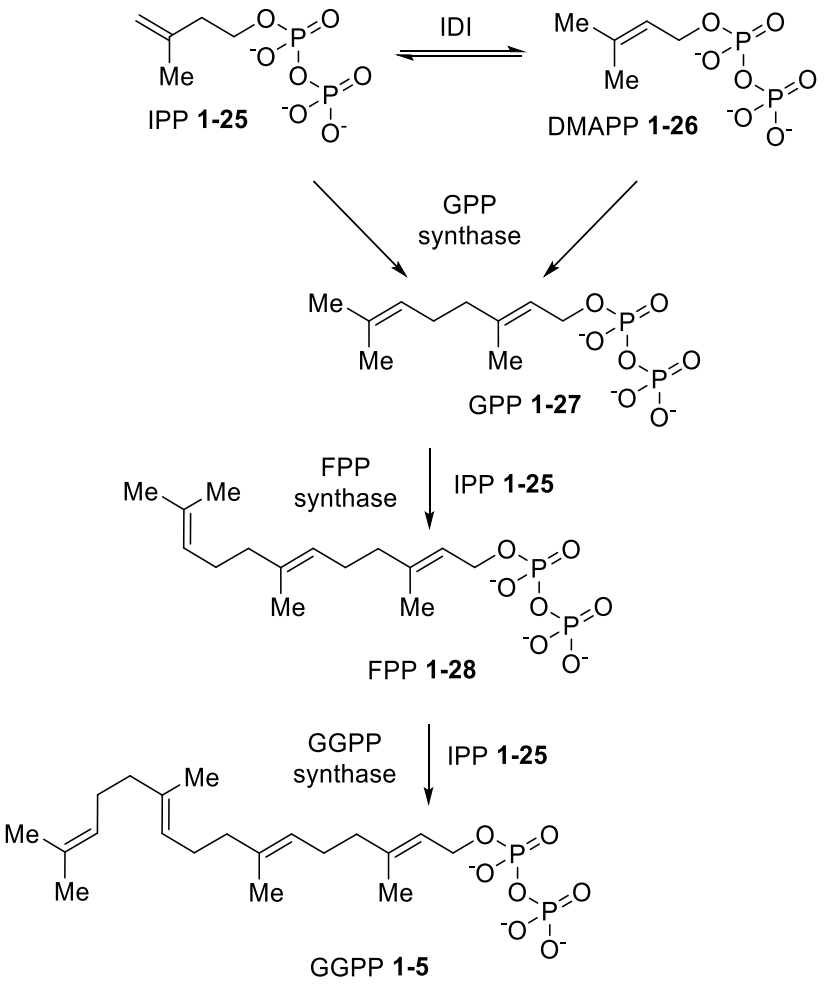

Figure I.5 Accepted major biosynthetic pathway leading to GGPP.

cyclization is expected to form the bridged tricycle in a concerted manner[24], although the intermediacy of alternative carbocationic structures cannot be ruled out, they are likely variable depending on the conformational dynamics of cyclase mutants across various species. In fact, reaction dynamics as affected by protein mutation and conformational dynamics can help explain how distinct, isomeric carbocyclic architectures all may selectively arise from linear GGPP **1-5**. Exocyclic alkene **1-30** provides a nucleophilic moiety to intramolecularly capture the cation

generated from ionic diphosphate departure, “tail-to-head” activation (class I cyclase activity), to

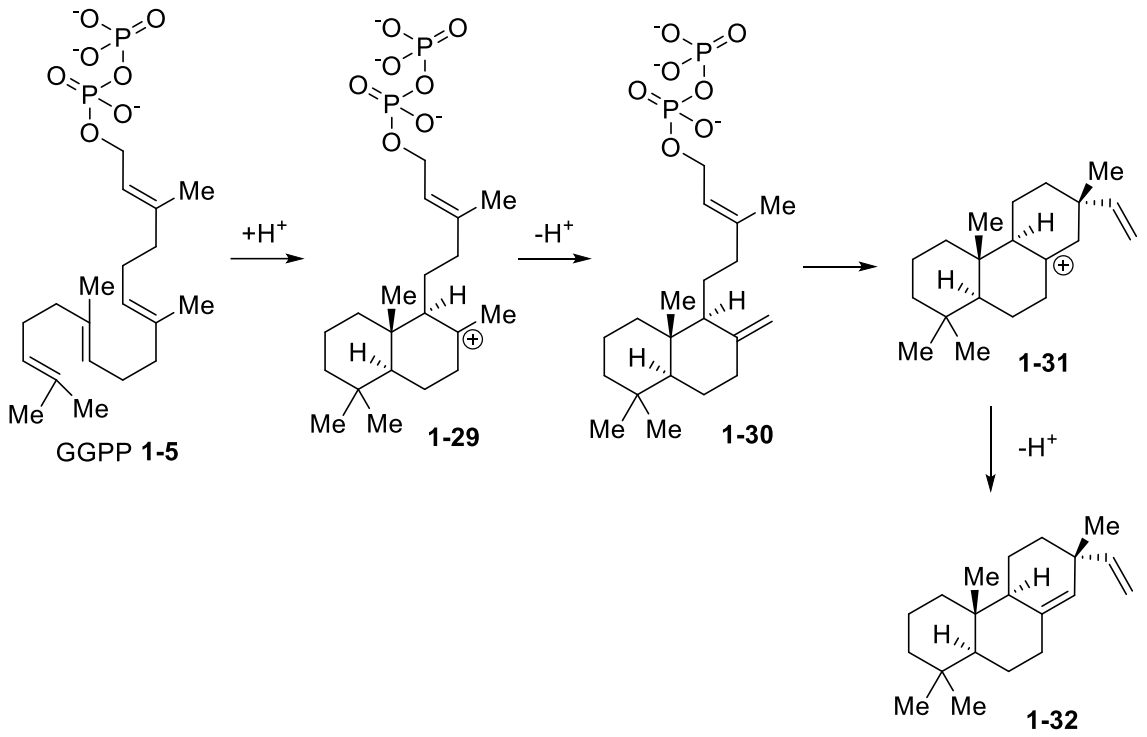

Figure I.6 Proposed biosynthetic pathway leading to scaffold **1-31**.

yield cationic intermediate **1-31** from species **1-30**. Deprotonation of carbocation **1-31** leads to alkene **1-32**, or a related isomer resulting from deprotonation of carbocation **1-31**. The implication of both class I and II cyclase activity would suggest the stabile intermediacy of species **1-30** during this biosynthesis. However, bifunctional enzymes that feature both class I and II cyclase activity have been reported to emerge in nature.[40] Nonetheless, the proposed biosynthetic pathway incorporating GGPP (**1-5**) to intermediates like **1-32** is mechanistically consistent with analogous, accepted diterpene biosyntheses.[9,41-43]

I.4 Selected Examples of Synthetic Biomimetic Tricyclization

Broadly speaking, the development of the synthetically relevant carbocyclization strategies owes its breadth to the equally diverse steroid hormone products[44-46] that compose both primary

and secondary metabolic pathways in nature. Steroids bear some structural similarly to diterpenes because of their polyene biosynthetic precursors that are also derived from the same mevalonate pathway as for all terpenes. This structural origination in a product of a biologically conserved pathway helps explains why terpenes are both common and diverse across the species. Consequently, even this single tricyclic core related to the isopimaranes provides a scaffold with access to a wide array of bioactivity. Due to potential medicinal use of the tricarbocyclic core, various synthetic groups have devoted effort to building analogous tricyclic diterpenes. Many synthetic contributions have been made towards the chemical synthesis of diterpenes and steroidal compounds alike. One major category of synthetic effort in this area is the biomimetic synthesis.[47] These syntheses are more analogous to the previously described biosynthetic cyclization of GGPP (**1**-**5**) which similarly leads to structurally complex compounds from polyene scaffolds. Although the natural cyclization is often proposed to invoke ionic cyclization via carbocation generation, both ionic and radical synthetic strategies have been achieved for synthetic biomimetic pathways. By establishing varying synthetic methodology to access these carbocyclic scaffolds, the associated pharmacophore can be structurally diversified to explore the changes that may alter the biological activity and efficacy of the molecule. The following synthetic examples are united in

their formation of an analogous fused tricyclic system associated with diterpene aspewentin A (**1-16**).

I.4.1 The van Tamelen Biomimetic Approach to the Diterpene Scaffold

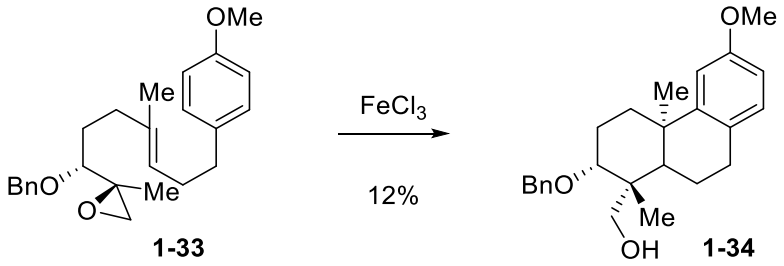

Figure I.7 Biomimetic van Tamelen key cyclization step.

For the synthesis of (±)-aphidicolin,[48] chiral epoxide **1-33** was cyclized via a Lewis acid-catalyzed ring closure to **1-34** in 12% yield mediated by $FeCl_3$ in PhMe (Figure I.7). The electron-rich methoxy arene moiety facilitates termination of the activated epoxide and yields an electrophilic aromatic substitution to generate cyclized product **1-34**. By designing this biomimetic synthesis, analogues of desirable complex molecules are made to rapidly generate complex scaffolds from selectively elongated polyene precursors.

I.4.2 The Corey Biomimetic Approach to the Diterpene Scaffold

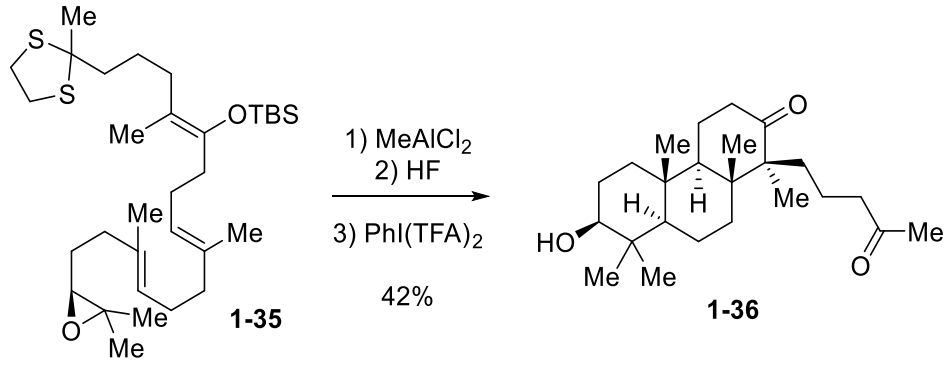

Figure I.8 Biomimetic Corey key cyclization step.

For the synthesis of dammarenediol II,[49] chiral epoxide **1-35** was cyclized via a Lewis acid-catalyzed ring closure mediated by $MeAlCl_2$ in DCM which was terminated by the silyl enol ether moiety of **1-35**. The resulting crude material was then subjected to aqueous HF in MeCN and then $PhI(TFA)_2$ in wet methanol to provide product **1-36** in 42% yield (Figure I.8). The conformational constraints on these highly substituted precursors affect the favorability of certain reaction transition states and yield the observed cyclized product with the observed diastereoselectivity.

I.4.3 Alternative Corey Biomimetic Approach to the Diterpene Scaffold

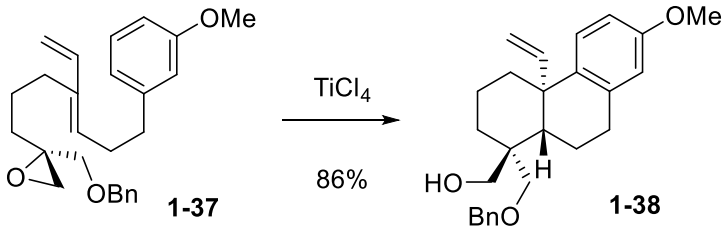

Figure I.9 Alternative biomimetic Corey key cyclization step.

For the synthesis of neotripterifordin[50] an approach similar to the previous van Tamelen synthesis (Figure I.7) was achieved by using chiral epoxide **1-37** was cyclized via a Lewis acid-catalyzed ring closure to **1-38** in 86% yield mediated by $TiCl_4$ in DCM (Figure I.9). Facile ionic cyclization of substrate **1-37** can be rationalized by the buildup of cationic character in anticipated intermediates through the annulation pathway. Participation of the trisubstituted olefin moiety of **1-37** in ionic opening of the activated epoxide adduct generates an intermediate with a buildup of an allylic carbocation character. The electron-rich methoxy arene moiety originating in **1-37** facilitates termination via an electrophilic aromatic substitution and the terminating C-C bond formation and is further accelerated by the *para*-methoxy group resonance effects when compared to the previous van Tamelen example leading to **1-34**. Furthermore, synthetic access to alkenyl

products like **1-38**, provides a functional handle for access to C-19 oxidation which is otherwise challenging to achieve selectively on inactivated substrates.

I.4.4 The Pattenden Biomimetic Radical Approach to the Diterpene Scaffold

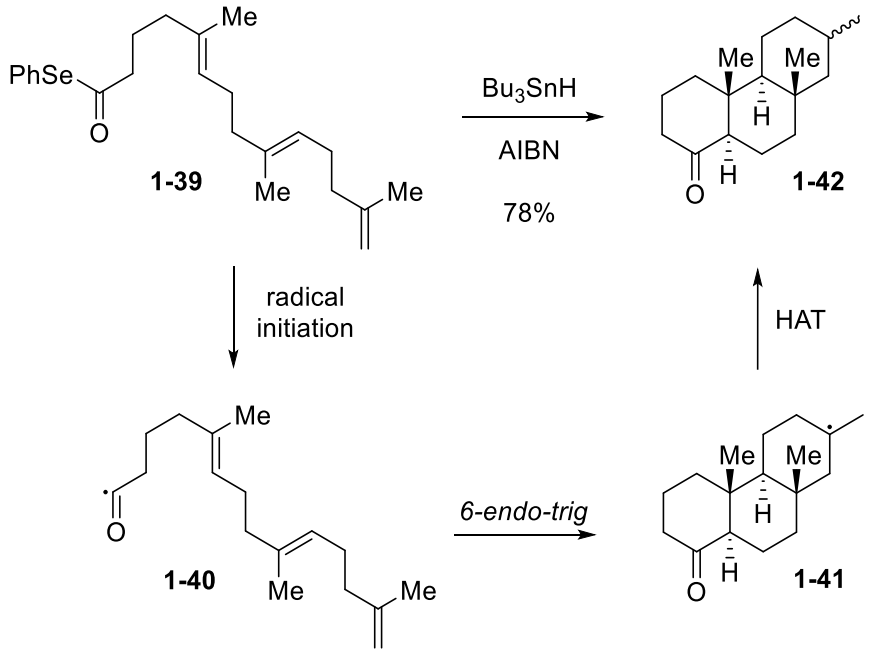

Figure I.10 The Biomimetic Pattenden key radical cyclization step.

During studies on radical polyene cyclization pathways,[51,52] selenoester **1-39** was cyclized via a radical ring closure to **1-42** in 78% yield as a mixture of epimers initiated by AIBN and terminated by tributyl stannane reductant in PhH under reflux conditions (Figure I.10). Radical initiation by AIBN results in the formation of acyl radical **1-40** and a subsequent *6-endo-trig* cyclization step yields radical **1-41**. Termination of radical **1-41** with the stannane provides the intended product and a resulting tin-centered radical to propagate the radical process. Notably, the radical mode of cyclization offered greater flexibility in the potential site of radical termination, unlike the ionic cyclization which more frequently relies on intramolecular nucleophilic trapping in practice, as in the prior examples. Depending on the olefin substitution patterns, different C-C

bond formation patterns led to the observation of either 5-member or 6-member cyclization products when this methodology was explored.

I.4.5 The MacMillan Biomimetic Radical Approach to the Diterpene Scaffold

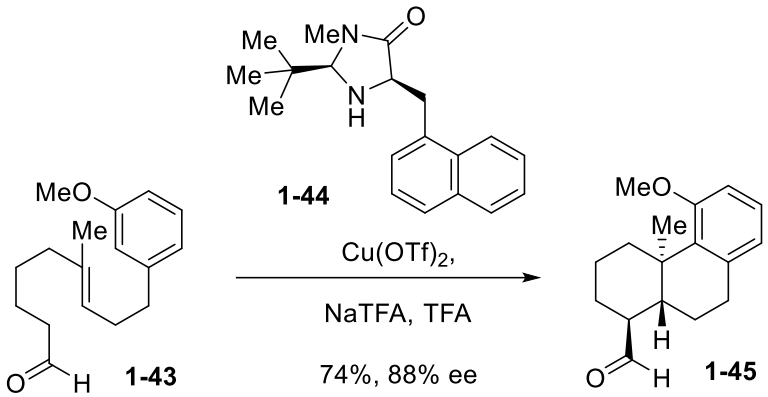

Figure I.11 The Biomimetic MacMillan key radical cyclization step.

During studies on enantioselective radical polyene cyclization pathways,[53] aldehyde **1-43** was stirred with a catalytic quantity of chiral imidazolidinone **1-44** to enantioselectively generate cyclized product **1-45** in 74% yield and 88% ee using $Cu(OTf)_2$ and a mixture of TFA and NaTFA in a 1:2 mixture of i-PrCN/DME (Figure I.11). Imidazolidinone catalyst **1-44** was found to broadly control product enantioselectivity and various electronic substitution patterns were tolerated when analogues of the tricyclic scaffold were generated via this method.

I.5 Selected Examples of Ionic Tricyclization

There similarly exist numerous alternative synthetic pathways designed for application during natural product total syntheses to access this tricyclic scaffold associated with isopimarane diterpenes. Each distinct total synthesis offers an approach to create these compounds with a unique diversity in chemical functionalization and chiral character, such that together complement

the overall synthetic accessibility to this structure of interest. These select syntheses have been chronologically arranged based on the mode of their key tricyclization step.

I.5.1 The Meyer Approach to the Diterpene Scaffold

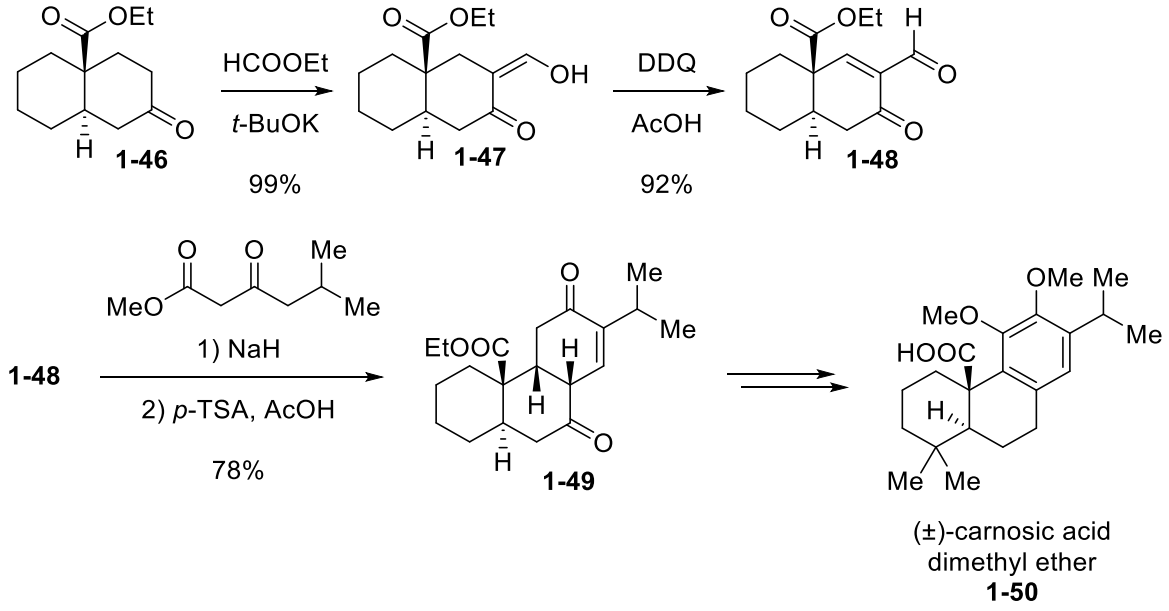

Figure I.12 The Meyer tricyclic scaffold synthesis.

A Robinson annulation strategy has been applied for a total synthesis of (±)-carnosic acid dimethyl ether (**1-50**) (Figure I.12).[54] To this end, ester **1-46** was formylated using ethyl formate and *t*-BuOK in *t*-BuOH to provide ketone **1-47** in quantitative yield. Ketone **1-47** was oxidized using DDQ and catalytic AcOH in 1,4-dioxane to provide the unsaturated product **1-48** in 92% yield. Methyl isovalerylacetate successfully underwent Robinson annulation via conjugate addition onto acceptor **1-48** using NaH in DMSO to afford an intermediate mixture that was then

subjected to an aldol reaction promoted by AcOH and *p*-TSA under refluxing conditions to give cyclized product **1-49** in 78% yield.

I.5.2 The Cai Approach to Diterpene Scaffold

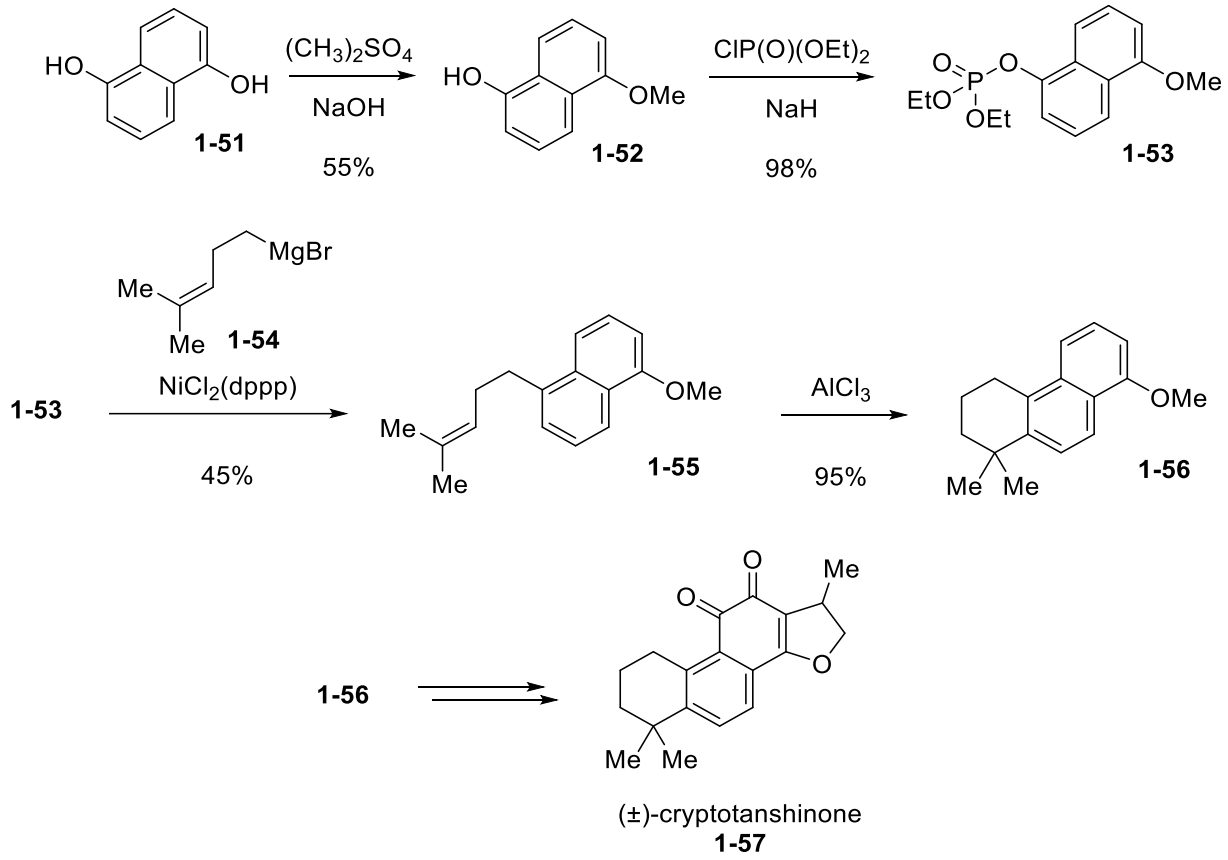

Figure I.13 The Cai tricyclic scaffold synthesis.

A Lewis acid-mediated electrophilic aromatic substitution strategy has been utilized for a total synthesis of (±)-cryptotanshinone (**1-57**),[55] beginning with monomethylation of 1,5-naphthalene-diol **1-51** using dimethyl sulfate and aqueous NaOH to yield naphthol **1-52** in 55% yield (Figure I.13). Naphthol **1-52** was converted to phosphate ester **1-53** using diethyl phosphorochloridate and NaH in THF in 98% yield. Phosphate **1-53** underwent cross-coupling with prepared organomagnesium bromide species **1-54** using catalytic $NiCl_2$(dppp) in Et_2O to provide coupled

product **1-55** in 45% yield. Key intramolecular electrophilic aromatic substitution was performed by subjecting adduct **1-55** to $AlCl_3$ in DCM to yield tricyclized material **1-56** in 95% yield.

I.5.3 The Overman Approach to the Diterpene Scaffold

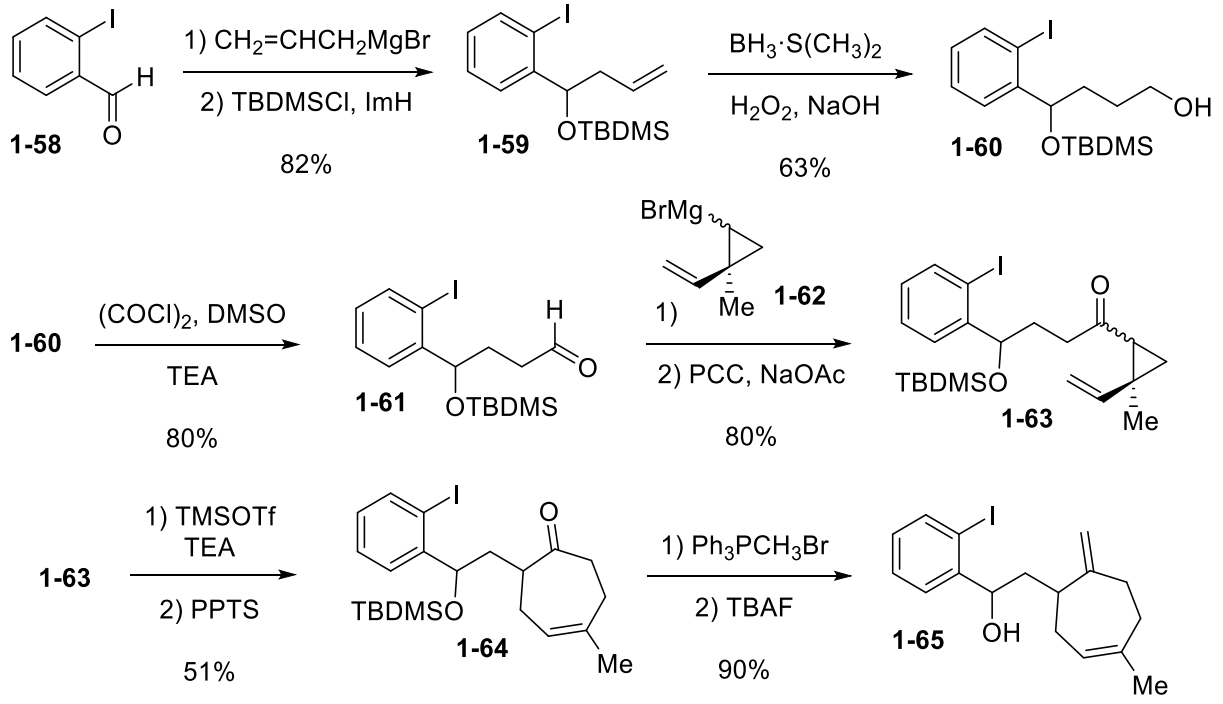

Figure I.14 The Overman synthesis of a precursor of scopadulcic acid B.

A palladium-mediated cyclization was accomplished to access the desired tricycle for a total synthesis of scopadulcic acid B (**1-72**) (Figure I.14).[56] Aldehyde **1-58** was treated with allylmagnesium bromide in THF and then subjected to TBDMSCl and ImH in DMF to generate product **1-59** in 82% yield. Alkene **1-59** was hydroborated using borane dimethyl sulfide complex in hexanes and then subjected to aqueous NaOH and H_2O_2 to provide alcohol **1-60** in 63% yield. Alcohol **1-60** was oxidized using Swern conditions of oxalyl chloride and DMSO with TEA in DCM to afford aldehyde **1-61** in 80% yield. Pre-made Grignard reagent **1-62** was subjected to substrate **1-61** in Et_2O to generate an intermediate alcohol, which was oxidized to ketone **1-63** in

80% yield using PCC and NaOAc in DCM. Ketone **1-63** was enolized to form a silyl enol ether using TMSOTf and TEA in DCM. The resulting crude silyl enol ether was refluxed in PhH prior to a transfer into EtOH, then subjected to wet PPTS to form a cyclized, Cope rearrangement product **1-64** in 51% yield. Ketone **1-64** was olefinated using methyltriphenylphosphonium bromide, deprotonated using *n*-BuLi, in THF and then exposed to TBAF in THF to provide alcohol **1-65** in 90% yield.

Alcohol **1-65** was oxidized using PCC and NaOAc in DCM to yield ketone **1-66** in 90% yield (Figure I.15). The key cyclization was then achieved by reacting ketone **1-66** with excess TEA and a catalytic quantity of $Pd(OAc)_2$ and PPh_3 under reflux in MeCN to provide a 1.5:1 ratio mixture of cyclized materials **1-70** and **1-71** in 83% yield. Cyclization can be understood as proceeding via an oxidative addition of the Pd metal onto the aryl halide bond to generate palladated intermediate **1-67**. Intramolecular migratory insertion leads to cyclized intermediate **1-68**, and a subsequent migratory insertion to intermediate **1-69** yields the observed carbocyclic product scaffold. β-Hydride elimination from **1-69** provides product **1-70**, and subsequent allylic isomerization by Pd likely converts product **1-70** to the more stable enone **1-71** to provide the observed product mixture. These two resulting products can be converged under oxidative conditions and were both implemented in the final total synthesis of scopadulcic acid B (**1-72**).

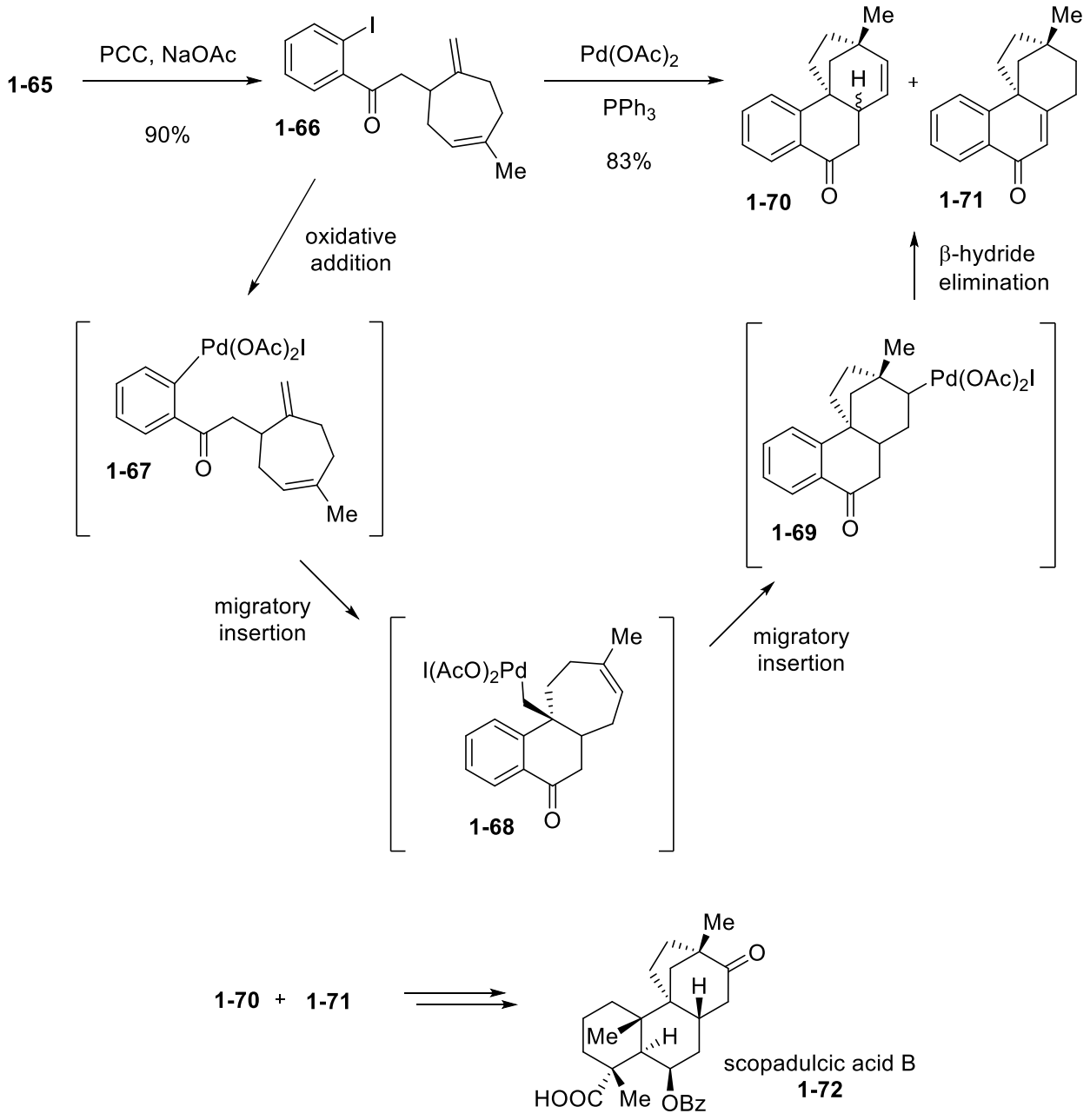

Figure I.15 The Overman synthesis of scopadulcic acid B.

I.5.4 The Pan Approach to the Diterpene Scaffold

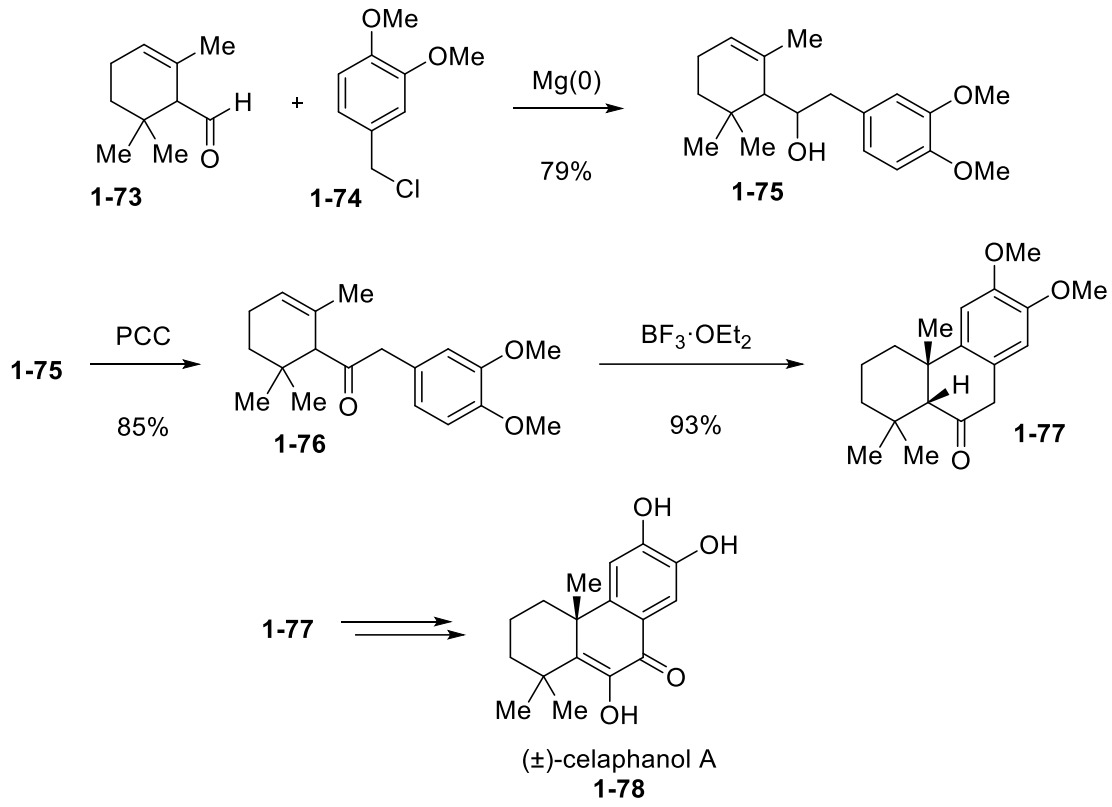

Figure I.16 The Pan synthesis of (±)-celaphanol A.

A Lewis acid-mediated isomerization and electrophilic aromatic substitution strategy has been applied for a total synthesis of (±)-celaphanol A (**1-78**) (Figure I.16).[57] Benzyl chloride **1-74** was subjected to magnesium powder in Et_2O and the resulting Grignard intermediate was subjected to aldehyde **1-73** in Et_2O which resulted in 79% yield of adduct **1-75**. Alcohol **1-75** was oxidized using PCC in DCM to generate ketone **1-76** in 85% yield. Key cyclization of ketone **1-76** was then achieved using boron trifluoride diethyl etherate in DCM to afford product **1-77** in 93% yield. This reaction process is likely achieved by an acid-mediated 1,3-isomerization of the alkene of starting material **1-76** by Lewis acid-assisted Brønsted acidity. Alkene isomerization can form a conjugated

enone intermediate from **1-76** that may undergo an intramolecular Michael addition leading to product **1-77**.

I.5.5 The Tu Approach to the Diterpene Scaffold

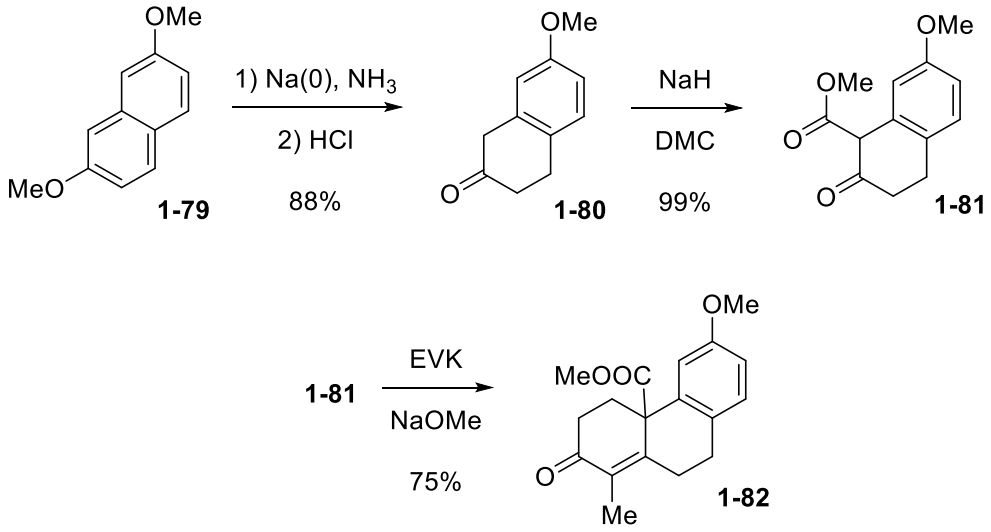

Figure I.17 The Tu tricyclic synthesis of pisiferic acid core scaffold.

A Robinson annulation strategy was implemented to access the core tricycle during studies on the total synthesis of pisiferic acid-type diterpenes (Figure I.17).[58] Ether **1-79** was reduced using liquid ammonia and metallic sodium in EtOH. The resulting crude material was hydrolyzed using aqueous HCl in acetone to provide ketone **1-80** in 88% yield. Ketone **1-80** was esterified using NaH and DMC in refluxing PhH to yield ketoester **1-81** in 99% yield. The key Robinson annulation was achieved by stirring ketoester **1-81** with EVK and NaOMe in MeOH to generate product **1-82** in 75% yield.

I.5.6 The Qin Approach to Diterpene Scaffold

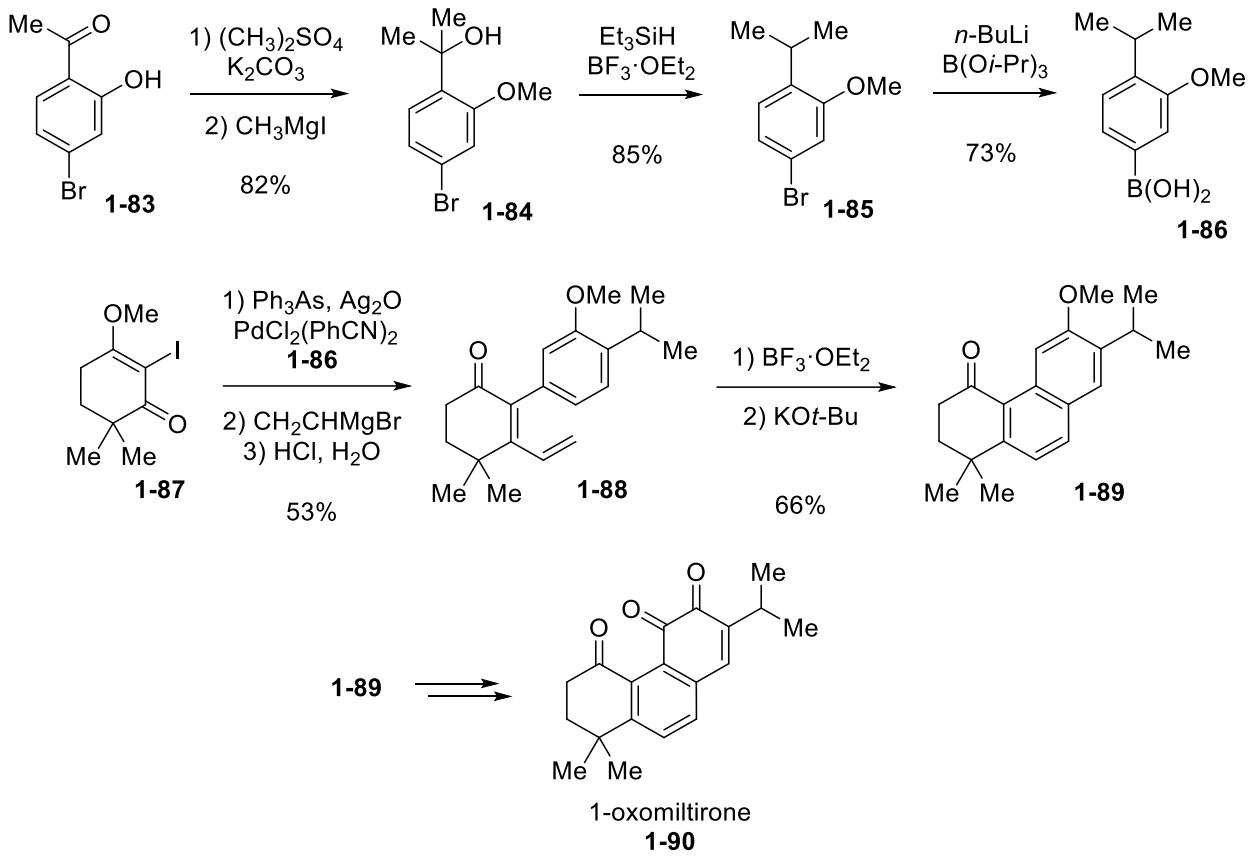

Figure I.18 The Qin synthesis of 1-oxomiltirone.

An electrophilic aromatic substitution/aromatization strategy was implemented for a total synthesis of 1-oxomiltirone (**1-90**) (Figure I.18).[59] Phenol **1-83** was methylated using dimethyl sulfate and potassium carbonate in acetone, and subsequently subjected to CH_3MgI to convert its ketone into a tertial alcohol **1-84** in 82% yield. Tertiary alcohol **1-84** was deoxygenated using triethyl silane and boron trifluoride diethyl etherate in DCM to provide product **1-85** in 85% yield. Aryl bromide **1-85** was made into boronic acid **1-86** using n-BuLi and triisopropylborate in THF in 73% yield. Separately, iodoalkene **1-87** was prepared using a previously reported synthesis.[60] Boronic acid **1-86** was coupled with iodoalkene **1-87** in the presence of stoichiometric quantities of silver oxide and catalytic quantities of triphenylarsine and $PdCl_2(PhCN)_2$ in wet THF to yield a

crude coupled product that was then subjected to vinyl magnesium bromide in THF. The intermediate product undergoes an acidic demethylation during upon exposure to aqueous HCl and ultimately results in product **1-88** in 53% yield. Key cyclization of material **1-88** was achieved using boron trifluoride diethyl etherate in carbon tetrachloride under refluxing conditions and then subsequentially refluxed in *t*-BuOH with *t*-BuOK (presumably in exposure to ambient atmosphere

to provide the oxidative conditions needed for final aromatization) which gave aromatized product **1-89** in 66% yield.

I.5.7 The Koert Approach to Diterpene Scaffold

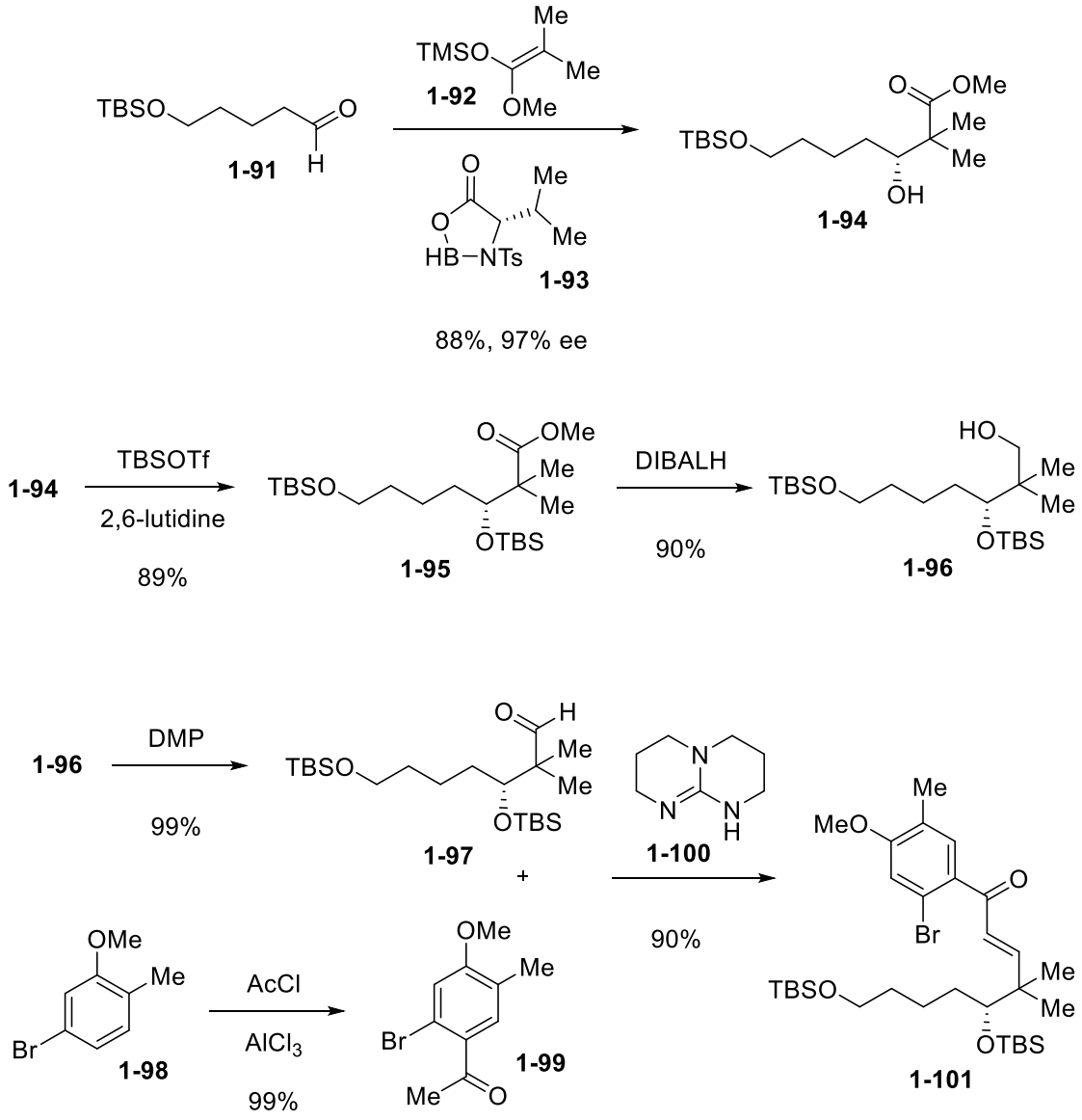

Figure I.19 The Koert synthesis of intermediate to (+)-elevenol.

A Pd-mediated enolate arylation strategy was employed for a total synthesis of (+)-elevenol (**1-107**) (Figure I.19).[61] Aldehyde **1-91** was stirred with silyl ketene acetal **1-92** and stoichiometric

quantities of chiral borane **1-93** in THF for a 88% yield of alcohol **1-94** in 97% ee via a borane-mediated aldol reaction.[62] Alcohol **1-94** was protected using TBSOTf and 2,6-lutidine in DCM to provide product **1-95** in 89% yield. Substrate **1-95** was reduced using DIBALH in DCM to alcohol **1-96** in 90% yield. The produced alcohol **1-96** was then oxidized using DMP in DCM to yield aldehyde **1-97** in 99% yield. Separately, aryl bromide **1-98** underwent acylation using acetyl chloride and $AlCl_3$ in DCM to provide ketone **1-99** in 99% yield. Ketone **1-99** and aldehyde **1-97** underwent an aldol condensation process using TBD (**1-100**) to generate enone **1-101** in 90% yield. The primary silyl ether moiety of enone **1-101** was deprotected using PPTS in EtOH to provide alcohol **1-102** in 98% yield (Figure I.20). Alcohol **1-102** was subsequently treated with DMP and then chiral pyrrolidine **1-103** facilitated an intramolecular Michael addition of an intermediate enamine onto the enone to provide an intermediate aldehyde species that was subjected to the next step without further purification. Then, a net disproportionation (Tishchenko-type) of the formyl and ketone groups of the *in-situ* generated material using *i*-Bu_2AlOMe in PhMe results in the formation of product **1-104** in 50% yield and >20:1 dr. Key cyclization of ester **1-104** is achieved

using NaHMDS, and catalytic quantities of both $Pd(dba)_2$ and SIPr ligand precursor **1-105** in PhMe to afford product **1-106** in 98% yield via an enolate arylation mechanism mediated by Pd.[63]

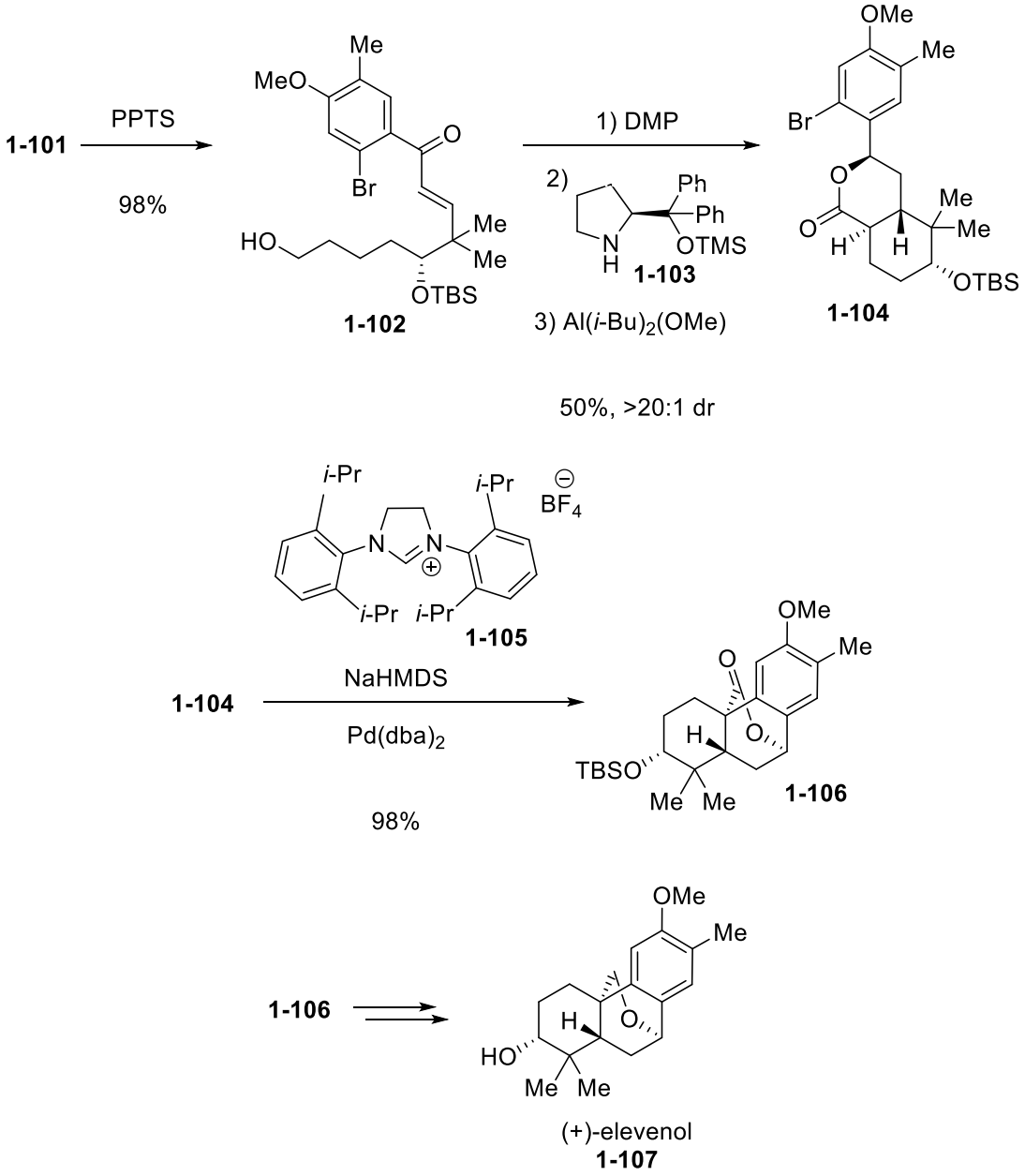

Figure I.20 The Koert synthesis of (+)-elevenol.

I.5.8 The Herzon Approach to Diterpene Scaffold

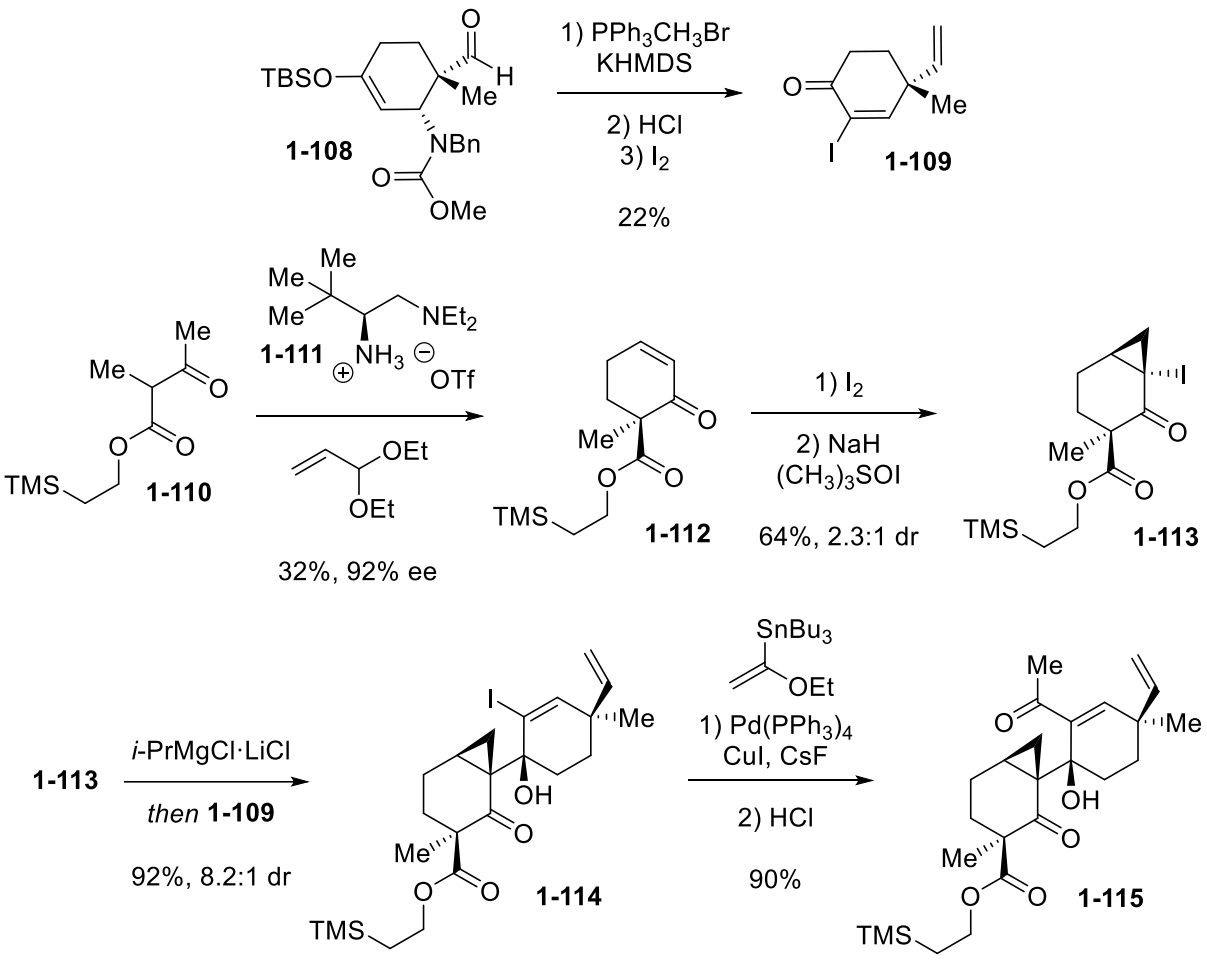

Figure I.21 The Herzon synthesis of intermediate to core of myrocin G.

A base-mediated aldol condensation was used to for the intended tricycle for a total synthesis of myrocin G (**1-118**).[64] An enantioenriched cyclic aldehyde **1-108** was prepared in four steps according to a reported procedure in 20% yield and 95% ee.[65] Aldehyde **1-108** was then olefinated using methyltriphenylphosphonium bromide and KHMDS in THF, deprotected using aqueous HCl in THF, and iodinated using I_2 in 5% (v/v) pyridine–DCM to provide enone **1-109** in 22% yield (Figure I.21). Separately, ester **1-110** was prepared according to a previously reported procedure in 77% yield.[66] Ester **1-110** was annulated using catalytic quantity of chiral amine **1-111** and excess

3-nitrobenzoic acid in MeCN for enamine catalysis with acrolein diethyl acetal to provide product **1-112** in 32% yield and 22% ee. The cyclic ester **1-112** was sequentially α-iodinated in 5% (v/v) pyridine–DCM and then its enone moiety was cyclopropanated using trimethylsulfoxonium iodide and NaH in DMF which gave alkylated product **1-113** in 64% yield and 2.3:1 dr. The formed alkyl iodide **1-113** was converted into a Grignard species *in-situ* using Mg/I exchange with *i*-PrMgCl·LiCl (Turbo Grignard) in PhMe and then coupled with **1-109** to provide product **1-114** in 92% yield and 8.2:1 dr. Stille coupling of substrate **1-114**, incorporating catalytic $Pd(PPh_3)_4$, excess CuI, stoichiometric CsF and tributyl(1-ethoxyvinyl)stannane in MeCN followed by an acidic hydrolysis of the resulting intermediate ethyl vinyl ether using aqueous HCl in THF generated product **1-115** in 90% yield. The alcoholic moiety of **1-115** was protected using TMSOTf and TEA in DCM, then the ketone moiety was oxidized using *m*-CPBA in DCM to an intermediate acyloin species which was immediately protected using AllocCl in 5% (v/v) pyridine–DCM to yield product **1-116** in 41% yield (Figure I.22). Key cyclization of **1-116** was achieved under basic condition using NaO*t*-Bu in THF leading to aldol condensation product **1-**

117 in 64% and an additional hydrated cyclized product in 15% yield. Deprotection of **1-117** using TBAF led to myrocin G (**1-118**) in 64% yield.

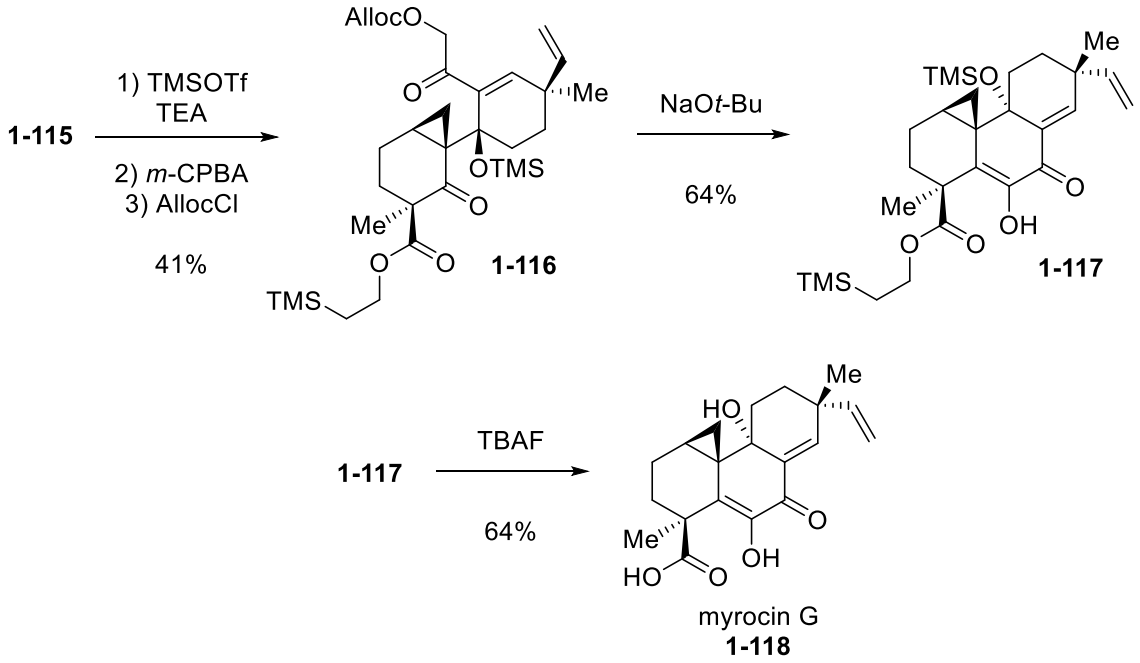

Figure I.22 The Herzon synthesis of myrocin G.

I.5.9 The Carter Approach to the Diterpene Scaffold

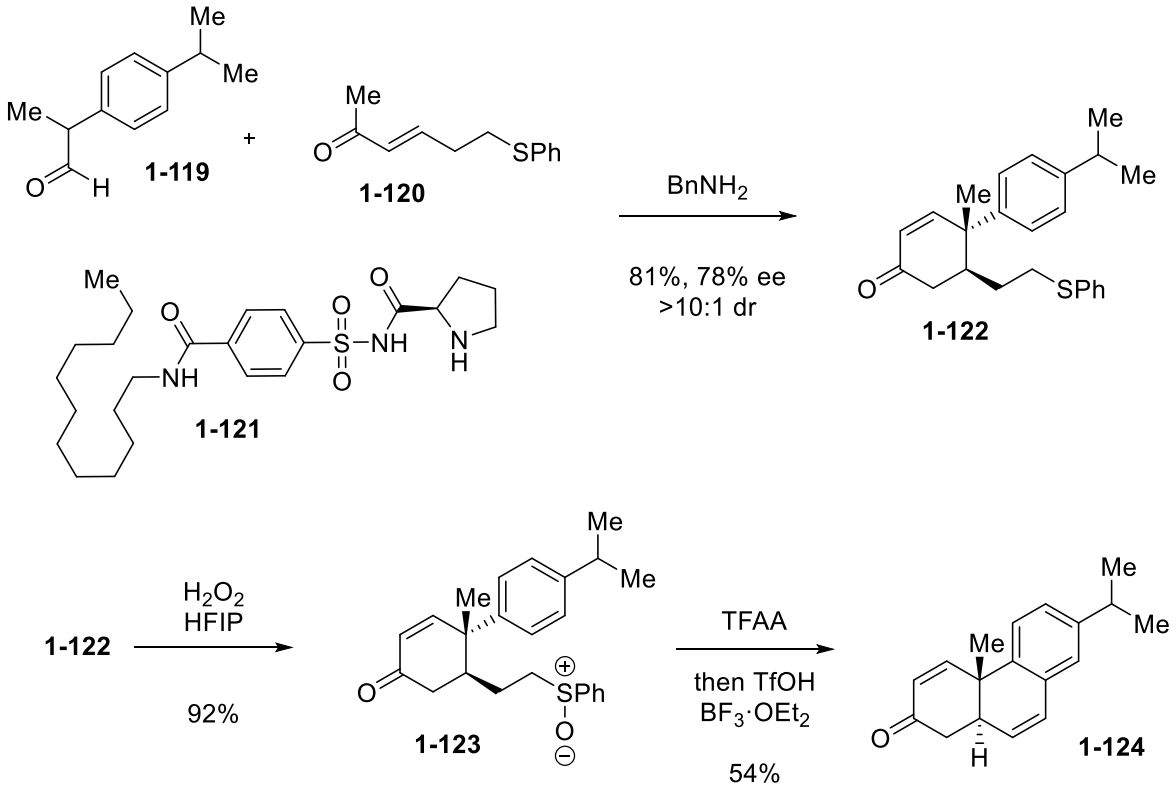

Figure I.23 The Carter synthesis of an aromatic abietane.

A tandem Pummerer rearrangement/electrophilic aromatic substitution strategy was implemented for the divergent total syntheses of aromatic abietane diterpenoids (Figure I.23).[67] Aldehyde **1-119** and enone **1-120** were stirred with benzyl amine and pyrrolidine catalyst **1-121** in DCE and DMSO to yield annulated product **1-122** in 81% yield, 78% ee, and >10:1 dr. The phenyl sulfide moiety of **1-122** was oxidized using H_2O_2 in HFIP and DCM to provide sulfoxide **1-123** in 92% yield. Key cyclization of substrate **1-123** was achieved using TFAA in DCE to facilitate a Pummerer rearrangement to an intermediate monothioacetal, followed by the addition of TfOH and boron trifluoride diethyl etherate to yield 54% of product **1-124**.

I.6 Selected Examples of Redox-Initiated Tricyclization

I.6.1 The Maimone Approach to the Diterpene Scaffold

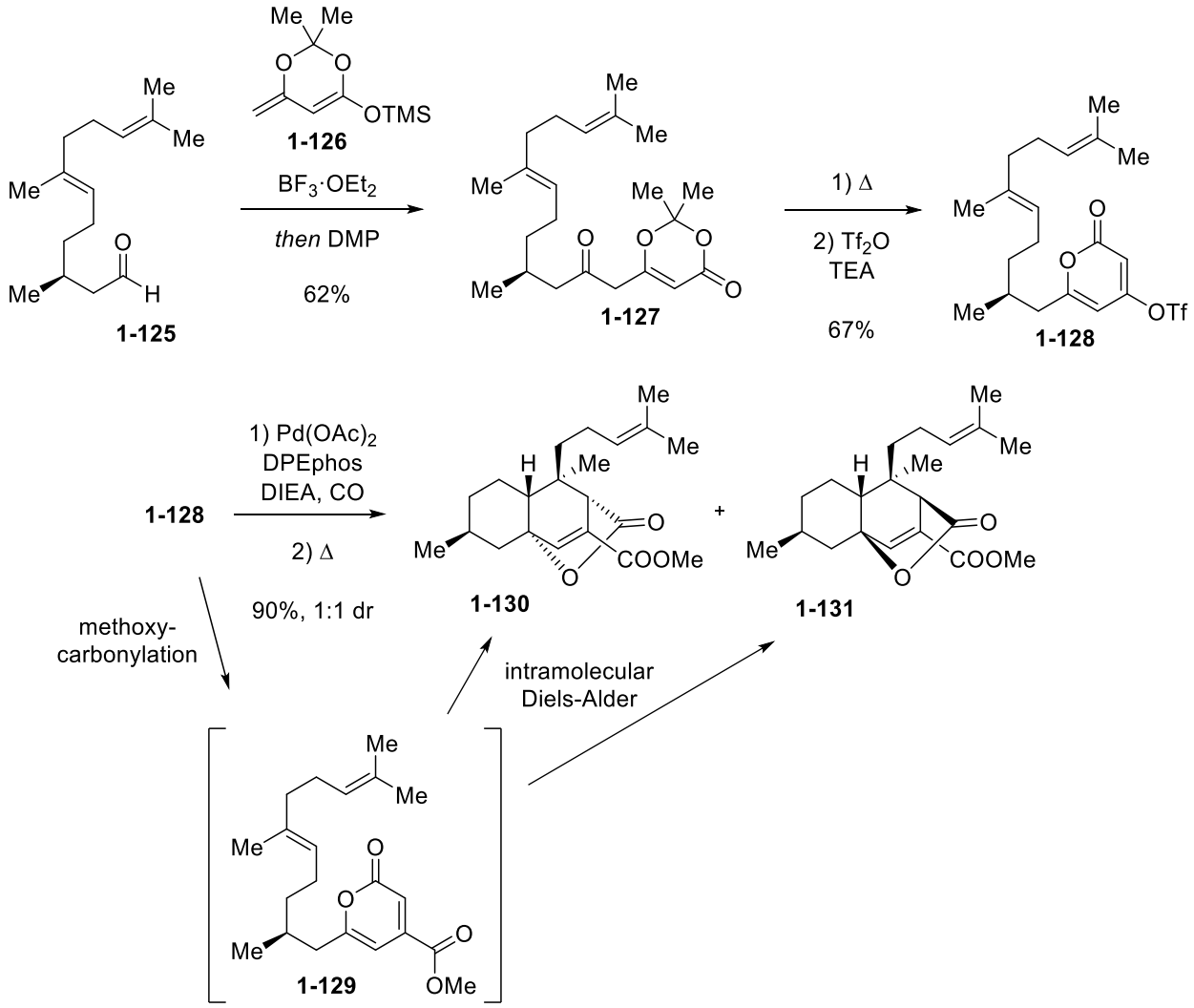

Figure I.24 The Maimone synthesis of precursor to (+)-chatancin.

A tandem chlorination/intramolecular Barbier coupling strategy was utilized during the total synthesis of (+)-chatancin (**1-135**).[68] Aldehyde **1-125** was stirred with silyl ketene acetal **1-126** in the presence of boron trifluoride diethyl etherate in DCM and the produced crude material was then oxidized using DMP and $NaHCO_3$ in DCM to afford ketone **1-127** in 62% yield (Figure I.24). Substrate **1-127** was refluxed in PhMe to produce an α-pyrone then subjected to triflic anhydride

and TEA in DCM to generate triflated pyrone **1-128** in 67% yield. Pyrone **1-128** was intramolecularly cyclized by stirring with DIEA and carbon monoxide with catalytic quantities of $Pd(OAc)_2$ and DPEphos in methanolic MeCN to form intermediate **1-129** via a previously established method of methoxycarbonylation,[69] then subsequently refluxed in PhMe to provide a 1:1 ratio of cycloaddition products **1-130** and **1-131** in 90% yield. Key cyclization of isomer **1-131** was advanced for their synthetic target and accomplished by subjecting the substrate to sulfuryl chloride and Na_2CO_3 in DCM to form an intermediate allyl chloride **1-132** which was subjected to Barbier conditions of metallic zinc in refluxing THF to yield 80% of product **1-134** from organozinc intermediate **1-133** (Figure I.25). The alkenyl moiety of **1-134** was reduced using H_2 and catalytic quantities of 5% Pd/C in MeOH to provide (+)-chatancin (**1-135**) in 80% yield.

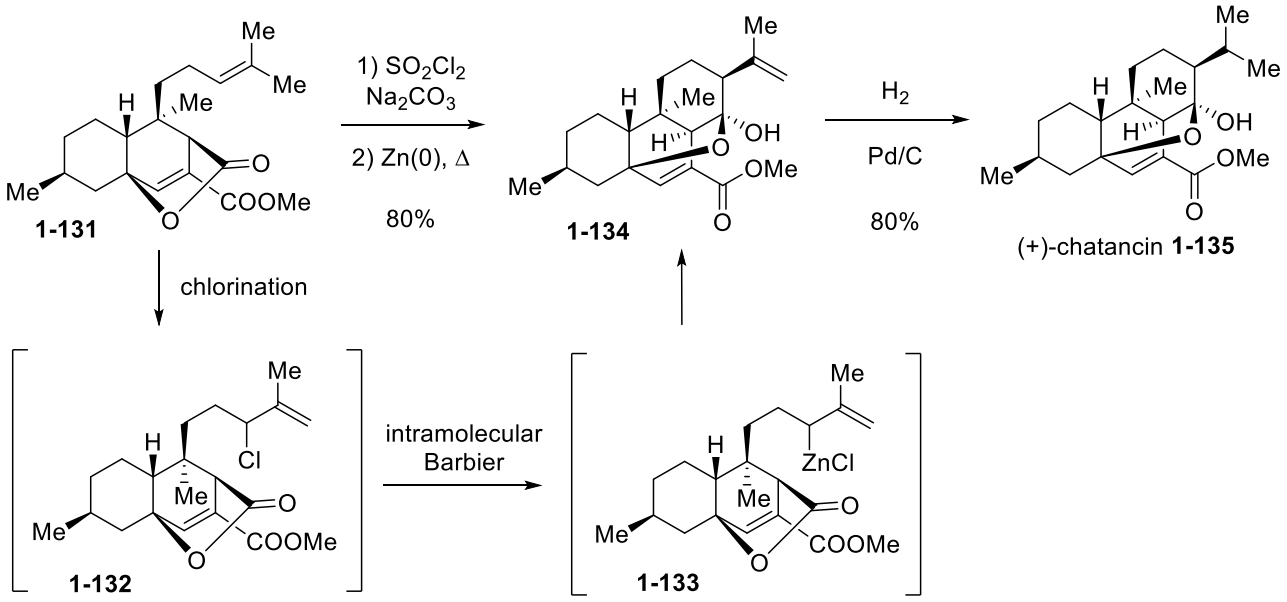

Figure I.25 The Maimone synthesis of (+)-chatancin.

I.6.2 The Xu Approach to the Diterpene Scaffold

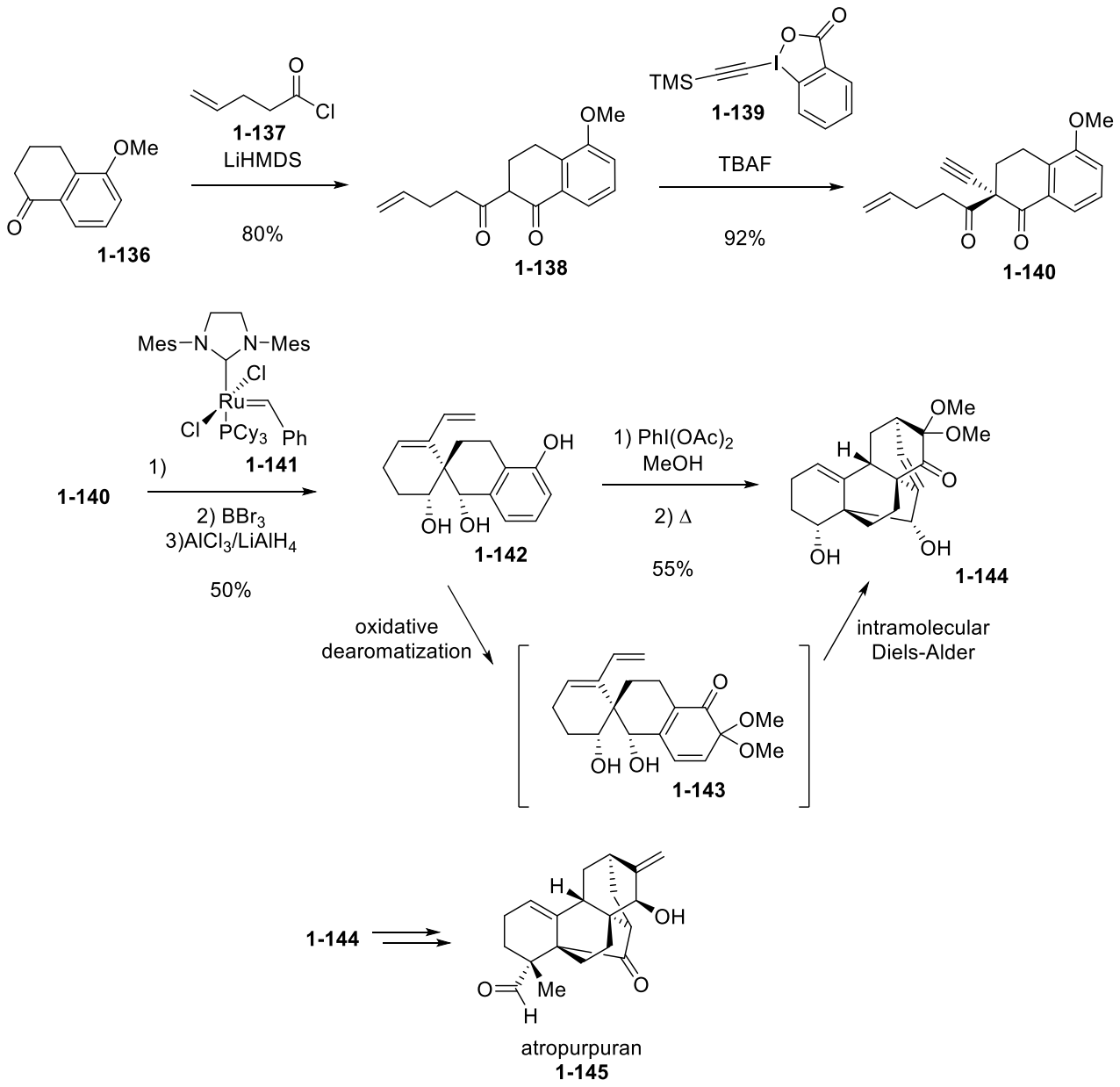

Figure I.26 The Xu synthesis of atropurpuran.

A tandem oxidative dearomatization/intramolecular Diels-Alder strategy was implemented to access the desired tricycle for a total synthesis of atropurpuran (**1-145**) (Figure I.26).[70] ketone **1-136** was acylated using acyl chloride **1-137** and LiHMDS in THF to generate diketone **1-138** in

80% yield. Diketone **1-138** was alkynylated using alkyne donor TMS-EBX (**1-139**) and TBAF in THF to yield product **1-140** in 92% yield. Alkyne **1-140** was subjected to ring-closing enyne metathesis using Grubbs 2nd generation catalyst (**1-141**) in DCM, demethylated using boron tribromide, and subsequently reduced using $AlCl_3$ and $LiAlH_4$ to afford spirocycle **1-142** in 50% yield. Key cyclization of **1-142** was accomplished using oxidative dearomatization conditions of $PhI(OAc)_2$ in MeOH to generate intermediate **1-143**, then subsequent refluxing in mesitylene to accomplish an intramolecular [4+2] cycloaddition and provide product **1-144** in 55% yield. This dearomatization/Diels-Alder cascade had previously been explored for another total synthesis of atropurpuran (**1-145**).[71]

I.6.3 The Luo Approach to the Diterpene Scaffold

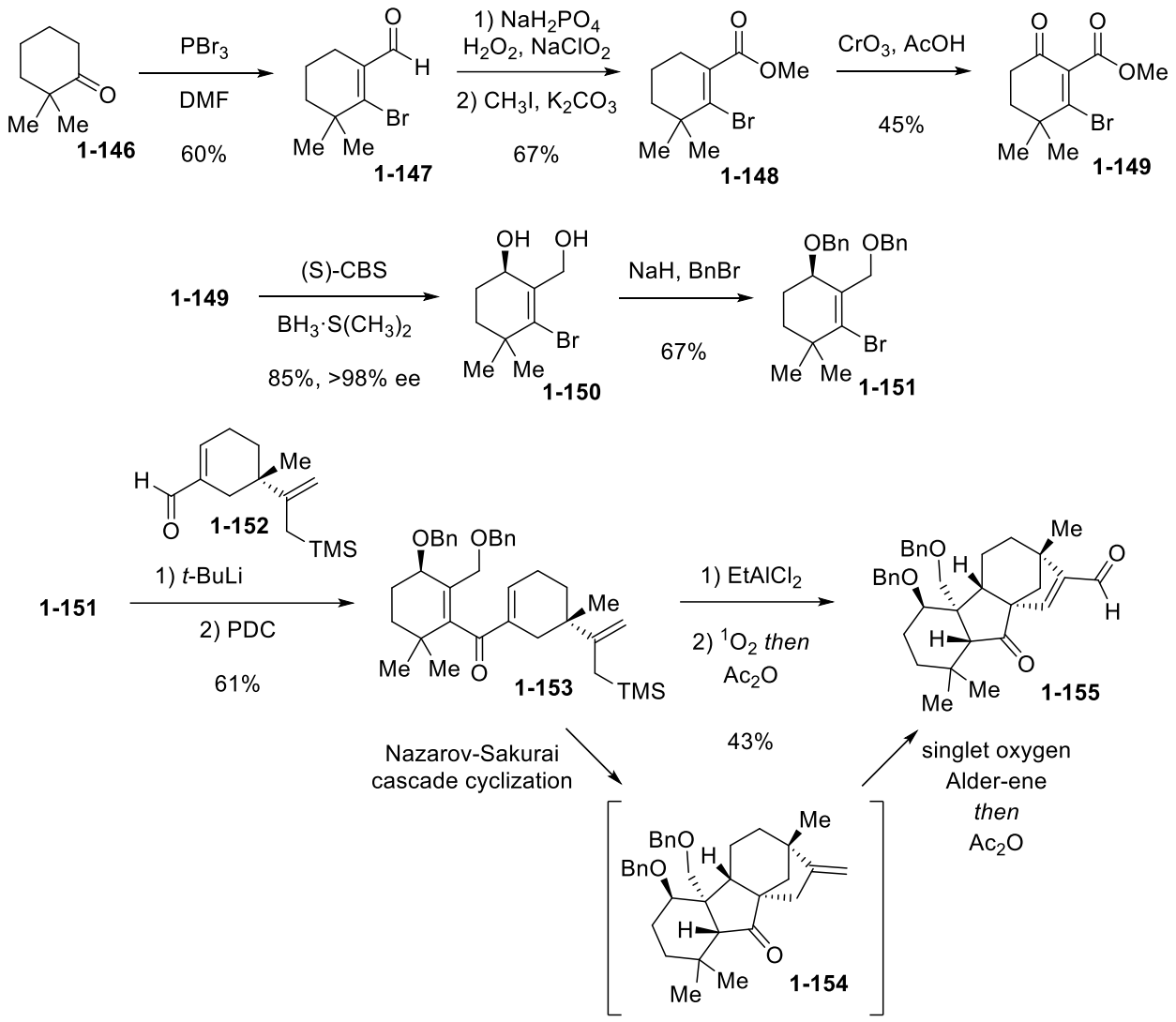

Figure I.27 The Luo synthesis of precursor to (−)-oridonin.

A tandem Nazarov-Sakurai cascade followed by a singlet oxygen Alder-ene rearrangement strategy was implemented for the key cyclization during a total synthesis of (−)-oridonin (**1-159**) (Figure I.27).[72] ketone **1-146** was brominated and formylated using phosphorus tribromide in DMF to yield aldehyde **1-147** in 60% yield. Aldehyde **1-147** was oxidized using NaH_2PO_4, H_2O_2, and $NaClO_2$ in wet MeCN and then subjected to MeI and K_2CO_3 in DMF to provide ester **1-148** in 67% yield. Allylic oxidation of ester **1-148** was achieved using CrO_3, AcOH, and Ac_2O in DCM

to generate ketone **1-149** in 45% yield. Borane dimethyl sulfide complex and (S)-CBS catalyst in THF were utilized to enantioselectively reduce substrate **1-149** to enriched alcohol **1-150** in 85% yield >98% ee. Alcohol **1-150** was benzylated using NaH and benzyl bromide in THF to yield 67% of product **1-151**. Separately, enal **1-152** was prepared using previously reported methodology.[73] Substrate **1-151** underwent lithium-halogen exchange using *t*-BuLi in Et_2O and was coupled to enal **1-152**. The resulting crude mixture was exposed to oxidizing conditions using PDC in DMF to provide dienone **1-153** in 61% yield. Dienone **1-153** was subjected to $EtAlCl_2$ in DCM to generate an intermediate Nazarov-Sakurai cascade product **1-154**. Then, singlet oxygen via molecular oxygen and TPP in chloroform is used to form an allyl hydrogen peroxide via a singlet oxygen Alder-ene reaction which can be converted to the corresponding enal **1-155** via oxidative rearrangement with Ac_2O and catalytic DMAP in pyridine in 43% yield. $RhCl(PPh_3)_3$ in refluxing PhMe was used to decarbonylate substrate **1-155** and generate product **1-156** in 67% yield (Figure I.28). Ketone **1-156** was alkylated using vinyllithium prepared in-situ and subsequently epoxidized using *m*-CPBA in DCM to provide product **1-157** in 70% yield. Key rearrangement of **1-157** was achieved using NBS in DCM to yield product **1-158** in 89% yield.

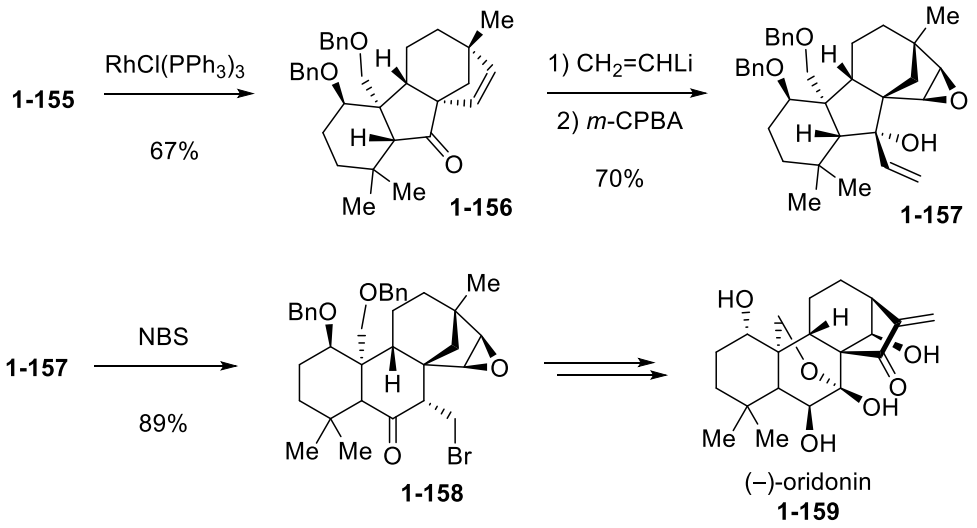

Figure I.28 The completion of (−)-oridonin by Luo et al.

I.6.4 The Liang Approach to the Diterpene Scaffold

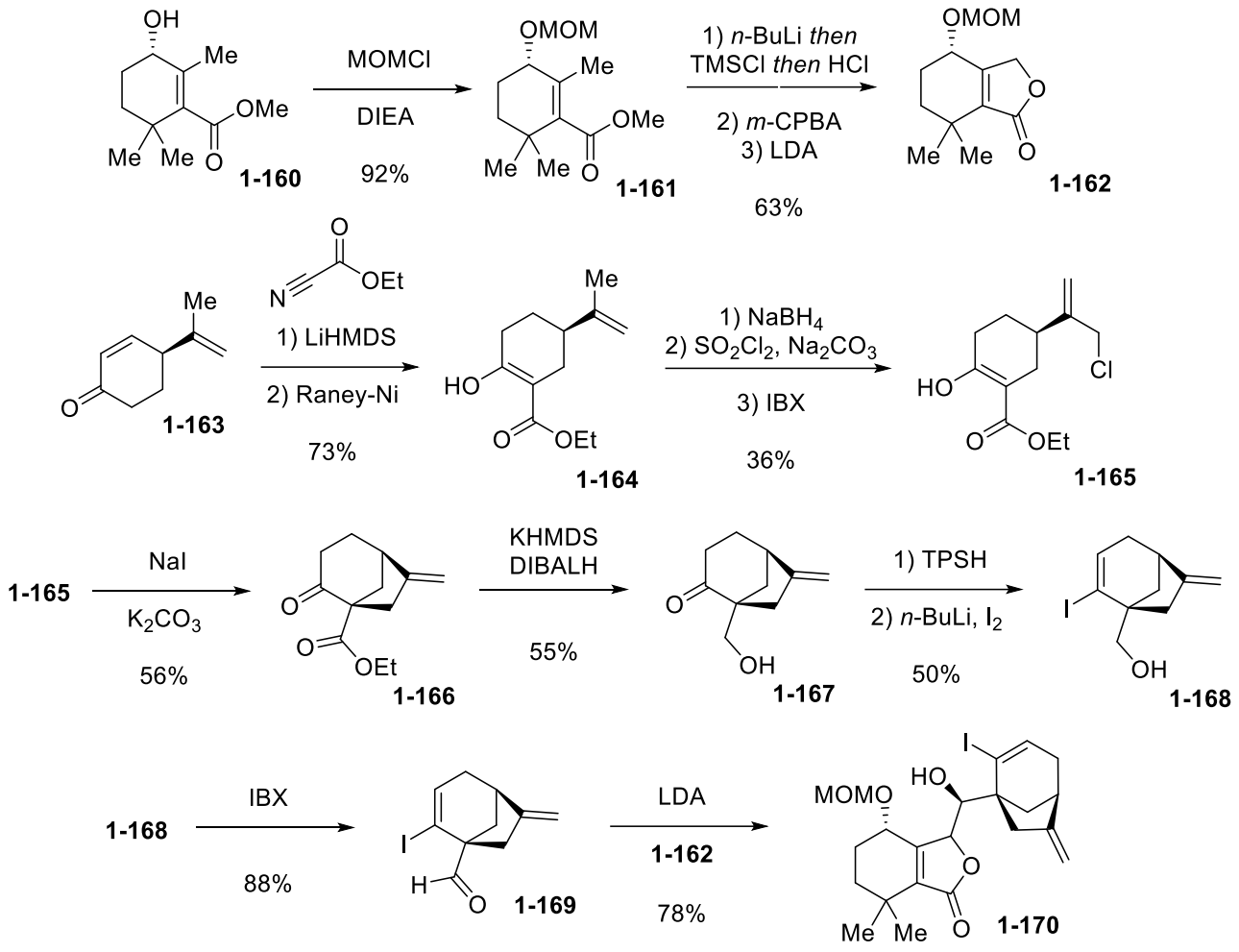

Figure I.29 The Liang synthesis of intermediate to isorosthin L.

An intramolecular pinacol coupling approach has been utilized for a total synthesis of isorosthin L (**1-179**).[74] Alcohol **1-160** was protected using MOMCl, NaI, and DIEA in DCM to afford ether **1-161** in 92% yield (Figure I.29). Substrate **1-161** was subjected to *n*-BuLi in THF, TMSCl, and then aqueous HCl. The resulting crude material was oxidized using *m*-CPBA in DCM and then exposed to LDA in THF to provide lactone **1-162** in 63% yield. Separately, enone **1-163** was esterified using LiHMDS and ethyl cyanoformate in THF and then reduced using Raney-Ni in THF to generate product **1-164** in 73% yield. Substrate **1-164** was further reduced via ethanolic

$NaBH_4$, subjected to sulfuryl chloride and Na_2CO_3 in DCM, and then oxidized using IBX in EtOAc to yield product **1-165** in 36% yield. Substrate **1-165** underwent an intramolecular annulation process in the presence of NaI and K_2CO_3 in acetone to provide bicycle **1-166** in 56% yield. Ester **1-166** was treated with KHMDS and then reduced in the presence of DIBALH in Et_2O to yield alcohol **1-167** in 55% yield. The ketone moiety of substrate **1-167** was converted to an intermediate hydrazone by exposure to TPSH in THF and then iodinated using *n*-BuLi and molecular iodine in Et_2O to afford iodoalkene **1-168** in 50% yield. The alcohol moiety of substrate **1-168** was oxidized using IBX in DMSO to provide aldehyde **1-169** in 88% yield. Then, lactone **1-169** was deprotonated using LDA in THF and coupled to **1-162** to yield 78% of adduct **1-170**. Intramolecular cyclization of **1-170** was accomplished using radical condition created by AIBN and terminated by tributyl stannane in PhMe (Figure I.30).

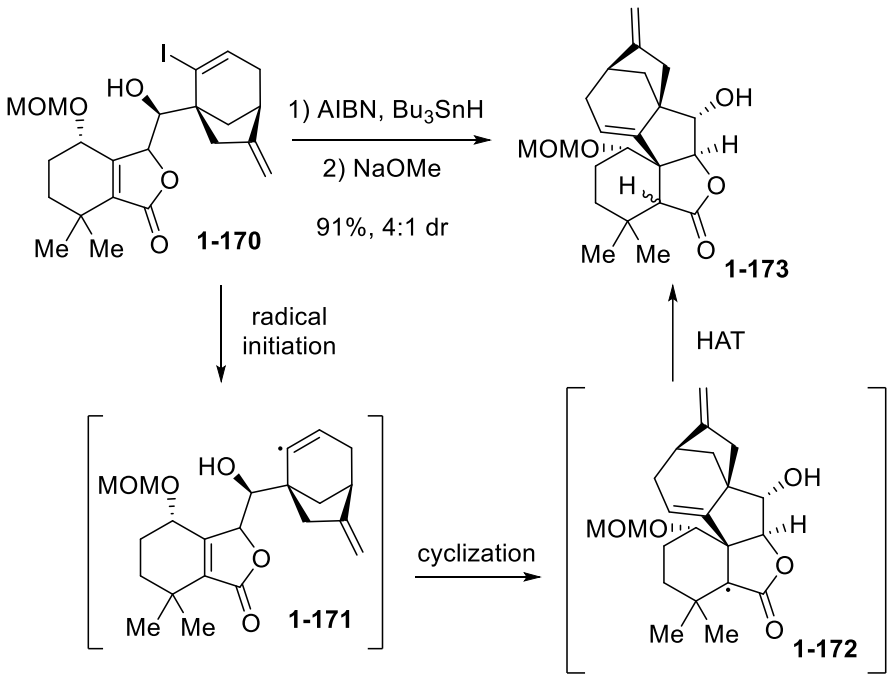

Figure I.30 The Liang radical cyclization of intermediate **1-170**.

The radical coupling is accomplished by forming organo-radical **1-171** *in-situ* which undergoes a subsequent intramolecular cyclization to form radical intermediate **1-172**. A HAT step from hydrogen atom donor tributylstannane terminates the carbon radical intermediate and the resulting tributyltin-centered radical can continue the radical propagation of this process. A subsequent epimerization step by NaOMe in MeOH leads to cyclized product **1-173** in 91% yield and 4:1 dr. Lactone **1-173** was reduced using $LiAlH_4$ in THF and then exposed to TBSCl and ImH in DCM to form diol **1-174** in 62% yield (Figure I.31). Diol **1-174** was selectively oxidized using IBX in DMSO and THF to provide acyloin **1-175** in 55% yield. Substrate **1-175** was deprotected using TBAF in THF and then a subsequent structural transformation was introduced via an oxidative cleavage of a C-C bond initiated by $Pb(OAc)_4$ in DCM and PhH which led to lactone **1-176** in 95% yield. Reduction of the formyl moiety of **1-176** using $LiBH_4$ in THF led to an intramolecular acyl transfer which was followed by exposure to oxidative conditions with DMP in DCM to generate

lactone **1-177** in 55% yield. Key intramolecular pinacol coupling of **1-177** was achieved by exposure to SmI_2 in THF to provide product **1-178** in 92% yield.

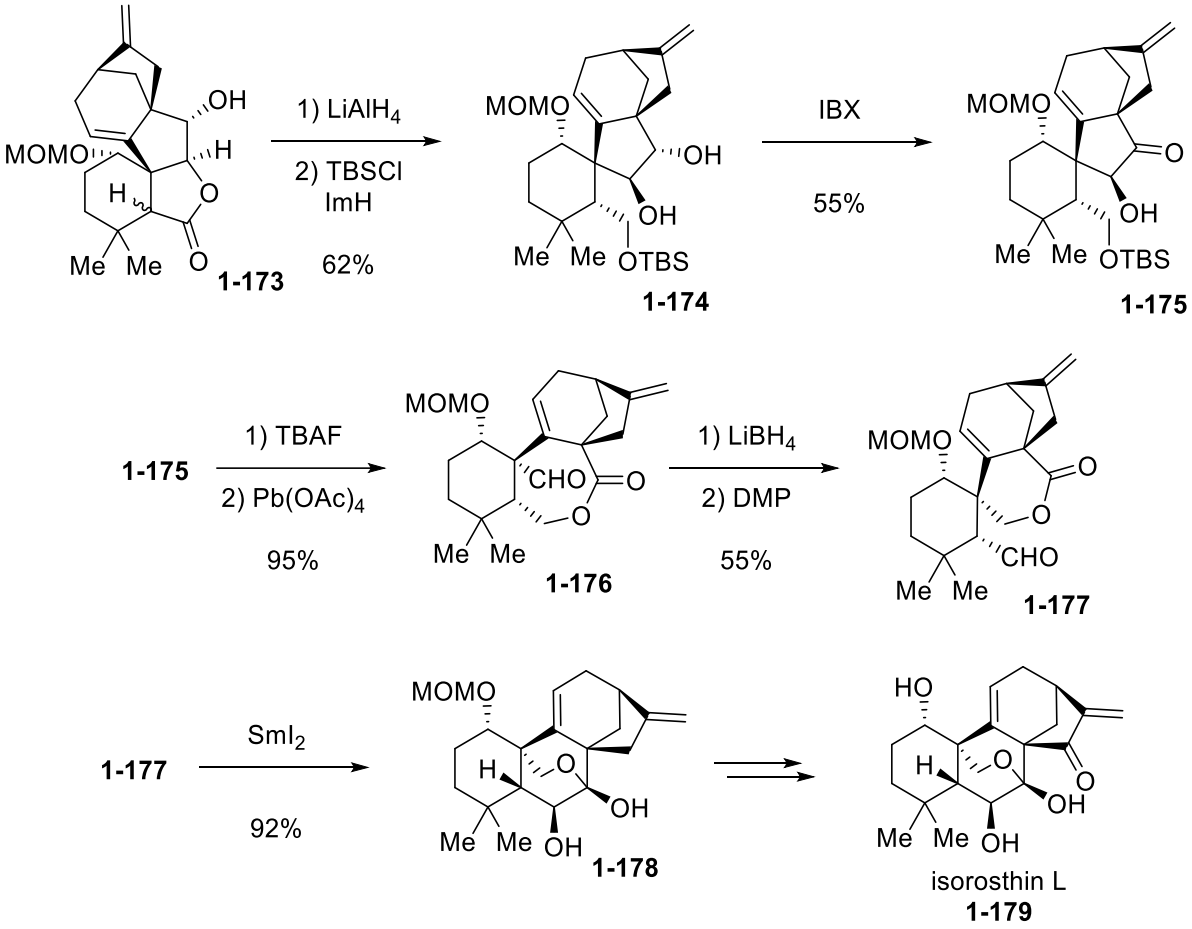

Figure I.31 The Liang synthesis of isorosthin L.

I.7 Selected Examples of Sigmatropic Tricyclization

I.7.1 The Zaragozá Approach to the Diterpene Scaffold

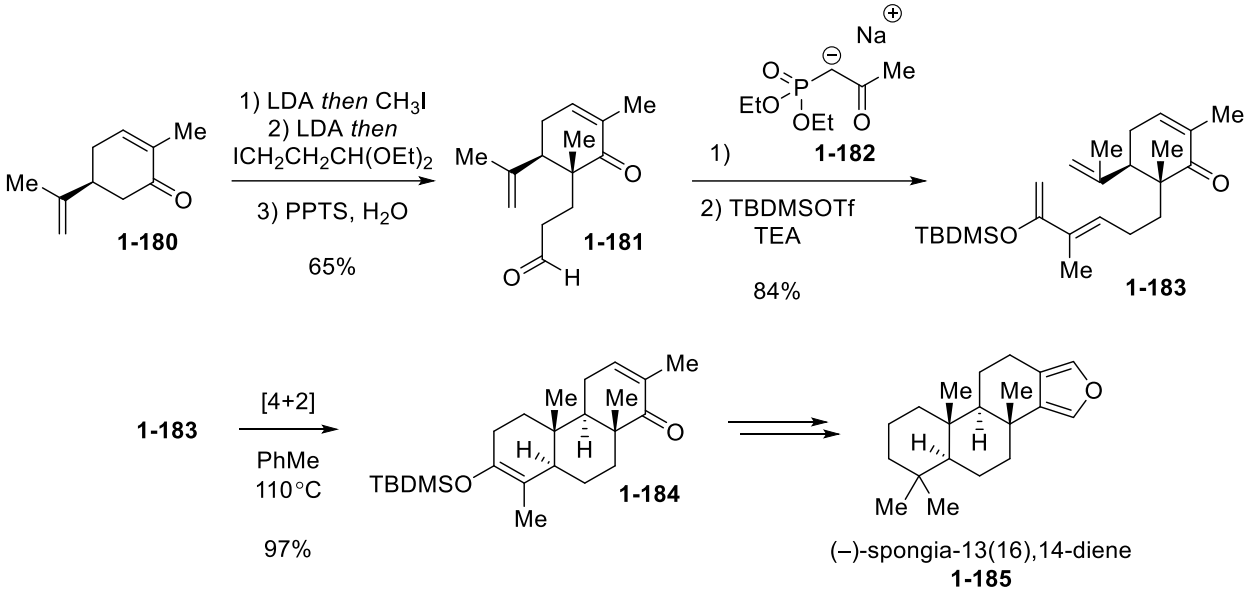

Figure I.32 The Zaragozá synthesis of steroidal core **1-185**.

An intramolecular Diels-Alder approach was implemented for the total synthesis of (−)-spongia-13(16),14-diene (**1-185**).[75] Enone **1-180** was subjected to LDA in THF and then methyl iodide, the alkylated intermediated was subjected once again to LDA in THF but with additional HMPA and then 3-iodopropanal diethyl acetal was added to the mixture (Figure I.32). Prior to product isolation, the crude material was subjected to PPTS in wet, refluxing acetone to yield aldehyde **1-181** in 65% yield. Aldehyde **1-181** was olefinated using Horner-Wadsworth-Emmons conditions of sodium ketophosphonate ester **1-182** in THF and then the resulting ketone was transformed into the corresponding silyl enol ether **1-183** in 84% yield using TBDMSOTf and

TEA in DCM. Key cyclization of substrate **1-183** was accomplished by refluxing conditions of 110°C in PhMe to yield cyclized product **1-184** in 97% yield.

I.7.2 The Deslongchamps Approach to the Diterpene Scaffold

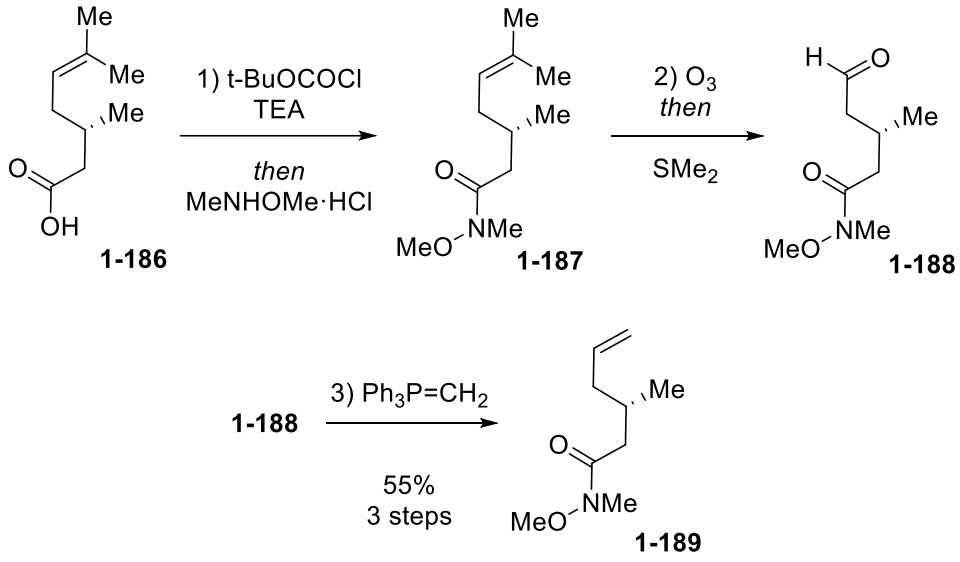

Figure I.33 The Deslongchamps synthesis of first intermediate for (+)-anhydrochatancin.

An intramolecular [4+2] cycloaddition was used to access the desired tricycle for a total synthesis of (+)-anhydrochatancin **1-210**.[76] Acid **1-186** was made into a mixed anhydride using *t*-butyl chloroformate and TEA in DCM and then *N*,*O*-dimethylhydroxylamine hydrochloride to generate an intermediate Weinreb amide **1-187** (Figure I.33). Weinreb amide **1-187** was subjected to ozonolysis in DCM with reductive quenching with Me_2S to produce intermediate aldehyde **1-188**. Finally, intermediate aldehyde **1-188** was methenylated using Wittig conditions of $MePPh_3^+Br^-$ with *n*-BuLi in THF to provide alkene **1-189** in 55% yield over the three steps. Synthesis of bromofuran **1-195** from amide **1-189** was accomplished by treatment with dilithio propargylate **1-190** in THF and HMPA to form intermediate **1-191** before acidification (Figure I.34). Protonation of **1-191** using HBr in PhH yields **1-192**, that undergoes addition of HBr to

generate intermediate enone **1-193**. Intramolecular cyclization of **1-193** yields hemiacetal **1-194** that can be dehydrated to reveal bromofuran **1-195**. This bromofuran synthesis based on ynone alcohol intermediates like **1-192** has been previously explored and the provided mechanism of bromofuran formation is based on the original proposal of the authors.[77] Subsequently, bromofuran **1-195** is lithiated using *n*-BuLi in THF and then subjected to CO_2 to provide acid **1-196** in 86% yield.

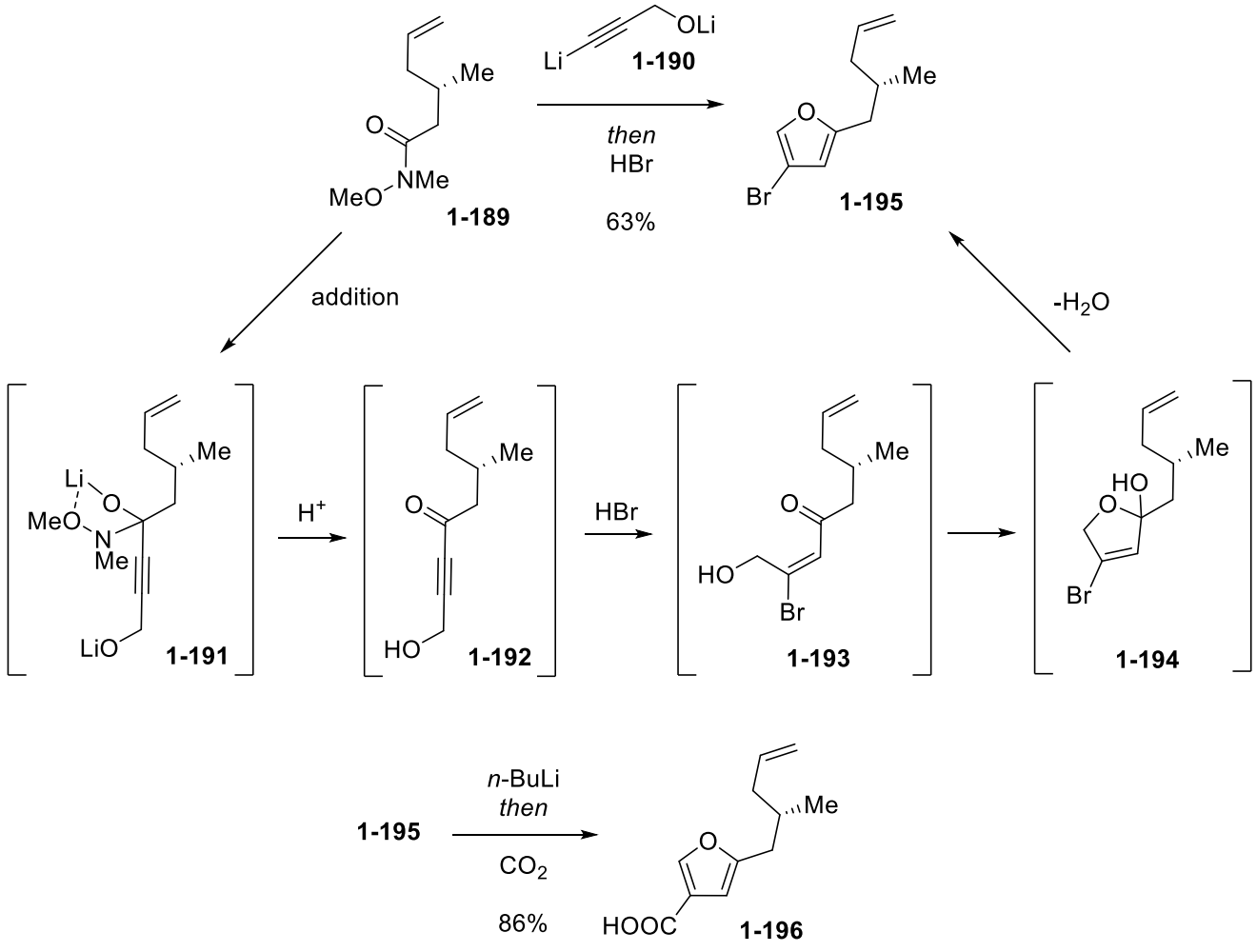

Figure I.34 Continued Deslongchamps synthesis of first intermediate for (+)-anhydrochatancin.

Separately, acid **1-197** was reduced using borane in THF and the resulting primary alcohol was selectively protected using TBDMSCl and ImH in DCM to give product **1-198** in 54% yield (Figure I.35). The secondary alcohol moiety of **1-198** was oxidized using Swern conditions of oxalyl chloride and DMSO with TEA in DCM to provide ketone **1-199** in 84% yield. Ketone **1-199** was methenylated using Wittig conditions of MeBr and PPh_3 with *n*-BuLi in THF to generate alkene **1-200** in 97% yield. The silyl ether protecting group of **1-200** was deprotected using TBAF in THF to provide alcohol **1-201** in 94% yield. Alcohol **1-201** was oxidized using Ley-Griffith conditions of TPAP and NMO to give aldehyde **1-202** in 83% yield.

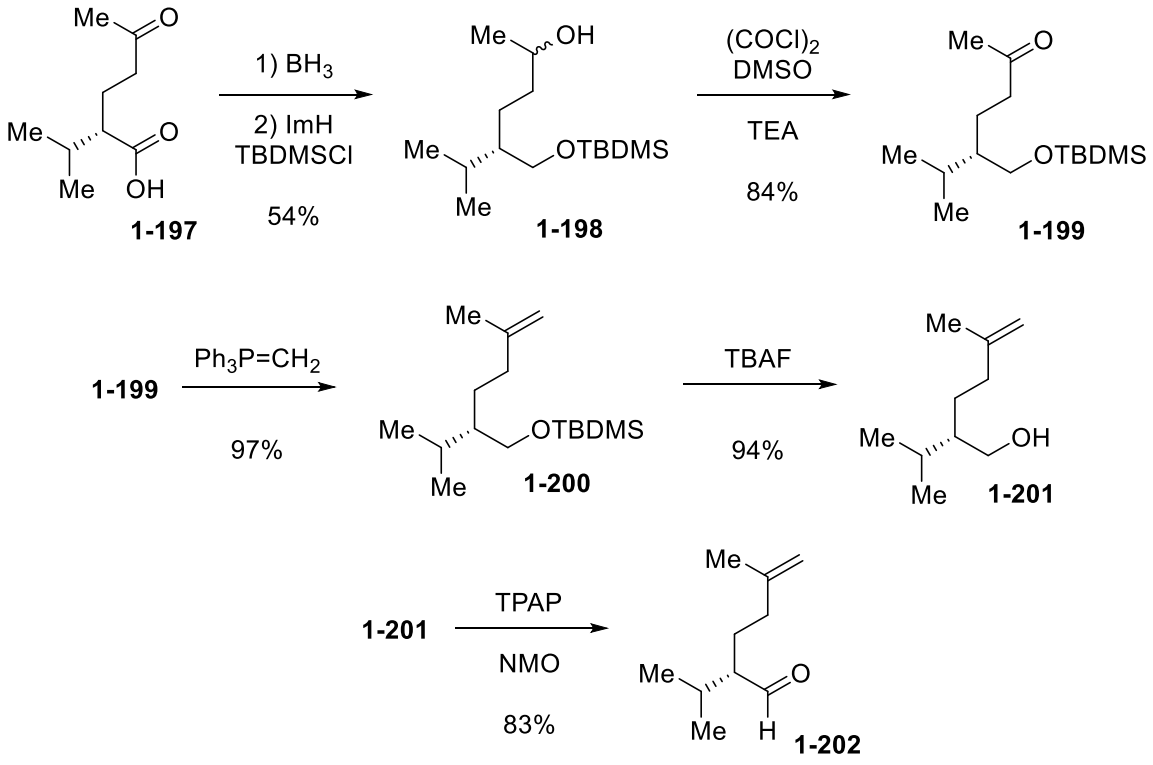

Figure I.35 The Deslongchamps synthesis of second intermediate for (+)-anhydrochatancin.

Coupling of **1-196** and **1-202** was achieved by subjecting **1-196** to two equivalents of LDA in THF followed by addition of **1-202** (Figure I.36). The resulting crude intermediate was exposed to diazomethane to methylate its acid moiety and yield methyl ester **1-203** in 96% yield and 2:1

dr. The alcohol moiety of **1-203** was oxidized using DMP in DCM to provide ketone **1-204** in 91% yield. Ring-closing metathesis of substrate **1-204** was accomplished using Grubbs 2nd generation catalyst (**1-141**) in DCM to provide a ~44:26 ratio of Z:E products (**1-205**:**1-206**) in 70% yield. Ketone **1-206** was reduced to **1-207** using methanolic $NaBH_4$ in 91% yield. Key transannular Diels-Alder reaction was performed by refluxing substrate **1-207** in a 2:1 mixture of DMSO/H_2O to yield cyclized product **1-208** in 70% yield. A pinacol-like rearrangement of substrate **1-208** is initiated by $SnCl_4$ in DCM to provide a 1,2-hydride shifted product which recyclizes to provide (+)-chatancin (**1-209**). Although (+)-chatancin (**1-209**) was the intended final target, acidic conditions used in this preparation led to its dehydration to provide (+)-anhydrochatancin (**1-210**) in 90% yield.

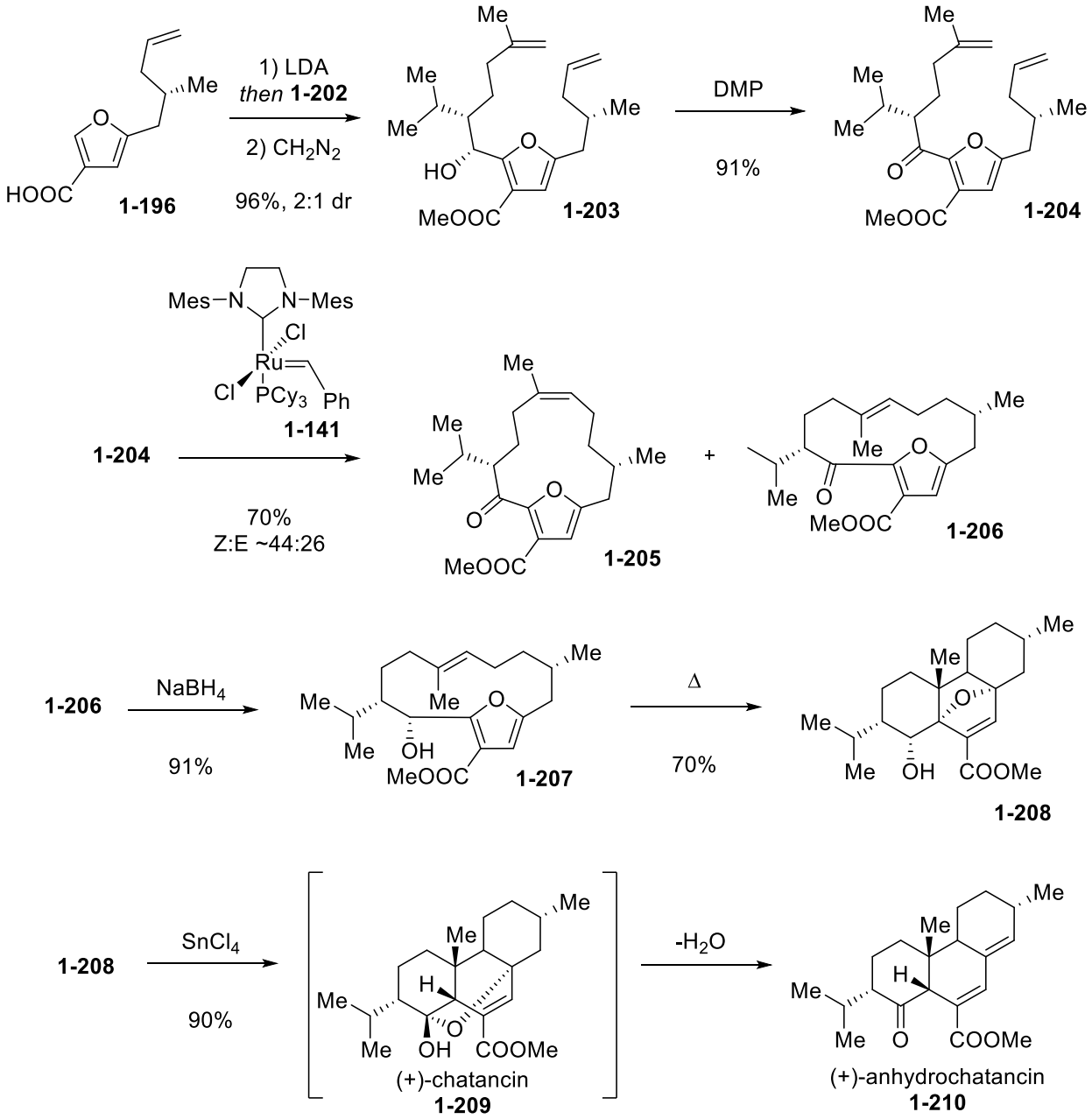

Figure I.36 The Deslongchamps synthesis of (+)-anhydrochatancin.

I.7.3 The Toyota Approach to the Diterpene Scaffold

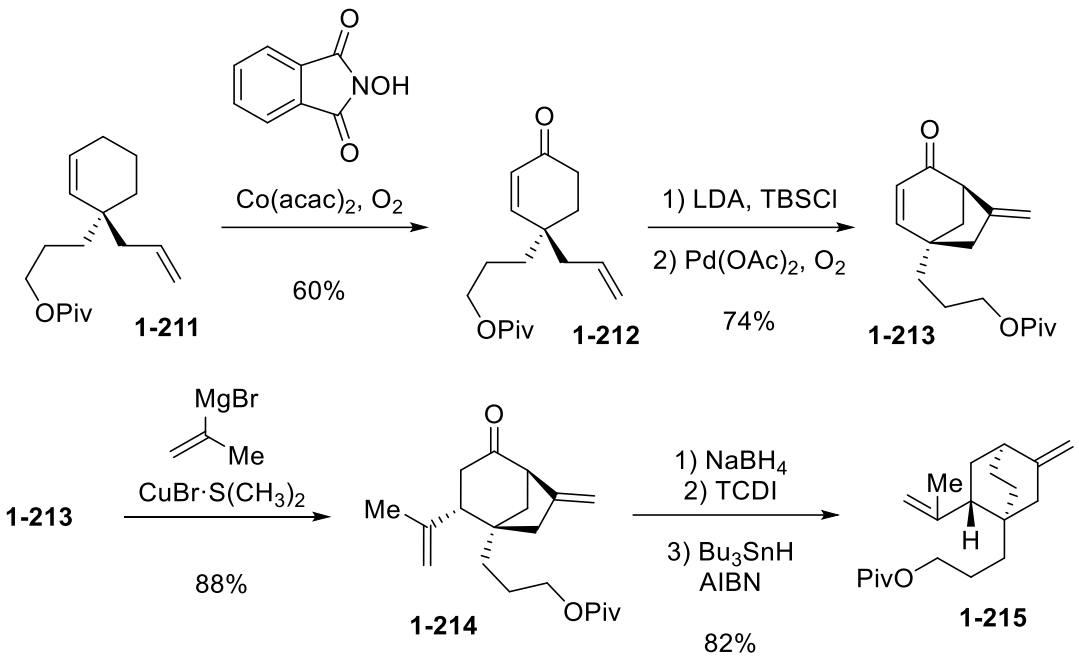

Figure I.37 The Toyota synthesis of intermediate to serofendic acids A and B.

A key intramolecular Diels-Alder cycloaddition was used for a total synthesis of serofendic acids A (**1-221**) and B (**1-222**),[78] alkene **1-211** was oxidized to the corresponding enone using *N*-hydroxypthalimide, oxygen gas, and $Co(acac)_2$ in MeCN to provide product **1-212** in 60% yield (Figure I.37). Enone **1-212** was exposed to LDA in THF, and a subsequent formation of an intermediate silyl enol ether was accomplished using TBSCl and HMPA. The generated intermediate underwent bicyclization with subsequent exposure to $Pd(OAc)_2$ and oxygen gas in DMSO to yield the cyclized material **1-213** in 74% yield. Treatment of product **1-213** with isopropenylmagnesium bromide and copper(I) bromide dimethyl sulfide complex in THF followed by a workup invoking TMSCl and 10% aqueous perchloric acid led to adduct **1-214** in 88% yield. A key homoallyl rearrangement of the substrate was achieved using stepwise treatment of **1-214** with $NaBH_4$ and TCDI to form a redox-active thiocarbonyl intermediate based on Barton-

McCombie conditions.[79] Then, AIBN with Bu_3SnH in PhMe was utilized to generate a radical species from the thiocarbonyl intermediate and provide the homoallyl rearrangement product **1-215** in 82% yield that reveals a 1,2-alkyl shift on the core scaffold. The pivalate ester moiety of **1-215** was reduced to reveal the corresponding alcohol **1-216** using $LiAlH_4$ in 92% yield (Figure I.38). Alcohol **1-216** was oxidized using sulfur trioxide pyridine complex, TEA, and DMSO in DCM and then the crude material was treated with phosphonate **1-217** and *t*-BuOK in THF to generate unsaturated ester **1-218** in 88% yield. The bromoalkene moiety of unsaturated ester **1-218** was transformed into a diene by treatment with potassium vinyltrifluoroborate and Cs_2CO_3 with catalytic $PdCl_2(dppf)_2$ in wet THF to provide the corresponding diene **1-219** in 51% yield.

Key intramolecular Diels-Alder of diene **1-219** was furnished by refluxed the substrate in PhMe to provide tricyclized product **1-220** in 84% yield.

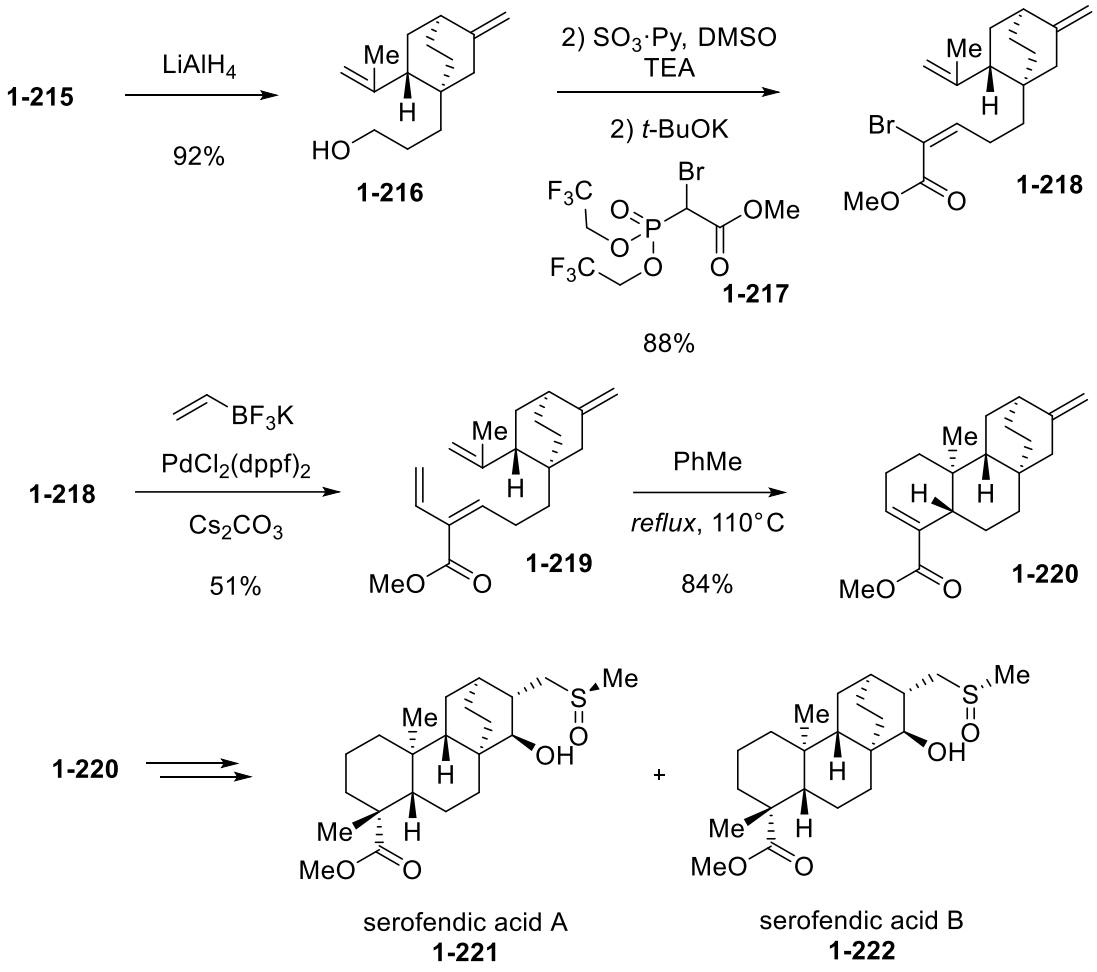

Figure I.38 The Toyota synthesis of serofendic acids A and B.

I.7.4 Alternative Deslongchamps Approach to the Diterpene Scaffold

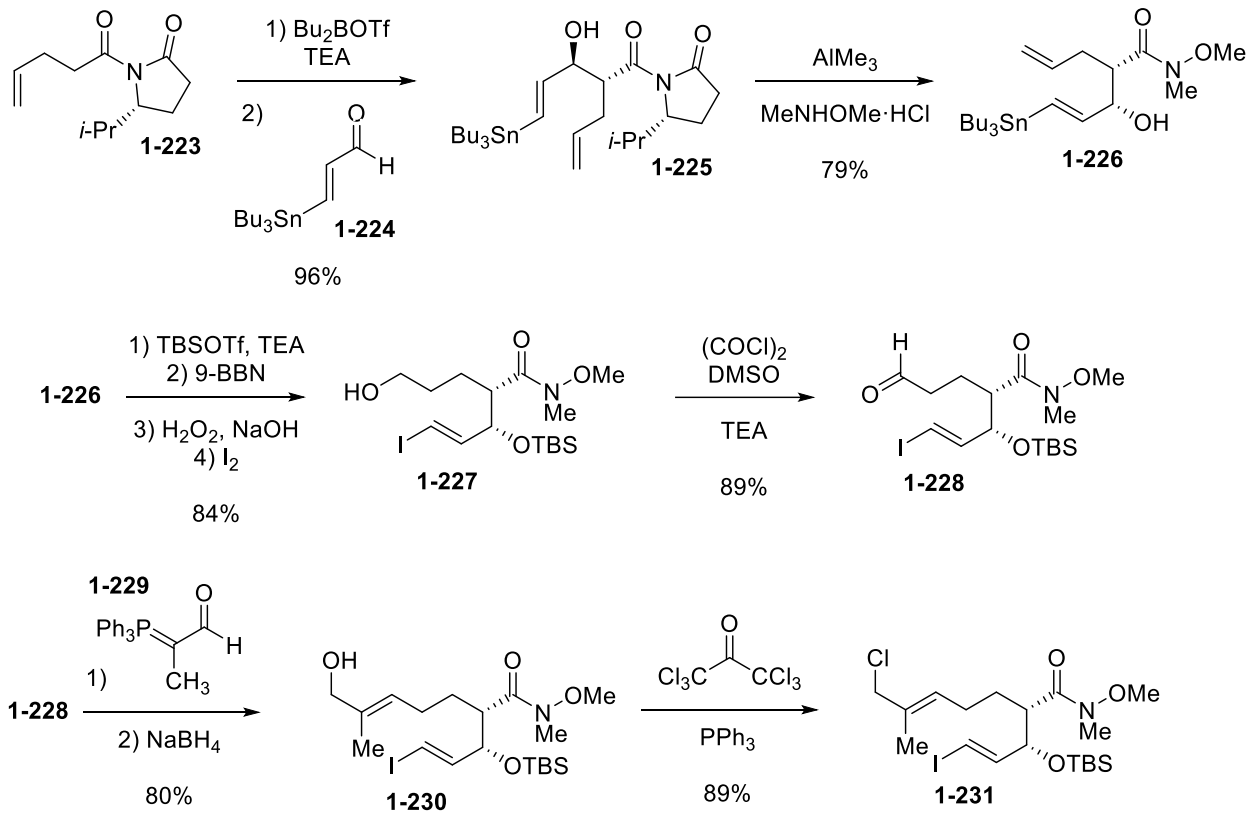

Figure I.39 Deslongchamps synthesis of intermediate to (+)-cassaine.

For a total synthesis of (+)-cassaine (**1-236**),[80] an asymmetric Evans-aldol approach was utilized to couple imide **1-223** and aldehyde **1-224** using dibutylboron trifluoromethanesulfonate and TEA in DCM to furnish alcohol **1-225** in 96% yield (Figure I.39). Transformation of imide **1-225** to the corresponding Weinreb amide **1-226** using $AlMe_3$ and *N*,*O*-dimethylhydroxylamine hydrochloride in DCM in 79% yield. The allylic alcohol moiety of amide **1-226** was protected using TBSOTf and TEA in DCM, then exposed to Brown hydroboration conditions of 9-BBN in THF followed by H_2O_2 and NaOH, then its stannane moiety was iodinated with I_2 in DCM to finally provide product **1-227** in 84% yield. The primary alcohol moiety of **1-227** was oxidized using Swern conditions of oxalyl chloride and DMSO with TEA in DCM to afford aldehyde **1-**

228 in 89% yield. Aldehyde **1-228** was subjected to Wittig conditions of phosphonium ylide **1-229** in refluxing PhH and then reduced using methanolic $NaBH_4$ to provide allylic alcohol **1-230** in 80% yield. Substrate **1-230** was chlorinated using previously described conditions[81] of hexachloroacetone and PPh_3 in THF to afford allyl chloride **1-231** in 89% yield. Separately, ketoester **1-232** was prepared in three steps according to a known procedure (Figure I.40).[82] Then, cesium salts were efficiently used to couple ester **1-232** and allyl chloride **1-231** with Cs_2CO_3, CsI, and 18-C-6 crown ether in acetone to generate coupled product **1-233** in 95% yield. Substrate **1-233** was intramolecularly coupled using Stille conditions of stoichiometric DIEA and catalytic quantities of triphenylarsine and $Pd_2(dba)_2$ in a mixture of THF and DMF to provide product **1-**

234 in 71% yield. The key transannular Diels-Alder step was achieved by refluxing **1-234** and PhMe in a seal reaction vessel to provide cyclized product **1-235** in 92% yield.

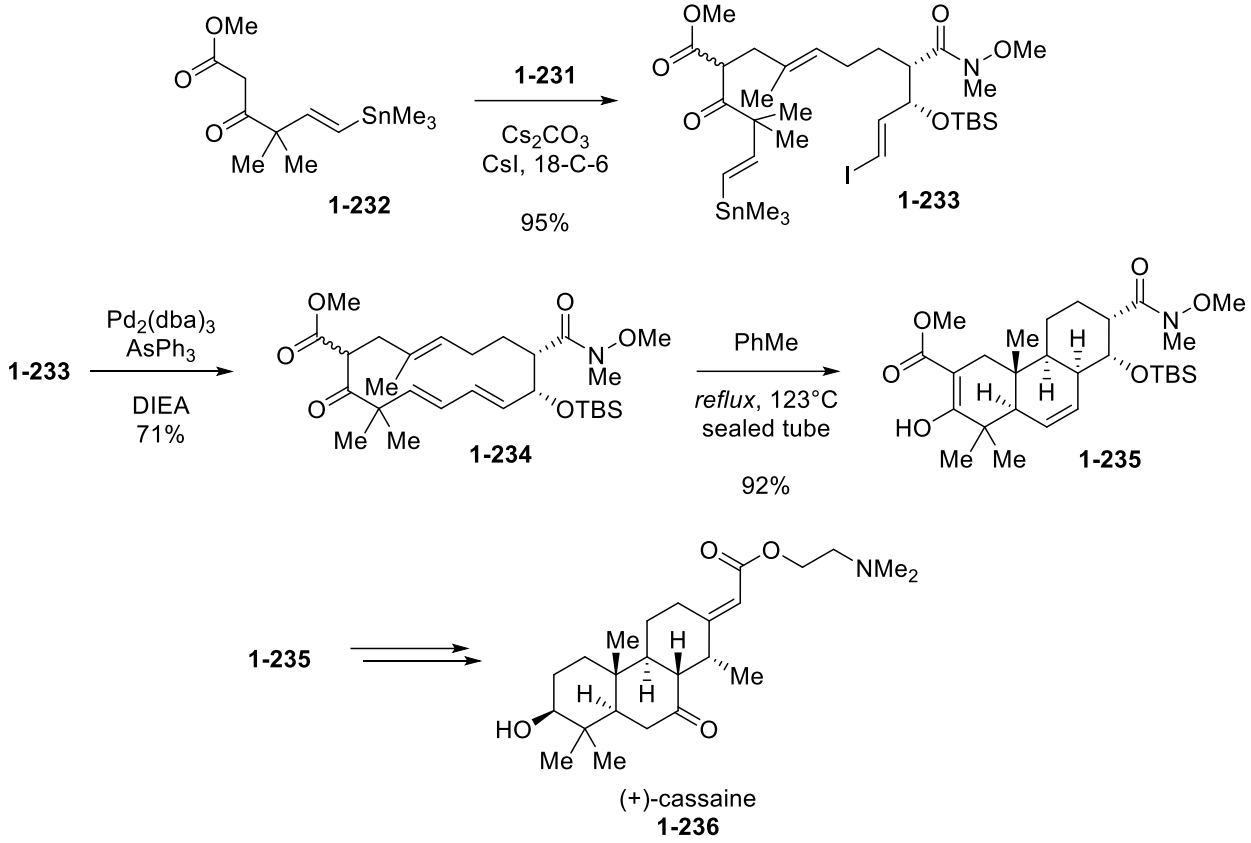

Figure I.40 Deslongchamps synthesis of (+)-cassaine.

I.7.5 The Fukuyama Approach to the Diterpene Scaffold

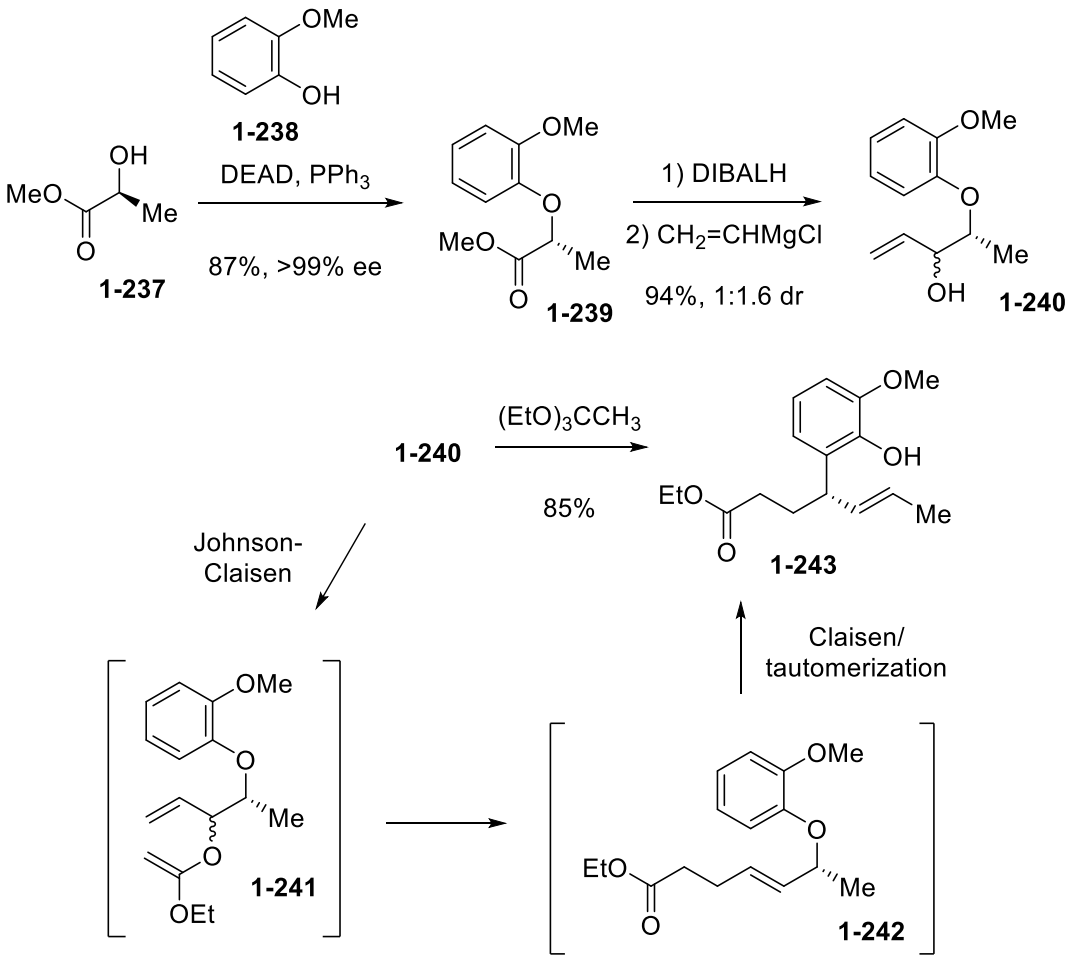

Figure I.41 The Fukuyama synthesis of intermediate to (−)-lepenine.

An intramolecular [4+2] cycloaddition strategy was utilized for a total synthesis of (−)-lepenine (**1-249**).[83] L-lactic acid methyl ester **1-237** used as a precursor to a Mitsunobu reaction with PPh_3, DEAD, and guaiacol **1-238** in PhMe to afford product **1-239** in 87% yield and >99% ee (Figure I.41). Ester **1-239** was reduced to an aldehyde using DIBALH in Et_2O and this aldehyde intermediate was then alkylated using vinylmagnesium chloride in THF to yield alcohol **1-240** in 94% yield and 1:1.6 dr. Alcohol **1-240** was refluxed with catalytic quantities of *p*-nitrophenol in triethyl orthoacetate to form intermediate ketene acetal **1-241** which underwent two cascading

[3,3]-sigmatropic rearrangements. The first sigmatropic rearrangement resulted from a Johnson-Claisen process to form intermediate ester **1-242**, which then undergoes a second Claisen rearrangement and tautomerization event to reveal ester **1-243** in 85% yield. Product **1-243** was protected using MsCl with TEA in DCM, subjected to ozonolysis in methanolic DCM, treated with $NaBH_4$ to reveal a crude alcohol, and then esterified using PivCl and pyridine with catalytic DMAP in DCM to yield desired product **1-244** in 58% yield and 91% ee (Figure I.42). Ethyl ester **1-244** was hydrolyzed using aqueous LiOH in methanolic THF and then subjected to TFAA and TFA in DCM to facilitate the formation of ketone **1-245** in 82% yield. Ketone **1-245** was subjected to vinylmagnesium chloride in THF and the resulting tertiary alcohol was refluxed with catalytic AgOTf in PhMe to generate the elimination product **1-246** in 53% yield. Substrate **1-246** was reduced using DIBALH in DCM and the corresponding alcohol was esterified using Steglich esterification conditions of DCC and catalytic DMAP in the presence of methacrylic acid in DCM to generate product **1-247** in 75% yield. The key intramolecular Diels-Alder reaction was achieved by subjecting diene **1-247** to refluxing PhMe to provide tricyclized product **1-248** in 84% yield.

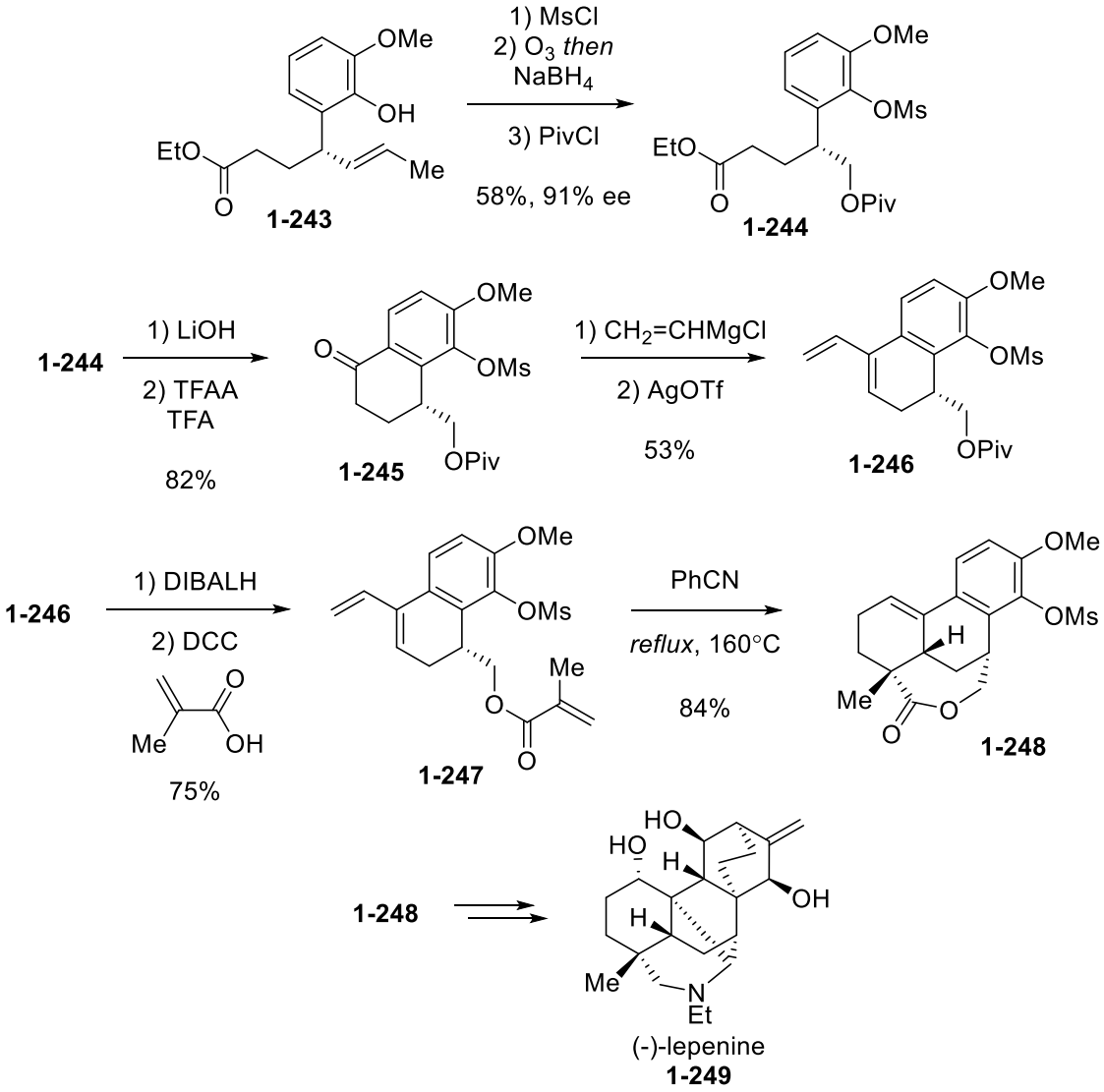

Figure I.42 The Fukuyama synthesis of (−)-lepenine.

I.7.6 The Li Approach to the Diterpene Scaffold

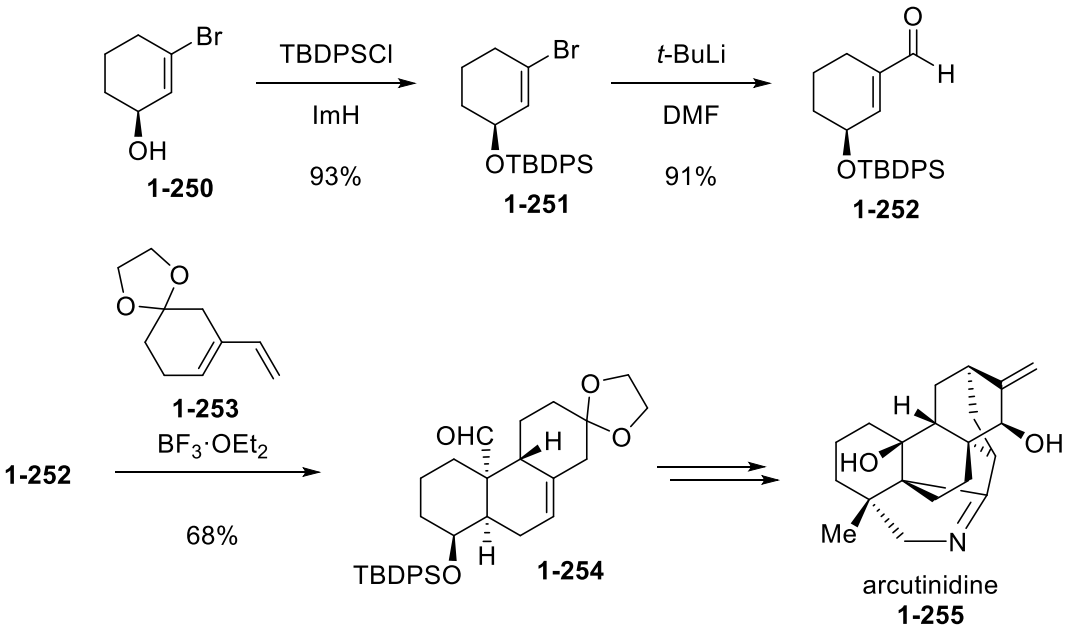

Figure I.43 The Li synthesis of arcutinidine.

An intramolecular [4+2] cycloaddition strategy was implemented during a total synthesis of arcutinidine (**1-255**).[84] Chiral alcohol **1-250** was protected using TBDPSCl and ImH in DMF to yield silyl ether **1-251** in 93% yield (Figure I.43). Substrate **1-251** was formylated via lithium-halogen exchange with *t*-BuLi in THF and then DMF was added to provide enal **1-252** in 91% yield. Key cyclization was achieved by stirring enal **1-252** and ketal **1-253** with boron trifluoride

diethyl etherate in DCM to provide intermolecular [4+2] cycloaddition product **1-254** in 68% yield.

I.7.7 Alternate Herzon Approach to the Diterpene Scaffold

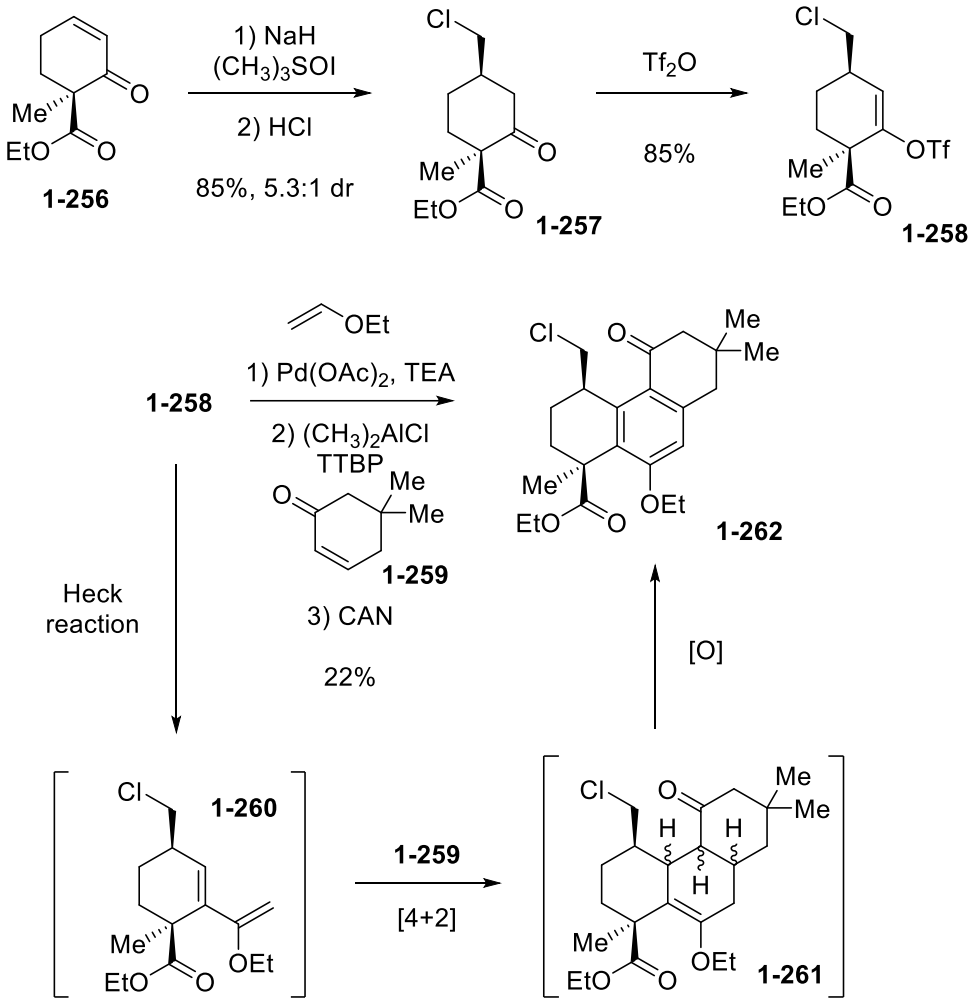

Figure I.44 Explored synthetic route during Herzon synthesis of myrocin G.

A tandem Heck reaction/intermolecular [4+2] cycloaddition/oxidative aromatization process was implemented during an enantioselective total synthesis of myrocin G.[85] This unused model synthetic route utilized ketoester **1-256** by addition to a suspension of NaH and trimethylsulfoxonium iodide in DMF and then subjected to HCl in 1,4-dioxane to generate alkyl

chloride **1-257** in 85% and 5.3:1 dr (Figure I.44). The ketone moiety of **1-257** was made into the corresponding vinyl triflate by reacting the substrate with triflic anhydride and 2,4,6-tri-*tert*-butylphenol in DCM to provide product **1-258** in 85% yield. Key cyclization of **1-258** was accomplished by a stepwise reaction with catalytic quantities of $Pd(OAc)_2$ and stoichiometric TEA and ethyl vinyl ether in DMSO to generate coupled intermediate **1-260**. Then, addition of dienophile **1-259** and dimethylaluminum chloride in DCM facilitates a Diels-Alder process to form cyclized intermediate **1-261**. 2,4,6-Tri-*tert*-butylphenol was used to stabilize **1-261** following isolation. The resulting crude material was then exposed to CAN in DMF to provide aromatized product **1-262** in 22% yield.

These are representative synthetic strategies though many more can be found in the literature. Each selected synthesis provides a varied approach and opportunity for functional group tolerance when considering an approach to the common tricyclic core that has been synthesized for these diterpenes. Each key tricycle shown above can be further functionalized to enable greater chemical diversity. In many of the mentioned examples the depicted key product served as an intermediate for functionalization or transformation to an alternative diterpene scaffold.

I.8 Summary

Natural product scaffolds continue to provide a valuable handle for drug discovery and for the many species that rely on the dynamics of those metabolites for their furthered survival. As we continue isolate and describe these structures, natural product synthesis will serve as an opportunity to improve access to these valuable complex molecules and elaborate on their bioactivity. Diterpenes are but one major family of complex molecules found expressed in nature, yet scaffold isomerization and chemical modification enabled by enzymes provides one family of

metabolites with a diverse range of bioactivity. To further enable medicinal and scientific study of these complex molecules, a range of synthetic strategies are continuously developed to enable access to these materials in the laboratory setting. Synthetic methods range from both biomimetic to *de novo* total syntheses, each of which enable varied structural modification and functional group tolerance.

CHAPTER II

Studies Towards the Synthesis of a Strategic Tricarbocyclic Motif via a Copper-Catalyzed Tandem Michael/Aldol Approach

II.1 Introduction

Provided the rich structural diversity of the isopimarane diterpenes, we envisioned that a general approach to the tricyclic scaffold would improve synthetic accessibility to these bioactive compounds. Specifically, we envisioned a Michael/aldol approach that would for the rapid synthesis of the phenolic B-ring-containing scaffold associated with (+)-aspewentin A (**1-16**). This chapter provides an overview of the history and prior synthetic work involving the aspewentins. The envisioned synthetic approach will be presented along with a key decarboxylative aromatization step related to this work. An overview of biological decarboxylation will be discussed along with its possible connection to the biosynthetic pathway that forms (+)-aspewentin A (**1-16**) in *Aspergillus wentii*. Novel synthetic results from the Cu(II)-Michael process will be reviewed in this chapter including unanticipated cyclization byproducts and some synthetic derivatives.

II.2 Overview of Aspewentin Biosynthesis

The initial report of the aspewentins followed activation of a cryptic genome pathway in an algicolous sample of *Aspergillus wentii* found in deep sea sediment soil.[35] In these studies media bearing isolated *Aspergillus wentii* was supplemented with additional suberoylanilide hydroxamic acid to function as a histone deacetylase inhibitor.[86] This chemical treatment was found to increase the variability and expression levels of secondary metabolites in this species via epigenetic

modification. The molecular dynamics of biological systems that contribute to epigenetic modification allow for an organism to respond to environmental changes and ultimately conserve its metabolite expression while still allowing for metabolite variability when it may be advantageous. The biomolecular events required to precede the formation and evolutionary selection of these epigenetic systems does not appear to be fully understood at this time.[87,88] However, knowledge of this biological property has contributed to the modern fields of bioinformatic genome mining,[89] biomolecular quorum sensing,[90] microbe co-culture,[91] and chemical epigenome manipulation[92] for natural product discovery. In this case, a single strain of *Aspergillus wentii* (GenBank accession no. KM409566, HM014129.1, KF9210087.1)[93] has produced all currently described aspewentins (A–M)[35,93,94] (Figure II.1). All members of the aspewentin family feature the 19-*nor*-isopimarane demethylation pattern which may suggest a common mechanism of decarboxylation in this strain. Of the currently described aspewentins, (+)-aspewentin A (**1-16**) bears the more potent and broad antimicrobial activity[93] with insignificant toxicity in brine shrimp assays[35] (safety indication), when compared to the other aspewentins. Structurally, **1-16** is distinct from some of its other members by the aromatized B-ring that forms its phenolic moiety. This hybridization state at the B-ring is only possible provided a preceding demethylation event to provide the requisite 20-nor-isopimarane scaffold. Further, the non-phenolic aspewentins bear a common C10-hydroxylation motif that may be derived from para-oxygenation of the corresponding phenol to a hydroxy cyclohexadienone moiety (as in the oxygenation of (+)-aspewentin A (**1-16**) to C (**2-2**)). It is unknown how the biological effects of standout diterpene compounds like (+)-aspewentin A (**1-16**) are affected by the presence of its phenolic moiety. Initial bioassays against some species of marine phytoplankton[35] appeared to suggest that the phenol might be critical for its bioactivity but broader *in-vitro* antimicrobial studies

do not clearly invoke a trend in activity necessitating the phenol. Nonetheless, as previously mentioned, structurally analogous phenolic diterpenes are one of the major electron-rich secondary metabolites associated with antioxidant activity in certain plants[36,37] and remain of interest to the greater health community.

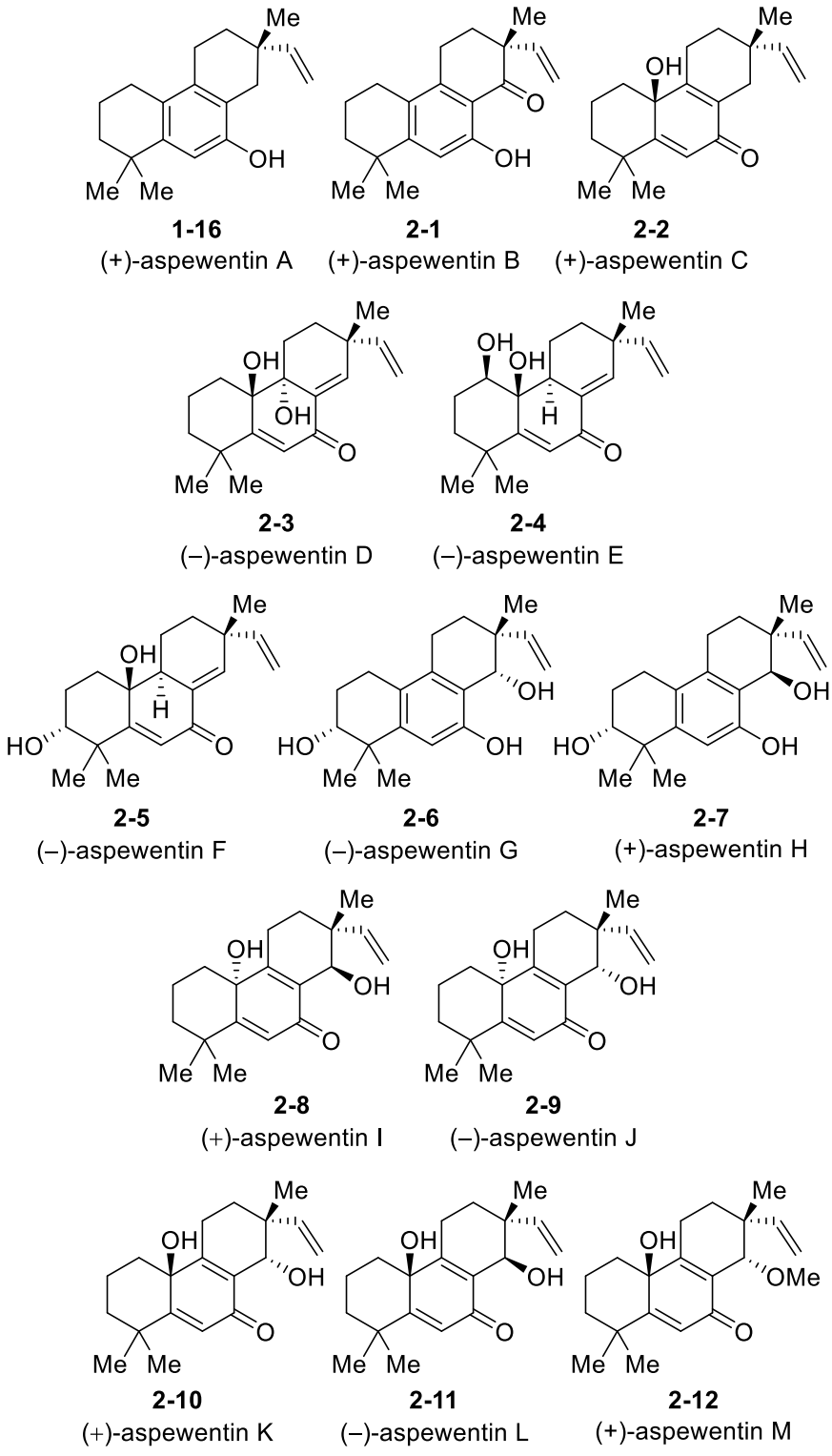

Figure II.1 Currently described members of the aspewentin family (A–M).

II.3 The Stoltz Approach to Aspewentins A–C

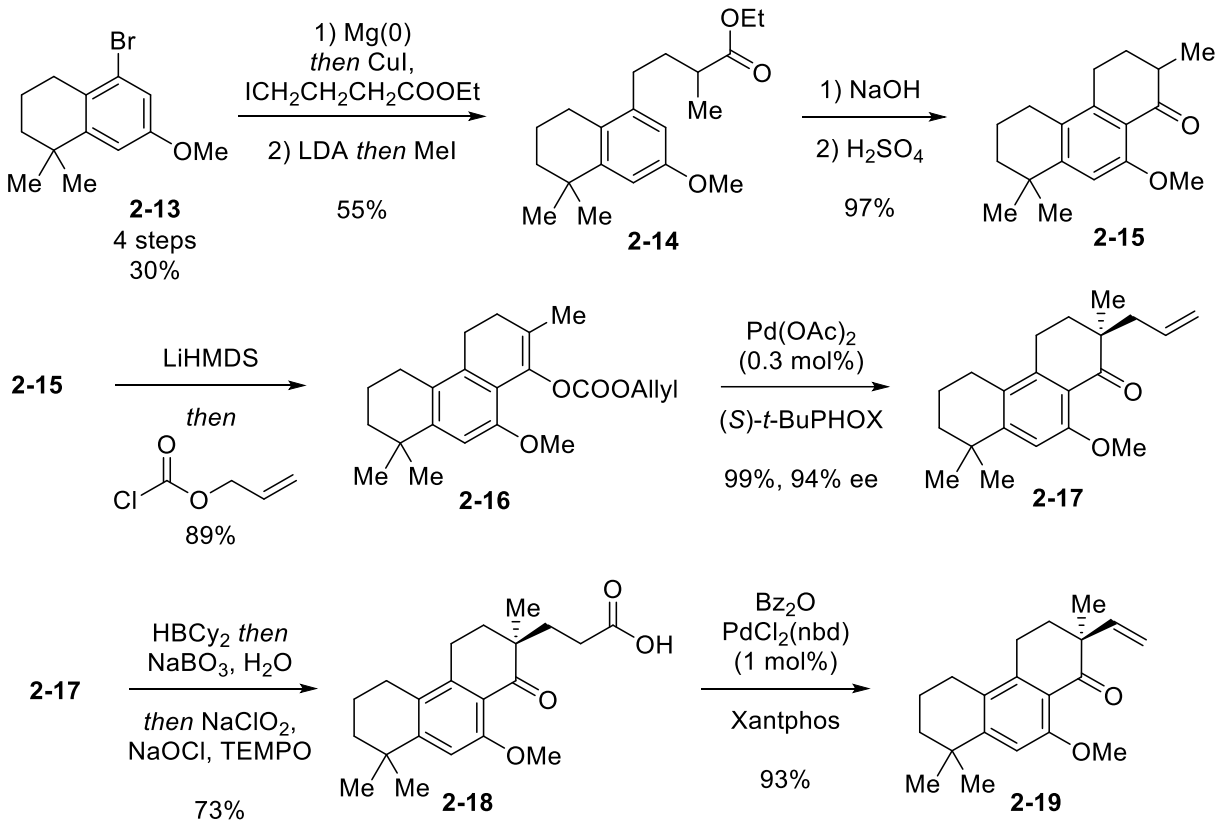

Figure II.2 The Stoltz total synthesis of (−)-aspewentins A–C.

The first reported total synthesis of (−)-aspewentin A (**(−)-1-16**), B (**(−)-2-1**), and C (**(−)-2-2**) was described by the Stoltz group implementing a key Pd-mediated decarboxylation to provide the pendant vinyl group (Figure II.2).[95] Aryl bromide **2-13** was prepared in four steps and 30% overall yield from known patent literature. Subsequently, **2-13** was alkylated by subjecting the substrate to metallic magnesium in THF and then CuI and ethyl 4-iodobutyrate was added to the reaction mixture. The resulting crude material was subjected to LDA in THF and then methyl iodide to methylate an intermediate enolate species and generate product **2-14** in 55% yield. Ester **2-14** was exposed to NaOH in MeOH and then aqueous H_2SO_4 to afford cyclized product **2-15** in 97% yield. The ketone moiety of **2-15** was transformed into the corresponding enol allyl carbonate

by deprotonating the substrate using LiHMDS in THF and then adding allyl chloroformate to furnish carbonate **2-16** in 89% yield. Decarboxylative rearrangement of enol allyl carbonate **2-16** was mediated by $Pd(OAc)_2$ (0.3 mol%) and (*S*)-*t*-BuPHOX (1.0 mol%) in MTBE to provide allylated ketone **2-17** in 99% yield and 94% ee. Brown hydroboration/oxidation of substrate **2-17** using dicyclohexylborane in THF followed by aqueous sodium perborate and then a subsequent exposure to aqueous sodium chlorite and catalytic quantities of sodium hypochlorite and TEMPO at 6.5 pH gave product **2-18** in 73% yield. Decarbonylative dehydration of **2-18** was mediated by catalytic quantities of $PdCl_2$(nbd) (1.0 mol%) and Xantphos (1.2 mol%) in the presence of benzoic anhydride and NMP to yield product **2-19** in 93% yield. Substrate **2-19** was demethylated using NaI and $AlCl_3$ in MeCN to yield (−)-aspewentin B (**(−)-2-1**) in 78% yield (Figure II.3). (−)-Aspewentin B (**(−)-2-1**) was then deoxygenated using $NaBH_4$ and TFA in DCM to provide (−)-aspewentin A (**(−)-1-16**) in 85% yield. Subsequent dearomative oxidation of (−)-aspewentin A

((−)-**1-16**) was accomplished using $Rh_2(cap)_4$ (1 mol%) and *t*-BuOOH to provide (−)-aspewentin C ((−)-**2-2**) in 13% yield along with (+)-10-*epi*-aspewentin C (**2-20**) in 7% yield, all over 16 steps.

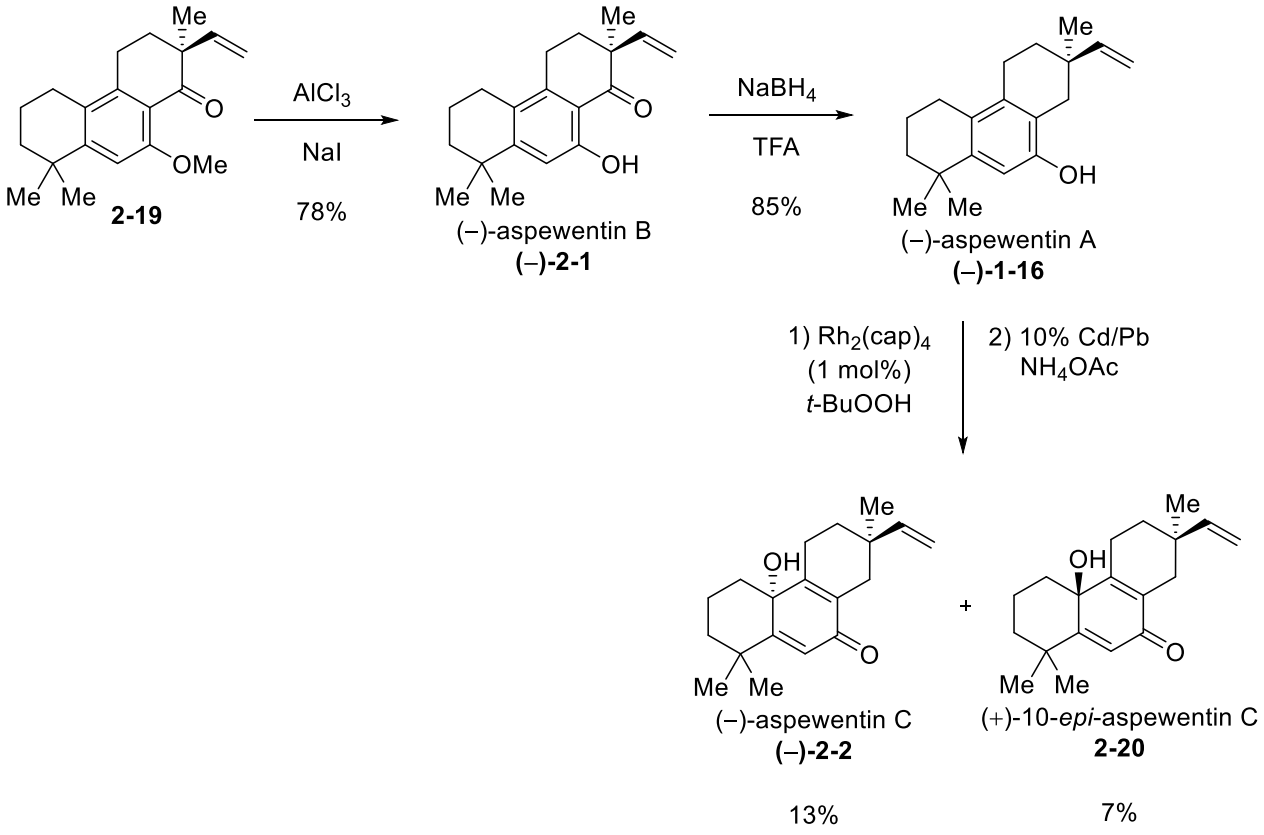

Figure II.3 The Stoltz total synthesis of (−)-aspewentins A–C.

II.4 Proposed Synthetic Route to the Strategic Intermediate and Isopimaranes

Using the prior work by the Nagorny group as the foundation of these studies, the work in this and subsequent chapters is based on the hypothesis that tandem Michal/aldol cascade reactions could be utilized to access a key tricyclic core of isopimarane diterpenes (Figure II.4). To rapidly generate this highly substituted and asymmetric scaffold, we envisioned that enantioenriched Michael acceptor **(R)-2-21** and Michael donor **2-22** could be coupled with Cu(II) as the catalyst under *neat* conditions to yield product **2-24** in a diastereoselective manner.

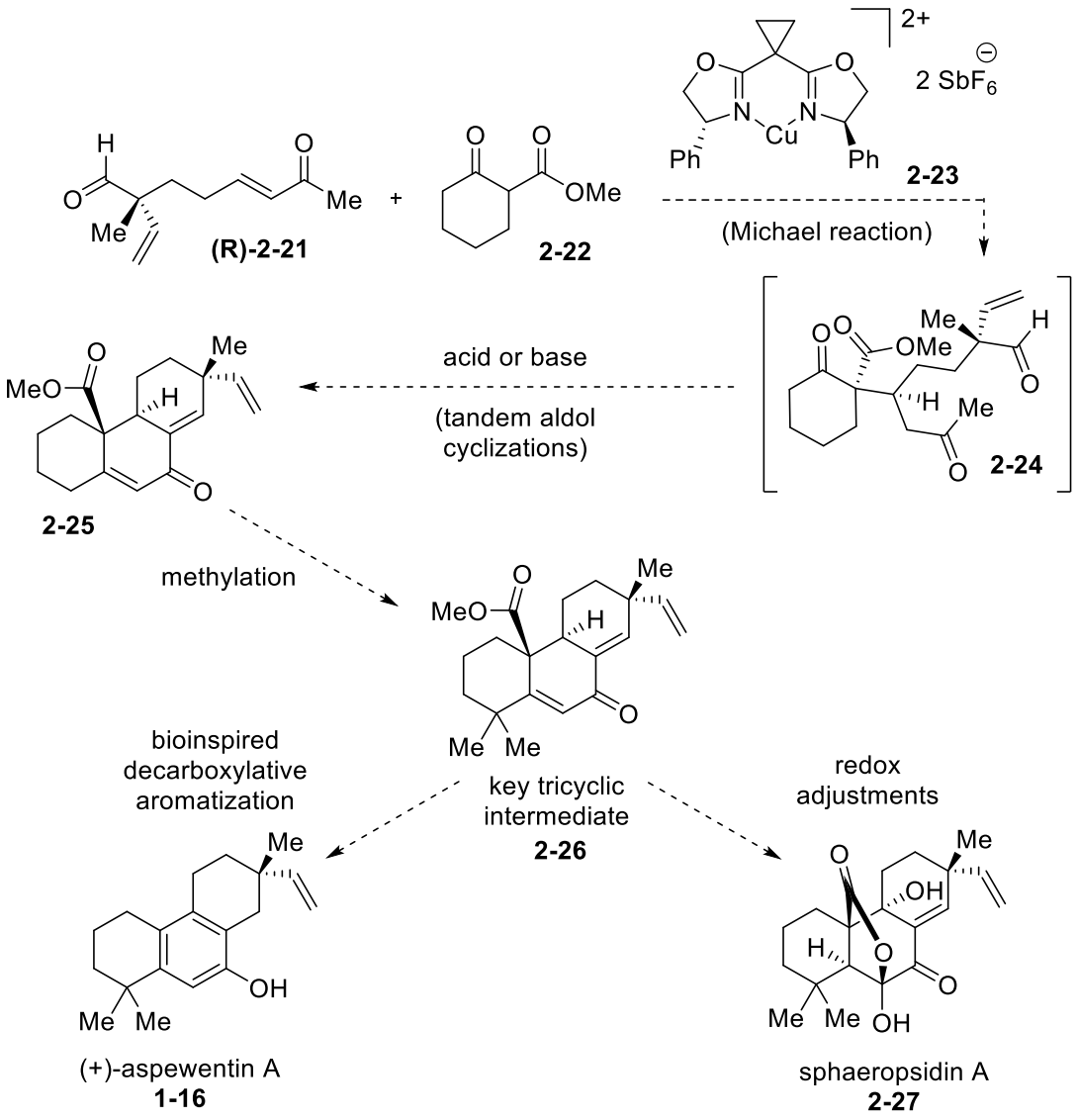

Figure II.4 Sequential Cu(II)-catalyzed Michael/aldol approach to isopimaranes.

The general Cu(II)-catalyzed Michael reaction process has a significant history as a powerful strategy for carbon-carbon bond formation.[96-99] Intermediate **2-24** can then be subject to acidic or basic conditions to afford a cyclized, condensed tricycle **2-25** via two intramolecular aldol condensation reactions. An alkylation strategy can then be implemented to access highly congested carbocycle **2-26** which mimics the alkyl substitution pattern associated with isopimaranes. (+)-Aspewentin A (**1-16**) can be directly formed from tricycle **2-26** through a decarboxylative

aromatization process. Alternatively, sphaeropsidin A (**2-27**) can be formed from tricycle **2-26** provided selective redox manipulations to the scaffold.

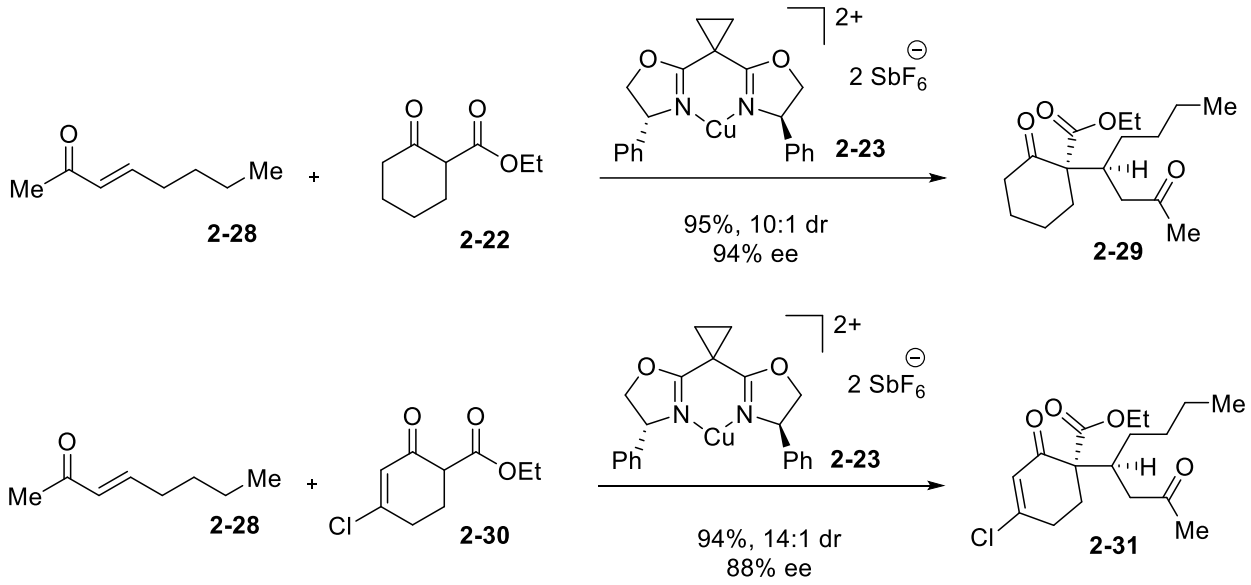

Figure II.5 Precedent Cu(II)-Michael addition results.

Synthetic interests within the Nagorny group broadly involve the development of synthetic methodology and strategies to enable the total syntheses of steroids and other natural products. Prior synthetic work by Nagorny and coworkers has focused on addressing the challenges involving the synthesis of sterically hindered Michael products within the context of steroidal synthesis. Our group has successfully implemented a high yielding and diastereoselective Cu(II)-Michael process to facilitate access to useful C-C coupled products as intermediates (Figure II.5). For example, a diastereoselective Cu(II)-Michael reaction can be achieved by stirring model Michael acceptor octenone **2-28** and keto-ester **2-22** under *neat* conditions with Cu(II)-BOX catalyst **2-23** to yield Michael adduct **2-29** in 95% yield, 10:1 dr, and 94% ee. Similarly, when octenone **2-28** and chloro keto-ester **2-30** were stirred under identical conditions, Michael adduct **2-31** was formed in 94% yield, 14:1 dr, and 88% ee.

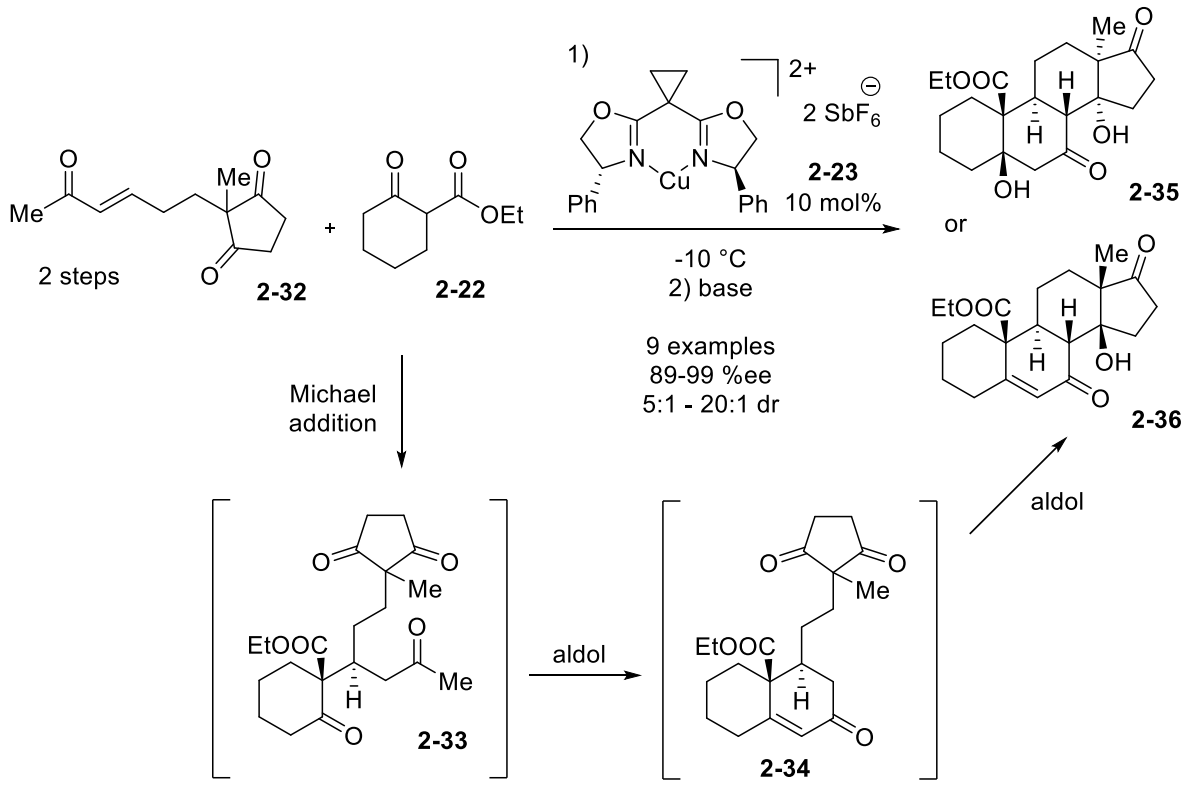

Figure II.6 Precedent tandem Cu(II)-Michael/aldol results.

The Cu(II)-Michael approach has been applied to steroid total synthesis by utilizing an enantioselective and diastereoselective Michael addition process mediated by (*R*,*R*)-Cu(II)-BOX catalyst **2-23** during model studies leading to the concise synthesis of oxygenated steroids (Figure II.6).[100] Michael acceptor **2-32**, can be stirred with donors like **2-22** and Cu(II)-BOX catalyst **2-23** (10 mol%) to generate intermediate **2-33** before being subjected to either acidic or basic conditions

to yield steroidal products like **2-35** or **2-36**, via intermediate **2-34**, with high enantioselectivity and diastereoselectivity.

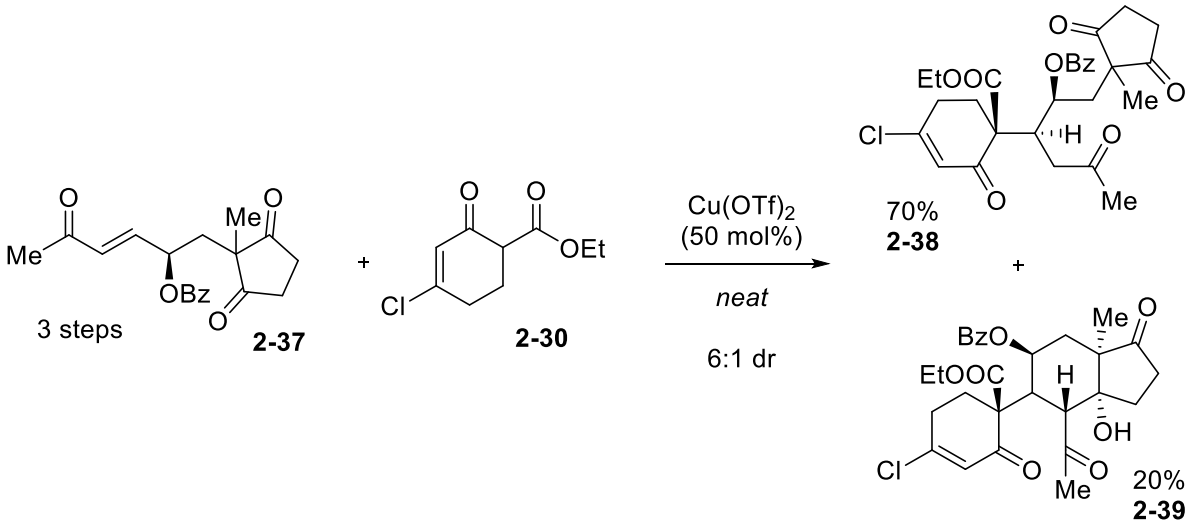

Figure II.7 Precedent total synthesis enabled by a Cu(II)-Michael/aldol condensation strategy.

The Cu(II)-Michael reaction has been made diastereoselective without the use of a chiral catalyst by implementing a chiral benzoyloxy stereocenter in the Michael acceptor (Figure II.7). Thus, Michael acceptor **2-37**, available in three synthetic steps, and chloro keto-ester **2-30** were applied to the Cu(II)-mediated process by stirring under *neat* conditions with $Cu(OTf)_2$ catalyst (50 mol%) to provide Michael adduct **2-38** in 70% yield and its corresponding aldol product **2-39** in 20% yield, both in 6:1 dr.[97] Cyclization of Michael adduct **2-38** can then be achieved using *p*-TSA in MeCN at 55 °C to provide a diastereoenriched product **2-40** in 68% yield and >20:1 dr (Figure II.8), while **2-39** was independently cyclized to **2-40** as well. Intermediate **2-40** has been

elaborated for the total syntheses of several cardinolides including the trewianin aglycone (**2-41**), panogenin (**2-42**), and ouabagenin (**2-43**).[97,99]

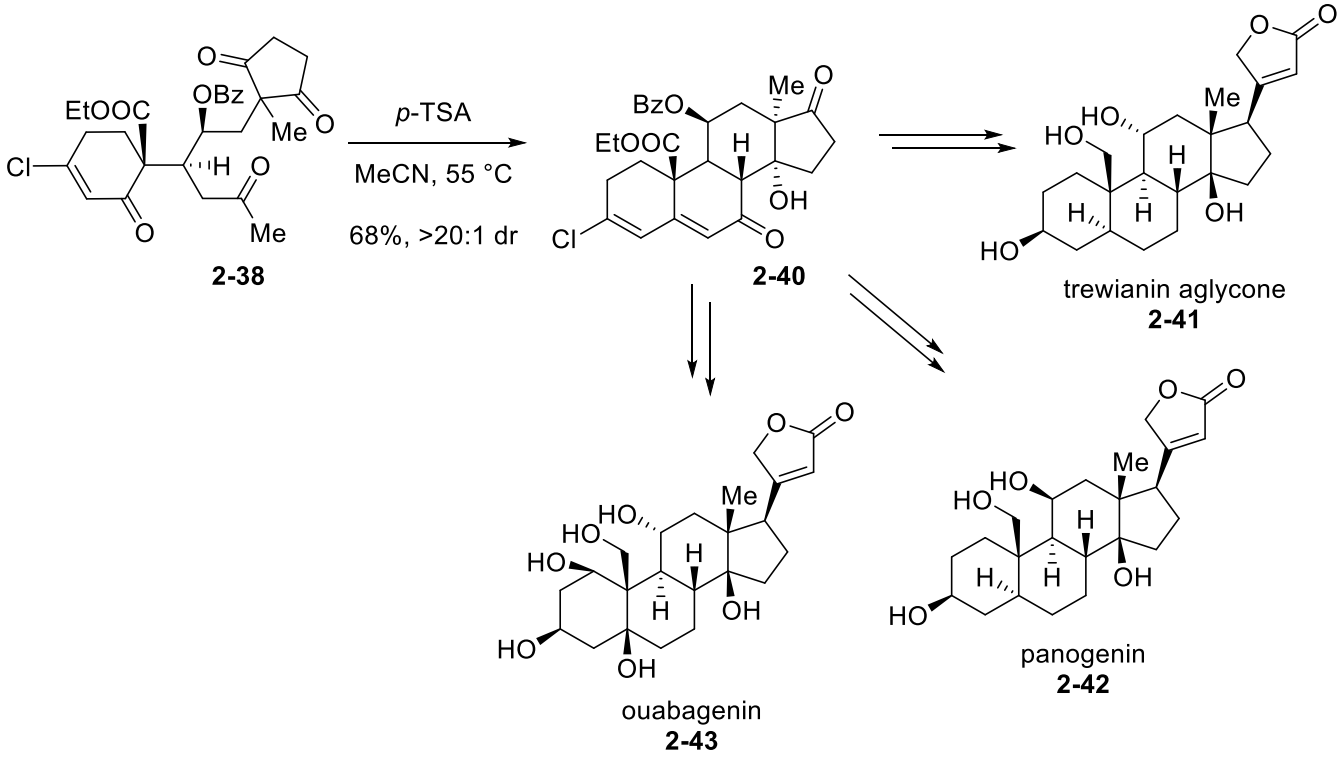

Figure II.8 Precedent total synthesis enabled by a Cu(II)-Michael/aldol condensation strategy.

Similarly, Michael acceptor **2-32**, accessible in two synthetic steps, has been stirred with ester **2-30** under *neat* conditions with catalytic (*R*,*R*)-Cu(II)-BOX **2-23** (10 mol%) to provide Michael adduct **2-44** in 92% yield, >20:1 dr, and 92% ee (Figure II.9).[101] Cyclization of Michael adduct **2-44** can be achieved using *p*-TSA in MeCN at 60 °C to provide product **2-45** in 57% yield. Intermediate **2-45** was then synthetically elaborated for the total synthesis of cannogenol (**2-46**).

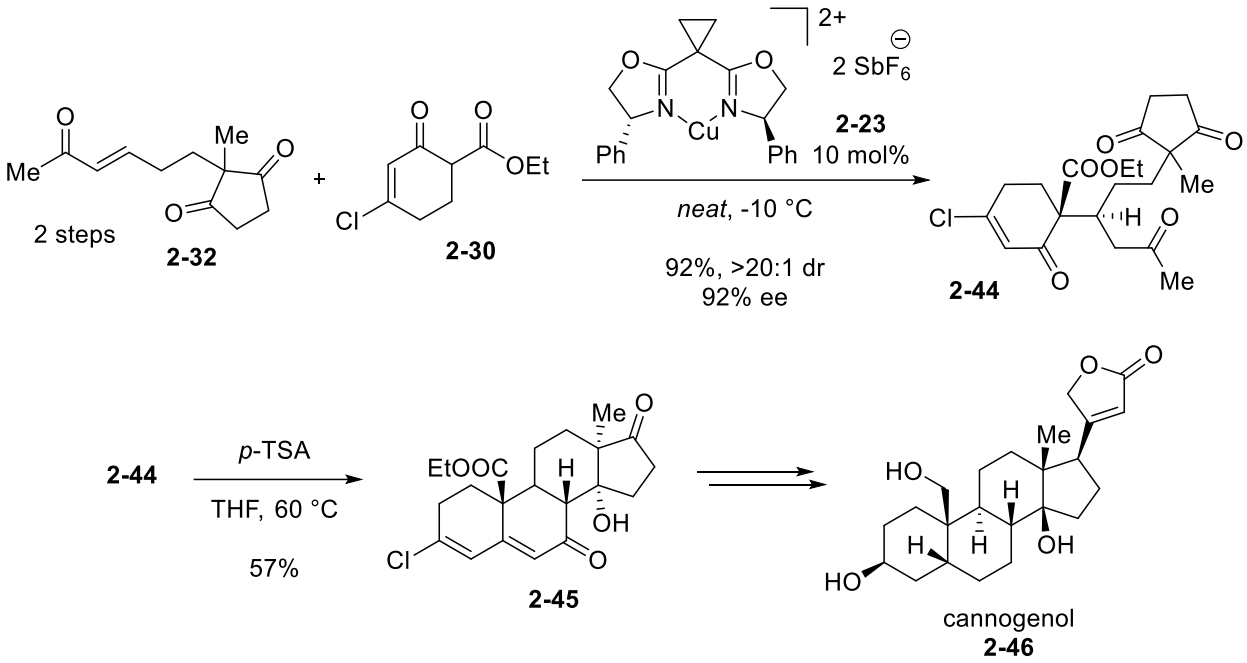

Figure II.9 Total synthesis of cannogenol (**2-46**) via a Cu(II)-Michael/aldol strategy.

These results suggest that the intended Michael/aldol process involving **(*R*)-2-21** and **2-22** leading to intermediate **2-26** (Figure II.4) would be similarly promoted by a Cu(II)-based catalyst and successive aldol cyclization conditions. While this approach would allow for synthetic access to the tricyclic skeleton related to isopimaranes, a subsequent decarboxylative aromatization step yielding phenols remains another key element in our synthetic design and enables the total

synthesis of (±)-aspewentin A (**(±)-1-16**. Considering its importance to our synthetic design, we provide an overview of decarboxylation reactions in the following subchapter.

II.5 Decarboxylation Overview

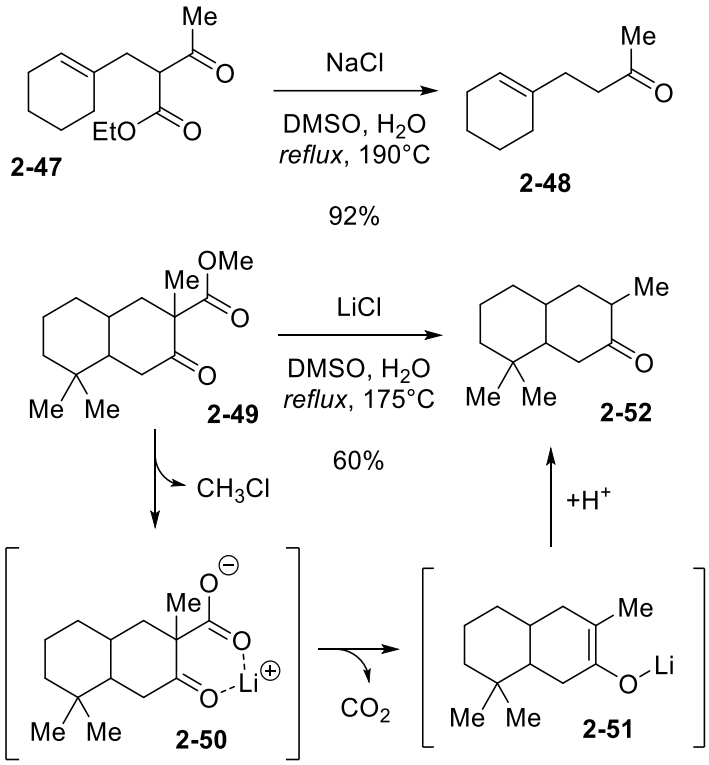

Figure II.10 Select examples of Krapcho Decarboxylation.

Synthetic decarboxylation finds its origins, and continued industrial application, in chemical feedstock pyrolysis leading to decarboxylation and structural diversification.[102-104] Synthetic methods, such as in the Krapcho decarboxylation, have been developed in detail to enable the decarboxylation of available scaffolds (Figure II.10).[105] For example, keto-ester **2-47** can be effectively decarboxylated by heating with NaCl in aqueous DMSO at 190°C to afford methyl ketone **2-48** in 92% yield.[106] Furthermore, bicycle **2-49** can be decarboxylated by heating with LiCl in aqueous DMSO at 175°C to afford ketone **2-52** in 60% yield.[107] The α-decarboxylation of bicycle **2-49** proceeds via ester dealkylation leading to byproduct chloromethane and intermediate

carboxylate **2-50**. Carboxylate **2-50** may then undergo the decarboxylation process leading to enolate **2-51** before protonation to the product ketone **2-52**. Thermal β-keto acid α-decarboxylation is known to invoke the intermediacy of a six-membered transition state that facilitates its thermal process.[108] For example, the thermal α-decarboxylation of β-keto acid **2-53** to acetone (**2-56**) invokes transition state **2-54** leading directly to enol **2-55** before tautomerization to the product acetone (**2-56**) (Figure II.11). Similarly, derivatives of 3-butenoic acid (**2-57**) are able to undergo thermal decarboxylation event that likewise utilizes a six-membered transition state (**2-58**) to facilitate a pyrolytic process, in this case leading to isobutene (**2-59**).[109-111] The mechanism of 3-butenoic acid (**2-57**) decarboxylation is analogous to the intended operation of decarboxylative aromatization of vinylogous ketones presented at the beginning of this chapter (Figure II.4). This strategy has synthetic precedence as during a stepwise synthesis implementing a decarboxylative aromatization step on Hagemann's ester (**2-60**) using heating in ethanolic NaOEt to provide enone **2-61** in 60% yield.[112] In this case, enone **2-61** was then aromatized by heating with palladium on carbon to facilitate chemical dehydrogenation and yield phenol **2-62** in 55% yield. Likewise, bicycle **2-63** has successfully been decarboxylated by refluxing in aqueous KOH to provide alkene **2-64** in 9% yield and enone **2-65** in 91% yield.[113] Although thermal decarboxylation has been the focus of this discussion, methodology for the analogous radical chemistry has also been developed for acids and "activated esters" via homolysis.[114-116]

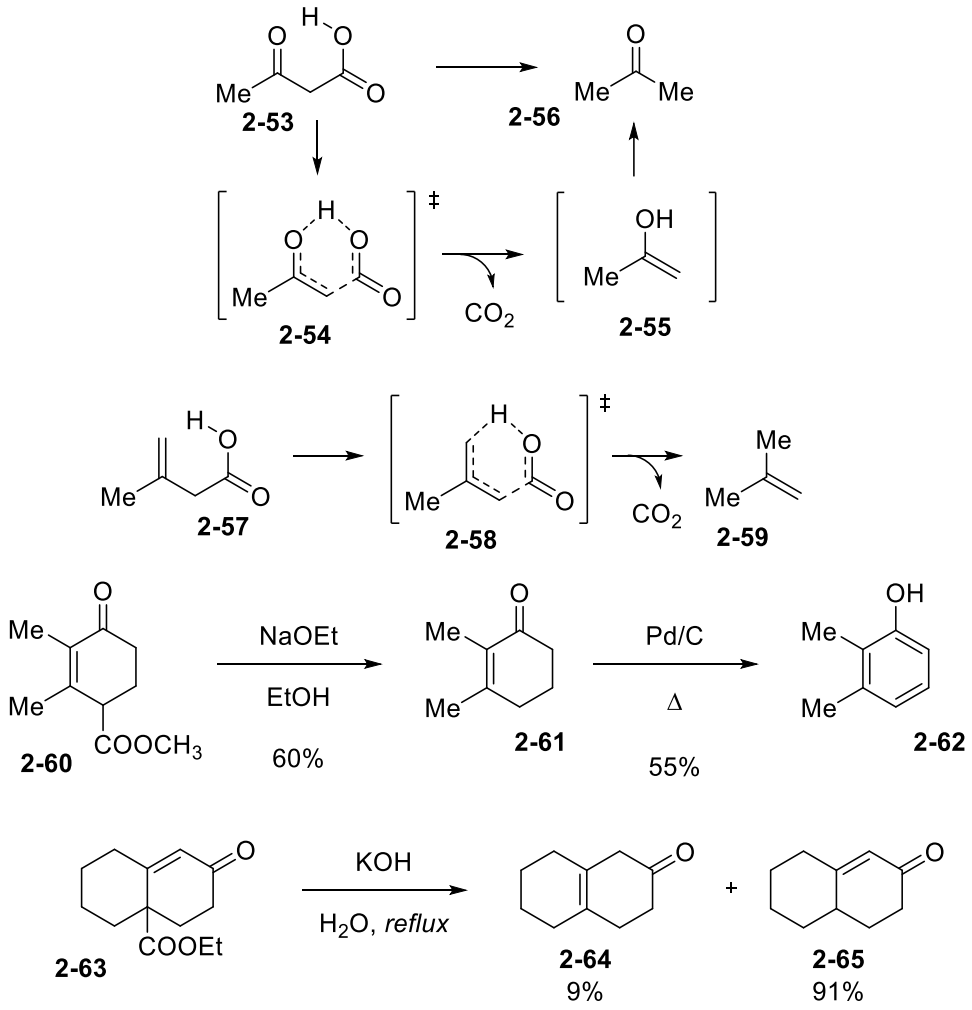

Figure II.11 Transition state of thermal decarboxylation and precedent γ-decarboxylation.

Decarboxylation processes in nature are mediated by a diverse set of enzymes that can be identified in a number of conserved, regulatory biological pathways.[117] Although the following examples of decarboxylation in nature are not exhaustive, they serve as a representation of the mechanistic requirements for various dynamic cellular activities to proceed.

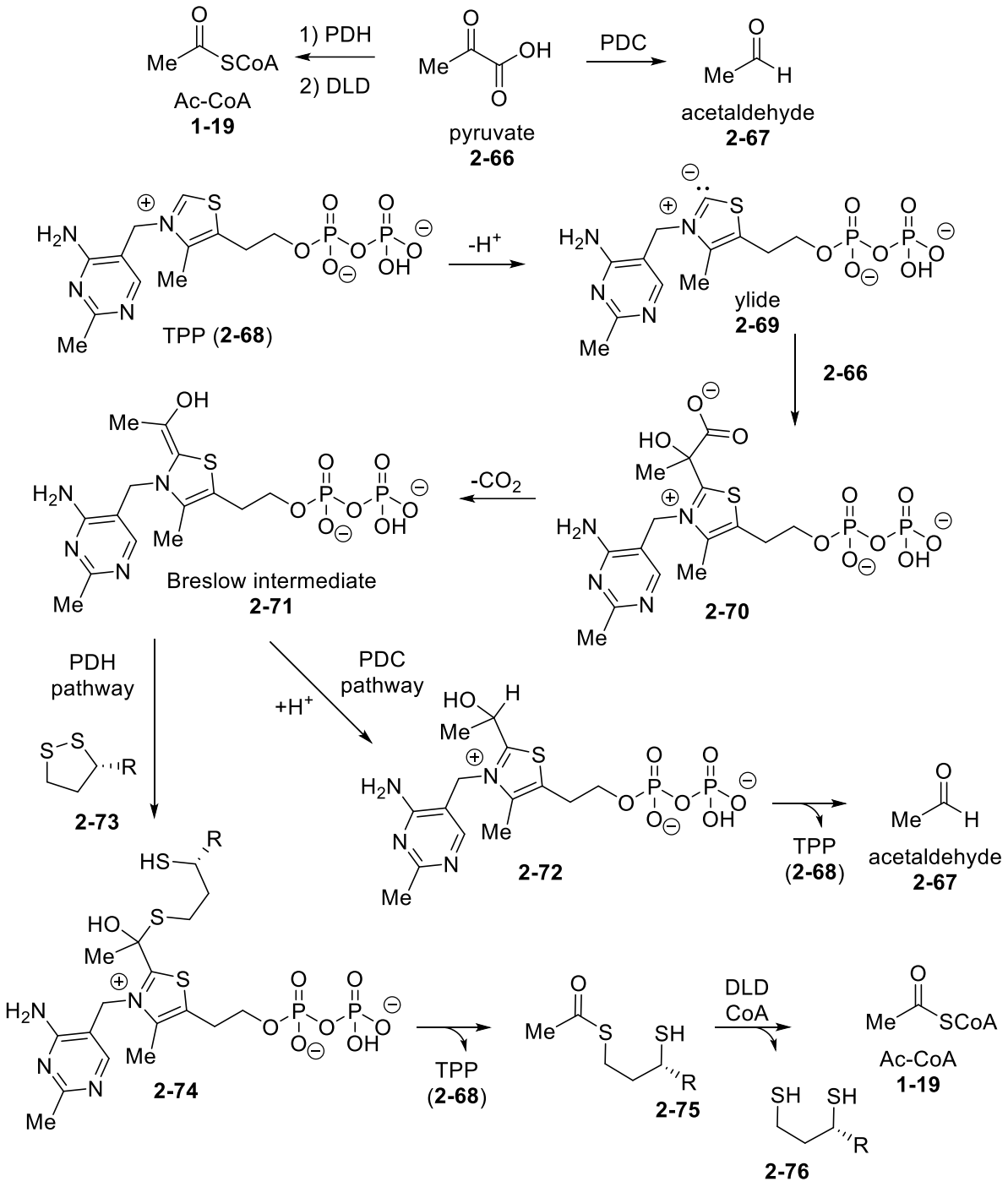

Figure II.12 Mechanism of pyruvate (**2-66**) decarboxylation mediated by either PDC or PDH.

During glycolysis, pyruvate (**2-66**) is formed as an intermediate metabolite. There are at least two well-known biosynthetic decarboxylation pathways leading away from pyruvate (**2-**

66), the PDC and PDH pathways (Figure II.12). The PDC enzyme is associated with the fermentation process in yeast and yields acetaldehyde (**2-67**) as an intermediate product involved in the fermentation of alcohol. Conversely, the PDH enzyme is associated the citric acid (Krebs) cycle in biochemistry and provides Ac-CoA (**1-19**) as a starting material for the biosynthesis of citric acid. Ac-CoA (**1-19**) was previously described as the biosynthetic starting material for steroids and terpenes in the first chapter. The mechanisms of PDC and PDH both invoke the cofactor TPP (**2-68**), which broadly functions to facilitate the decarboxylation step in these enzymes by the formation of nucleophilic ylide **2-69**. Coupling of ylide **2-69** and pyruvate (**2-66**) yields intermediate **2-70** that then undergoes a key decarboxylative step to provide the Breslow intermediate **2-71**.[118] If the PDC pathway is in operation, the Breslow intermediate **2-71** is then protonated to intermediate **2-72** before eliminating TPP (**2-68**) to reveal acetaldehyde (**2-67**).[119] Conversely, if the PDH pathway is in operation, the Breslow intermediate **2-71** is then coupled to disulfide **2-73** (associated with lipoamide) forming intermediate **2-74** before eliminating TPP (**2-68**) to reveal thioester carrier **2-75**.[120] The enzyme DLD mediates the biosynthesis of Ac-CoA (**1-19**) using the thioester carrier **2-75** and CoA with dithiol **2-76** (reduced form of lipoamide) as a byproduct of the process. When the PDH enzyme participates in this fundamental biological process it is referred to as the pyruvate dehydrogenase complex.

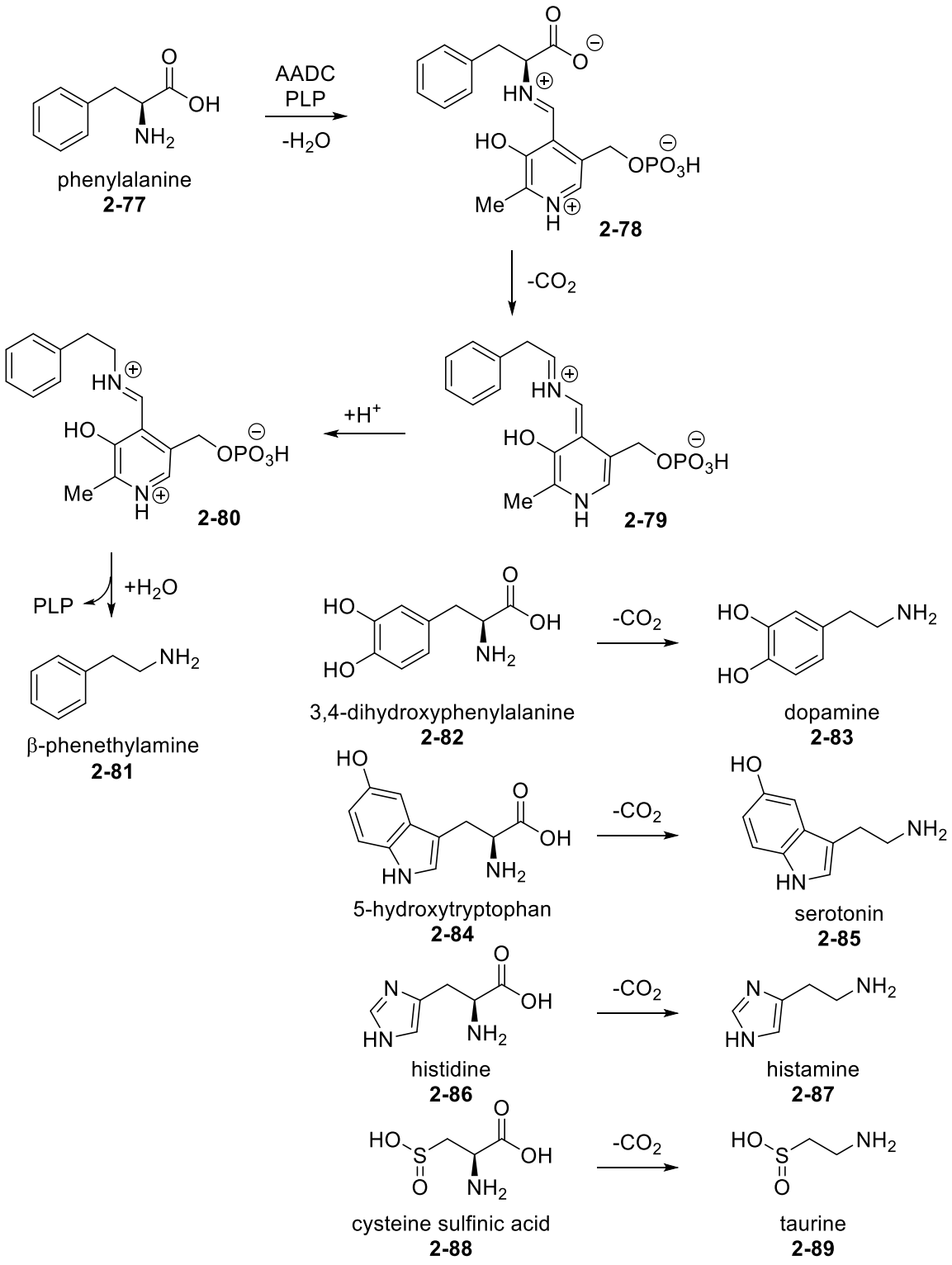

Figure II.13 General aromatic L-amino acid and neurotransmitter decarboxylation.

Decarboxylation is a fundamental part of the biosynthesis of monoamine neurotransmitters that are derived from their corresponding L-amino acid precursors (Figure II.13). The enzyme AADC mediates several necessary biosynthetic decarboxylation events that provide monoamine neurotransmitters in nature. AADC accomplishes its decarboxylation process by invoking the PLP cofactor which directly forms iminium species **2-78** from substrate phenylalanine (**2-77**).[121] Decarboxylation from iminium **2-78** leads to intermediate **2-79** which can then be protonated to generate iminium **2-80**. Hydrolysis of iminium **2-80** reveals β-phenethylamine (**2-81**) and reforms the starting PLP cofactor. AADC can accomplish these L-amino acid decarboxylation on several substrates, including 3,4-dihydroxyphenylalanine (**2-82**, L-DOPA) to dopamine (**2-83**, DA), 5-hydroxytryptophan (**2-84**, 5-HTP) to serotonin (**2-85**, 5-HT), and histidine (**2-86**) to histamine (**2-87**). However, the transformation of histidine (**2-86**) to histamine (**2-87**) is generally regulated by the conserved enzyme HDC. The transformation of cysteine sulfinic acid (**2-88**) to taurine (**2-89**) is accomplished by decarboxylation of the enzyme CSAD, similarly invoking a mechanism with the cofactor PLP.

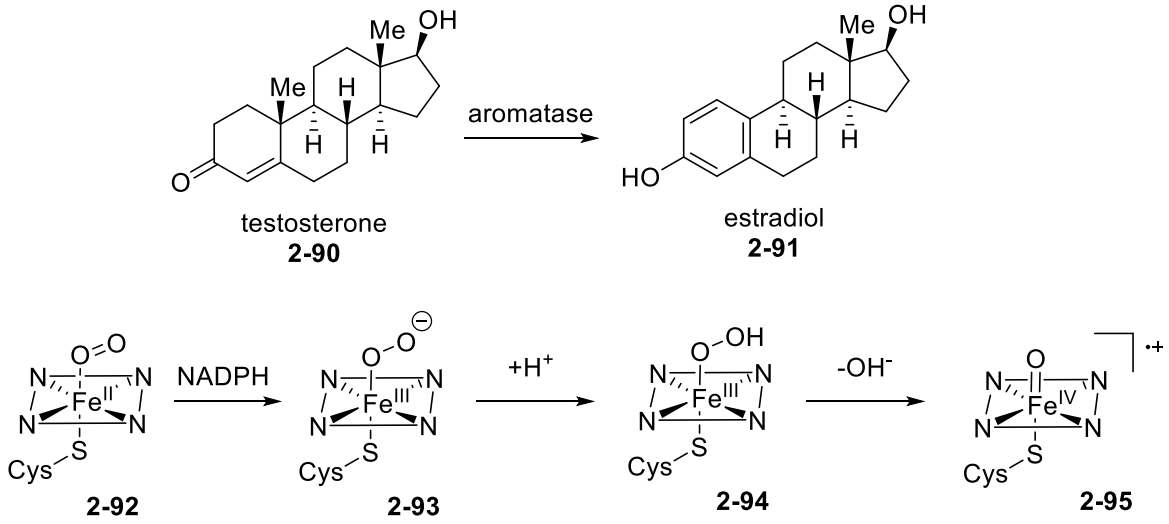

Figure II.14 Oxidation of testosterone **2-90** and select CYP active-site species.

Oxidative C19-demethylation of testosterone (**2-90**) is a fundamental aromatization step leading to estradiol (**2-91**) (Figure II.14). Aromatase is a biologically conserved oxidative CYP enzyme that is involved in the biosynthesis and regulation of the estrogen steroid hormones from available androgens. Sequence homology and alignment studies across vertebrates and invertebrates suggest that the evolutionary conservation of the proximal active site residues in CYP19 (aromatase) occurred early on in certain phylogenetic branches.[122] Although the entire CYP catalytic cycle is not shown, the relevant active species have been provided. Complexation of molecular oxygen in the heme active site of these CYPs leads to the generation of oxy-ferrous complex **2-92** (iron(II)-oxo complex) which can be reduced by cofactor NADPH to reveal the peroxo-ferric species **2-93** (iron(III)-peroxo).[123,124] Protonation of the peroxo-ferric species **2-93** leads to the formation of hydroperoxo-ferric species **2-94** (iron(III)-hydroperoxo). The first oxidation step of decarboxylation via CYPs, like aromatase (CYP19), generally invokes the formation of a high-valence oxyferryl species **2-95** (iron(IV)–oxo porphyrin cation radical species, also conventionally referred to as "Compound 1" when in reference to the active C-H insertion species of CYPs) for the initial hydrogen atom abstraction. The elimination of a hydroxide ion from hydroperoxo-ferric species **2-94** produces the high-valence oxyferryl species **2-95**. Oxyferryl species **2-95** then hydroxylates testosterone **2-90** to an initial primary alcohol **2-96** (Figure II.15). Then, oxyferryl species **2-95** once again hydroxylates alcohol **2-96** to an intermediate hydrate which rapidly eliminates water to form aldehyde **2-97**. The nucleophilic peroxo-ferric species **2-93** is implicated in the third, and final, oxidation step of electrophilic aldehyde **2-97** leading to aromatization and the formation of radical **2-99**, byproduct formic acid from C19, and the iron(III)-oxyl radical species **2-100** via coupled intermediate **2-98**.[125] Notably, the nucleophilic peroxo-ferric species **2-93** is suggested to persist for longer lifetimes in aromatase,[126] whereas its protonation to

hydroperoxo-ferric species **2-94** (iron(III)-hydroperoxo species) occurs more rapidly to in other CYPs. A final hydrogen atom transfer event from radical **2-99** to iron(III)-oxyl radical species **2-100** yields estradiol (**2-91**) and hydroxy-ferric species **2-101** (iron(III)-hydroxide species).

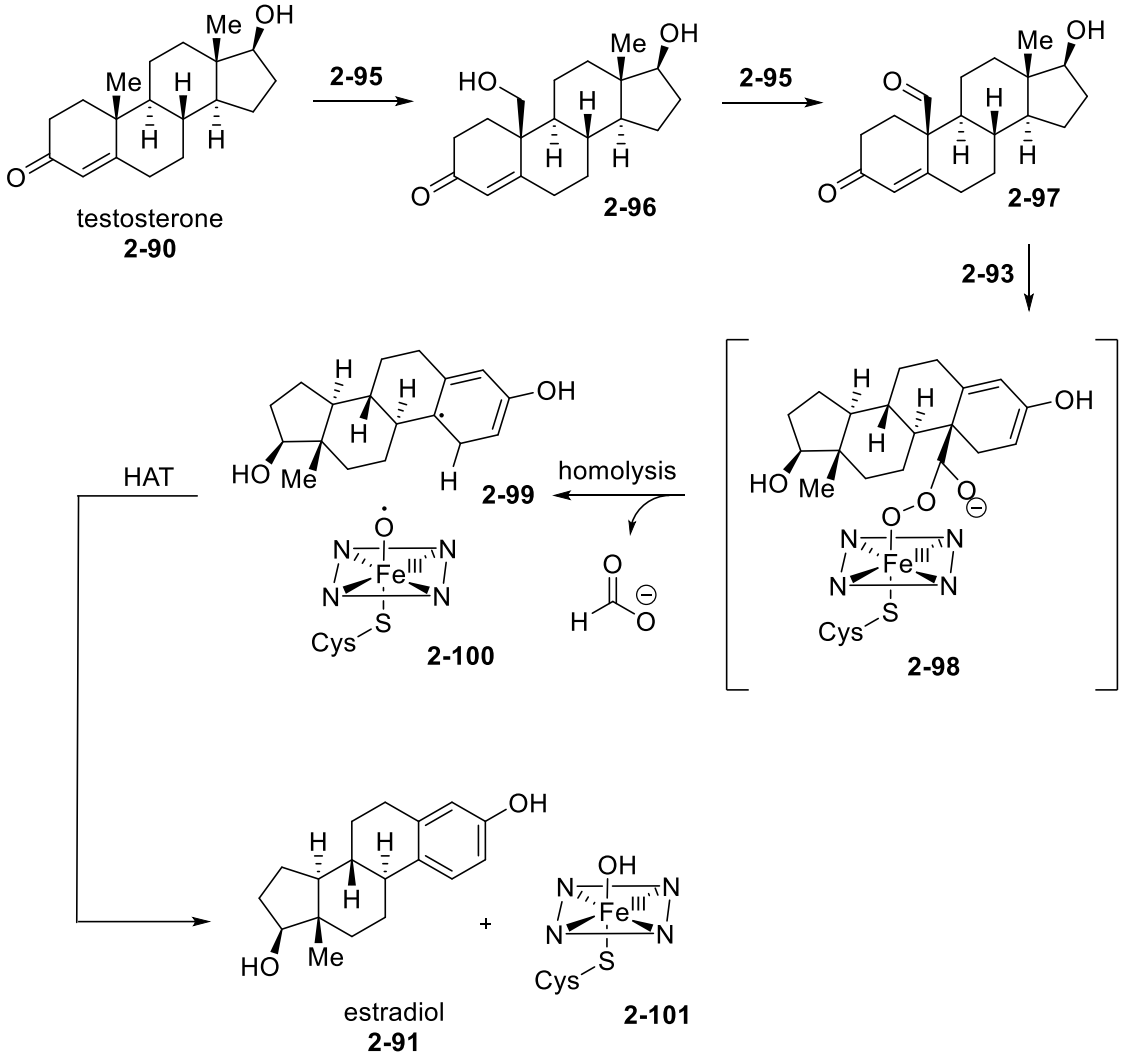

Figure II.15 Accepted biosynthetic mechanism of oxidation for testosterone **2-90**.

Although the biosynthetic oxidation of terpenes and other natural product classes invoke diverse enzymes within single or across coexisting species, CYPs are most frequently implicated in these oxidation networks leading to the observed secondary metabolites.[127-130] Provided the involvement of CYPs in the biosynthesis of (+)-aspewentin A (**1-16**), oxidation of the biosynthetic

intermediate **1-32** would lead to aldehyde **2-102** as an intermediate (Figure II.16). Then, a CYP-mediated mechanism of isopimarane scaffold C20-deformylation/ HAT would lead to the transformation of **2-102** to (+)-aspewentin A (**1-16**). Alternatively, another undefined oxidoreductase enzyme might facilitate the oxidation of C20 from **1-32** to an acid, as in **2-103**, which may then undergo a decarboxylation/ aromatization step similarly leading to (+)-aspewentin A (**1-16**). This oxidation and decarboxylation pathway, corresponding with intermediate **2-84**, has been previously suggested as a viable biosynthetic pathway for analogous aromatic diterpene cycloethers[41] from *Aspergillus wentii* (GenBank accession no. KM409566, HM014129.1, KF9210087.1)[93] whose structural members also predominantly bear the phenolic B-ring motif. For these aromatized diterpenes, aromatization is thought to invoke the oxidation phase of the biosynthesis and oxidative demethylation of C20, however, it is notable that benzyloxymethylated ($BnOCH_2$-) analogues of the aromatized scaffold of **1-16** have been synthetically generated by chemical modifications (dehydrating conditions) via a 1,2-methyl shift from an appropriately oxygenated isomer.[28]

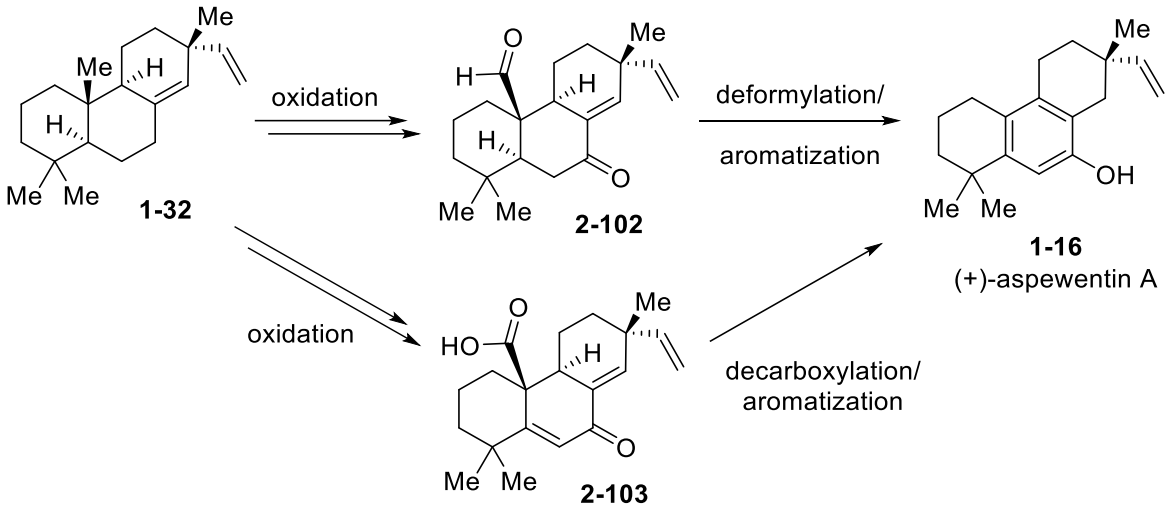

Figure II.16 Biosynthetic elaboration of **1-32** to (+)-aspewentin A (**1-16**).

II.6 Model Studies of the Michael/Aldol Cascades

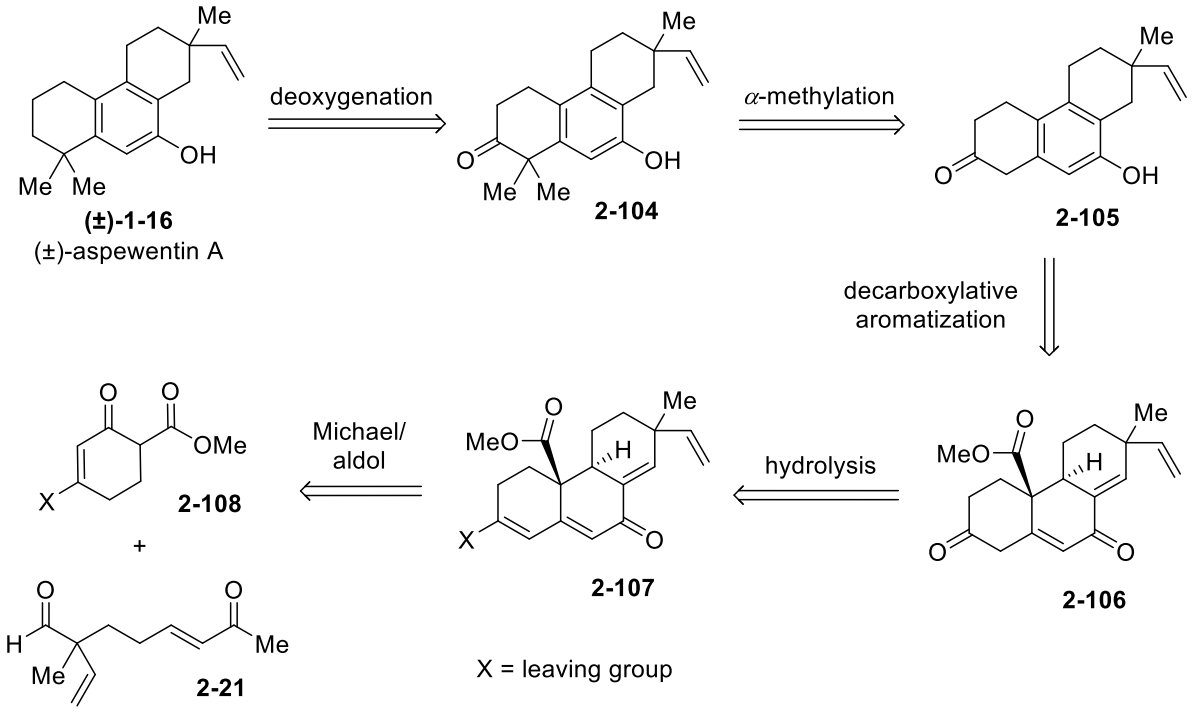

Figure II.17 First-generation retrosynthetic analysis of (±)-aspewentin A (**(±)-1-16**).

Based on the proposed biosynthetic considerations (*vide supra*), first-generation retrosynthetic analysis of (±)-aspewentin A (**(±)-1-16**) provides a pathway via deoxygenation from ketone **2-104**, itself accessible by dimethylation of intermediate **2-105** (Figure II.17). The phenolic moiety of ketone **2-105** can be made by decarboxylative aromatization from the tricyclic analogue **2-106**. Diketone **2-106** can be generated from hydrolysis of the corresponding substituted intermediate **2-107**. Scaffold **2-107** can be directly furnished from the Michael-aldol process if the appropriate

conjugated donor **2-108** and acceptor **2-21** are successfully implemented in the proposed reaction cascade.

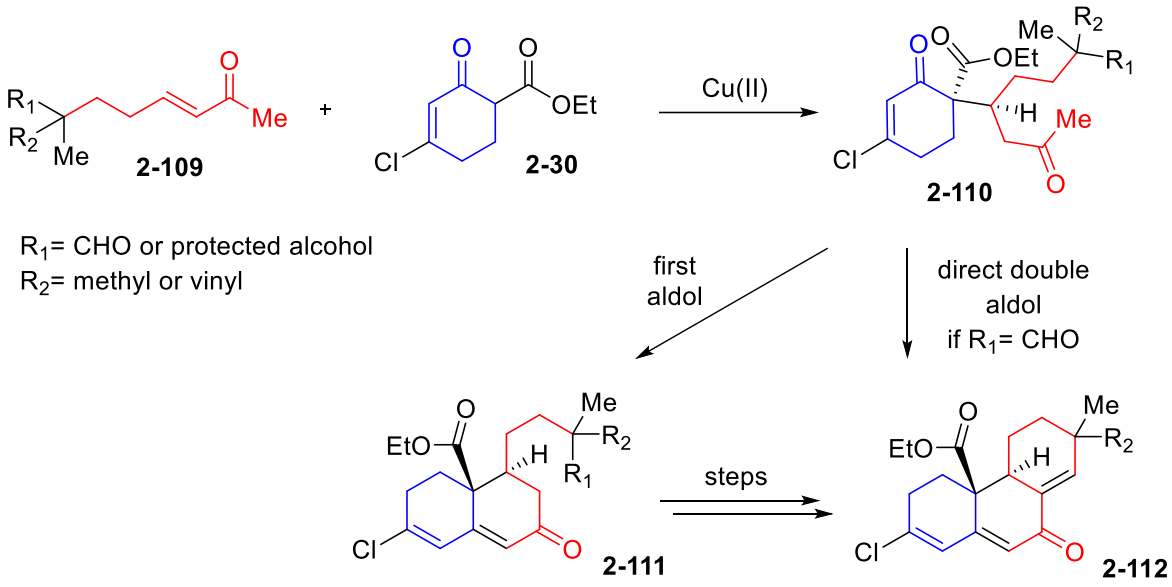

Figure II.18 Proposed Michael-aldol-aldol process leading to key scaffold **2-112**.

Thus, the envisioned plan involved reacting Michael acceptor (**2-109**) and donor (**2-30**) using Cu(II)-Michael chemistry to generate an intermediate Michael adduct **2-110** that may then be cyclized to form the desired carbocycle (Figure II.18). Cyclization can be accomplished through a stepwise approach, as in single annulation to intermediate **2-111**. Synthetic elaboration of scaffold **2-111** would then allow for the second cyclization to occur generating the key intermediate **2-112**. Alternatively, if Michael adduct **2-110** bears a formyl moiety at the appropriate position (R_2), then

the double annulation event can be accomplished in one synthetic operation directly leading to the condensation of **2-110** to **2-112**.

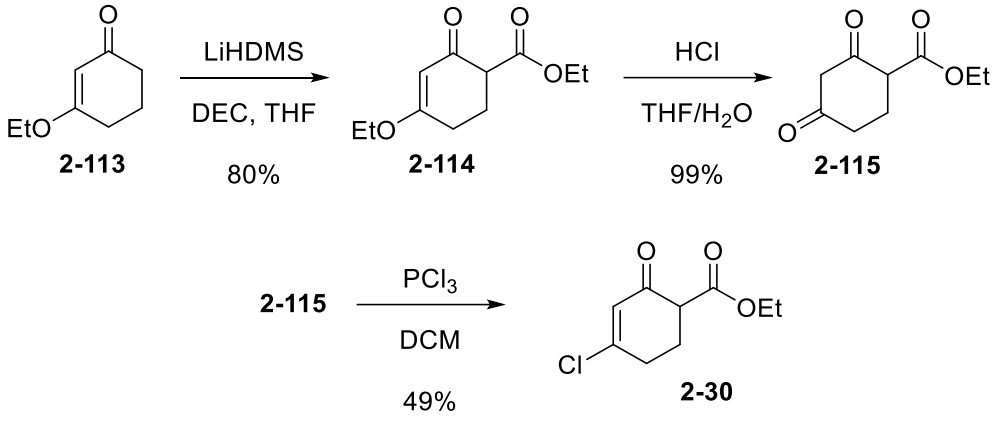

Figure II.19 Synthesis of donor **2-30**.

To synthetically access donor **2-30**, enone **2-113** was deprotonated using LiHDMS and DEC in THF to provide keto-ester **2-114** in 80% yield (Figure II.19). Keto-ester **2-114** was hydrolyzed using HCl in aqueous THF to yield diketone **2-115** in quantitative yield. Then, chlorination of diketone **2-115** was achieved using PCl_3 in DCM to afford donor **2-30** in 49% yield. An attempt to perform the Cu(II)-Michael operation with acceptor **2-28** and donor **2-30** found that equimolar loading of the two components gave 65% yield of adduct **2-31** (Table II.1, entry 1). Conversely, 2.0 equivalents of donor **2-30** lead to a diminished yield of 45% yield (entry 2).

Table II.1 Effect of donor **2-30** stoichiometry in Cu(II)-Michael process.

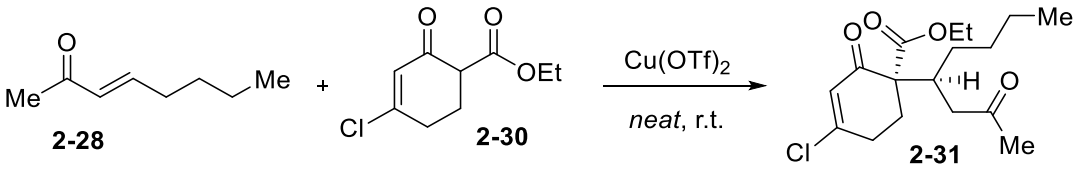

entry	catalyst	catalyst loading	**2-30**	dr	yield
1	$Cu(OTf)_2$	0.3 equiv.	1.0 equiv.	>20:1	65%
2	$Cu(OTf)_2$	0.3 equiv.	2.0 equiv.	>20:1	45%

Additionally, treatment of Michael acceptor **2-116** and donor **2-30** with $Cu(OTf)_2$ (0.3 equiv.) under *neat* conditions for 120 h gave adduct **2-117** in 11% yield (Figure II.20). Although this Michael product would avoid difficulty associated with the annulation steps and lead to aldol products like **2-118**, its low reactivity in the Cu(II)-Michael process meant that the double aldol condensation remained the favorable option.

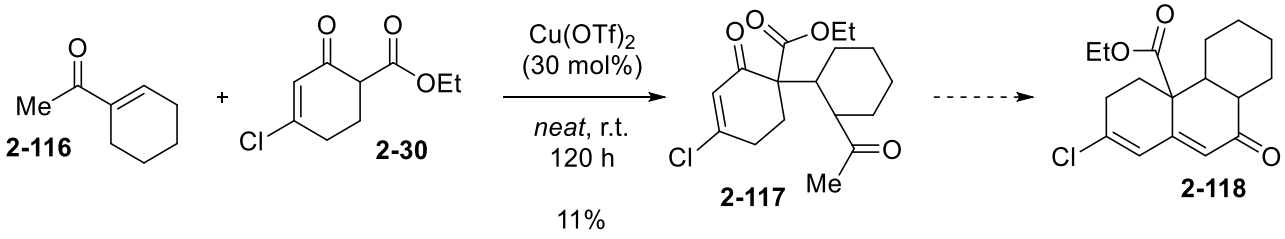

Figure II.20 Screening of Michael acceptor **2-116**.

Subsequently, aldol condensation of adduct **2-31** leading to **2-119** was screened using several acidic dehydrating conditions (Table II.2). The use of dry *p*-TSA versus the monohydrate was not found to affect the reaction outcome when a Dean-Stark trap for the azeotropic removal of water was in use (entries 1, 2). Extending the reaction time from 6 h up to 30 h appeared to show a buildup of condensed product over time (45–68% yield) (entries 3–6). If this condition was

performed at a lower temperature, such as during refluxing in THF rather than PhMe, the reaction was not observed to proceed (entry 7). An analogous soft enolization approach led to the treatment of adduct **2-31** to stoichiometric quantities of Lewis acid and excess TEA in DCM with $TiCl_4$ (44% yield), $SnCl_4$ (64% yield), or Bu_2BOTf (9% yield) (entries 8–10). Is the aldol reaction of adduct **2-31** was attempted with an excess of either NaOEt or NaO*t*-Bu in THF each led to less than 1% isolated yield of the intended bicyclic product **2-118** (entries 11–12). In addition to the observed reaction dynamics, two diastereomeric products consistently emerged following the acidic, annulative process. The erosion of product diastereoselectivity was consistently observed when cyclization of an adducts derived from donor **2-30** were attempted in acidic media.

Table II.2 Aldol condensation screening of adduct **2-31**.

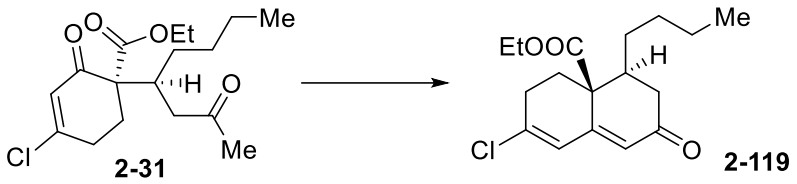

entry	activator	solvent	temperature	time	dr	yield
1	*p*-TSA (0.3 equiv.)	PhMe	reflux*	3 h	1.3:1	46%
2	*p*-TSA·H_2O (0.3 equiv.)	PhMe	reflux*	3 h	1.3:1	45%
3	*p*-TSA (0.3 equiv.)	PhMe	reflux*	6 h	1.3:1	48%
4	*p*-TSA (0.3 equiv.)	PhMe	reflux*	12 h	1.6:1	51%
5	*p*-TSA (0.3 equiv.)	PhMe	reflux*	30 h	1.8:1	46%
7	*p*-TSA (0.3 equiv.)	PhH	reflux*	24 h	1.2:1	45%
8	*p*-TSA (0.3 equiv.)	THF	reflux	24 h	--	no reaction
9	$TiCl_4$ (1.0 equiv.), TEA (2.0 equiv.)	DCM	0 °C → r.t.	16 h	2.3:1	44%
10	$SnCl_4$ (1.0 equiv.), TEA (2.0 equiv.)	DCM	0 °C → r.t.	16 h	2.9:1	64%
11	Bu_2BOTf (1.0 equiv.), TEA (2.0 equiv.)	DCM	0 °C → r.t.	16 h	1.1:1	9%
12	NaOEt (5.0 equiv.)	THF	r.t.	16 h	--	<1%
13	NaO*t*-Bu (5.0 equiv.)	THF	r.t.	16 h	--	<1%

*Azeotropic removal of water was accomplished using a Dean-Stark trap.

Although loss of diastereoselectivity was neither anticipated nor fully understood in its mechanism, a ring opening event of bicycle **2-119** was envisioned as proceeding through a tautomerization event to **2-120** and an electrocyclic ring-opening process that may open to alkene

2-121 (Figure II.21). Although this ring-opening event would explain a loss in enantioselectivity, a loss in diastereoselectivity would be achieved by an acid-mediated alkene isomerization event from intermediate **2-121** to **2-122**. The reversal of this process leading to ring closure and reformation of material **2-119**, may provide the observed loss in diastereoselectivity. The vinyl chloride moiety may play some role in the unanticipated reaction dynamics as electronic effects caused by variable donors or acceptors can shift the observed outcomes of sigmatropic processes.[131]

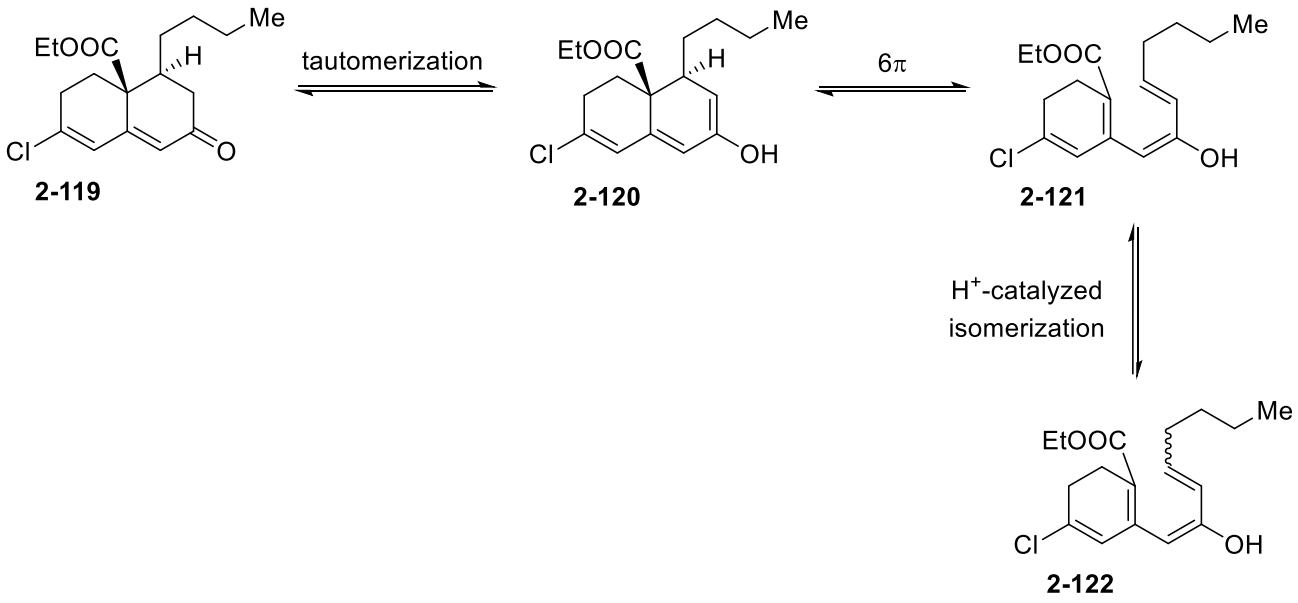

Figure II.21 Hypothesized mechanism for loss of diastereoenrichment in **2-118**.

Despite the observed loss of diastereoselectivity, we opted to test the possibility of combining the Michael reaction with a tandem aldol cyclization based on the strategy previously applied for steroidal synthesis (Figures II.6–9). To test the capability of a tandem Michael-aldol-aldol process implementing donor **2-30** in a facile operation, aldehyde **2-130** was prepared to function as a Michael acceptor in the copper-catalyst addition process (Figure II.22). Thus, halide **2-125** was synthesized in 61% yield via ruthenium cross-coupling with Grubbs 2nd generation catalyst (**1-**

141) from bromoalkene **2-123** and silyl ether **2-124** in DCM. Then, ester **2-126** was added to halide **2-125** via an enolate addition to generate adduct **2-127** in 76% yield. Ester **2-127** was then reduced using LAH to the corresponding primary alcohol **2-128** in 98% yield. The silyl ether moiety of **2-128** was deprotected using TBAF in THF to reveal an allylic alcohol **2-129** in 81% yield. The diol **2-129** underwent successful bis-oxidation using Dess-Martin conditions and afford aldehyde **2-130** in 88% yield.

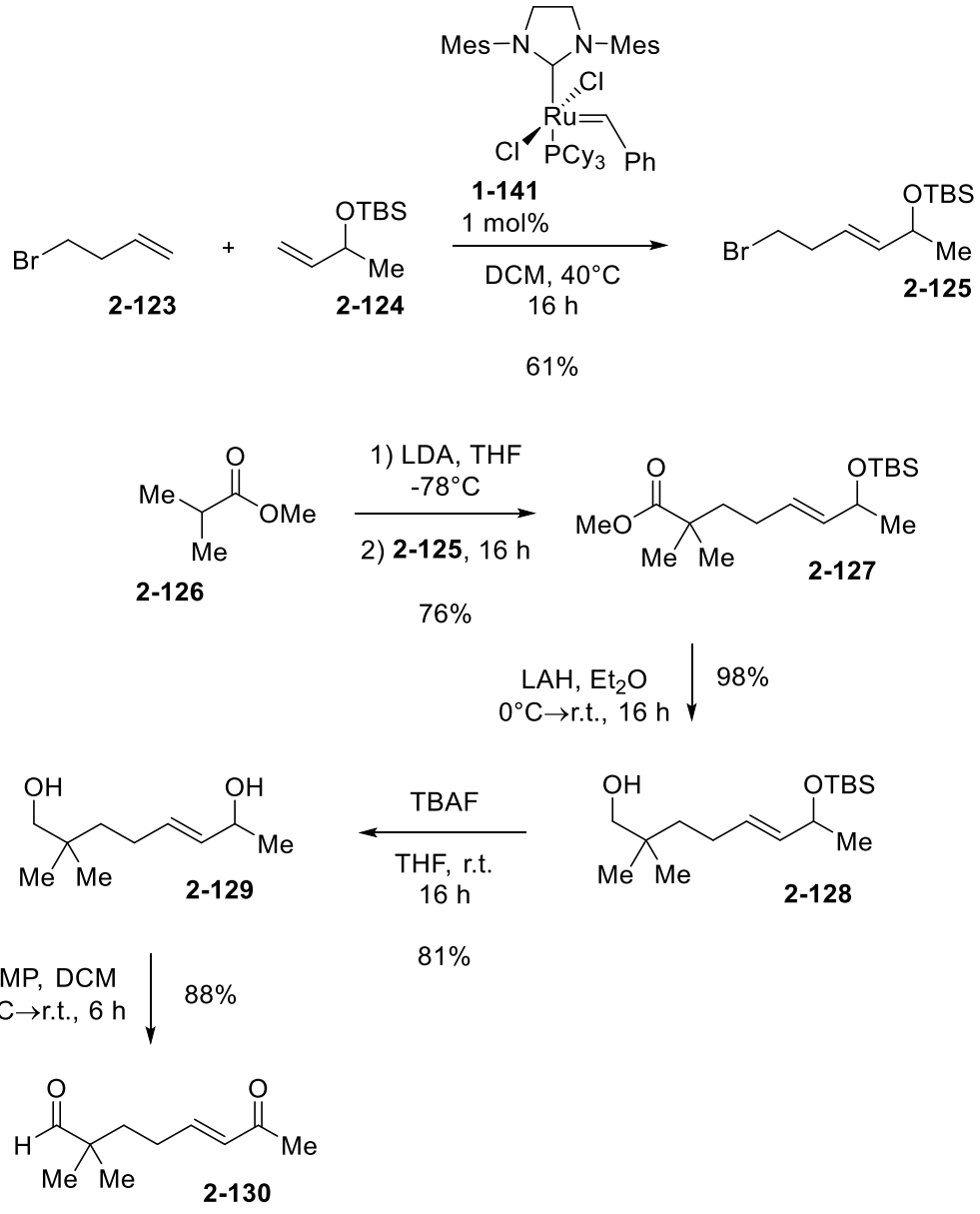

Figure II.22 Synthesis of Michael acceptor **2-130**.

Following the successful synthesis of **2-130**, its coupling with keto-ester **2-30** was investigated (Figure II.23). Reactivity of acceptor **2-130** and donor **2-30** in the presence of $Cu(OTf)_2$ (0.3 equiv.) to form intermediate **2-131**, followed by dehydrating conditions of catalytic *p*-TSA (0.3 equiv.) in refluxing PhMe, equipped with a Dean-Stark trap for the azeotropic removal of water, gave tricyclized product **2-133** in 15% and 2:1 dr via intermediate **2-132**.

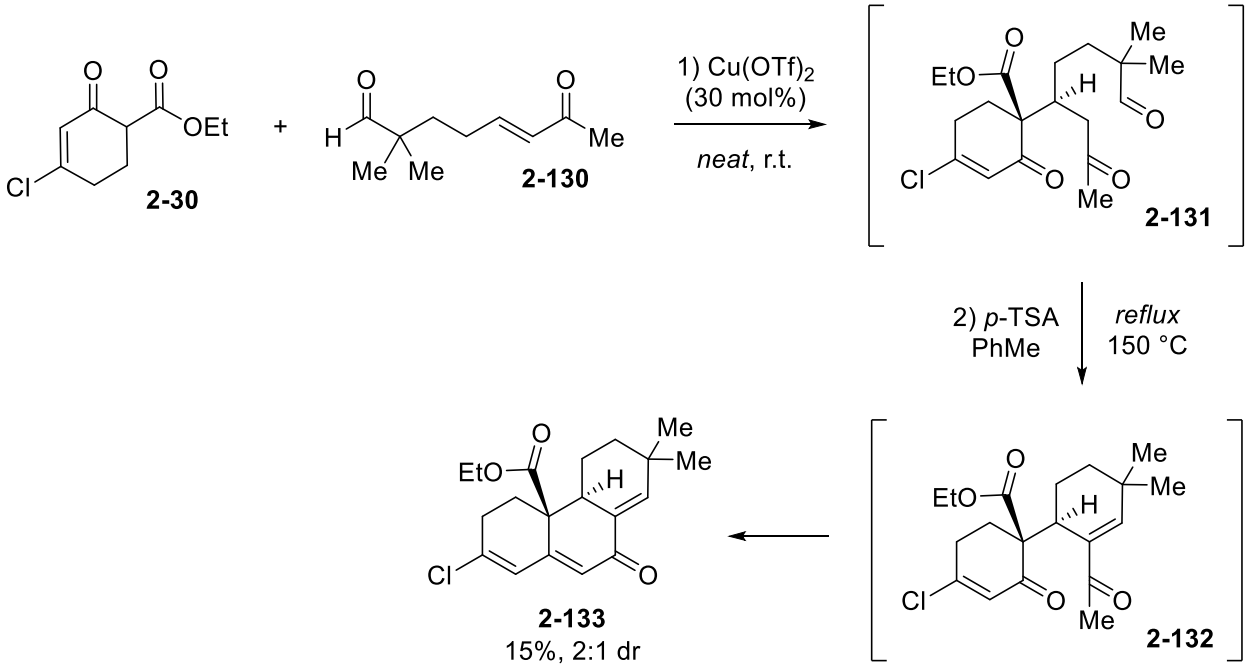

Figure II.23 Screening of Michael-aldol reaction implementing donor **2-30** acceptor **2-130**.

To improve annulation yields leading to **2-133**, a stepwise strategy was investigated (Figure II.24). By utilizing Michael acceptors bearing variable protecting groups, **2-134**, we intended to better control the reactivity of the Michael/aldol process. Donor **2-30** and protected acceptor **2-134** can be reacted using the Cu(II)-Michael reactivity to yield adduct **2-135**. The first aldol condensation of adduct **2-135** would provide bicycle **2-136** which would then be deprotected to reveal alcohol **2-137**. An oxidation of alcohol **2-137** using Dess-Martin conditions would generate

aldehyde **2-138** that is then ready for the subsequent aldol condensation leading to the desired intermediate, **2-133**.

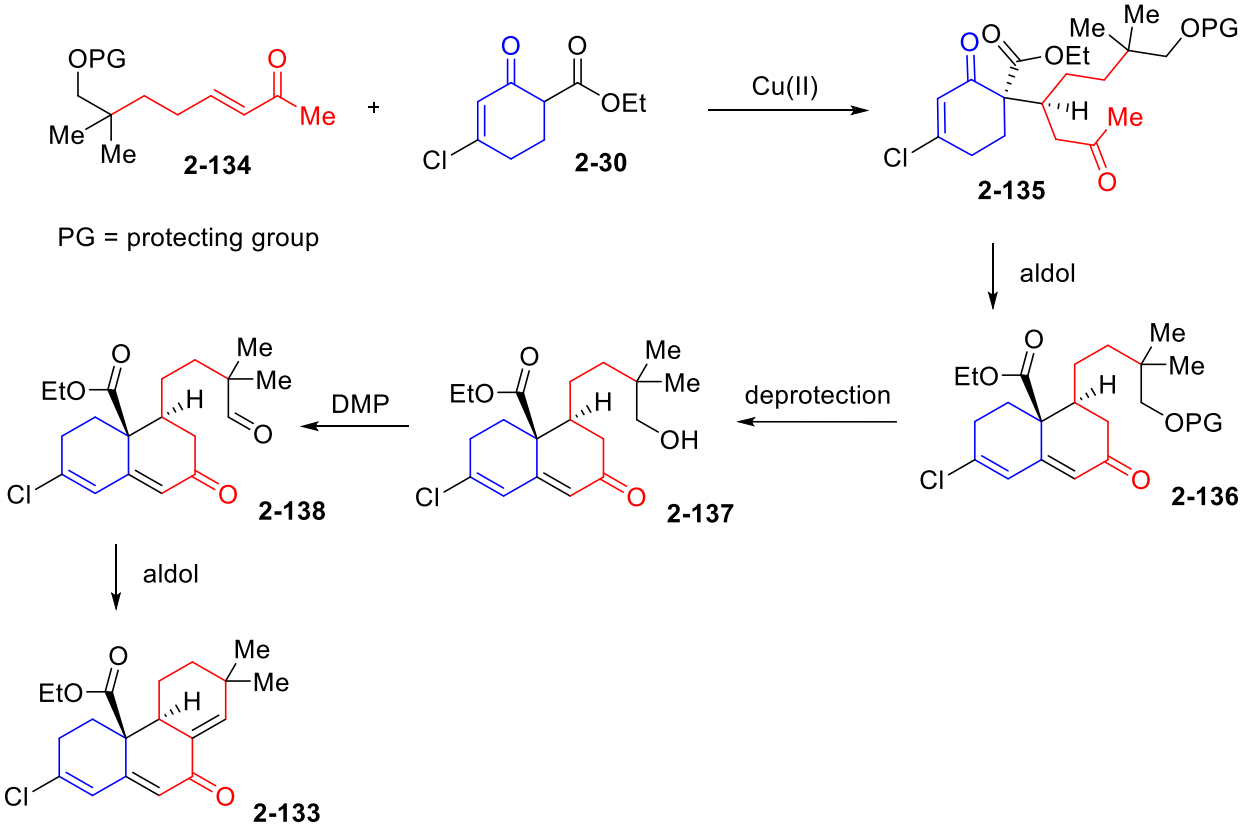

Figure II.24 Proposed stepwise synthesis leading to key scaffold **2-133**.

A benzoate-protected analogue was the first to be investigated for this process (Figure II.25). Thus, alcohol **2-139** was accessed from known[132] starting materials and transformed into benzoate **2-140** in 85% yield using acylating conditions with pyridine and BzCl. Michael acceptor **2-142** was then synthesized in 93% yield via cross-metathesis with Grubbs 2nd generation catalyst (**1-141**) from ketone **2-141** and ester **2-140**. Treatment of Michael acceptor **2-142** and donor **2-30** with $Cu(OTf)_2$ (0.3 equiv.) under *neat* conditions gave adduct **2-143** in 83% yield and >20:1 dr. Aldol condensation conditions of catalytic *p*-TSA (0.3 equiv.) in refluxing PhMe, equipped with a Dean-Stark trap for the azeotropic removal of water, gave cyclized product **2-144** in 57% and

2:1 dr from **2-143**, continuing the observed loss of diastereoenrichment when utilizing donor **2-30**. If solvolysis of **2-143** using either acidic or basic conditions was attempted, no deprotected product **2-145** or desired aldol adducts were observed.

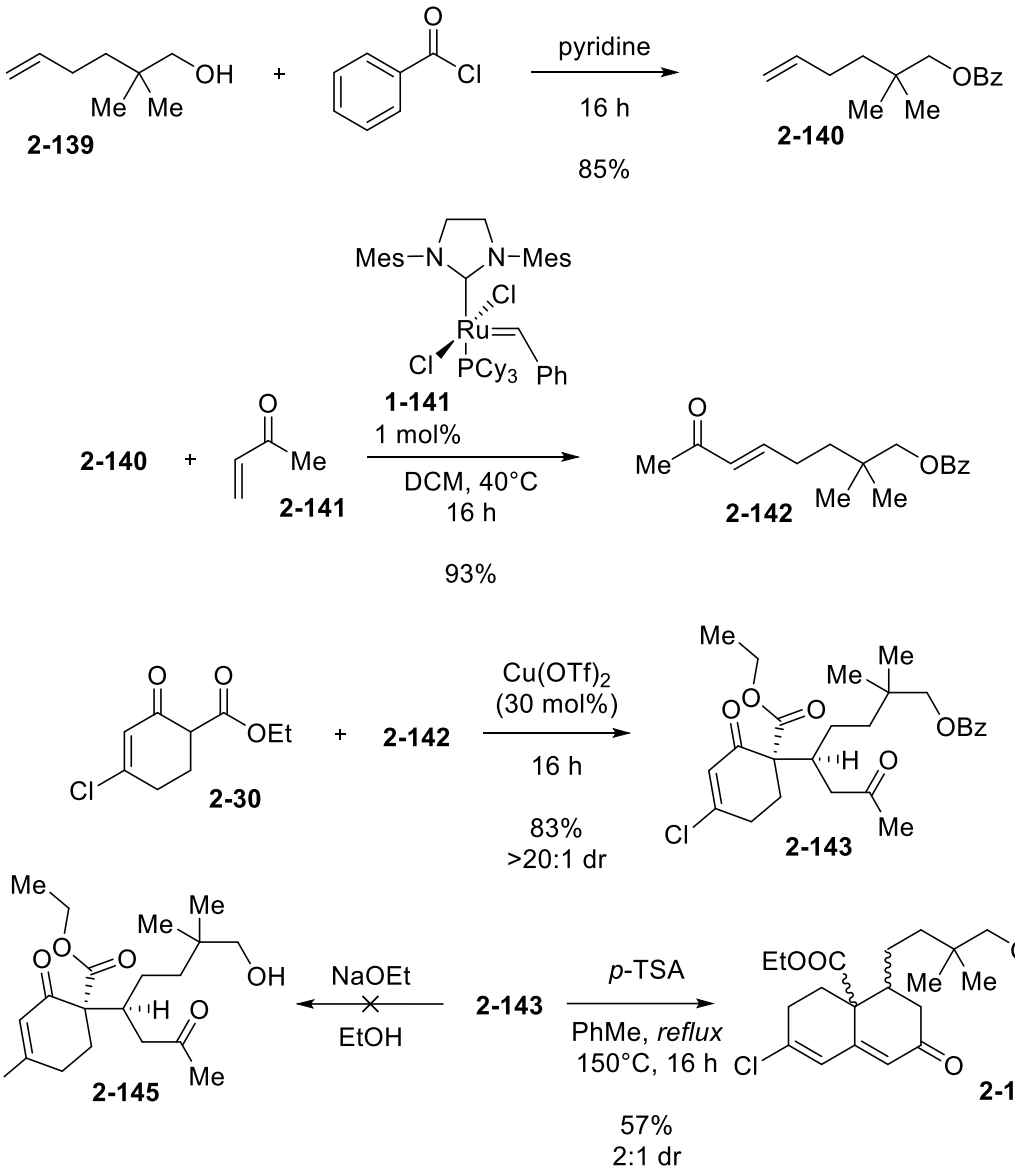

Figure II.25 Synthesis and reactivity of acceptor **2-142**.

To address the challenges associated with the benzoate group, alternative protecting groups were investigated (Figure II.26). Thus, alcohol **2-139** was transformed into silyl ether **2-146** in

84% yield using silylating conditions of ImH and TIPSCl in DCM. Michael acceptor **2-147** was then synthesized in 57% yield via cross-metathesis with Grubbs 2nd generation catalyst (**1-141**) from ketone **2-141** and silyl ether **2-146**. Treatment of Michael acceptor **2-147** and donor **2-30** with $Cu(OTf)_2$ (0.3 equiv.) under *neat* conditions gave adduct **2-148** in 66% yield and >20:1 dr.

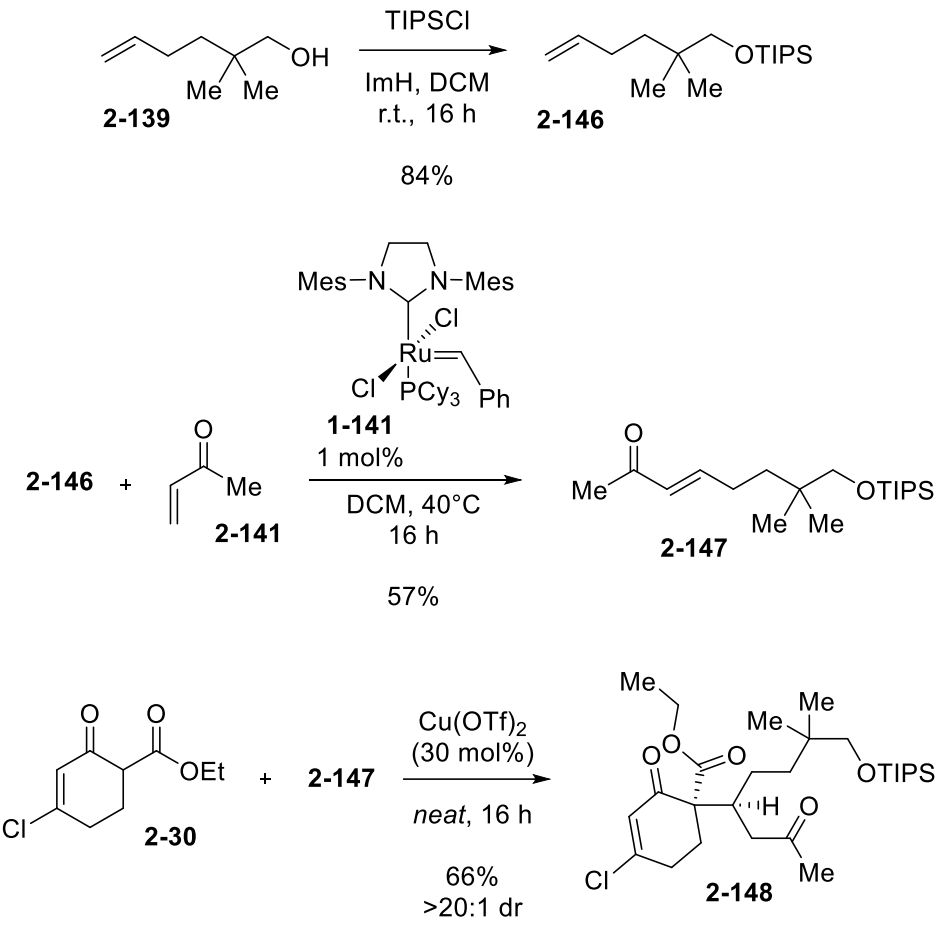

Figure II.26 Synthesis and reactivity of acceptor **2-147**.

Following the synthesis of Michael adduct **2-148**, an attempt to deprotect its silyl ether protecting group using TBAF led to the intended deprotection, but also led to a shift in the ^1H NMR spectra that appears to correspond with a rigid carbocyclic scaffold with new and highly diverse proton coupling patterns (Figure II.27). Spectral investigation supported the tentative

assignment of product **2-151** as a bridged bicycle arising from the formation of a vinylogous enolate **2-149** before undergoing an intramolecular γ-aldol addition step with the proximal ketone to provide intermediate **2-150** that can be protonated to the product. Thus, **2-151** was formed from **2-148** in the presence of TBAF (4.4 equiv.) and THF in 51% yield.

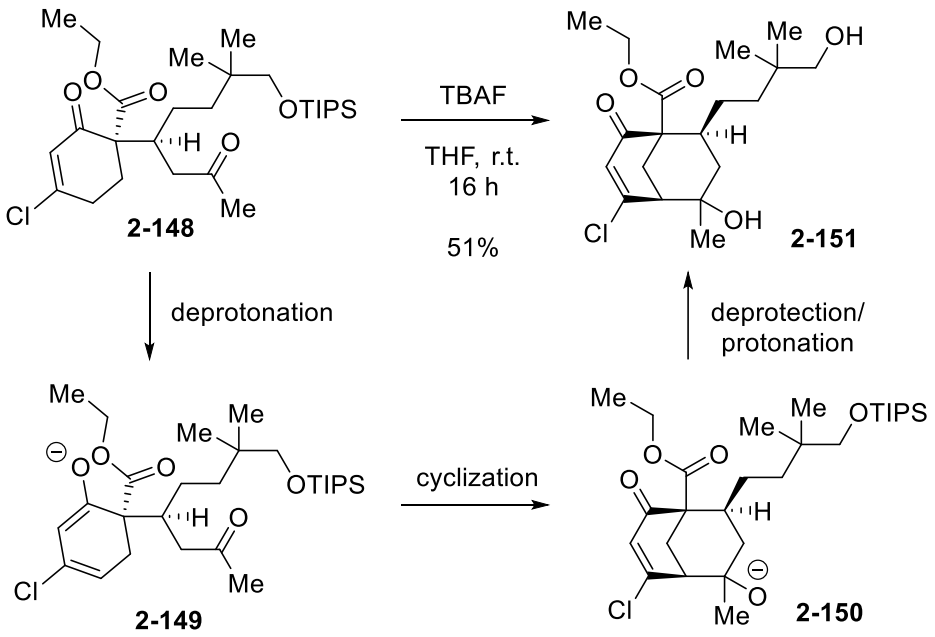

Figure II.27 Pathway leading to the formation of **2-151**.

To form a substrate with a more readily cleavable protecting group, methoxyacetate was investigated as a more sensitive protecting group for the primary alcohol moiety (Figure II.28). Methoxyacetate is known to allow for its orthogonal deprotection by solvolysis, including in the presence of other esters,[133] and has been previously implemented in the Nagorny Group during the synthesis of the cardiotonic steroid cannogenol (**2-46**) (Figure II.9).[101] Then, alcohol **2-139** was transformed into ester **2-152** in 96% yield using acylating conditions of pyridine and $O(MAc)_2$. Michael acceptor **2-153** was then synthesized in 79% yield via cross-metathesis with Grubbs 2nd generation catalyst (**1-141**) from ketone **2-141** and ester **2-152**.

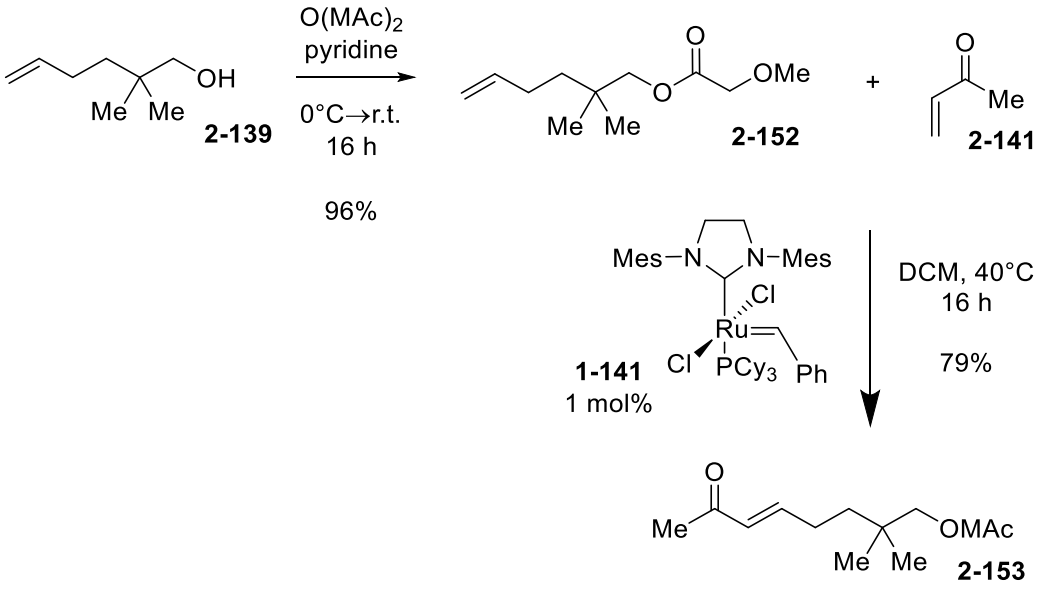

Figure II.28 Synthesis of Michael acceptor **2-153**.

When acceptor **2-153** and donor **2-22** were utilized in the Cu(II)-Michael reaction with $Cu(OTf)_2$ (0.3 equiv.) under *neat* conditions, adduct **2-154** was isolated in 84% yield and 3.7:1 dr (Figure II.29). When the Cu(II)-Michael process was attempted with acceptor **2-153** and donor **2-30** with $Cu(OTf)_2$ (0.3 equiv.) catalyst under *neat* conditions, adduct **2-155** was isolated in 79% yield and >20:1 dr.

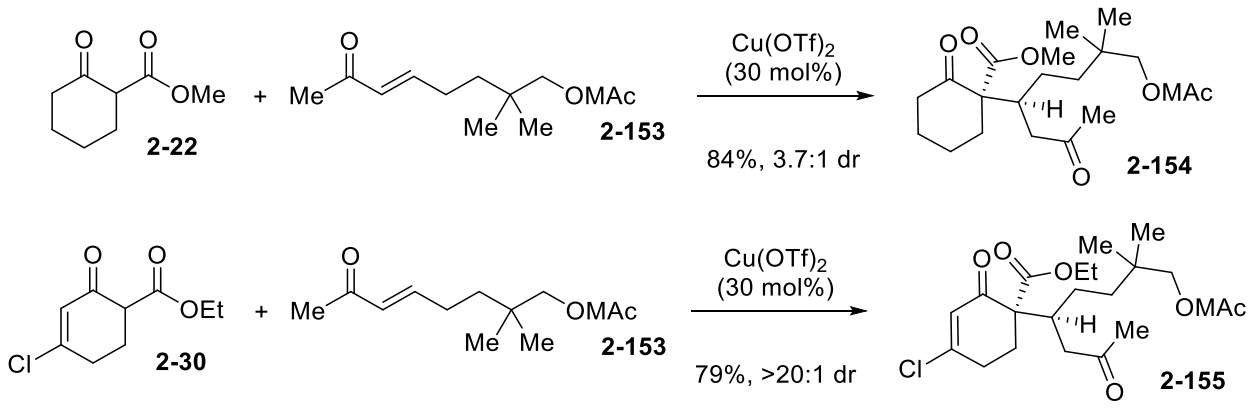

Figure II.29 Screening of Michael reaction implementing acceptor **2-153**.

When methoxyacetate moiety of Michael intermediate **2-155** was subjected to deprotection using (7N) ammonia in MeOH, side-product **2-156** resulting from an intramolecular γ-aldol addition was generated in 12% yield (Figure II.30). The methoxyacetate group of **2-156** was then subjected to lithium hydroxide (5.0 equiv.) in 2:1 THF:MeOH resulting in side-product **2-157** resulting from the intramolecular γ-aldol reaction and displacement of the chloro group for a methoxy group in 33% yield. The same methoxy-substituted side-product **2-157** was isolated in 22% yield when the deprotection of **2-155** was attempted using $Yb(OTf)_3$ (0.3 equiv.) in MeOH. Finally, an attempt to remove the methoxyacetate protecting group of adduct **2-155** using lithium phenylthiolate (3.0 equiv.) (prepared immediately prior to use from thiophenol and *n*-BuLi) at –78 °C resulted in a mixture of deprotected adducts **2-158** and **2-159** in 23% and 50% yield, respectively.

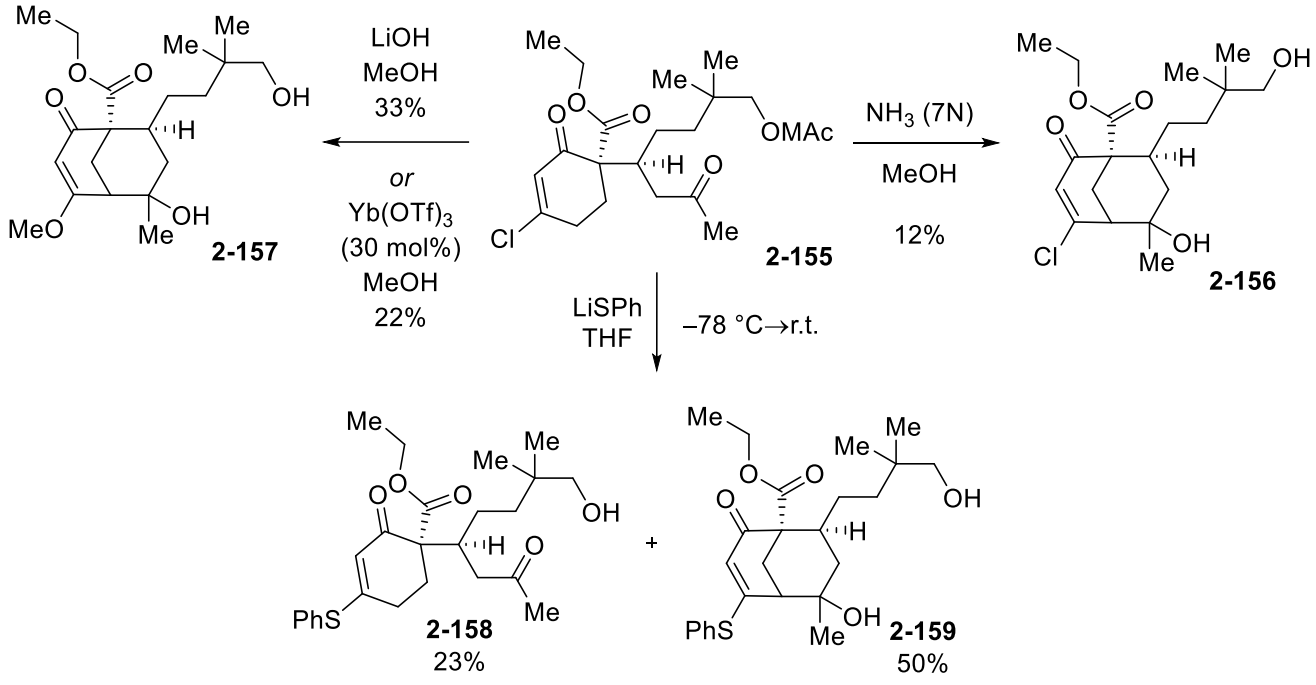

Figure II.30 Deprotection approaches of adduct **2-155**.

Considering that both basic and Lewis acidic conditions for the deprotection of the methoxyacetate group resulted in significant side-reactions, deprotection under reductive conditions was examined next (Figure II.31). When Michael adduct **2-155** was subjected to reduction with DIBALH (2.0 equiv.) in DCM (–78 °C to r.t.) the resulting product was found to bear an unexpected alkenyl signal, and dichlorination was observed. This was attributed to the formation of product **2-162**, resulting from a Stork-Danheiser transposition of the starting material in 76% yield. The reductive transposition is enabled by a rapid 1,2-reduction of the enone moiety of **2-155** that occurs along with the intended deprotection step, resulting in intermediate species **2-160**. A protonation event during the product isolation process may facilitate the formation cationic intermediate **2-161** before a hydrolysis event reveals the product of reductive transposition, **2-162**.

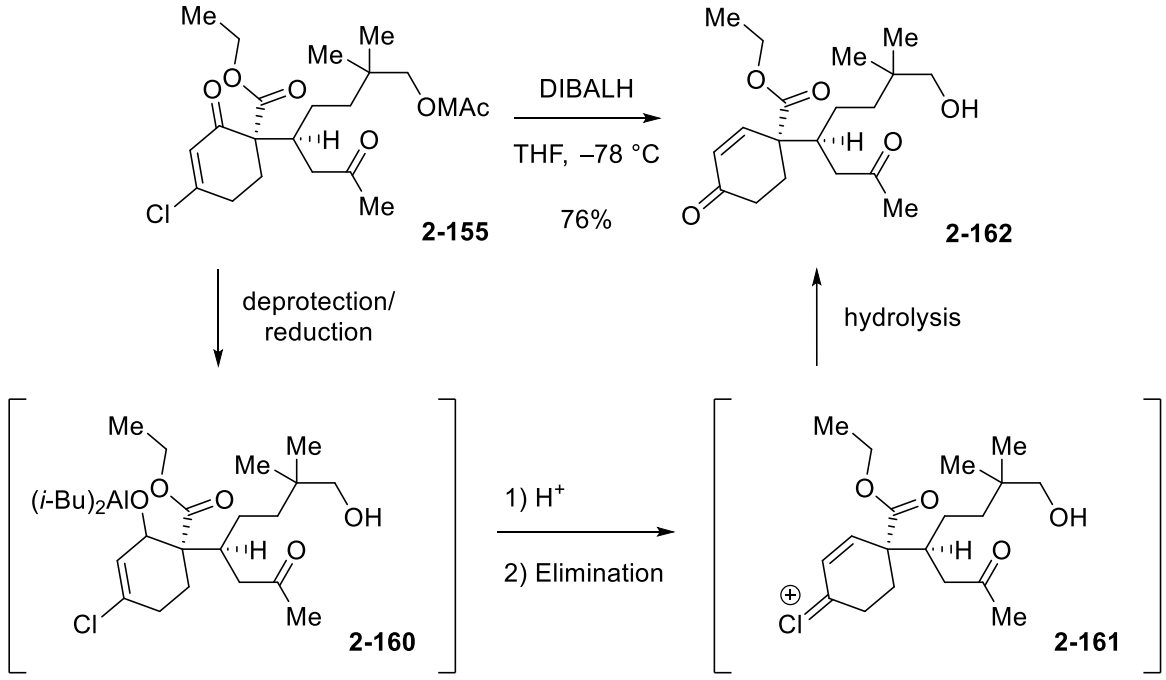

Figure II.31 Reductive transposition of adduct **2-155**.

Based on these observations, we opted to investigate the reactivity of donor **2-163**, use of which might avoid the undesired side-reactions observed for donor **2-30**. Treatment of Michael acceptor

2-153 and donor **2-163** with $Cu(OTf)_2$ (0.3 equiv.) under *neat* conditions gave adduct **2-164** in 52% yield and 3:1 dr (Figure II.32). Michael adduct **2-164** was condensed using aldol condensation with catalytic *p*-TSA (0.3 equiv.) in refluxing PhMe with a Dean-Stark trap for the azeotropic removal water gave cyclized product **2-165** in 27%. Solvolysis of **2-164** using NaOMe in MeOH gave **2-166** in 51% yield. Alcohol **2-166** was oxidized using DMP and pyridine in DCM to generate aldehyde **2-167** in 72% yield. Attempting to perform a double aldol condensation of **2-167** with catalytic *p*-TSA (0.3 equiv.) in refluxing PhMe at 110 °C with a Dean-Stark trap resulted in an unidentified side-product, and no desired tricyclic product **2-168** was observed under these conditions.

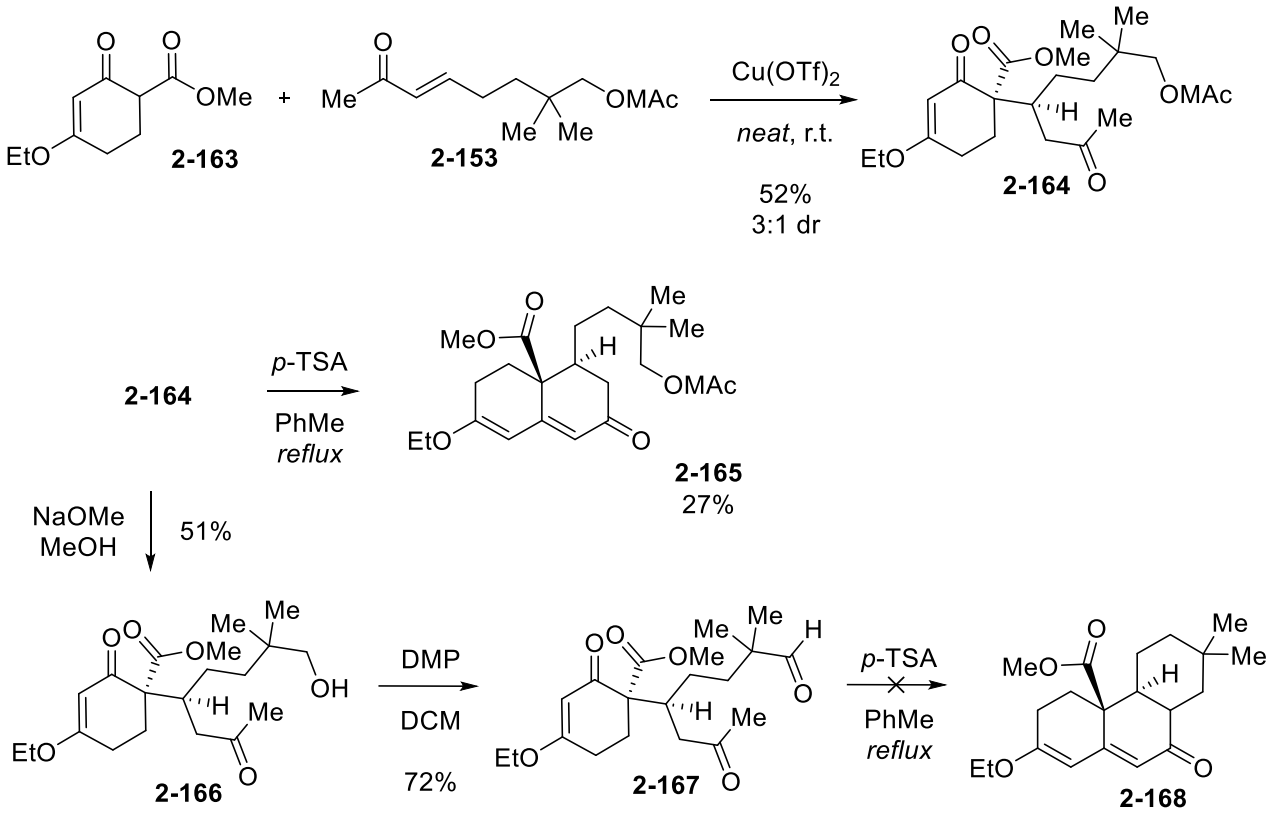

Figure II.32 Synthesis and attempted modification of adduct **2-164**.

With this observation in hand, we decided to pursue an alternative, stepwise route for the elaboration of **2-164** into the tricyclic core of aspewentin A (Figure II.33). Hydrolysis of **2-164** with aqueous HCl in THF gave **2-169** in 20% yield and **2-170** in 75% yield. Intermediate **2-170** was methylated using methyl iodide and K_2CO_3 to provide **2-171** in 41% yield. Attempts to cyclize **2-171** in *p*-TSA and refluxing PhMe at 110 °C did not provide **2-172** but only resulted in complex mixtures of decomposition products.

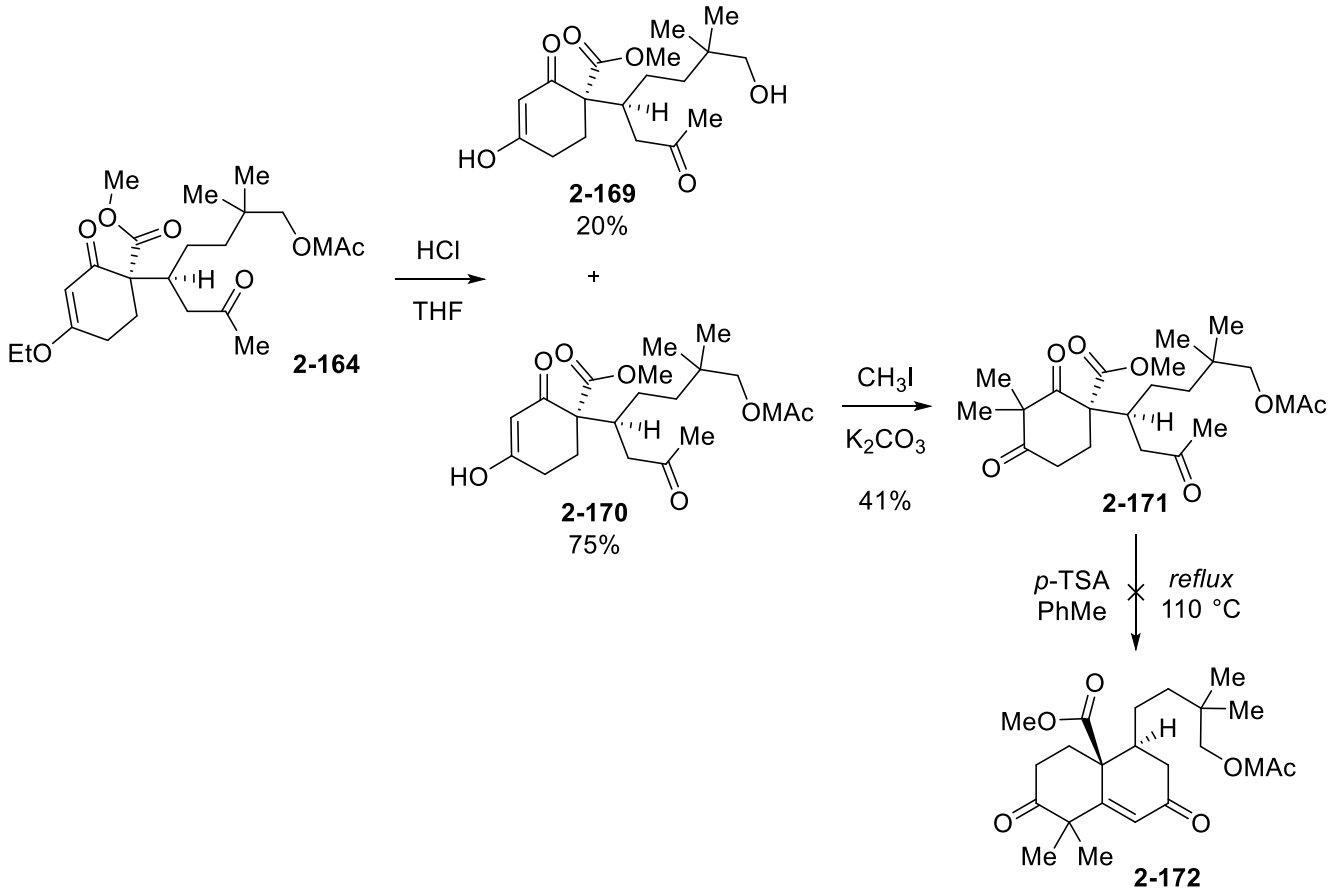

Figure II.33 Continued chemical modification of adduct **2-164**.

In addition to the enone Michael donors, **2-30** and **2-163**, we investigated the possibility of employing donor **2-174** (Figure II.34). Ester **2-174** was synthesized by treatment of bromoalkene **2-173** with LiHMDS in THF and then methyl cyanoformate (Mander's reagent) in 50% yield.

Then, acceptor **2-28** and donor **2-174** with $Cu(OTf)_2$ (0.3 equiv.) under *neat* conditions have crude adduct **2-175** that was exposed to catalytic *p*-TSA (0.3 equiv.) in refluxing PhMe at 110 °C with a Dean-Stark trap for the azeotropic removal of water to provide bridged bicycle **2-176** by a second intramolecular conjugate addition when refluxed in PhMe and *p*-TSA.

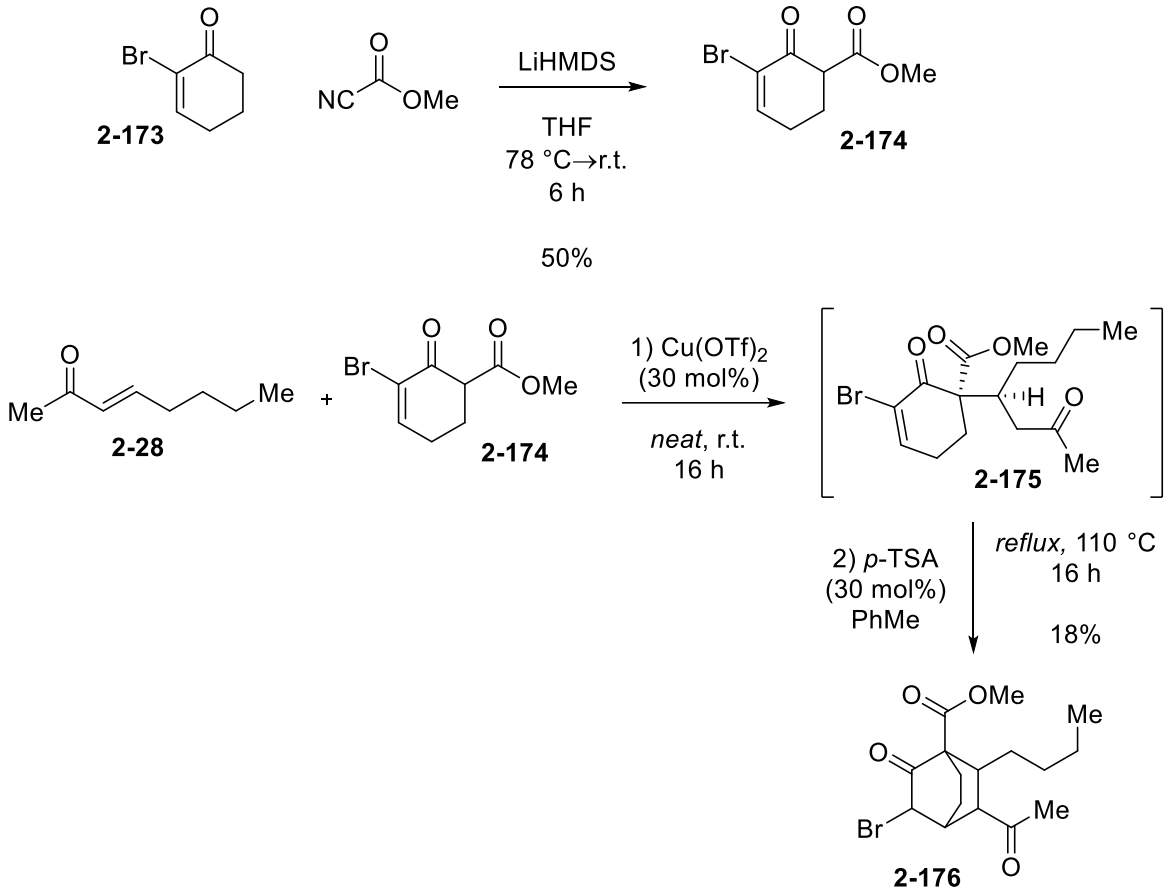

Figure II.34 Observed reactivity of donor **2-174**.

These studies on the reactivity of unsaturated keto-ester donors like **2-30**, **2-163**, or **2-174** find that despite their promising reactivity in the Cu(II)-Michael process, their adduct products are liable to undertake various intramolecular coupling pathways which are not conducive to forming the intended cyclization patterns associated with the isopimarane skeleton. Thus, a second-generation retrosynthetic analysis of (±)-aspewentin A (**(±)-1-16**) implementing less

functionalized donor **2-22** was envisioned as requiring the use of an oxidation step to assist in a subsequent functionalization (Figure II.35). Thus, (±)-aspewentin A (**(±)-1-16**) is formed through a *gem*-dimethylation step of ketone **2-177** and is itself accessible by decarboxylative aromatization of the tricyclic dione **2-178.** Dione **2-178** is accessible via allylic oxidation of intermediate **2-25**, which can be directly furnished from the Michael/aldol process if donor **2-22** and acceptor **2-21** are successfully implemented in the proposed reaction cascade.

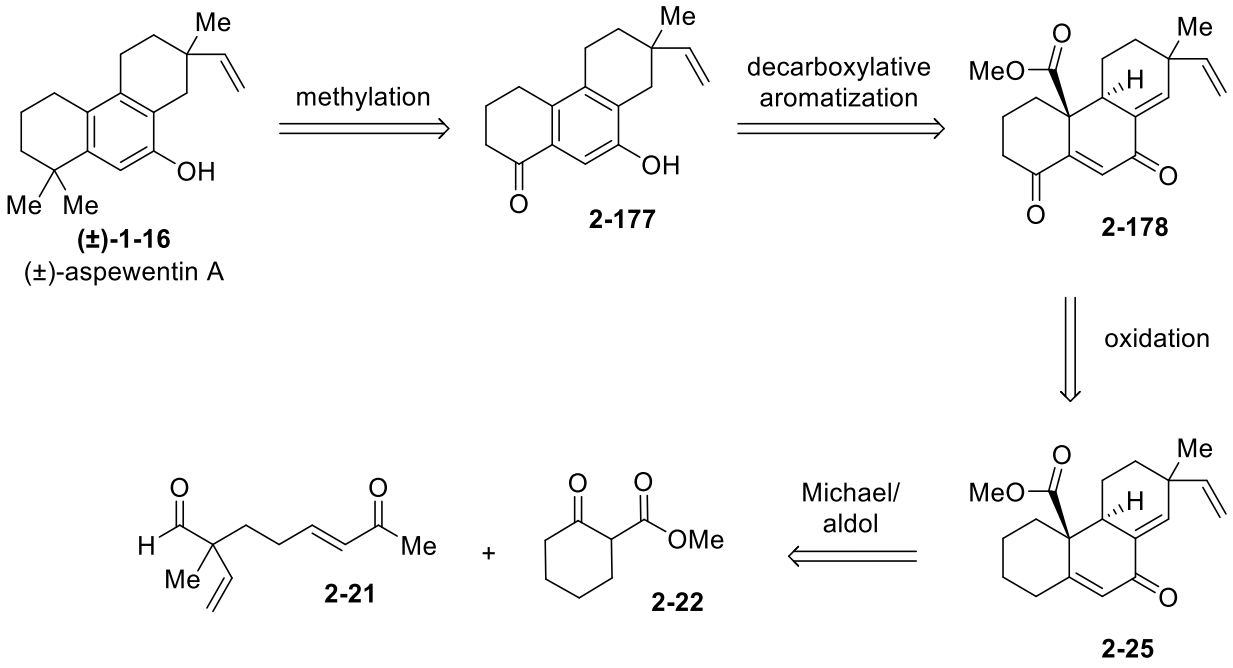

Figure II.35 Second-generation retrosynthetic analysis of (±)-aspewentin A (**(±)-1-16**).

To investigate the proposal depicted in Figure II.35, we first studied the Michael-aldol process implementing model aldehyde **2-130** in lieu of **2-21** (Figure II.36). Donor **2-22** and acceptor **2-130** were reacted using the Cu(II)-Michael process with $Cu(OTf)_2$ (0.3 equiv.) under *neat* conditions to form **2-179**, and the resulting crude was exposed to catalytic *p*-TSA (0.3 equiv.) in refluxing PhMe at 110 °C with a Dean-Stark trap for the azeotropic removal of water and proceeds via aldol intermediate **2-180** to yield carbocycle **2-181** in 46% yield and 4:1 dr.

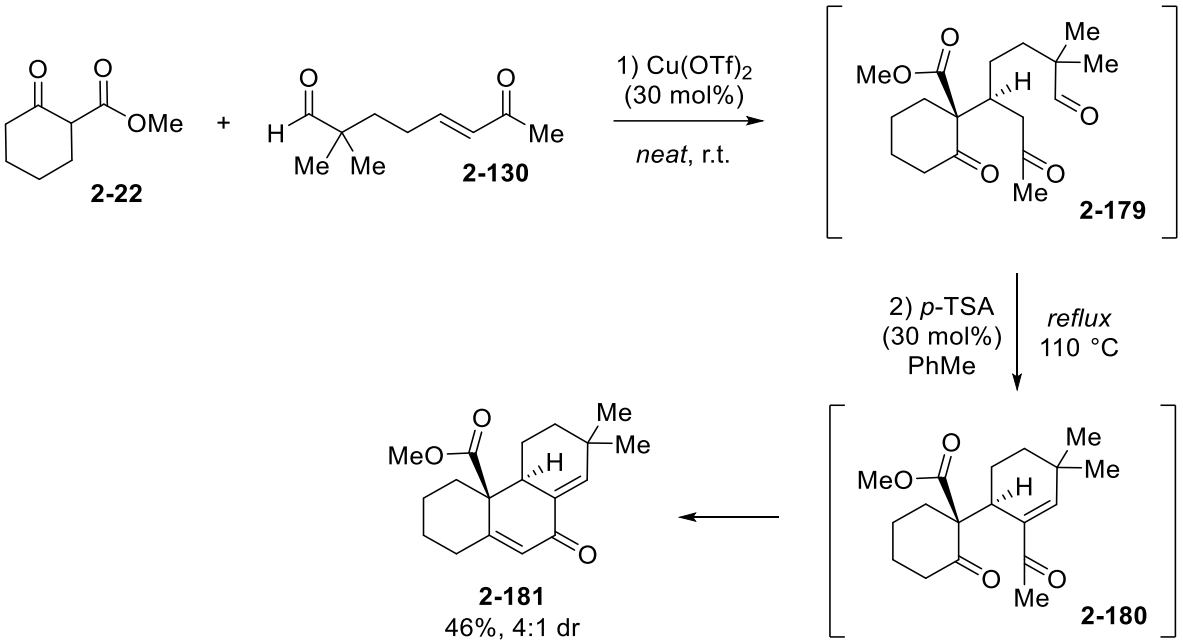

Figure II.36 Synthesis of model tricycle **2-181**.

With the tricyclic substrate **2-181** in hand, we then focused on the allylic oxidation of the enone moiety implementing a previously developed $Rh_2(cap)_4$-based oxidation.[134,135] The studies summarizing the oxidation of scaffold **2-181** using $Rh_2(cap)_4$ and T-HYDRO under various conditions leading to **2-183** are provided in Table II.3. During the oxidation process, starting material **2-181** was found to have undergone an acid-mediated 1,3-hydrogen shift via intermediate **2-182**, leading to the more substituted alkenyl product isomer corresponding to the observed **2-183**. This alkenyl rearrangement was expected to further facilitate a subsequent decarboxylative aromatization process via an increased inductive effect. However, when substrate **2-181** was oxidized with $Rh_2(cap)_4$ (0.01 equiv.) and T-HYDRO (8 equiv.) in DCE at 40 °C for 24 h, we first observed a degradation product **2-184** corresponding to alkene isomerization and overoxidation (entry 1). However, if substrate **2-181** was stirred at room temperature and using less reagent loading (T-HYDRO (4 equiv.)) in DCE for 24 h, product **2-183** in observed in 28% yield (entry 2). This yield was increased to 41% yield if T-HYDRO loading was again increased to 8 equiv.

while remaining at room temperature (entry 3). The addition of catalytic quantities of K_2CO_3 (0.5 equiv.) diminished the reaction yield to 28% (entry 4). If the reaction time was doubled and the catalyst was recharged at the halfway point, product **2-183** was isolated in 65% yield in DCE (entry 5) and 45% yield in H_2O (entry 6).

Table II.3 Rhodium-mediated oxidation studies of **2-181**.

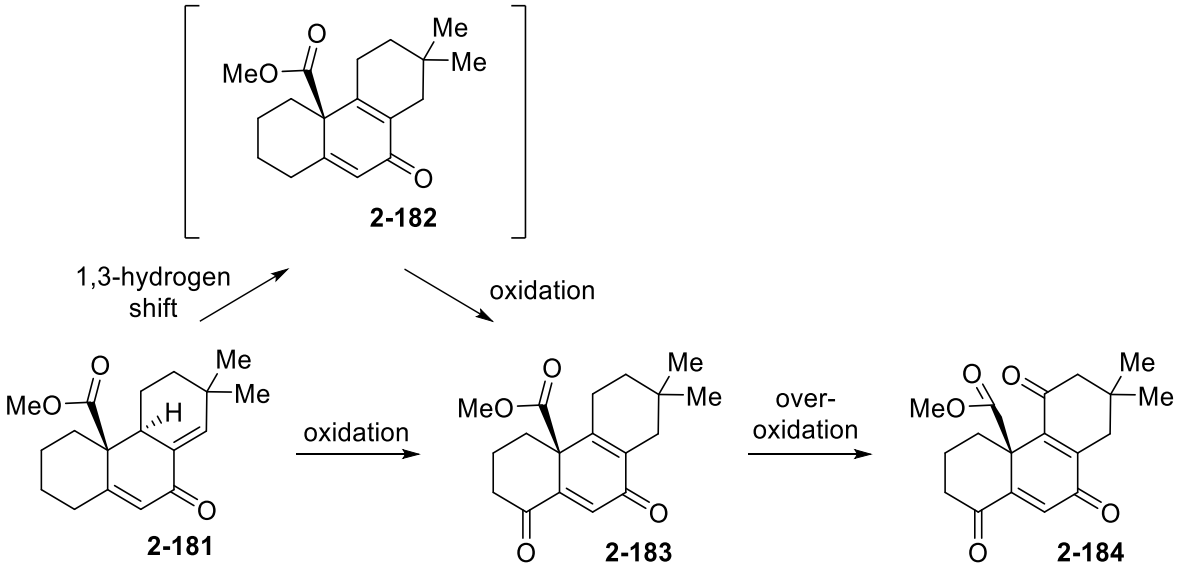

Entry	Catalyst	Reagent	Solvent	Temperature	Time	Yield **2-183**
1	$Rh_2(cap)_4$ (0.01 equiv.)	T-HYDRO (8 equiv.)	DCE	40 °C	24 h	overoxidation observed
2	$Rh_2(cap)_4$ (0.01 equiv.)	T-HYDRO (4 equiv.)	DCE	r.t.	24 h	28%
3	$Rh_2(cap)_4$ (0.01 equiv.)	T-HYDRO (8 equiv.)	DCE	r.t.	24 h	41%
4	$Rh_2(cap)_4$ (0.01 equiv.)	T-HYDRO (8 equiv.), K_2CO_3 (0.5 equiv.)	DCE	r.t.	24 h	28%
5	$Rh_2(cap)_4$ (0.01 equiv.)*	T-HYDRO (8 equiv.)	DCE	r.t.	48 h	65%
6	$Rh_2(cap)_4$ (0.01 equiv.)*	T-HYDRO (8 equiv.)	H_2O	r.t.	48 h	45%

*Catalyst was recharged at 24 h, doubling overall loading shown.

The rearranged alkene geometry of dienone **2-183**, and the additional electronic demand created by the additional oxo group in conjugation to the dienone pi-system was expected to facilitate the reaction process leading to decarboxylative aromatization of this substrate. Consequently, when methyl ester **2-183** was refluxed in DMSO and excess LiCl at 180 °C, the decarboxylative aromatization pathway leading to phenol **2-189** was observed in 60% yield (Figure II.37). The reaction is expected to proceed through the formation of a carboxylate intermediate **2-185** by nucleophilic displacement of the methyl group of **2-183**. Carboxylate **2-185** is then ready for subsequent decarboxylation leading to the aromatization and formation of phenolate resonance pairs **2-186** and **2-187**. Protonation of phenolate **2-187** then provides product **2-189**. The successful formation of **2-189** validates our retrosynthetic proposal and sets a strong foundation for the completion of (±)-aspewentin A (**(±)-1-16**) described in the subsequent chapter (*vide infra*).

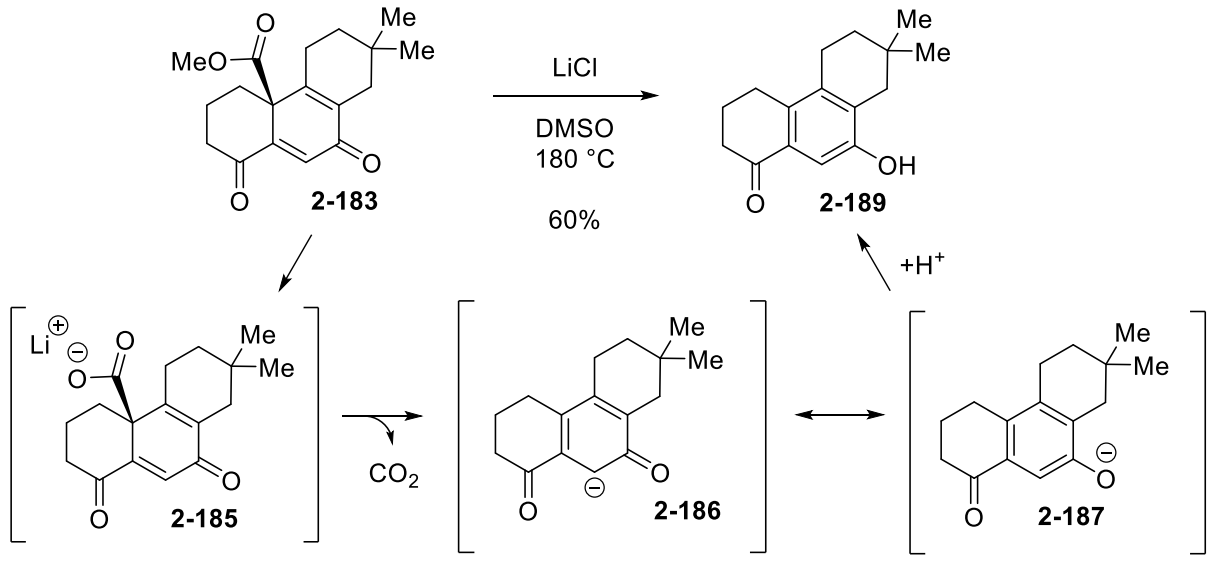

Figure II.37 Decarboxylative aromatization to phenol **2-189**.

II.7 Conclusion/Summary

In summary, this chapter summarizes our studies focused on exploring a tandem Cu(II)-Michael/aldol approach to synthetize (±)-aspewentin A (**(±)-1-16**). The intended pathway for total synthesis involves a decarboxylative aromatization pathway and has been compared to the natural biosynthetic route that is invoked for the formation of this diterpene, (±)-aspewentin A (**(±)-1-16**). The functionalized carbocycle necessary for the decarboxylative aromatization step was expected to be furnished either directly through a tandem Michael-aldol-aldol process or through an iteration of synthetic steps that would allow for the strategic carbocycle to be formed in a more controlled manner. Although the direct, tandem Michael-aldol-aldol process would be the most desirable path forward, the substrates featuring multiple (ambident) electrophilic and acidic sites might contribute to diminished efficiency for the intended process if they contribute to byproduct formation. These model studies explored several Michael acceptors and donors for this synthetic work. Although various unsaturated keto-esters were found to successfully undergo the Cu(II)-Michael event, they performed less efficiency during the aldol steps and were liable to form alternative intramolecular cyclization patterns not useful for the total synthesis of (±)-aspewentin A (**(±)-1-16**). These cyclization dynamics were unobserved during prior steroidal total syntheses that utilized similar Cu(II)-Michael donors and may be result of increased conformational flexibility in the synthons involved in synthesizing the diterpene scaffold. The attempt to utilize these donors for a stepwise pathway involving deprotection steps further revealed dynamics that facilitated the formation of undesired bridged bicyclic motifs. The synthetic pathway was then modified to allow for the use of saturated Michael donors that were expected to participate in the desired aldol pathways. However, this synthetic option necessitates the oxidation of the tricyclic intermediate so that the *gem*-dimethyl substitution pattern associated with these isopimaranes can be achieved. A solution

to the oxidation involved a $Rh_2(cap)_4$-mediated process to yield the more reactive substrate that is both suitable for subsequent methylation and decarboxylate aromatization necessary for the total synthesis of (±)-aspewentin A (**(±)-1-16**). The intended decarboxylative aromatization was successfully performed under Krapcho conditions using a model substrate which indicated that the strategy would be applicable in the synthesis of (±)-aspewentin A (**(±)-1-16**).

II.8 Graphical Summary

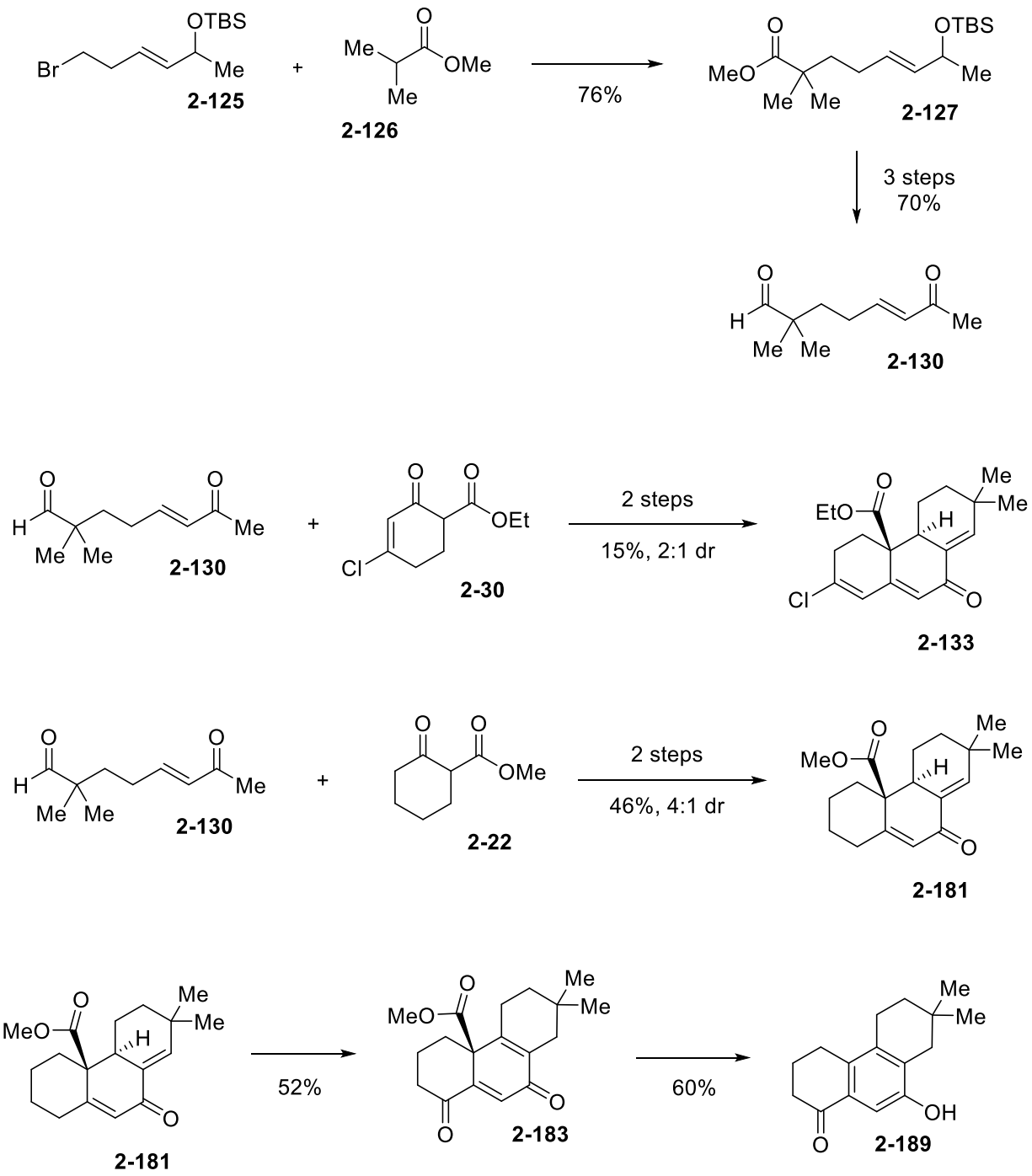

II.9 Experimental

Methods and Reagents:

Unless otherwise stated, all reagents and solvents were purchased from commercial sources and were used as received without further purification unless otherwise specified. DCM, DMF, Et_2O, THF, PhMe, were purified by Innovative Technology's Pure-Solve System using basic alumina. All reactions were carried out under a positive pressure of nitrogen in flame- or oven-dried glassware with magnetic stirring. Reactions were cooled using an external cooling bath of ice water (0 °C), sodium chloride/ice water (–20 °C), dry ice/acetonitrile (–40 °C), or dry ice/acetone (–78 °C). Heating was achieved by use of a silicone oil bath with heating controlled by an electronic contact thermometer. Deionized water was used in the preparation of all aqueous solutions and for all aqueous extractions. Solvents used for extraction and chromatography were ACS or HPLC grade. Purification of reaction mixtures was performed by flash chromatography using SiliCycle SiliaFlash P60 (230-400 mesh). Yields indicate the isolated yield of the title compound with ≥95% purity as determined by ^{1}H NMR analysis. Diastereomeric ratios were determined by ^{1}H NMR analysis. ^{1}H NMR spectra were recorded on a Varian vnmrs 700 (700 MHz), 600 (600 MHz), 500 (500 MHz), 400 (400 MHz), Varian Inova 500 (500 MHz), or a Bruker Advance Neo 500 (500 MHz) spectrometer and chemical shifts (δ) are reported in parts per million (ppm) with solvent resonance as the internal standard ($CDCl_3$ at δ 7.26, CD_3OD at δ 3.31, C_6D_6 at δ 7.16). Tabulated 1H NMR Data are reported as s = singlet, d = doublet, t = triplet, q = quartet, qn = quintet, sext = sextet, m = multiplet, ovrlp = overlap, and coupling constants in Hz. Proton-decoupled ^{13}C NMR spectra were recorded on Varian vnmrs 700 (700 MHz) spectrometer and chemical shifts (δ) are reported in ppm with solvent resonance as the internal standard ($CDCl_3$ at δ 77.06, CD_3OD at δ 49.0, C_6D_6 at δ 128.1). High resolution mass spectra (HRMS) were performed and recorded on

Micromass AutoSpec Ultima or VG (Micromass) 70-250-S Magnetic sector mass spectrometers in the University of Michigan mass spectrometry laboratory. Infrared (IR) spectra were recorded as thin films a Perkin Elmer Spectrum BX FT-IR spectrometer. Absorption peaks are reported in wavenumbers (cm^{-1}).

Instrumentation:

All spectra were recorded on Varian vnmrs 700 (700 MHz), Varian vnmrs 500 (500 MHz), Varian MR400 (400 MHz), Varian Inova 500 (500 MHz) spectrometers and chemical shifts (δ) are reported in parts per million (ppm) and referenced to the ^{1}H signal of the internal tetramethylsilane according to IUPAC recommendations. Data are reported as (br = broad, s = singlet, d = doublet, t = triplet, q = quartet, qn = quintet, sext = sextet, m = multiplet; coupling constant (*S*) in Hz; integration). High resolution mass spectra (HRMS) were recorded on MicromassAutoSpecUltima or VG (Micromass) 70-250-S Magnetic sector mass spectrometers in the University of Michigan mass spectrometry laboratory. Infrared (IR) spectra were recorded as thin films on NaCl plates on a Perkin Elmer Spectrum BX FT-IR spectrometer. Absorption peaks were reported in wavenumbers (cm^{-1}).

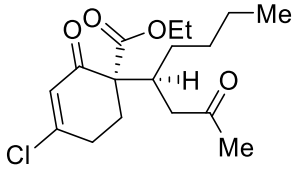

Ethyl (*S*)-4-chloro-2-oxo-1-((*S*)-2-oxooctan-4-yl)cyclohex-3-ene-1-carboxylate (2-31): A flame-dried round-bottom flask was charged with compound **2-30** (1.00 g, 4.94 mmol, 1.0 equiv.) and compound **2-28** (0.62 g, 4.94 mmol, 1.0 equiv.). The round bottom flask was then transferred

to a glovebox and $Cu(OTf)_2$ (0.55 g, 1.48 mol, 0.3 equiv.) was added to the mixture and the contents were removed from the glovebox and left to stir at room temperature under *neat* conditions for 16 h. The crude material was purified by column chromatography with 10% to 33% EtOAc/hexanes. (1.06 g, 3.23 mmol, 65%, >20:1 dr).

^{1}H NMR (500 MHz, $CDCl_3$) δ 6.20 (d, J = 2.3 Hz, 1H), 4.17 – 4.11 (m, 1H), 4.11 – 4.04 (m, 1H), 2.93 (t, J = 5.7 Hz, 1H), 2.83 (dddd, J = 19.3, 10.0, 5.2, 2.3 Hz, 1H), 2.61 (dd, J = 18.2, 5.8 Hz, 2H), 2.40 (ddd, J = 13.8, 5.1, 3.7 Hz, 1H), 2.34 (dd, J = 18.2, 5.0 Hz, 1H), 2.11 (s, 3H), 2.07 – 1.99 (m, 2H), 1.26 – 1.21 (m, 7H), 0.85 (t, J = 7.0 Hz, 3H).

HRMS (ESI-TOF) $[M+Na]^+$ m/z: calcd for $C_{17}H_{25}ClO_4$ 351.1339; Found 351.1335.

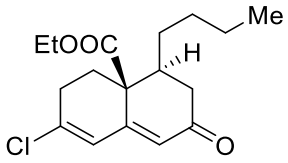

Ethyl (4*S*,4a*S*)-4-butyl-7-chloro-2-oxo-3,4,5,6-tetrahydronaphthalene-4a(2*H*)-carboxylate (2-118): Compound **2-31** (50 mg, 0.15 mmol, 1.0 equiv.) was loaded into a round-bottom flask and dissolved in toluene (2 mL) and then *p*-TSA (0.01 mg, 0.05 mmol, 0.3 equiv.) was added. The reaction flask was equipped with a Dean-Stark trap for the azeotropic removal of water and a reflux condenser to be refluxed at 110 °C for 16 h. The crude material was concentrated *in vacuo* and purified by column chromatography with 10% to 33% EtOAc/hexanes. (19 mg, 0.06 mmol, 45%, 2:1 dr).

^{1}H NMR (500 MHz, $CDCl_3$) δ 6.36 (s, 1H), 5.90 (s, 1H), 4.21 (dq, J = 10.6, 7.1 Hz, 1H), 4.13 (dq, J = 10.8, 7.1 Hz, 1H), 2.87 – 2.78 (m, 1H), 2.74 (dd, J = 12.8, 5.5 Hz, 1H), 2.59 (dd, J = 17.5, 4.6 Hz, 1H), 2.48 (dd, J = 18.8, 5.6 Hz, 1H), 2.29 (dd, J = 17.5, 13.5 Hz, 1H), 1.99 – 1.90 (m, 1H),

1.76 (qt, J = 9.7, 4.4 Hz, 1H), 1.54 (td, J = 12.0, 5.6 Hz, 1H), 1.35 – 1.17 (m, 6H), 0.89 (t, J = 7.3 Hz, 3H).

^{13}C NMR (126 MHz, $CDCl_3$) δ 199.0, 169.9, 153.2, 143.3, 126.3, 126.3, 61.6, 48.6, 43.2, 39.8, 32.0, 31.9, 30.9, 30.0, 29.8, 29.4, 22.7, 22.6, 14.3, 14.2, 14.0.

HRMS (ESI-TOF) $[M+Na]^+$ m/z: calcd for $C_{17}H_{23}O_3$ 333.1233; Found 333.1233.

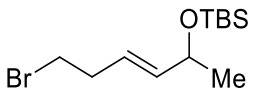

(*E*)-((6-Bromohex-3-en-2-yl)oxy)(*tert*-butyl)dimethylsilane (2-125): A flame-dried round-bottom flask was charged with Grubbs 2nd generation catalyst (**1-141**) (0.23 g, 0.27 mmol, 0.01 equiv.) under the inert atmosphere of a glove box. The flask was removed from the glovebox anhydrous DCM (100 mL) was added. Then, 75% compound **2-124** (6.67 g, 26.83 mmol, 1.0 equiv.) and 97% bromide **2-123** (3.73 g, 26.83 mmol, 1.0 equiv.). The contents were left to stir under reflux conditions at 55 °C for 24 h. After this time, the heating was removed, and the reaction was left to cool to room temperature. The reaction was then directly dry loaded onto silica by concentration *in vacuo*. The crude material was purified by column chromatography with 10% to 33% EtOAc/hexanes. (4.82 g, 16.42 mmol, 61%).

^{1}H NMR (600 MHz, $CDCl_3$) δ 5.57 (d, J = 2.6 Hz, 1H), 5.56 (d, J = 1.7 Hz, 1H), 4.27 (qd, J = 6.3, 3.8 Hz, 1H), 3.38 (t, J = 7.1 Hz, 2H), 2.57 (q, J = 6.9 Hz, 2H), 1.20 (d, J = 6.2 Hz, 3H), 0.89 (s, 9H), 0.06 (d, J = 3.2 Hz, 6H).

^{13}C NMR (126 MHz, $CDCl_3$) δ 139.7, 124.5, 68.1, 32.5, 25.8, 25.7, 24.1, -4.6, -4.8.

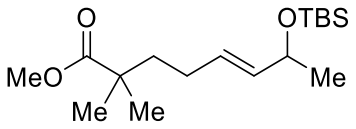

Methyl (*E*)-7-((*tert*-butyldimethylsilyl)oxy)-2,2-dimethyloct-5-enoate (2-127): A flame-dried round-bottom flask was utilized to prepare LDA (34.09 mmol, 2.0 equiv.) with HMPA (7.5 mL) in THF (100 mL) at –78 °C. Compound **2-126** (4.96 mL, 37.50 mmol, 2.2 equiv.) was added to the cooled solution dropwise over the course of 5 minutes. The reaction flask was warmed to 0 °C and allowed to stir for 30 minutes and then cooled again to –78 °C. Compound **2-125** (5.0 g, 17.05 mmol, 1.0 equiv.) was added to the cooled solution dropwise. The contents were left to slowly warm to room temperature and left to stir for 16 h. The reaction was then quenched with NH_4Cl (sat.) and extracted with EtOAc (3x 20 mL). The organic layer was washed with NH_4Cl (sat.) (2x 10 mL), NaCl (sat.) (2x 10 mL), dried over Na_2SO_4, decanted, and then concentrated *in vacuo*. The crude material was purified by column chromatography with 10% to 33% EtOAc/hexanes. (4.26 g, 13.27 mmol, 76%).

^{1}H NMR (600 MHz, $CDCl_3$) δ 5.51 (dt, J = 15.4, 6.5 Hz, 1H), 5.43 (dd, J = 16.3, 5.6 Hz, 1H), 4.23 (p, J = 6.2 Hz, 1H), 4.12 (s, 3H), 1.93 (dt, J = 11.3, 5.8 Hz, 2H), 1.60 – 1.53 (m, 2H), 1.17 (s, 6H), 1.08 (d, J = 6.7 Hz, 3H), 0.88 (s, 9H), 0.04 (d, J = 4.1 Hz, 6H).

^{13}C NMR (126 MHz, $CDCl_3$) δ 177.6, 132.3, 131.7, 72.7, 51.6, 42.2, 40.7, 31.0, 25.8, 25.8, 25.8, 24.6, 24.6, 24.0, 18.3, -5.0, -5.0.

HRMS (ESI-TOF) $[M+H]^+$ m/z: calcd for $C_{17}H_{34}O_3Si$ 315.2355; Found 315.2351.

IR (film, cm^{-1}) 1260, 1720, 2860, 2880, 2900, 2910.

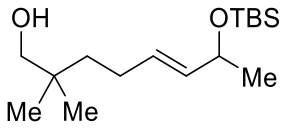

(*E*)-7-((*tert*-Butyldimethylsilyl)oxy)-2,2-dimethyloct-5-en-1-ol (2-128): A flame-dried round-bottom flask was charged with 95% LAH (1.03 g, 25.89 mmol, 2.0 equiv.) and Et_2O (100 mL) and cooled to 0 °C. Compound **2-127** (4.25 g, 12.95 mmol, 1.0 equiv.) was added dropwise to the cooled mixture. The reaction mixture was allowed to slowly warm to room temperature with vigorous stirring while being monitored for uncontrolled production of hydrogen gas byproduct. The contents were left to stir at room temperature for 4 h. The reaction was then cooled to 0 °C and DI H_2O was slowly added dropwise to the reaction mixture until bubbling slows. Then, NH_4Cl (sat.) was added to the reaction mixture slowly until bubbling stops and aluminum clumping is dispersed. The organic layer was washed by NaCl (sat.) (2x 10 mL), dried over Na_2SO_4, decanted, and then concentrated *in vacuo*. The crude material was purified by column chromatography with 10% to 33% EtOAc/hexanes. (3.64 g, 12.69 mmol, 98%).

^{1}H NMR (400 MHz, $CDCl_3$) δ 5.57 – 5.48 (m, 1H), 5.43 (dd, J = 15.3, 5.7 Hz, 1H), 4.23 (q, J = 5.5 Hz, 1H), 3.31 (d, J = 6.1 Hz, 2H), 2.02 – 1.90 (m, 2H), 1.34 – 1.21 (m, 4H), 1.17 (d, J = 6.3 Hz, 3H), 0.87 (s, 9H), 0.87 (s, 6H), 0.03 (d, J = 1.8 Hz, 6H).

^{13}C NMR (126 MHz, $CDCl_3$) δ 132.6, 131.8, 72.7, 72.1, 38.6, 32.8, 31.2, 26.0, 26.0, 26.0, 24.6, 24.6, 23.9, 18.3, -4.9, -4.9.

HRMS (ESI-TOF) $[M+H]^+$ m/z: calcd for $C_{16}H_{34}O_2Si$ 287.2406; Found 287.2413.

IR (film, cm^{-1}) 1280, 1330, 2850, 2870, 2960.

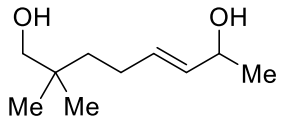

(*E*)-2,2-Dimethyloct-5-ene-1,7-diol (2-129): A flame-dried round-bottom flask was charged with compound **2-128** (3.25 g, 11.35 mmol, 1.0 equiv.) in THF (18 mL) and cooled to 0 °C. 1M TBAF (39.75 mL, 39.75 mmol, 3.5 equiv.) was slowly added to the cooled mixture. The reaction flask was then allowed to slowly warm to room temperature and left to stir at room temperature for 16 h. NH_4Cl (sat.) was added to quench the reaction mixture. Et_2O (20 mL) was used to partition the organic materials into an organic layer. The organic layer was isolated, washed by NaCl (sat.) (2x 10 mL), dried over Na_2SO_4, decanted, and then concentrated *in vacuo*. The crude material was purified by column chromatography with 10% to 33% EtOAc/hexanes. (1.58 g, 9.20 mmol, 81%).

^{1}H NMR (500 MHz, $CDCl_3$) δ 5.63 (dt, J = 13.0, 6.5 Hz, 1H), 5.51 (dd, J = 14.7, 5.9 Hz, 1H), 4.24 (t, J = 6.4 Hz, 1H), 3.30 (s, 2H), 1.98 (q, J = 7.8, 7.3 Hz, 2H), 1.71 (br s, 2H), 1.35 – 1.28 (m, 2H), 1.23 (d, J = 6.4 Hz, 3H), 0.87 (s, 6H).

^{13}C NMR (126 MHz, $CDCl_3$) δ 134.0, 131.6, 71.8, 69.0, 38.2, 35.2, 26.8, 23.9, 23.5.

HRMS (ESI-TOF) $[M+Na]^+$ m/z: calcd for $C_{10}H_{20}O_2$ 195.1361; Found 195.1374.

IR (film, cm^{-1}) 2860, 2890, 2970, 3330, 3350, 3410.

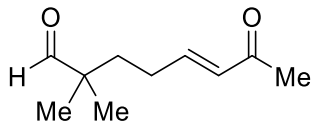

(*E*)-2,2-Dimethyl-7-oxooct-5-enal (2-130): A flame-dried round-bottom flask was transferred to a glovebox. There, 95% DMP (4.72 g, 10.56 mmol, 2.6 equiv.) was added to the reaction flask and removed from the glove box. The solid material was dissolved in DCM (40 mL) and cooled to 0

°C. Compound **2-129** (700 mg, 4.06 mmol, 1.0 equiv.) was added to the cooled mixture followed by a dropwise addition of pyridine (1.31 mL, 16.25 mmol, 4.0 equiv.). The reaction flask was allowed to slowly warm to room temperature and left to stir at room temperature for 16 h. $NaHCO_3$ (sat.) and $Na_2S_2O_3$ (sat.) was added to quench the reaction mixture and let stir 30 minutes. The organic layer was washed by $NaHCO_3$ (sat.) (2x 10 mL), NaCl (sat.) (2x 10 mL), dried over Na_2SO_4, decanted, and then concentrated *in vacuo*. The crude material was purified by column chromatography with 10% to 33% EtOAc/hexanes. (0.57 g, 3.37 mmol, 83%).

^{1}H NMR (400 MHz, $CDCl_3$) δ 9.44 (s, 1H), 6.74 (dtd, J = 15.9, 6.9, 2.3 Hz, 1H), 6.06 (d, J = 16.0 Hz, 1H), 2.22 (s, 3H), 2.14 (q, J = 8.7, 7.7 Hz, 2H), 1.70 – 1.57 (m, 2H), 1.07 (s, 6H).

^{13}C NMR (100 MHz, $CDCl_3$) δ 205.4, 200.8, 147.1, 131.4, 45.6, 35.2, 27.4, 26.9, 21.4, 21.4.

HRMS (ESI-TOF) $[M+H]^+$ m/z: calcd for $C_{10}H_{16}O_2$ 169.1229; Found 169.1234.

IR (film, cm^{-1}) 1260, 1670, 1720, 2700, 2850, 3000.

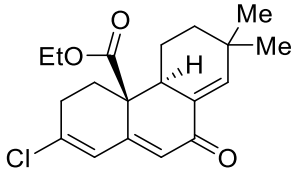

Ethyl (4a*S*,4b*S*)-2-chloro-7,7-dimethyl-9-oxo-3,4b,5,6,7,9-hexahydrophenanthrene-4a(4*H*)-carboxylate (2-133): A flame-dried round-bottom flask was added compound **2-130** (27.0 mg, 0.16 mmol, 1.0 equiv.) and compound **2-30** (32.5 mg, 0.16 mmol, 1.0 equiv.). The round bottom flask was then transferred to a glovebox and 98% $Cu(OTf)_2$ (17.8 mg, 0.05 mmol, 0.3 equiv.) was added to the mixture and the contents were removed from the glovebox and left to stir at room temperature under *neat* conditions for 16 h. The crude material was passed through a short silica

plug using Et_2O as eluant. The resulting solution was evaporated into a round-bottom flask and dissolved in PhMe (4 mL) and *p*-TSA (6.3 mg, 0.05 mmol, 0.3 equiv.) was added. The reaction flask was equipped with a Dean-Stark trap for the azeotropic removal of water and a reflux condenser to be refluxed at 110 °C for 16 h. The crude material was concentrated *in vacuo* and purified by column chromatography with 10% to 33% EtOAc/hexanes. (8.3 mg, 0.02 mmol, 15%, 2:1 dr).

^{1}H NMR (500 MHz, $CDCl_3$) δ 6.36 (d, J = 2.6 Hz, 1H), 5.92 (s, 1H), 4.91 – 4.83 (m, 1H), 4.34 – 4.26 (m, 1H), 4.17 (ddd, J = 10.7, 6.0, 3.0 Hz, 1H), 2.54 – 2.46 (m, 2H), 2.36 (t, J = 7.6 Hz, 1H), 2.11 – 2.08 (m, 2H), 1.65 (p, J = 7.6 Hz, 1H), 1.55 – 1.49 (m, 3H), 1.27 (br s, 6H), 0.89 (t, J = 7.0 Hz, 3H).

^{13}C NMR (126 MHz, $CDCl_3$) δ 200.8, 172.8, 152.0, 150.3, 144.3, 133.3, 125.7, 120.3, 62.0, 52.2, 42.4, 38.2, 33.5, 32.9, 29.2, 29.3, 27.8, 20.5, 14.2.

HRMS (ESI-TOF) $[M+Na]^+$ m/z: calcd for $C_{19}H_{23}ClO_3$ 357.1233; Found 357.1227.

IR (film, cm^{-1}) 1270, 1360, 1690, 2890, 2910.

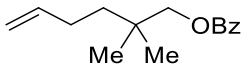

2,2-Dimethylhex-5-en-1-yl benzoate (2-140): A flame-dried round-bottom flask was charged with compound **2-139** (0.50 g, 3.90 mmol, 1.0 equiv.) and pyridine (2.5 mL) before being cooled to 0 °C. Then, benzoyl chloride (0.59 mL, 5.07 mmol, 1.3 equiv.) was added to the solution dropwise at 0 °C. The reaction was then allowed to warm to room temperature and stirred for 16 h. The reaction was then quenched with NH_4Cl (sat.) and extracted with EtOAc (3x 5 mL). The organic layer was washed with NH_4Cl (sat.) (2x 5 mL), NaCl (sat.) (2x 5 mL), dried over Na_2SO_4,

decanted, and concentrated *in vacuo*. The crude material was purified by column chromatography with 10% to 33% EtOAc/hexanes. (0.77 g, 3.30 mmol, 85%).

^{1}H NMR (500 MHz, $CDCl_3$) δ 8.05 (d, J = 7.0 Hz, 2H), 7.57 (t, J = 7.4 Hz, 1H), 7.45 (t, J = 7.7 Hz, 2H), 5.88 – 5.78 (m, 1H), 5.03 (dd, J = 17.1, 1.8 Hz, 1H), 4.94 (dd, J = 10.1, 2.0 Hz, 1H), 4.06 (s, 2H), 2.14 – 2.04 (m, 2H), 1.50 – 1.45 (m, 2H), 1.03 (s, 3H), 1.03 (s, 3H).

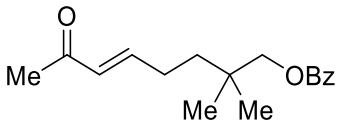

(*E*)-2,2-Dimethyl-7-oxooct-5-en-1-yl benzoate (2-142): A flame-dried round-bottom flask was charged with Grubbs 2nd generation catalyst (**1-141**) (0.03 mg, 0.03 mmol, 0.01 equiv.) under the inert atmosphere of a glove box. The flask was removed from the glovebox anhydrous DCM (20 mL) was added. Then, compound **2-140** (0.74 g, 3.17 mmol, 1.0 equiv.) and ketone **2-141** (0.26 mL, 3.17 mmol, 1.0 equiv.) were added to the flask and were left to stir under reflux conditions at 55 °C for 24 h. After this time, the heating was removed, and the reaction was left to cool to room temperature. The reaction was then directly dry loaded onto silica by concentration *in vacuo*. The crude material was purified by column chromatography with 10% to 33% EtOAc/hexanes. (0.87 g, 3.17 mmol, 93%).

^{1}H NMR (500 MHz, $CDCl_3$) δ 8.04 (d, J = 7.0 Hz, 2H), 7.57 (t, J = 7.4 Hz, 1H), 7.46 (t, J = 7.7 Hz, 2H), 6.80 (dt, J = 15.9, 6.7 Hz, 1H), 6.09 (d, J = 15.9 Hz, 1H), 4.07 (s, 2H), 2.29 – 2.25 (m, 2H), 2.23 (s, 3H), 1.57 – 1.51 (m, 2H), 1.05 (s, 3H), 1.05 (s, 3H).

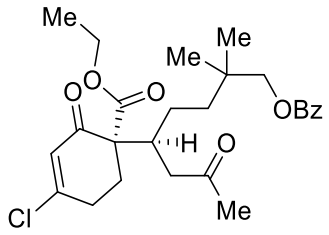

(*S*)-5-((*S*)-4-Chloro-1-(ethoxycarbonyl)-2-oxocyclohex-3-en-1-yl)-2,2-dimethyl-7-oxooctyl benzoate (2-143): A flame-dried round-bottom flask was charged with compound **2-30** (0.20 g, 0.73 mmol, 1.0 equiv.) and compound **2-142** (0.15 g, 0.73 mmol, 1.0 equiv.). The round bottom flask was then transferred to a glovebox and $Cu(OTf)_2$ (0.08 g, 0.22 mmol, 0.3 equiv.) was added to the mixture and its contents were removed from the glovebox and left to stir at room temperature under *neat* conditions for 16 h. The crude material was purified by column chromatography with 10% to 33% EtOAc/hexanes. (0.29 g, 0.61 mmol, 83%, >20:1 dr).

^{1}H NMR (500 MHz, $CDCl_3$) δ 8.04 (d, J = 8.3 Hz, 2H), 7.57 (t, J = 7.4 Hz, 1H), 7.45 (t, J = 7.8 Hz, 2H), 6.19 (s, 1H), 4.13 (ddd, J = 13.4, 7.3, 3.8 Hz, 1H), 4.08 (dd, J = 11.9, 7.1 Hz, 1H), 4.04 – 3.94 (m, 2H), 2.93 – 2.85 (m, 1H), 2.85 – 2.76 (m, 1H), 2.63 (dd, J = 18.3, 6.0 Hz, 1H), 2.60 – 2.53 (m, 1H), 2.39 (dt, J = 13.8, 4.4 Hz, 1H), 2.31 – 2.22 (m, 1H), 2.05 (s, 3H), 2.03 – 1.96 (m, 1H), 1.30 – 1.25 (m, 2H), 1.21 (t, J = 7.1 Hz, 3H), 0.98 (s, 3H), 0.95 (s, 3H).

HRMS (ESI-TOF) $[M+Na]^+$ m/z: calcd for $C_{26}H_{33}ClO_6$ 499.1863; Found 499.1859.

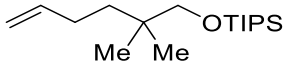

((2,2-Dimethylhex-5-en-1-yl)oxy)triisopropylsilane (2-146): A flame-dried round-bottom flask was charged with compound **2-139** (0.50 g, 3.90 mmol, 1.0 equiv.) and dissolved with anhydrous DCM (8 mL) before being cooled to 0 °C. Then, 97% TIPSCl (1.55 g, 7.80 mmol, 2.0 equiv.) was

added at 0 °C followed by the slow addition of ImH (0.53 g, 7.80 mmol, 2.0 equiv.) was added to the solution slowly at 0 °C. The reaction was then allowed to warm to room temperature and stirred for 16 h. The reaction was then quenched with NH_4Cl (sat.) and extracted with EtOAc (3x 5 mL). The organic layer was washed with NH_4Cl (sat.) (2x 5 mL), NaCl (sat.) (2x 5 mL), dried over Na_2SO_4, decanted, and concentrated *in vacuo*. The crude material was purified by column chromatography with 10% to 33% EtOAc/hexanes. (0.77 g, 3.26 mmol, 84%).

^{1}H NMR (500 MHz, $CDCl_3$) δ 5.84 (ddt, J = 16.8, 10.3, 6.5 Hz, 1H), 5.01 (dq, J = 17.1, 1.7 Hz, 1H), 4.95 – 4.89 (m, 1H), 3.37 (s, 2H), 2.03 (ddt, J = 17.3, 6.6, 1.5 Hz, 2H), 1.39 – 1.32 (m, 2H), 1.08 (s, 21H), 0.88 (s, 3H), 0.88 (s, 3H).

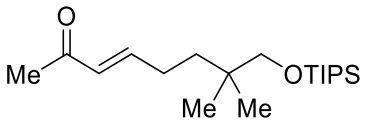

(*E*)-7,7-Dimethyl-8-((triisopropylsilyl)oxy)oct-3-en-2-one (2-147): A flame-dried round-bottom flask was charged with Grubbs 2nd generation catalyst (**1-141**) (0.01 mg, 0.01 mmol, 0.01 equiv.) under the inert atmosphere of a glove box. The flask was removed from the glovebox anhydrous DCM (5 mL) was added. Then, compound **2-146** (0.20 g, 0.70 mmol, 1.0 equiv.) and ketone **2-141** (0.06 mL, 0.70 mmol, 1.0 equiv.) were added to the flask and were left to stir under reflux conditions at 55 °C for 24 h. After this time, the heating was removed, and the reaction was left to cool to room temperature. The reaction was then directly dry loaded onto silica by concentration *in vacuo*. The crude material was purified by column chromatography with 10% to 33% EtOAc/hexanes. (0.13 g, 0.40 mmol, 57%).

^{1}H NMR (500 MHz, $CDCl_3$) δ 6.81 (dt, J = 16.0, 6.8 Hz, 1H), 6.07 (d, J = 15.9 Hz, 1H), 3.38 (s, 2H), 2.24 (s, 3H), 2.23 – 2.17 (m, 2H), 1.46 – 1.38 (m, 2H), 1.07 (s, 21H), 0.88 (s, 3H), 0.88 (s, 3H).

HRMS (ESI-TOF) $[M+H]^+$ m/z: calcd for $C_{19}H_{38}O_2Si$ 327.2714; Found 327.2713.

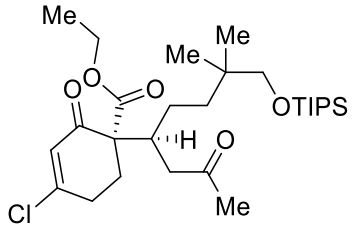

Ethyl (*S*)-4-chloro-1-((*S*)-7,7-dimethyl-2-oxo-8-((triisopropylsilyl)oxy)octan-4-yl)-2-oxocyclohex-3-ene-1-carboxylate (2-148): A flame-dried round-bottom flask was charged with compound **2-30** (0.25 g, 1.22 mmol, 1.0 equiv.) and compound **2-147** (0.40 g, 1.22 mmol, 1.0 equiv.). The round bottom flask was then transferred to a glovebox and 98% $Cu(OTf)_2$ (0.13 g, 0.37 mmol, 0.3 equiv.) was added to the mixture and the contents were removed from the glovebox and left to stir at room temperature under *neat* conditions for 16 h. The crude material was purified by column chromatography with 10% to 33% EtOAc/hexanes. (0.43 g, 0.81 mmol, 60%, >20:1 dr).

^{1}H NMR (500 MHz, $CDCl_3$) δ 6.20 (s, 1H), 4.17 – 4.02 (m, 2H), 3.33 – 3.22 (m, 2H), 2.87 – 2.78 (m, 2H), 2.62 (dt, J = 17.7, 5.2 Hz, 2H), 2.48 (d, J = 5.5 Hz, 1H), 2.46 – 2.38 (m, 1H), 2.34 (dd, J = 18.4, 4.6 Hz, 1H), 2.09 (s, 3H), 1.30 – 1.25 (m, 2H), 1.22 (t, J = 7.0 Hz, 3H), 1.19 – 1.14 (m, 2H), 1.05 (s, 21H), 0.81 (s, 3H), 0.78 (s, 3H).

HRMS (ESI-TOF) $[M+H]^+$ m/z: calcd for $C_{28}H_{50}ClO_5Si$ 529.3111; Found 529.3109.

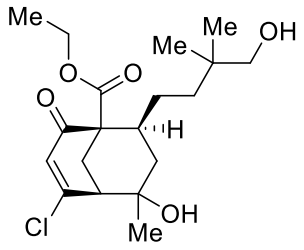

Ethyl (1*S*,5*S*,8*S*)-4-chloro-6-hydroxy-8-(4-hydroxy-3,3-dimethylbutyl)-6-methyl-2-oxobicyclo[3.3.1]non-3-ene-1-carboxylate (2-151): A flame-dried round bottom flask was charged with compound **2-148** (0.04 g, 0.10 mmol, 1.0 equiv.), dissolved with THF (0.3 mL) and cooled to 0 °C. 1M TBAF (0.35 mL, .35 mmol, 3.5 equiv.) was added to the cooled mixture. The reaction flask was allowed to slowly warm to room temperature and left to stir at room temperature for 16 h. The reaction flask was allowed to stir at 0 °C for 4 h. NH_4Cl (sat.) was added to quench the reaction mixture. Et_2O (10 mL) was used to partition the organic materials into an organic layer. The organic layer was isolated, washed by NaCl (sat.) (2x 5 mL), dried over Na_2SO_4, decanted, and then concentrated *in vacuo*. The crude material was purified by column chromatography with 10% to 33% EtOAc/hexanes. (0.02 g, 0.05 mmol, 51%).

^{1}H NMR (500 MHz, $CDCl_3$) δ 6.31 (s, 1H), 4.23 (dq, J = 10.7, 7.2 Hz, 1H), 4.19 – 4.10 (m, 2H), 3.34 (d, J = 9.2 Hz, 1H), 3.27 (d, J = 9.2 Hz, 1H), 2.66 (t, J = 3.8 Hz, 1H), 2.60 (dd, J = 12.6, 3.0 Hz, 1H), 2.48 (dd, J = 12.7, 3.3 Hz, 1H), 2.28 (dddd, J = 12.7, 10.3, 4.8, 2.1 Hz, 1H), 1.89 (dd, J = 15.0, 4.9 Hz, 1H), 1.73 (tdd, J = 13.2, 4.6, 2.1 Hz, 1H), 1.57 (s, 1H), 1.40 (s, 3H), 1.44 – 1.37 (m, 1H), 1.31 (dd, J = 15.3, 13.1 Hz, 1H), 1.25 (t, J = 7.1 Hz, 3H), 0.85 (s, 3H), 0.79 (s, 3H), 0.75 – 0.64 (m, 1H).

^{13}C NMR (126 MHz, $CDCl_3$) δ 193.87, 172.61, 159.90, 130.85, 71.33, 69.93, 69.90, 61.42, 57.63, 51.00, 38.43, 38.40, 36.47, 36.37, 36.26, 35.18, 30.10, 25.86, 24.51, 23.71, 14.14.

HRMS (ESI-TOF) $[M+Na]^+$ m/z: calcd for $C_{19}H_{29}ClO_5$ 395.1601; Found 395.1591.

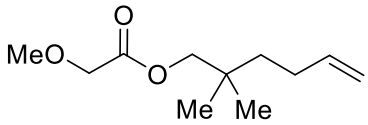

2,2-Dimethylhex-5-en-1-yl 2-methoxyacetate (2-152): A flame-dried round-bottom flask was charged with compound **2-139** (1.00 g, 7.80 mmol, 1.0 equiv.) and pyridine (6.0 mL), then cooled to 0 °C. Methoxyacetic anhydride (1.90 g, 11.70 mmol, 1.5 equiv.) was added to the reaction flask dropwise at 0 °C. The contents were left to slowly warm to room temperature and stir 6 h. The reaction was then quenched with NH_4Cl (sat.) and extracted with Et_2O (3x 20 mL). The organic layer was washed with NH_4Cl (sat.) (2x 10 mL), NaCl (sat.) (2x 10 mL), dried over Na_2SO_4, decanted, and concentrated *in vacuo*. The crude material was purified by column chromatography with 10% to 33% EtOAc/hexanes. (1.49 g, 7.48 mmol, 96%).

^{1}H NMR (700 MHz, $CDCl_3$) δ 5.80 (td, J = 16.9, 6.5 Hz, 1H), 5.01 (d, J = 17.1 Hz, 1H), 4.93 (d, J = 10.1 Hz, 1H), 4.05 (s, 2H), 3.91 (s, 2H), 3.46 (s, 3H), 2.02 (q, J = 7.0 Hz, 2H), 1.36 (dd, J = 9.5, 7.7 Hz, 2H), 0.93 (s, 6H).

^{13}C NMR (176 MHz, $CDCl_3$) δ 170.4, 139.0, 114.2, 72.6, 69.7, 59.4, 38.2, 33.8, 28.2, 24.1, 24.1.

HRMS (ESI-TOF) $[M+Na]^+$ m/z: calcd for $C_{11}H_{20}O_3$ 223.1310; Found 223.1299.

IR (film, cm^{-1}) 1130, 1190, 1760, 2890, 2930, 2960.

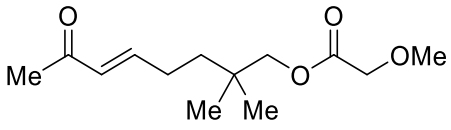

(*E*)-2,2-Dimethyl-7-oxooct-5-en-1-yl 2-methoxyacetate (2-153): A flame-dried round-bottom flask was charged with Grubbs 2nd generation catalyst (**1-141**) (169.2 mg, 0.200 mmol, 0.01 equiv.)

under the inert atmosphere of the glove box. Following removal from the glove box, compound **2-152** (4.0 g, 19.97 mmol, 1.0 equiv.) and ketone **2-141** (1.66 mL, 19.97 mmol, 1.0 equiv.) were added to the flask and dissolved in anhydrous DCM (12 mL). The contents were left to stir under refluxing conditions of 55 °C for 24 h. After this time, the heating was removed, and the reaction was left to cool to room temperature. The reaction was then directly dry loaded onto silica by concentration *in vacuo*. The crude material was purified by column chromatography with 10% to 33% EtOAc/hexanes. (3.81 g, 15.78 mmol, 79%).

^{1}H NMR (500 MHz, $CDCl_3$) δ 6.80 (dt, J = 16.0, 6.8 Hz, 1H), 6.09 (d, J = 15.9 Hz, 1H), 4.07 (s, 2H), 3.93 (s, 2H), 3.48 (s, 3H), 2.25 (s, 3H), 2.22 (ddd, J = 17.0, 6.7, 1.6 Hz, 2H), 1.48 – 1.41 (m, 2H), 0.96 (s, 6H).

^{13}C NMR (176 MHz, $CDCl_3$) δ 200.8, 170.6, 147.5, 130.9, 72.6, 69.7, 59.4, 38.2, 33.8, 28.2, 27.4, 24.1, 24.1, 23.7.

HRMS (ESI-TOF) $[M+Na]^+$ m/z: calcd for $C_{13}H_{22}O_4$ 265.1416; Found 265.1411.

IR (film, cm^{-1}) 1130, 1190, 1750, 2890, 2940.

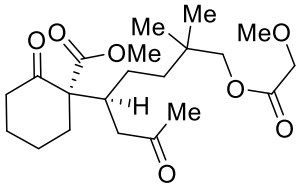

Methyl (*S*)-1-((*S*)-8-(2-methoxyacetoxy)-7,7-dimethyl-2-oxooctan-4-yl)-2-oxocyclohexane-1-carboxylate (2-154): A flame-dried round-bottom flask was charged with 90% compound **2-22** (71.6 mg, 0.41 mmol, 1.0 equiv.) and compound **2-153** (100 mg, 0.41 mmol, 1.0 equiv.). The round bottom flask was then transferred to a glovebox and $Cu(OTf)_2$ (0.12 mg, 0.12 mmol, 0.3 equiv.) was added to the mixture and the contents were removed from the glovebox and left to stir at room

temperature under *neat* conditions for 16 h. The crude material was purified by column chromatography with 10% to 33% EtOAc/hexanes. (138.1 mg, 0.35 mmol, 84%, 3.7:1 dr).

^{1}H NMR (500 MHz, $CDCl_3$) δ 4.05 (s, 2H), 3.90 (s, 2H), 3.74 (s, 3H), 3.45 (s, 3H), 2.30 – 2.24 (m, 4H), 2.24 – 2.19 (m, 2H), 2.05 – 1.97 (m, 2H), 1.71 – 1.64 (m, 2H), 1.60 (t, J = 5.7 Hz, 2H), 1.40 – 1.31 (m, 4H), 1.14 – 1.03 (m, 2H), 0.93 (s, 6H).

^{13}C NMR (176 MHz, $CDCl_3$) δ 207.6, 205.4, 171.6, 170.6, 73.1, 70.3, 63.4, 58.8, 52.6, 43.4, 41.2, 38.0, 37.2, 34.1, 33.3, 32.7, 30.1, 27.5, 24.7, 24.7, 23.7.

HRMS (ESI-TOF) $[M+Na]^+$ m/z: calcd for $C_{21}H_{34}O_7$ 421.2202; Found 421.2196.

IR (film, cm^{-1}) 1220, 1240, 1720, 1740, 2850, 2930.

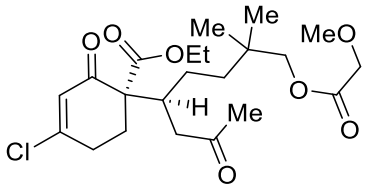

Ethyl (*S*)-4-chloro-1-((*S*)-8-(2-methoxyacetoxy)-7,7-dimethyl-2-oxooctan-4-yl)-2-oxocyclohex-3-ene-1-carboxylate (2-155): A flame-dried round-bottom flask was charged with compound **2-30** (1.0 g, 4.13 mmol, 1.0 equiv.) and compound **2-153** (0.84 g, 4.13 mmol, 1.0 equiv.). The round-bottom flask was then transferred to a glovebox and $Cu(OTf)_2$ (45.7 mg, 1.24 mmol, 0.3 equiv.) was added to the mixture and the contents were removed from the glovebox and left to stir at room temperature under *neat* conditions for 16 h. The crude material was purified by column chromatography with 10% to 33% EtOAc/hexanes. (1.45 g, 3.26 mmol, 79%, >20:1 dr).

^{1}H NMR (500 MHz, $CDCl_3$) δ 6.20 (s, 1H), 4.11 – 4.08 (m, 2H), 4.06 (d, J = 5.7 Hz, 2H), 4.05 (d, J = 3.4 Hz, 2H), 3.84 (d, J = 10.6 Hz, 1H), 3.82 (s, 1H), 3.46 (s, 3H), 2.88 – 2.81 (m, 2H), 2.67 –

2.61 (m, 2H), 2.40 (dt, J = 13.7, 4.3 Hz, 1H), 2.27 (dd, J = 18.3, 4.8 Hz, 1H), 2.11 (s, 3H), 2.00 (ddd, J = 13.7, 10.3, 5.4 Hz, 1H), 1.23 – 1.08 (m, J = 7.2 Hz, 5H), 0.86 (s, 6H).

^{13}C NMR (126 MHz, $CDCl_3$) δ 206.8, 192.6, 170.4, 170.2, 157.1, 128.4, 72.1, 69.7, 61.8, 59.7, 59.4, 44.6, 37.5, 36.1, 33.8, 31.7, 30.0, 27.0, 26.6, 24.3, 24.2, 13.9.

HRMS (ESI-TOF) $[M+Na]^+$ m/z: calcd for $C_{22}H_{33}ClO_7$ 467.1813; Found 467.1803.

IR (film, cm^{-1}) 1180, 1200, 1690, 1720, 1730, 2930, 2950, 2960.

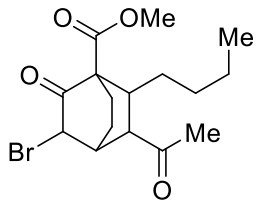

Methyl 3-acetyl-5-bromo-2-butyl-6-oxobicyclo[2.2.2]octane-1-carboxylate (2-176): A flame-dried round-bottom flask was charged with compound **2-174** (0.11 g, 0.47 mmol, 1.0 equiv.) and compound **2-28** (0.06 g, 0.47 mmol, 1.0 equiv.). The round-bottom flask was then transferred to a glovebox and $Cu(OTf)_2$ (0.05 g, 0.14 mmol, 0.3 equiv.) was added to the mixture and the contents were removed from the glovebox and left to stir at room temperature under *neat* conditions for 16 h. The resulting crude was dissolved in PhMe (5 mL) and *p*-TSA (0.02 g, 0.14 mmol, 0.3 equiv.) was added. The reaction flask was equipped with a Dean-Stark trap for the azeotropic removal of water and a reflux condenser to be refluxed at 110 °C for 16 h. The crude material was concentrated *in vacuo* and purified by column chromatography with 10% to 33% EtOAc/hexanes. (0.03 g, 0.08 mmol, 18%).

^{1}H NMR (500 MHz, $CDCl_3$) δ 1H NMR (500 MHz, cdcl3) δ 4.50 (s, 1H), 3.71 (s, 3H), 3.03 (s, 1H), 2.87 – 2.80 (m, 1H), 2.65 (s, 1H), 2.23 (s, 3H), 2.12 (tq, J = 6.4, 3.7, 3.2 Hz, 2H), 1.83 – 1.61

(m, 2H), 1.35 – 1.13 (m, 2H), 1.07 (p, J = 7.3 Hz, 2H), 0.96 – 0.87 (m, 1H), 0.82 (t, J = 7.3 Hz, 3H).

^{13}C NMR (126 MHz, $CDCl_3$) δ 207.5, 201.3, 170.3, 57.8, 52.8, 52.5, 52.2, 40.4, 38.0, 33.3, 28.8, 28.3, 26.6, 22.3, 21.2, 13.9.

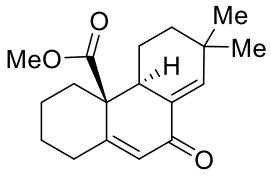

Methyl (4a*S*,4b*S*)-7,7-dimethyl-9-oxo-1,3,4,4b,5,6,7,9-octahydrophenanthrene-4a(2*H*)-carboxylate (2-181): A flame-dried round-bottom flask was charged with compound **2-130** (1.00 g, 5.94 mmol, 1.0 equiv.) and 90% compound **2-22** (1.03 g, 5.94 mmol, 1.0 equiv.). The round-bottom flask was then transferred to a glovebox and 98% $Cu(OTf)_2$ (0.66 g, 1.78 mmol, 0.3 equiv.) was added to the mixture and the contents were removed from the glovebox and left to stir at room temperature under *neat* conditions for 16 h. The crude material was passed through a short silica plug using Et_2O as eluant. The resulting solution was evaporated into a round-bottom flask and dissolved in PhMe (60 mL) and *p*-TSA (0.23 g, 1.78 mmol, 0.3 equiv.) was added. The reaction flask was equipped with a Dean-Stark trap for the azeotropic removal of water and a reflux condenser to be refluxed at 110 °C for 16 h. The crude material was concentrated *in vacuo* and purified by column chromatography with 10% to 33% EtOAc/hexanes. (0.78 g, 2.73 mmol, 46%yield of 90% pure mass, 4:1 dr).

^{1}H NMR (400 MHz, $CDCl_3$) δ 6.68 (s, 1H), 6.07 (s, 1H), 3.60 (s, 3H), 2.75 (dd, J = 13.5, 1.9 Hz, 1H), 2.45 (d, J = 12.3 Hz, 2H), 2.14 – 2.02 (m, 2H), 1.93 – 1.72 (m, 2H), 1.68 – 1.45 (m, 2H), 1.35 (d, J = 9.9 Hz, 2H), 1.21 (td, J = 13.4, 4.2 Hz, 2H), 1.06 (s, 3H), 0.96 (s, 3H).

^{13}C NMR (126 MHz, $CDCl_3$) δ 187.8, 171.7, 161.6, 144.6, 131.5, 128.0, 52.8, 52.1, 45.1, 40.7, 35.6, 35.4, 34.9, 29.9, 28.0, 26.0, 23.3, 21.0.

HRMS (ESI-TOF) $[M+Na]^+$ m/z: calcd for $C_{18}H_{24}O_3$ 311.1623; Found 311.1621.

IR (film, cm^{-1}) 1220, 1670, 1730, 2860, 2930, 2950.

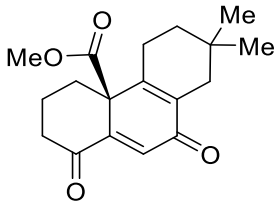

Methyl (*S*)-7,7-dimethyl-1,9-dioxo-1,3,4,5,6,7,8,9-octahydrophenanthrene-4a(2*H*)-carboxylate (2-183): A flame-dried round-bottom flask was transferred to a glovebox and 97% $Rh_2(cap)_4$ (1.4 mg, 0.002 mmol, 0.02 equiv.) was added to flask and then removed from the glovebox. Compound **2-181** (6.0 mg, 0.21 mmol, 1.0 equiv.) and DCE (0.6 mL) were added to the reaction flask followed by T-HYDRO (0.23 mL, 1.66 mmol, 8.0 equiv.). The reaction flask was stirred at room temperature for 48 h. The crude material was extracted using DCM and concentrated *in vacuo*, then purified by column chromatography with 10% to 33% EtOAc/hexanes. (32.5 mg, 0.11 mmol, 52% yield of 90% pure mass).

^{1}H NMR (500 MHz, $CDCl_3$) δ 6.35 (s, 1H), 3.60 (s, 3H), 2.50 (qt, J = 13.7, 4.7 Hz, 2H), 2.45 – 2.39 (m, 1H), 2.26 (td, J = 13.7, 13.0, 5.4 Hz, 1H), 2.11 – 2.04 (m, 1H), 2.00 – 1.88 (m, 1H), 1.78 (dtd, J = 15.9, 8.7, 7.7, 3.8 Hz, 1H), 1.69 – 1.63 (m, 2H), 1.40 (qt, J = 13.2, 4.2 Hz, 2H), 1.27 (d, J = 5.0 Hz, 2H), 1.25 (s, 3H), 1.24 (s, 3H).

^{13}C NMR (126 MHz, $CDCl_3$) δ 199.2, 197.5, 183.1, 169.2, 160.2, 153.7, 134.6, 128.4, 126.9, 53.1, 51.5, 48.0, 37.4, 33.7, 29.2, 24.4, 24.0, 21.7.

HRMS (ESI-TOF) $[M+H]^+$ m/z: calcd for $C_{18}H_{22}O_4$ 303.1596; Found 303.1609.

IR (film, cm^{-1}) 1660, 1720, 1750, 2880, 2930, 2950, 2990.

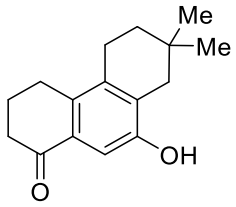

9-Hydroxy-7,7-dimethyl-3,4,5,6,7,8-hexahydrophenanthren-1(2*H*)-one (2-189): A flame-dried round-bottom flask was transferred to a glovebox and LiCl (22.1 mg, 0.52 mmol, 15.0 equiv.) was added to flask and then removed from the glovebox. Compound **2-183** (10.5 mg, 0.03 mmol, 1.0 equiv.) and DMSO (0.5 mL) were added to the reaction flask. The reaction flask was equipped with a reflux condenser and heated at 180 °C for 24 h. The crude material was extracted using DCM and concentrated *in vacuo*, then purified by column chromatography with 10% to 33% EtOAc/hexanes. (19.5 mg, 0.02 mmol, 60% of 80% pure mass).

^{1}H NMR (500 MHz, $CDCl_3$) δ 12.58 (s, 1H), 6.96 (s, 1H), 3.04 – 2.99 (m, 2H), 2.85 (s, 2H), 2.56 – 2.49 (m, 2H), 2.34 (t, J = 7.6 Hz, 2H), 2.26 – 2.18 (m, 2H), 1.77 (d, J = 3.5 Hz, 1H), 1.75 (d, J = 3.5 Hz, 1H), 1.32 (s, 6H).

^{13}C NMR (126 MHz, $CDCl_3$) δ 198.9, 156.5, 138.7, 132.8, 130.9, 129.5, 107.4, 39.9, 38.5, 35.3, 34.1, 28.0, 28.0, 25.9, 23.6, 22.4.

HRMS (ESI-TOF) $[M-H]^-$ m/z: calcd for $C_{18}H_{20}O_2$ 243.1385; Found 243.1377.

IR (film, cm^{-1}) 1460, 1650, 2850, 2890, 2920, 2950, 3010.

CHAPTER III

Total Synthesis of (±)-Aspewentin A

III.1 Introduction

The outcomes of the studies in the prior chapter indicated that strategic tricyclic intermediate **2-25** might be utilized in the total synthesis of (±)-aspewentin A (**(±)-1-16**); however, the undesired aldol reactivity of the explored unsaturated keto-ester donors meant that they were not readily applicable to the intended isopimarane scaffold synthesis. This chapter explores the challenges associated with the installation of the *gem*-dimethyl substitution pattern and the final route utilized to synthesize (±)-aspewentin A (**(±)-1-16**). The synthesis of vinylic acceptor **2-21** remains key to accomplishing the intended total synthesis and will be described in this chapter. The Rh-oxidation pathway established in the prior chapter will be explored to its application in leading to the natural product. Ultimately, this chapter will present several alternative synthetic strategies focused on raising the yield of the initial Michael C-C bond forming step.

Based on the encouraging model studies resulting in the formation of tricyclic product 2-189, our initial studies were focused on implementing this approach using actual substrates **2-21** and **2-22** (Figure III.1). By utilizing the Cu(II)-Michael process with donor **2-22** and acceptor **2-21**, intermediate **3-1** can directly undergo a double aldol condensation to yield tricyclic intermediate **2-25**. Allylic oxidation of **2-25** would provide product **2-178** that is then ready for decarboxylative aromatization to phenol **2-177**. Methylation of the ketone moiety of **2-177** would then yield (±)-aspewentin A (**(±)-1-16**).

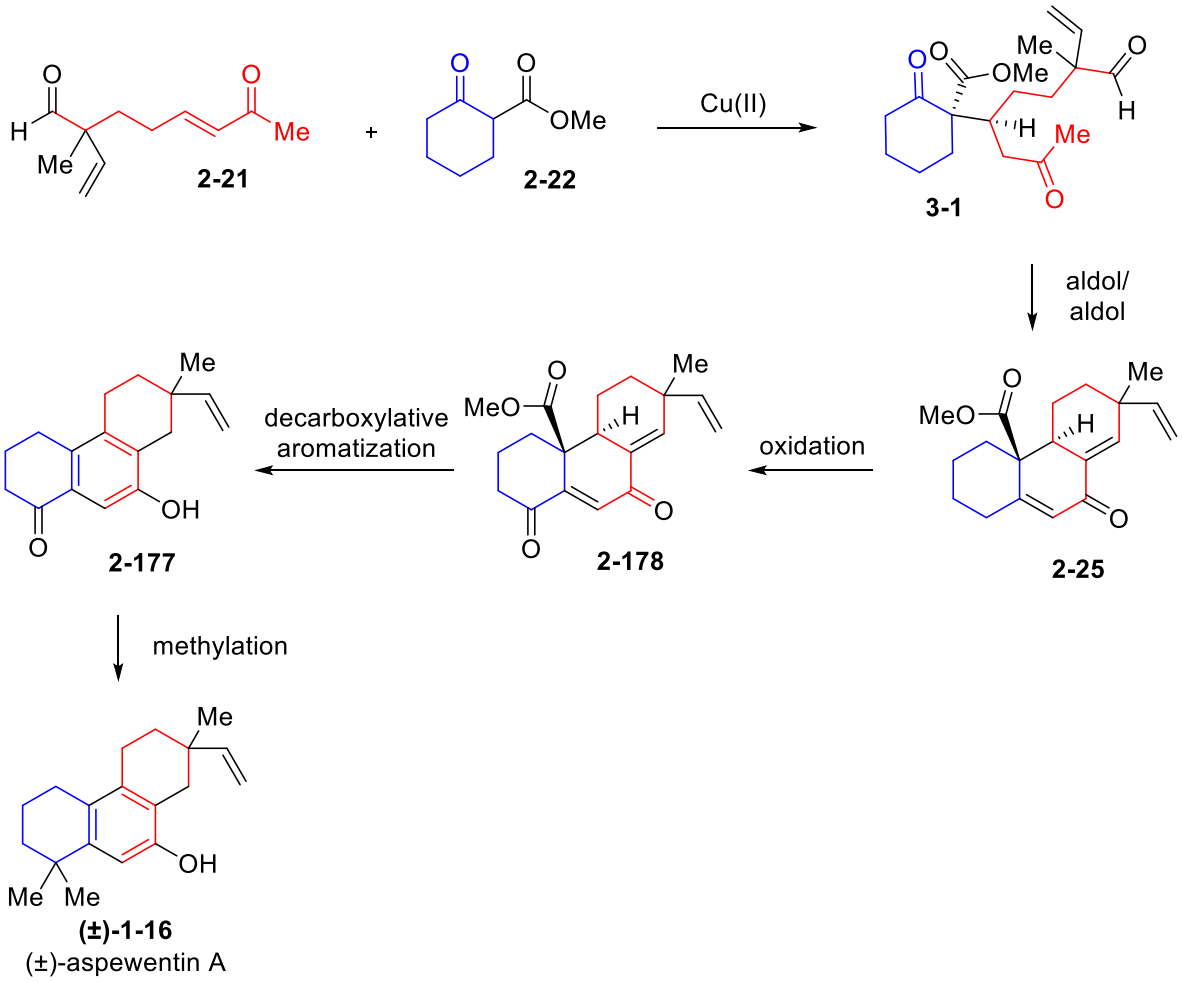

Figure III.1 Proposed synthetic pathway leading to (±)-aspewentin A (**(±)-1-16**).

Our attention turned toward the preparation of acceptor **2-21** to be utilized in the Cu(II)-Michael process. The first-generation synthesis targeting aldehyde **2-21** was initiated by stirring tiglic acid **3-2** with methyl iodide and K_2CO_3 in aqueous DMF to yield tiglate ester **3-3** in 59% yield (Figure III.2). Tiglate ester **3-3** was added to halide **2-123** via an enolate addition in HMPA and THF at –78 °C to generate adduct **3-4**, containing the desired quaternary stereocenter, in 84% yield. An attempt to selectively oxidize diene **3-4** using Lemieux-Johnson conditions of stoichiometric 1,6-lutidine and $NaIO_4$ along with catalytic quantities of potassium osmate(VI) dihydrate (0.02 equiv.) in 1,4-dioxane and H_2O gave aldehyde **3-5** in 24% yield. A major

byproduct, might arise from an osmium-mediated oxidative cyclization has been reported to produce both pyrrolidines and furans from dienes.[136] The 6-membered cyclization is significantly less reported, but has been observed for the proposed starting materials and intermediates in ruthenium-mediated[137] and rhenium-mediated[138] systems. Aldehyde **3-5** was intended to be applied for Wittig olefination with 1-(triphenylphosphoranylidene)-2-propanone (**3-6**) to provide adduct **3-7**; however, the low yield of this process lead to interest in an alternative synthetic route to acceptor **2-21**. Elaboration of enone **3-7** to aldehyde **2-21** would have involved a bis-reduction with LAH to diol **3-8** before a bis-oxidation with DMP to reveal aldehyde **2-21**.

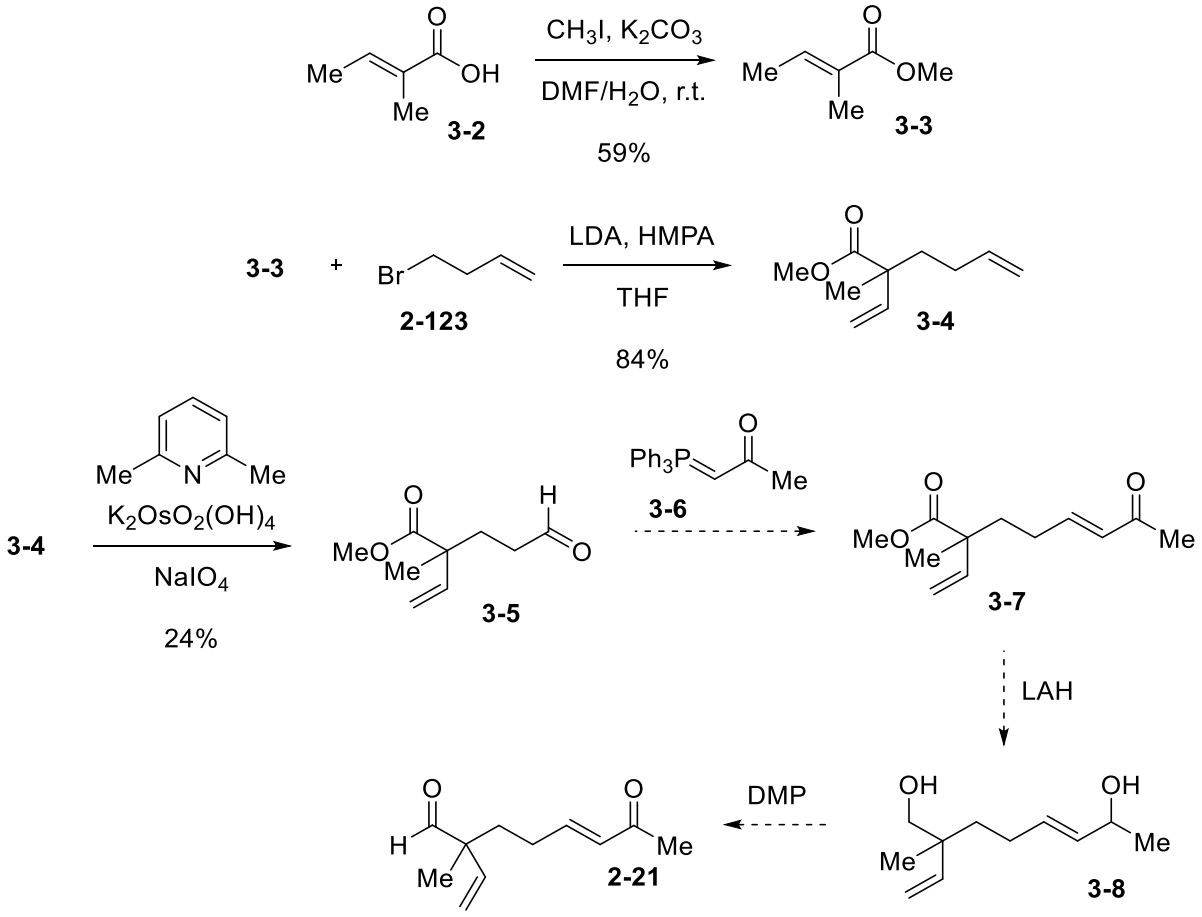

Figure III.2 First-generation synthesis of Michael acceptor **2-21**.

A subsequent second-generation approach to acceptor **2-21** resulted in more efficient access to this material (Figure III.3). Tiglate ester **3-3** was added to halide **2-125** via an enolate addition to generate adduct **3-9**, containing the desired C13-quaternary stereocenter, in 71% yield. Ester **3-9** was then reduced using LAH to the corresponding primary alcohol **3-10** in 93% yield. The silyl ether moiety of **3-10** was cleaved using TBAF to reveal an allylic alcohol **3-8** in 90% yield. The diol **3-8** underwent successful bisoxidation using DMP conditions and afford aldehyde **2-21** in 82% yield.

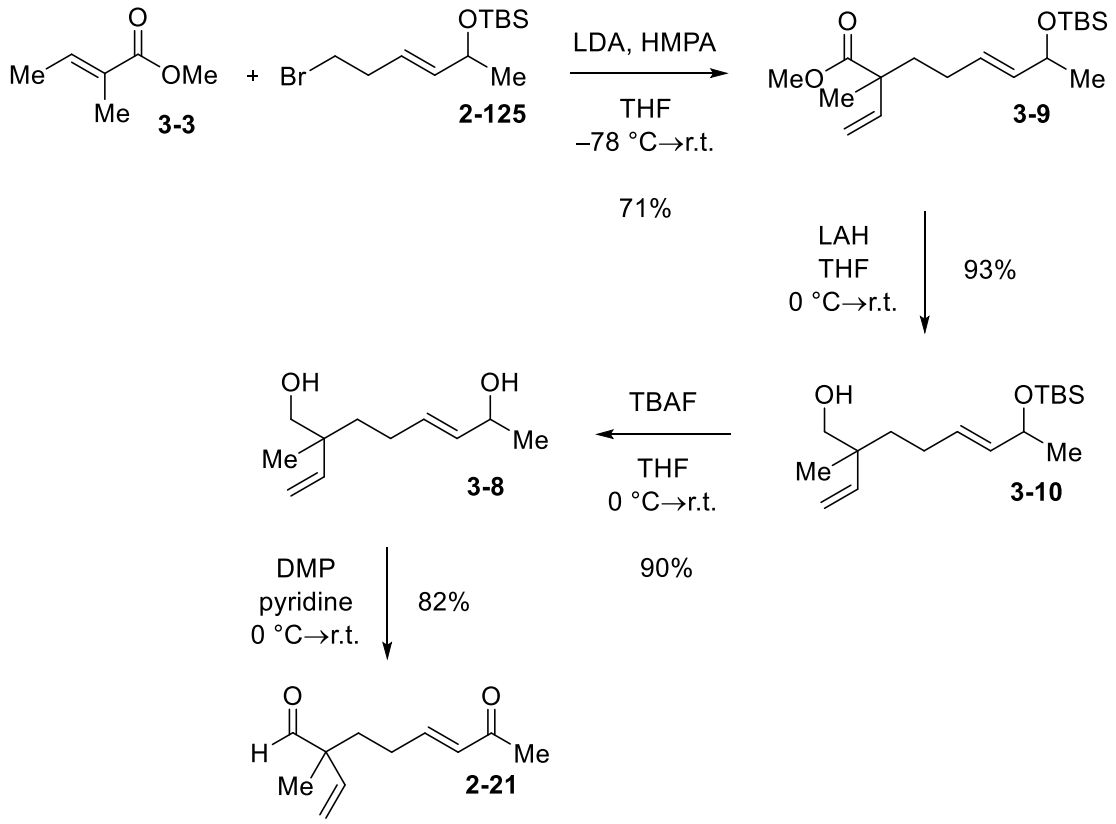

Figure III.3 Second-generation synthesis of Michael acceptor **2-21**.

Thus, ester **2-22** and acceptor **2-21** were stirred with $Cu(OTf)_2$ (0.3 equiv.) under *neat* conditions, and the resulting crude Michael reaction product was exposed to catalytic *p*-TSA (0.3 equiv.) in refluxing PhMe at 110 °C with a Dean-Stark trap for the azeotropic removal of water,

to provide carbocycle **2-25** in 42% yield and 4:1 dr (Figure III.4). Then, substrate **2-25** was oxidized under optimized conditions with $Rh_2(cap)_4$ (0.01 equiv., recharged at 24 h) and T-HYDRO (8 equiv.) in DCE at room temperature for 48 h to give **2-178** in 36% yield. However, subjecting **2-178** to the decarboxylative process only produced a mixture, and no desired product **2-177** was observed. Failure of the intended decarboxylative aromatization may involve reactivity of the vinylic group in **2-25** which was not present in the model system developed in the prior chapter (Figure II.37). Product **2-177** was intended to participate in a subsequent methylation event that would provide (+)-aspewentin A (**(+)-1-16**). The possibility of such a reaction was tested using model substrate, α-tetralone (**3-11**), which was efficiently alkylated utilizing previously reported[139] conditions of $TiCl_4$ (2.2 equiv.) and $Zn(CH_3)_2$ (2.2 equiv.) in DCM to generate *gem*-dimethyl product **3-12** in 90% yield. Considering that the installation of the C13-vinyl group has significantly reduced the yield for the allylic oxidation and interfered with the formation of **2-177**, the modification of this strategy was required.

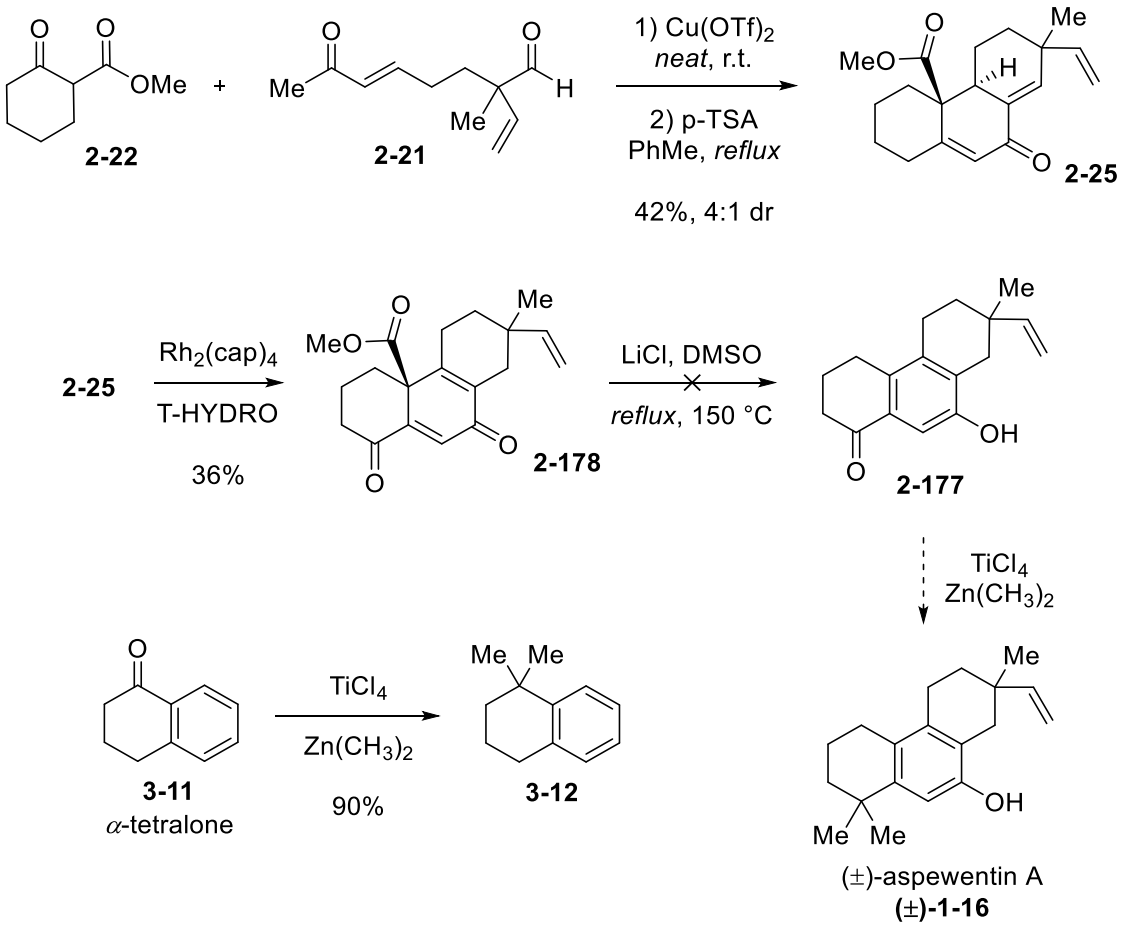

Figure III.4 Synthesis and attempted oxidation of tricycle **2-25**.

III.2 Model Studies of *gem*-Dimethyl Michael Donors

To mitigate these new challenges, we opted to investigate the possibility of the *gem*-dimethyl substitution pattern associated with isopimaranes being directly carried into the Cu(II)-Michael process with the intention that this concise synthetic approach would enable the total of (±)-Aspewentin A (**1-16**) (Figure III.1). The electronic and steric effect of the *gem*-dimethyl substitution pattern of **3-13** on the decarboxylative step is expected to impede the intended process but will remain favorable given the stability of the aromatized product. The hindered tricycle **3-13**

can be formed directly from the Michael-aldol-aldol cascade if hindered donor **3-14** and acceptor **2-21** are directly implemented in the Cu(II)-Michael process.

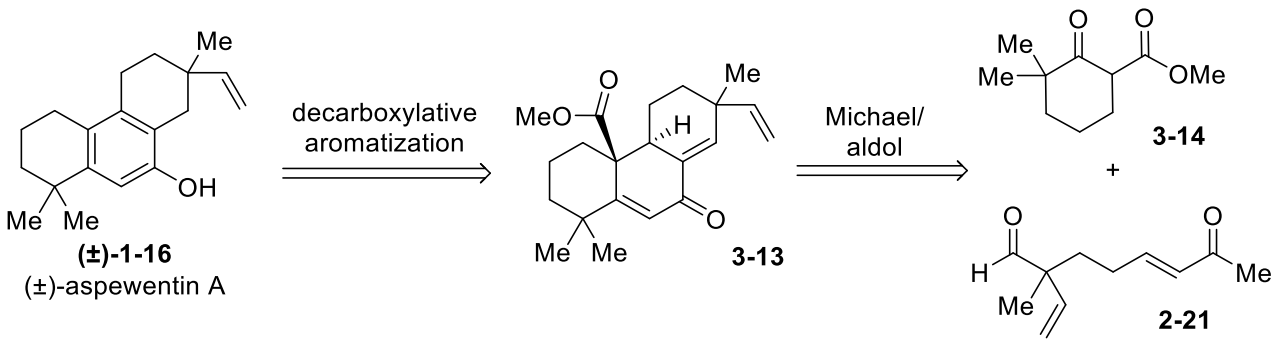

Figure III.5 Third-generation retrosynthetic analysis of (±)-aspewentin A (**(±)-1-16**).

Synthesis of gem-dimethyl donor **3-14** was achieved by deprotonating ketone **3-15** using NaH in THF and then the addition of dimethyl carbonate to yield the product ester **3-14** in 58% yield (Figure III.6).

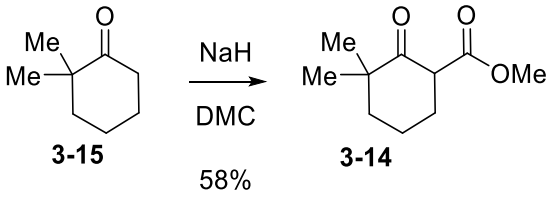

Figure III.6 Synthesis of *gem*-dimethyl keto-ester donor **3-14**.

When the Cu(II)-Michael reaction process was tested using sterically hindered *gem*-dimethyl Michael donor **3-14** and acceptor **3-15**, coupled product **3-16** was isolated with 1:1 diastereoselectivity (Table III.1). The loss in yield and diastereoselectivity for these reaction participants, relative to the vinyl chloride donor **2-30**, was broadly attributed to the steric bulk of *gem*-dimethyl donor **3-14**. When Michael donor **3-14** (1.2 equiv.) and acceptor **3-15** (1.0 equiv.) were stirred with $Cu(OTf)_2$ (0.5 equiv.) for 7 h adduct **3-16** was isolated in 35% (entry 1), or 31% yield (entry 2), if stirred for 24h. If $Cu(OTf)_2$ loading was reduced to 0.3 equivalents and stirred

for 24 h, product **3-16** was isolated in 23% yield (entry 3). If Michael donor **3-14** was increased to 2.0 equivalents, with $Cu(OTf)_2$ (0.3 equiv.), and the reaction stirred for 48 h then product **3-16** was isolated in 24% yield (entry 4) and 20% yield (entry 5) if stirred for 120h. Aldol condensation adduct **3-17**, resulting from the *homo*-dimerization of enone **3-15**, was generally observed as a byproduct when hindered donor **3-14** was implemented. Increasing the catalyst loading of this transformation carried out under *neat* conditions was found to greatly affect the viscosity of the reaction mixture and affect its ability to stir as these processes proceeded. This observation may indicate that as some reaction complexes or intermediates were formed, the bulk properties of the material mixture became more viscous and hindered magnetic stirring.

Table III.1 Reactivity study of donor **3-14** in the Cu(II)-Michael process.

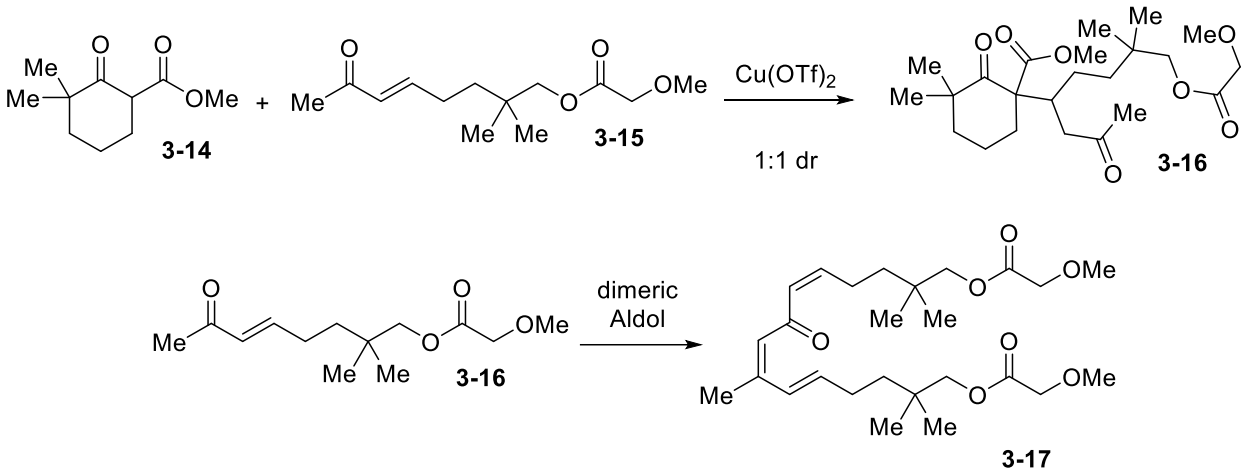

entry	catalyst	catalyst loading	**3-14**	time	Yield **3-16**
1	$Cu(OTf)_2$	0.5 equiv.	1.2 equiv.	7 h	35%
2	$Cu(OTf)_2$	0.5 equiv.	1.2 equiv.	24 h	31%
3	$Cu(OTf)_2$	0.3 equiv.	1.2 equiv.	24 h	23%
4	$Cu(OTf)_2$	0.3 equiv.	2.0 equiv.	48 h	24%
5	$Cu(OTf)_2$	0.3 equiv.	2.0 equiv.	120 h	20%

In addition to the synthetic plan depicted in Figure III.5, a more direct decarboxylative Michael-aldol approach, previously studied by our research group,[140] was implemented towards the desired tricyclic scaffold by utilizing donor **3-18** and acceptor **2-21** (Figure III.7). The reaction was envisioned to proceed through the initial Cu(II)-mediated formation of adduct **3-19** before an α-decarboxylation event forms **3-20**. Intermediate **3-20** may then undergo a double annulation event and tautomerization to reveal (±)-aspewentin A (**(±)-1-16**).

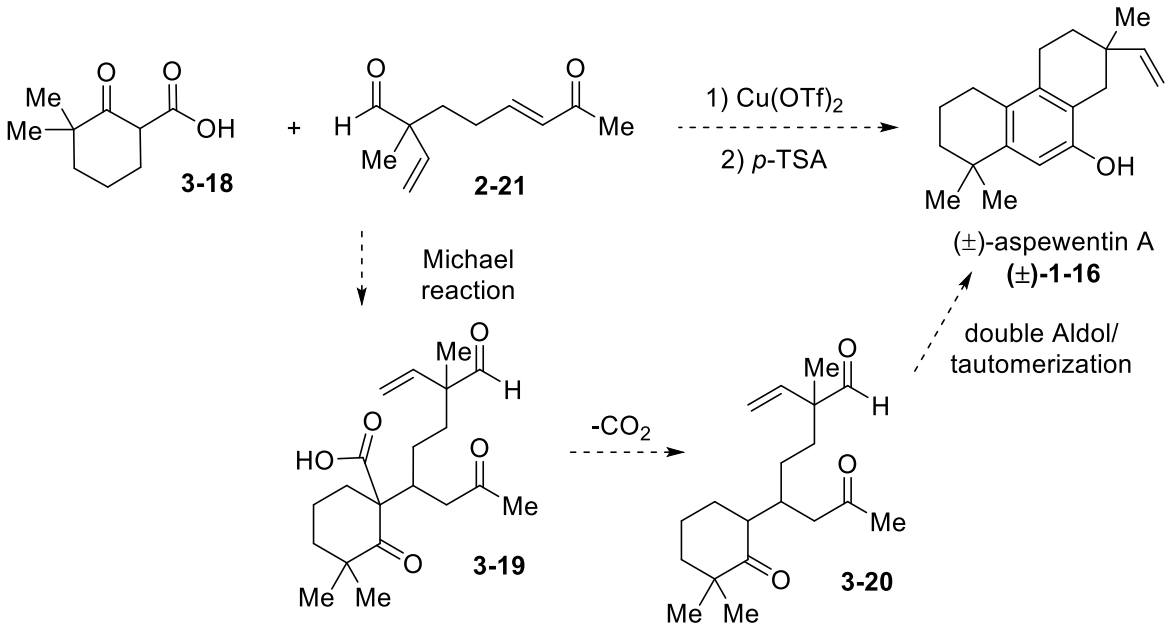

Figure III.7 Decarboxylative Michael approach towards a tricyclic scaffold.

The keto-acid donor **3-18** can be derived from **3-14** under hydrolytic conditions of aqueous NaOH to provide in 48% yield (Figure III.8).

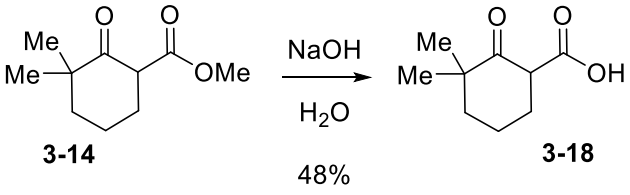

Figure III.8 Synthesis of *gem*-dimethyl keto-acid donor **3-18**.

However, when keto-acid **3-18** and enone **3-130** were subjected to the Cu(II)-Michael conditions with $Cu(OTf)_2$ (0.3 equiv.) and then dehydrating conditions of catalytic *p*-TSA (0.3 equiv.) in refluxing PhMe, only condensation product **3-22** was isolated in 42% yield from the mixture (Figure III.9). Similarly, if keto-acid **3-23** and enone **2-130** were subjected to the same conditions, condensation product **3-22** was isolated in quantitative yield from the mixture, and no desired tricyclic product **3-24** was observed.

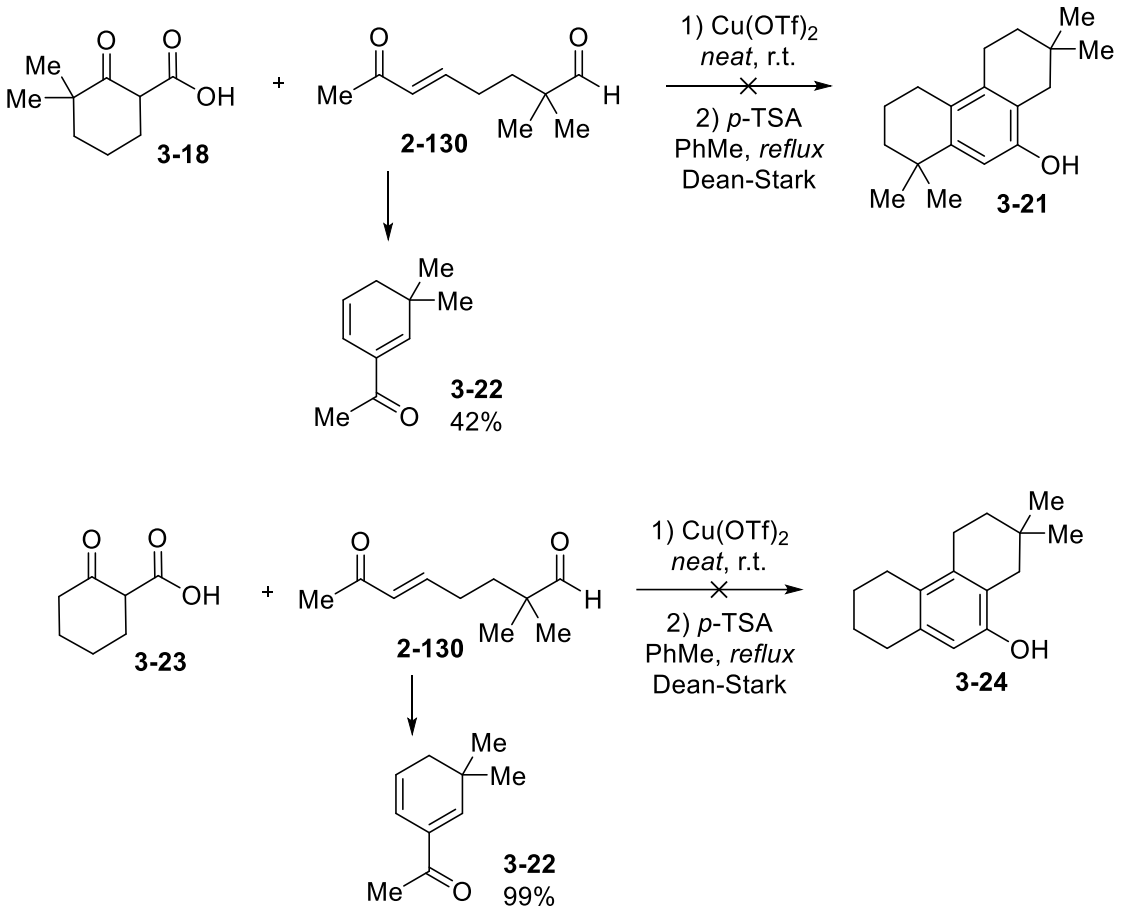

Figure III.9 Attempted decarboxylative cascade to construct aspewentin.

Intending that the Michael reaction with an alkyne rather than alkene-containing acceptors may proceed faster, a decarboxylative Michael approach implementing ynones and keto-acids was investigated (Figure III.10). To test this hypothesis, model ketoacid **3-23** and ynone **3-25** were subjected to $Cu(OTf)_2$ (0.3 equiv.). The anticipated Cu(II)-Michael process would lead to the initial formation of intermediate **3-26** followed by its decarboxylation to **3-27**. Intermediate **3-27** was then expected to provide an aromatized product **2-29** via deprotonation of aldol condensation intermediate **2-28**. However, a bicyclic side-product assigned to be compound **2-30** was observed. Similarly, when the corresponding *gem*-dimethyl donor **3-18** was implemented in this process, no formation of aromatized product **3-31** was observed.

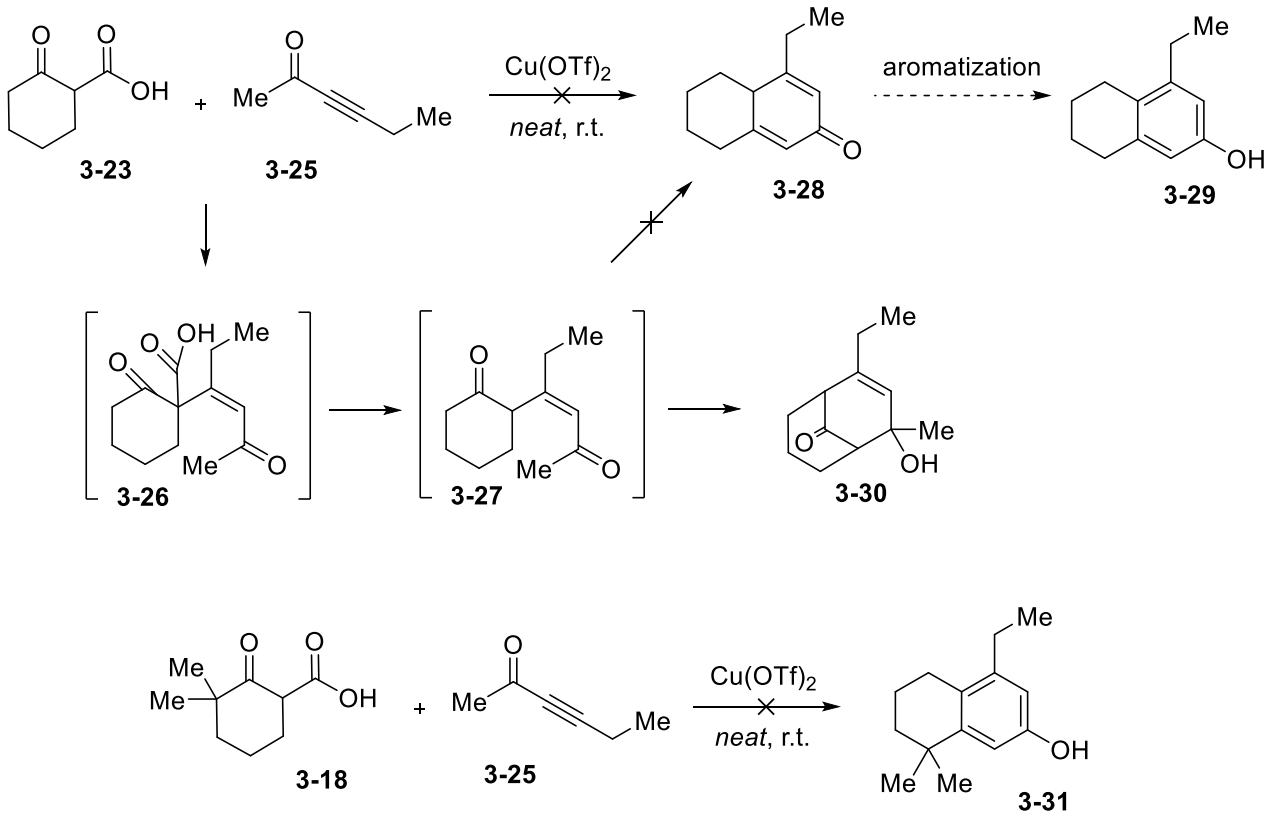

Figure III.10 Decarboxylative Cu(II)-catalyzed coupling of ynones and keto-acids.

Surmising that a simple Mukaiyama variant of a Michael reaction may also produce precursor **3-20** (Figure III.7), the possibility of utilizing this reaction was investigated next (Figure III.11). Successful application of silyl enol ether **3-32** and **2-21** to this process, followed by a double aldol/tautomerization event would directly furnish (±)-aspewentin A (**(±)-1-16**) via intermediate **3-33**.

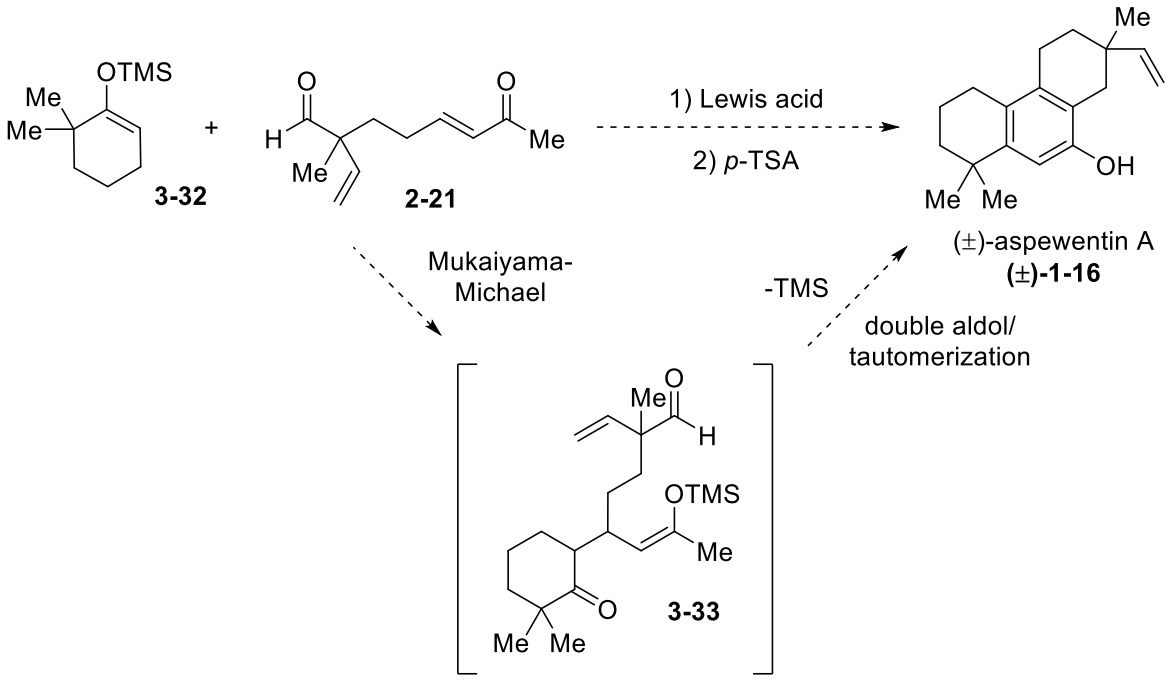

Figure III.11 Mukaiyama-Michael approach to (±)-aspewentin A (**(±)-1-16**).

To achieve the synthesis of **3-36**, alcohol **2-139** was oxidized using DMP (1.2 equiv.) and pyridine (2.2 equiv.) in DCM and the resulting crude was subjected to 2-methoxy-1,3-dioxolane (**3-34**) and ethylene glycol under acidic conditions to yield dioxolane **3-35** in 65% yield (Figure III.12). Ruthenium cross-coupling using Grubbs 2nd generation catalyst (**1-141**) synthesized Michael acceptor **3-36** in 64% yield via from ketone **2-141** and dioxolane **3-35**. Silyl enol ether **3-32** was produced from ketone **3-15** by deprotonation with LDA and then stirred with TMSCl in THF to provide product **3-32** in quantitative yield (Figure III.13).

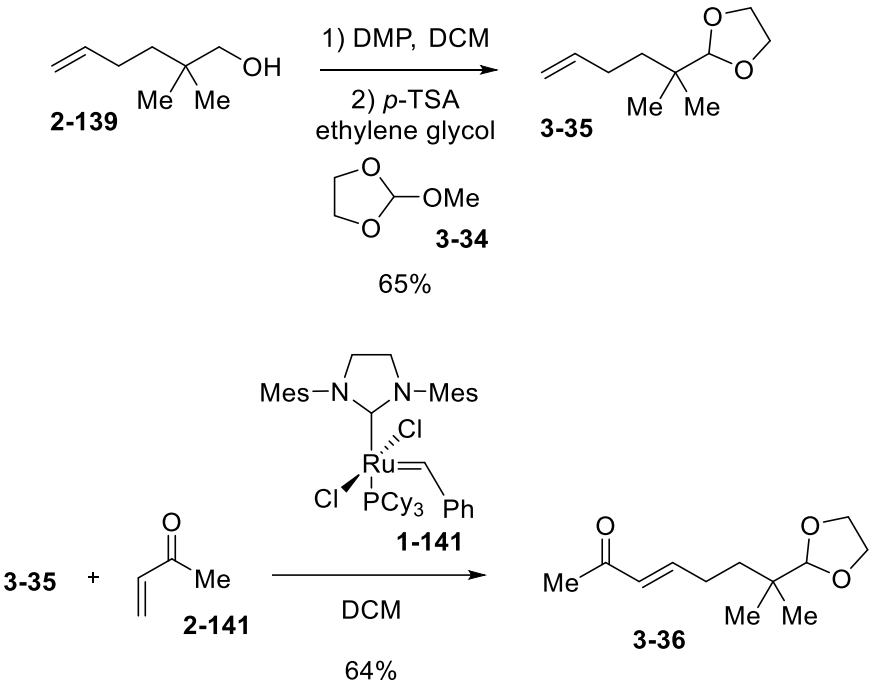

Figure III.12 Synthesis of acceptor **3-36**.

When the Mukaiyama-Michael of silyl enol ether **3-32** and acceptors **3-36** or **2-130** was initiated with either $TiCl_4$ or $Zn(OTf)_2$ at –78 °C only complex mixtures were observed and no desired Michael products were isolated.

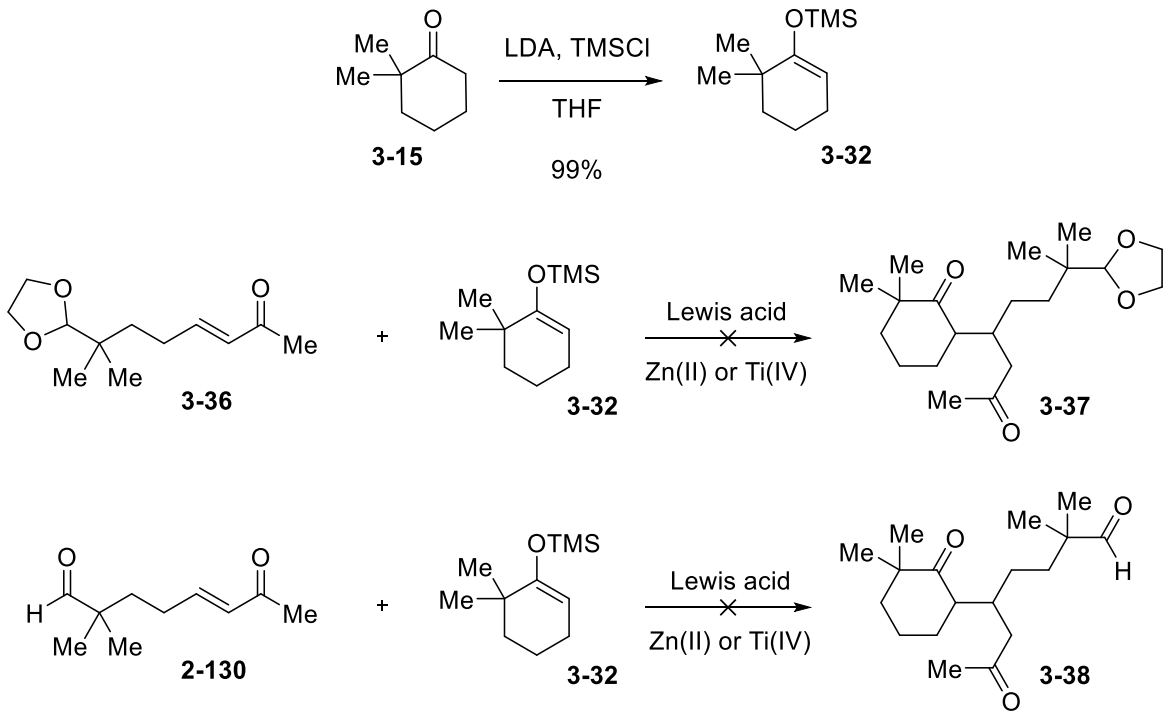

Figure III.13 Reactivity of silyl ether donor **3-32**.

Considering that the Cu(II)-catalyzed Michael reaction of **2-22** and aldehyde-containing enone **2-21** were successfully coupled to produce tricyclic skeleton **2-25**, our final third-generation approach focused on achieving a similar transformation between keto-ester **3-14** and enone **2-21** (Figure III.14). The successful coupling of 3-14 and 2-21 would result in advanced intermediate 3-31, which could then be subjected to decarboxylative aromatization to yield (±)-aspewentin A

((±)-**1-16**). However, the low yields previously observed with **3-14** prompted us to investigate non-classical methods for achieving more efficient Michael reactions.

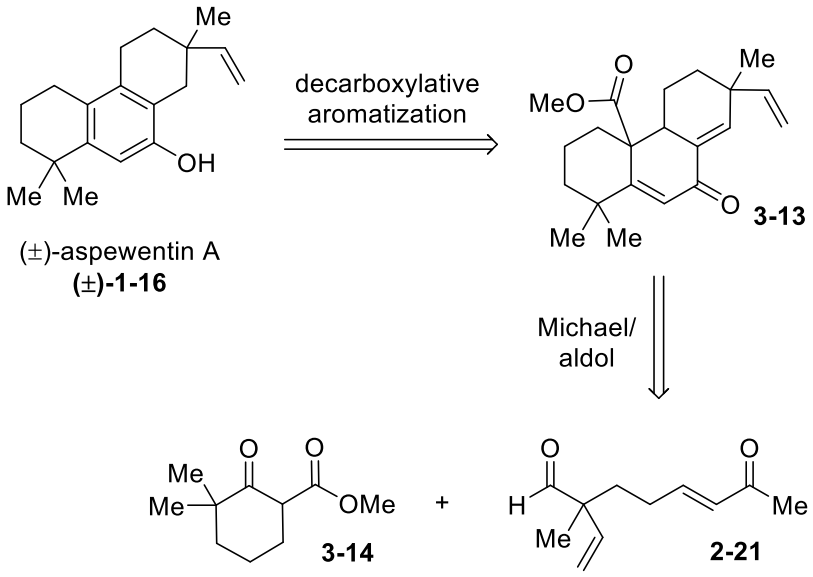

Figure III.14 Third-generation retrosynthetic analysis of (±)-aspewentin A (**(±)-1-16**).

Analogous Michael-aldol processes, yielding compact carbocyclic products that implemented β,β'-disubstituted Michael acceptors have been known to proceed efficiently at 15 kbar of pressure.[141] The effect of high-pressures in organic synthesis is rationalized by a shift in the equilibrium position for processes based on differences in the volumes of the starting materials to products but also the catalytic effects on reactivity as described by the volume of activation for reaction transition states.[142,143] Notably, cyclic β,β'-disubstituted Michael acceptors and $MeNO_2$ as nucleophilic donor has also been found to enantioselectively couple in the presence of an organocatalyst at 10 kbar of pressure.[144] In attempt to activate our C-C bond forming process, donor **3-14** and acceptor **2-28** were reacted with $Cu(OTf)_2$ (0.3 equiv.) under 60,000 psi (4.1 kbar) of pressure (Figure III.15). Although this model system did appear to show a slight increase in the yield of the desired adduct **3-39** at the increased pressure, a switch to more functionally complex

substrate **2-21** was not found to increase yield at these pressures. However, it should be noted that higher reaction pressures, such as 10 kbar or 15 kbar, may still prove useful in enabling synthesis of this hindered scaffold, despite prior literature examples not incorporating functionally complex substrates. Separately, $Mn(OAc)_3$ was utilized in the presence of donor **3-18** and acceptor **2-28** to form a radical intermediate from donor **3-18** and enable a radical addition pathway with **2-28** and provide product **3-39** following a terminating HAT process.[145,146] The reaction was found not to proceed in MeCN but gave trace product **3-39** in EtOH at ambient conditions. The addition of catalytic $Cu(OTf)_2$ did not improve the results of the intended radical addition process.

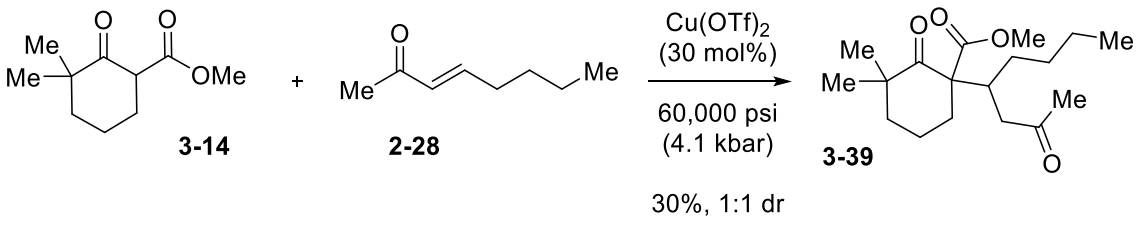

Figure III.15 High-pressure synthetic approach.

III.3 Total Synthesis of (±)-Aspewentin A ((±)-1-16)

This Michael-aldol process continued to reflect the steric challenges associated with *gem*-dimethyl donor **3-14** as its reaction with acceptor **2-130** in the presence of $Cu(OTf)_2$ (0.3 equiv.) under *neat* conditions to form intermediate **3-40**, followed by dehydrating conditions of catalytic *p*-TSA (0.3 equiv.) in refluxing PhMe at 110 °C with a Dean-Stark trap for the azeotropic removal

of water to give tricyclized product **3-42** in 16% and 1:1 dr via aldol intermediate **3-41** (Figure 111.16).

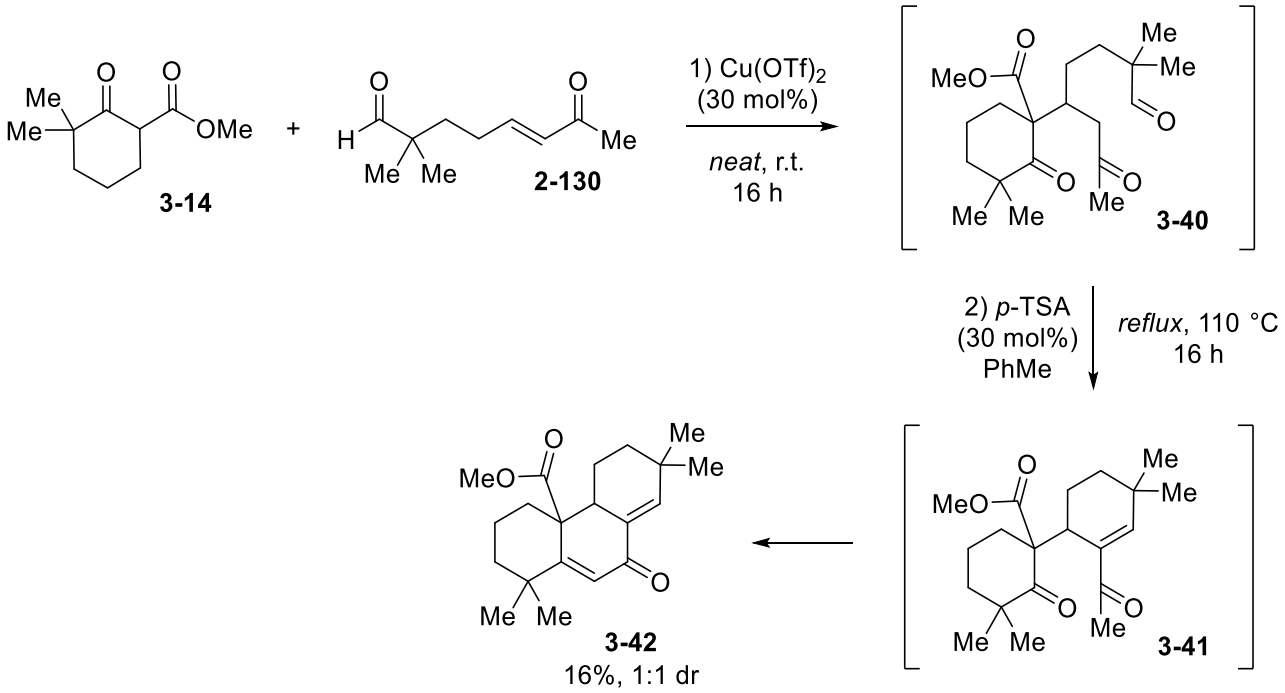

Figure III.16 Synthesis of model intermediate **3-42**.

In attempts to optimize this process, *gem*-dimethyl donor **3-14** and acceptor **2-130** were treated with $Cu(OTf)_2$ (0.3 equiv.) under *neat* conditions to form intermediate **3-40**, which was followed by basic conditions to achieve the aldol reaction. Under these conditions, both the double-dehydration product **3-42** and mono-dehydration product **3-42** were isolated from the mixture (Table III.2). When donor **3-14** (1.2 equiv.) and acceptor **2-130** (1.0 equiv.) were treated with $Cu(OTf)_2$ (0.3 equiv.) under *neat* conditions, followed by LiHMDS (2.0 equiv.) in THF or Cs_2CO_3 (2.0 equiv.) in DMF and heated to reflux, **3-42** can be isolated in 13–17% yield and **3-43** in 5–14% yield (entry 1–4). The combined yields of **3-42** and **3-43** indicate that there are no significant advantages of one set of conditions versus the others; however, further optimization may enhance these yields.

Table III.2 Base-mediated aldol approach.

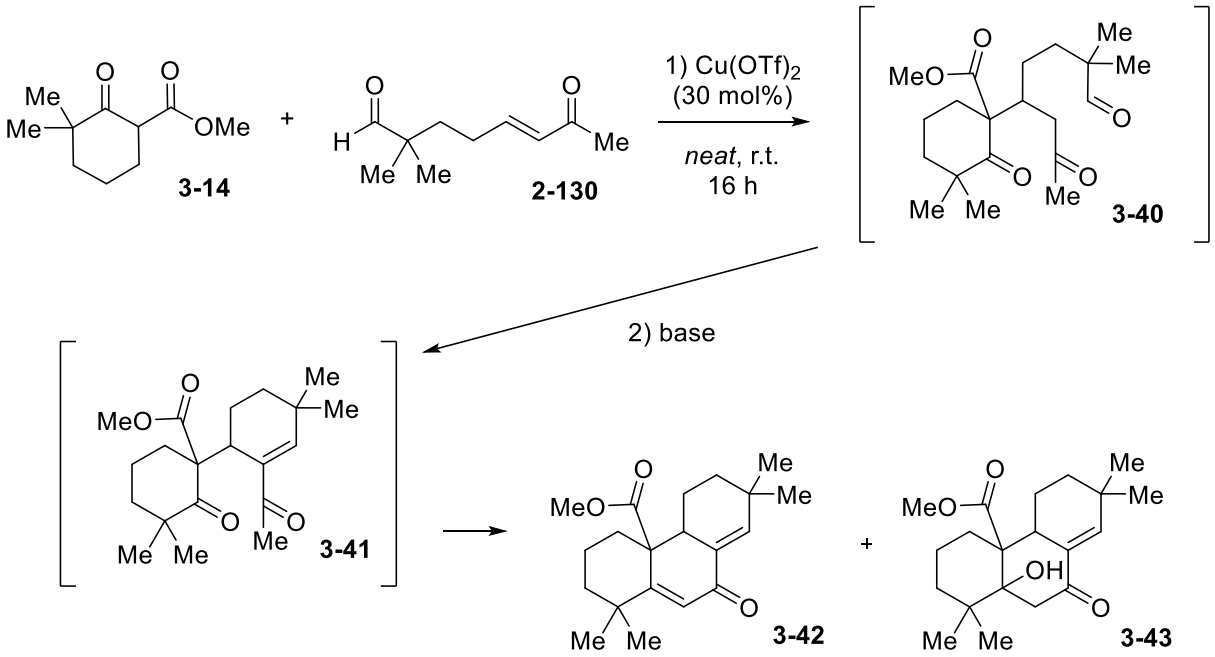

entry	base	solvent	**3-14**	temperature	time	yield
1	LiHMDS (2.0 equiv.)	THF	1.2 equiv.	*reflux* (80 °C)	1 h	**3-42**: 15% **3-43**: 5%
2	LiHMDS (2.0 equiv.)	THF	1.2 equiv.	*reflux* (80 °C)	16 h	**3-42**: 14% **3-43**: 9%
3	Cs_2CO_3 (2.0 equiv.)	DMF	1.2 equiv.	*reflux* (180 °C)	1 h	**3-42**: 17% **3-43**: 7%
4	Cs_2CO_3 (2.0 equiv.)	DMF	1.2 equiv.	*reflux* (180 °C)	16 h	**3-42**: 13% **3-43**: 14%

With advance intermediate **3-42** in hand, its decarboxylative aromatization was attempted using DMSO heated to 180 °C and excess LiCl (Figure III.17). Although **3-42** lacks a γ-oxo moiety that reduced the barrier for decarboxylation, product phenol **3-47** was still isolated in 35% yield. Following the previously stated mechanistic hypothesis, the decarboxylation process would first be mediated by a nucleophilic displacement of the methyl group to generate carboxylate **3-44**

before the decarboxylative aromatization step generates the phenolate resonance pairs **3-45** and **3-46**. The protonation of phenolate **3-46** then provides the observed product **3-47**. The diminished yield of this decarboxylative aromatization when compared to the example presented in the prior chapter was attributed to the steric impedance associated with the *gem*-dimethyl substitution pattern, but also the loss of electronic demand associated with the dione substrate **2-183** (Figure II.37).

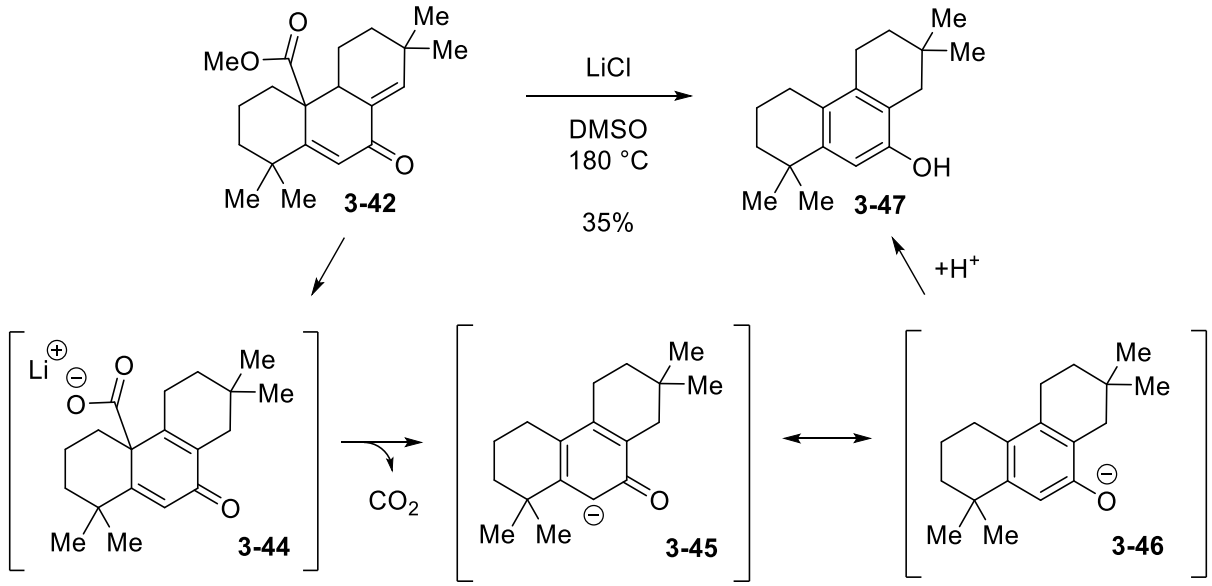

Figure III.17 Decarboxylative aromatization leading to phenol **3-47**.

Provided the successful aromatization of the model intermediate **3-42**, we next explored conditions directly leading to (±)-aspewentin A (**(±)-1-16**) by implementing acceptor **2-21** and donor **3-14** to the Cu(II)-Michael and aldol process (Figure III.18). When donor **3-14** and acceptor **2-21** were stirred *neat* in the presence of $Cu(OTf)_2$ (0.3 equiv.) to generate intermediate **3-48**, followed by dehydrating conditions of catalytic *p*-TSA (0.3 equiv.) in refluxing PhMe at 110 °C with a Dean-Stark trap for the azeotropic removal of water, the desired dehydrated aldol product **3-13** was obtained in 9% yield and 1.4:1 dr. However, if the crude product mixture from this aldol

process was subjected to the decarboxylative aromatization step with DMSO at 180 °C and excess LiCl, this protocol directly furnished (±)-aspewentin A (**(±)-1-16**) in 2% yield over the three steps. Although this synthetic route enables the rapid generation of complex molecular architecture, the yield of (±)-aspewentin A (**(±)-1-16**) was likely impacted by the steric impedance of Michael donor **3-14** as well as the chemical reactivity of the vinylic substituent of Michael acceptor **2-21**, often not present during the prior model studies. Spectral features of the newly synthesized (±)-aspewentin A (**(±)-1-16**) matched those of both previously reported natural and synthetically generated aspewentin A.[35,95]

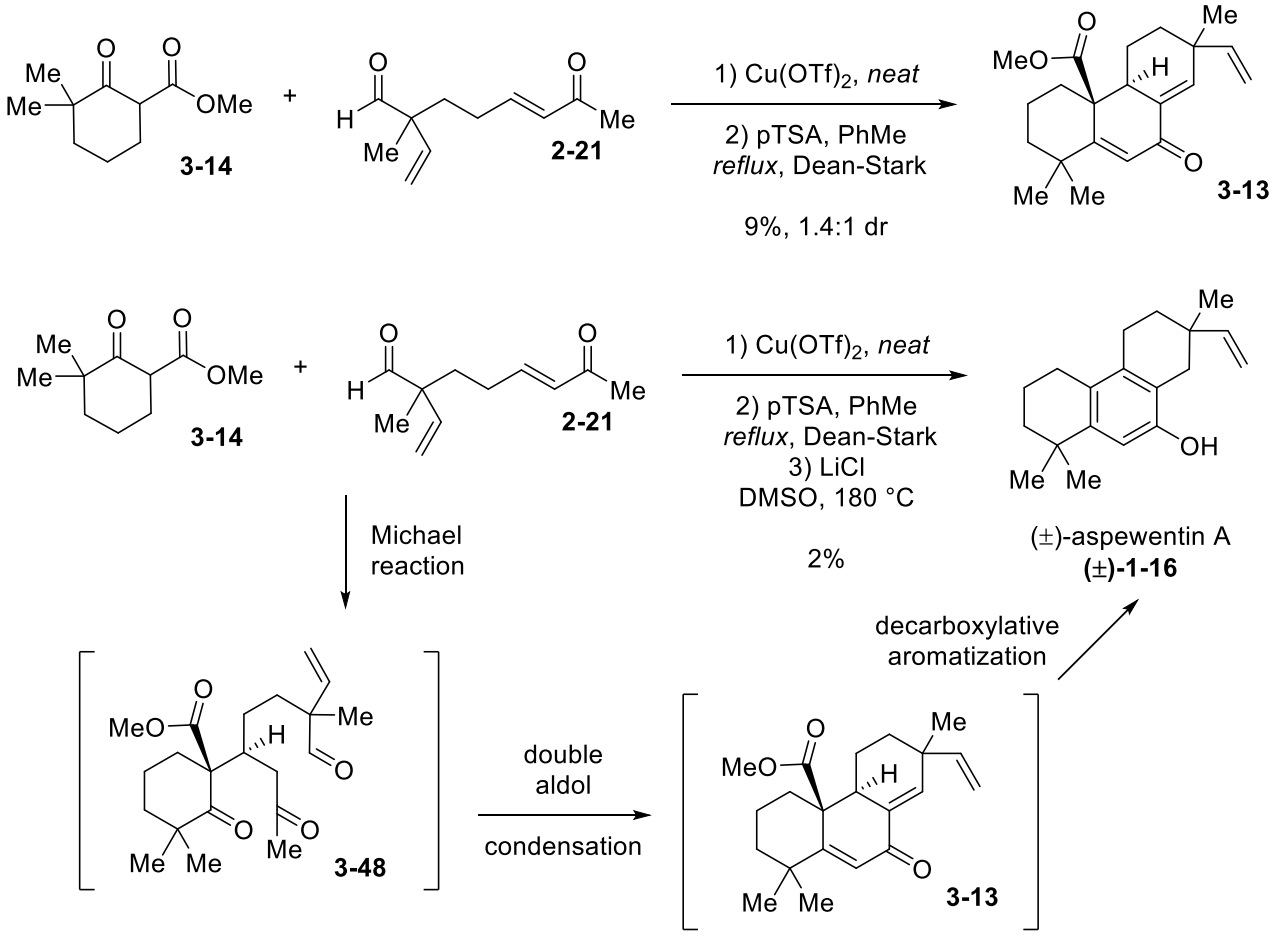

Figure III.18 Key cyclization generating (±)-aspewentin A (**(±)-1-16**).

III.4 Conclusion/Summary

Thus, a tandem Cu(II)-Michael/aldol strategy to rapidly access highly congested carbocycles was applied for the total synthesis of (±)-aspewentin A (**(±)-1-16**). The key synthetic reaction was achieved using $Cu(OTf)_2$ as the catalyst under *neat* conditions to enable an initial C-C bond formation and then condense the intermediate to generate a highly substituted fused tricycle under the dehydrative aldol conditions. This newly established route to access (±)-aspewentin A (**(±)-1-16**) can potentially be made enantioselective by enantioenriching Michael acceptor **2-21**. Previous work in our group by Brian Larsen has established a synthetic pathway to **(*R*)-2-21** via diastereoselective synthesis of intermediate amide **3-51** from butenamide **3-49** and iodoalkane **3-50** (Figure III.19).[147] Implementation of **(*R*)-2-21** in the described synthetic pathway offers rapid access to natural, enantioenriched (+)-aspewentin A (**1-16**).

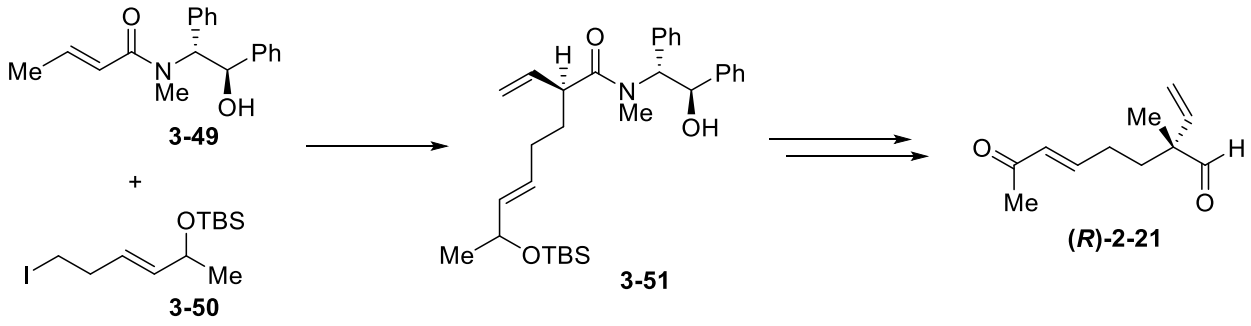

Figure III.19 Precedent synthesis of enantioenriched Michael acceptor **(*R*)-2-21**.

During the total synthesis of (±)-aspewentin A (**(±)-1-16**), establishing a synthetic route to racemic **2-21** became necessary to enable synthetic studies on the isopimarane scaffold. Although the vinylic scaffold appeared to tolerate the Rh-mediated allylic oxidation chemistry, the high temperature reflux associated with the Krapcho conditions in DMSO may have impacted the viability of this synthetic pathway. The final yield resulting from each decarboxylative aromatization pathway may be improved if either the proper alkenyl masking group is applied or

if an appropriate nucleophile can enable the process of ester demethylation under more mild conditions. An alternative to the Rh-oxidation pathway was the direct implementation of a *gem*-dimethyl donor to the Cu(II)-Michael and aldol cascade. Although the *gem*-dimethyl substitution pattern was expected to inhibit the reactivity of these processes it would circumvent the issues associated with alternative functionalization of the tricyclic intermediate, as described in the prior chapter and in implementation of acceptor **2-21** to this chemistry. Several alternative synthetic strategies to better enable the C-C coupling of the initial Michael process were investigated but none were found to significantly enable the desired process using a *gem*-dimethyl donor. By directly implementing donor **3-14** and acceptor **2-21** in the tandem Michael, aldol, and decarboxylative process (±)-aspewentin A (**(±)-1-16**) can be synthesized in 8 overall steps in a convergent manner. Establishment of this synthetic methodology helps to improve the general accessibility to these structures and to possible structural analogues that may be desirable for therapeutic or other industrial applications. The development of novel synthetic approaches may also help to better inform the next generation of improved synthetic pathways to these aspewentins and other desirable isopimaranes.

III.5 Graphical Summary

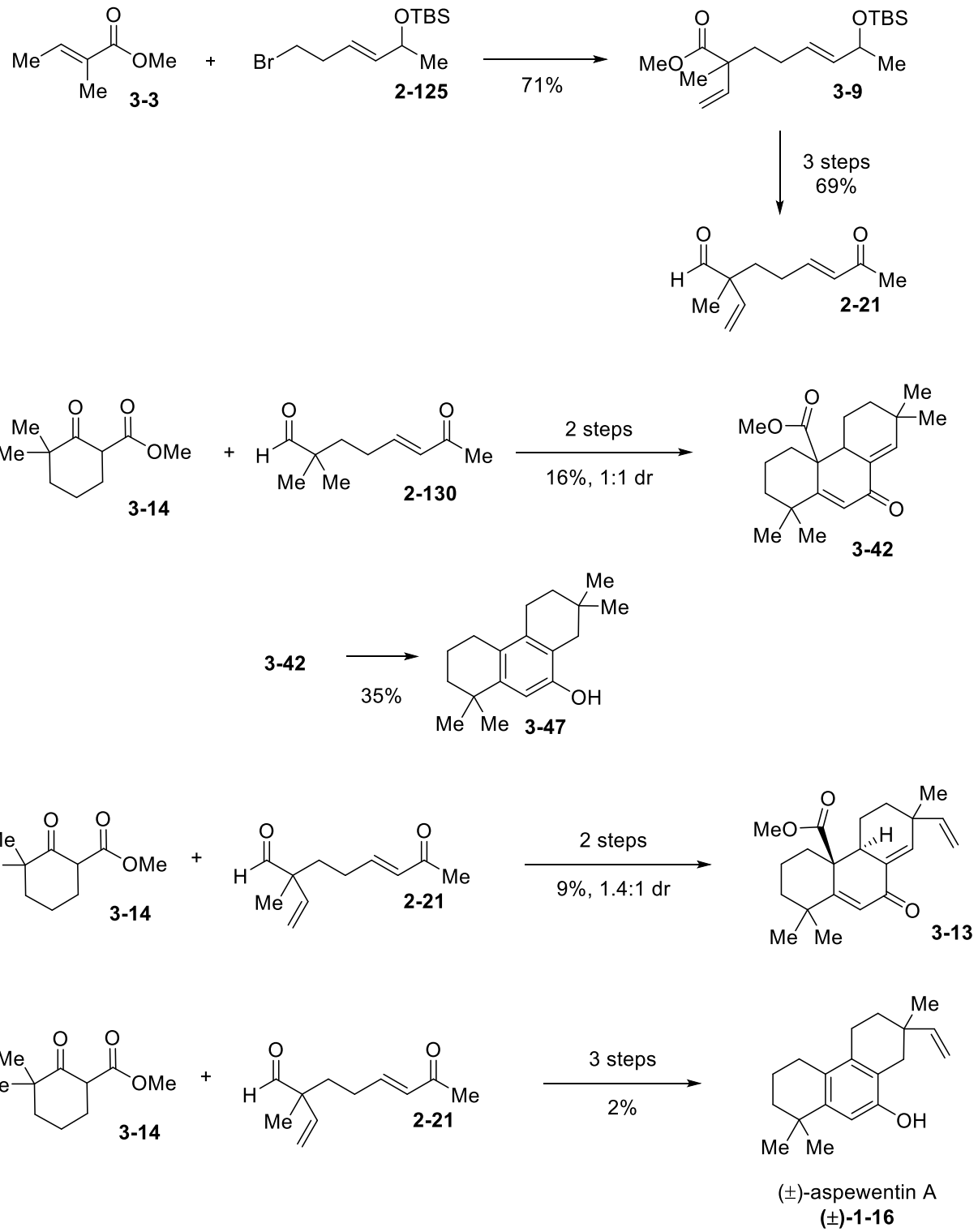

III.6 Experimental

Methods and Reagents:

Unless otherwise stated, all reagents and solvents were purchased from commercial sources and were used as received without further purification unless otherwise specified. DCM, DMF, Et_2O, THF, PhMe, were purified by Innovative Technology's Pure-Solve System using basic alumina. All reactions were carried out under a positive pressure of nitrogen in flame- or oven-dried glassware with magnetic stirring. Reactions were cooled using an external cooling bath of ice water (0 °C), sodium chloride/ice water (–20 °C), dry ice/acetonitrile (–40 °C), or dry ice/acetone (–78 °C). Heating was achieved by use of a silicone oil bath with heating controlled by an electronic contact thermometer. Deionized water was used in the preparation of all aqueous solutions and for all aqueous extractions. Solvents used for extraction and chromatography were ACS or HPLC grade. Purification of reaction mixtures was performed by flash chromatography using SiliCycle SiliaFlash P60 (230-400 mesh). Yields indicate the isolated yield of the title compound with ≥95% purity as determined by ^{1}H NMR analysis. Diastereomeric ratios were determined by ^{1}H NMR analysis. ^{1}H NMR spectra were recorded on a Varian vnmrs 700 (700 MHz), 600 (600 MHz), 500 (500 MHz), 400 (400 MHz), Varian Inova 500 (500 MHz), or a Bruker Advance Neo 500 (500 MHz) spectrometer and chemical shifts (δ) are reported in parts per million (ppm) with solvent resonance as the internal standard ($CDCl_3$ at δ 7.26, CD_3OD at δ 3.31, C_6D_6 at δ 77.06). Tabulated 1H NMR Data are reported as s = singlet, d = doublet, t = triplet, q = quartet, qn = quintet, sext = sextet, m = multiplet, ovrlp = overlap, and coupling constants in Hz. Proton-decoupled ^{13}C NMR spectra were recorded on Varian vnmrs 700 (700 MHz) spectrometer and chemical shifts (δ) are reported in ppm with solvent resonance as the internal standard ($CDCl_3$ at δ 77.16, CD_3OD at δ 49.0, C_6D_6 at δ 128.1). High resolution mass spectra (HRMS) were performed and recorded on

Micromass AutoSpec Ultima or VG (Micromass) 70-250-S Magnetic sector mass spectrometers in the University of Michigan mass spectrometry laboratory. Infrared (IR) spectra were recorded as thin films a Perkin Elmer Spectrum BX FT-IR spectrometer. Absorption peaks are reported in wavenumbers (cm^{-1}).

Instrumentation:

All spectra were recorded on Varian vnmrs 700 (700 MHz), Varian vnmrs 500 (500 MHz), Varian MR400 (400 MHz), Varian Inova 500 (500 MHz) spectrometers and chemical shifts (δ) are reported in parts per million (ppm) and referenced to the ^1H signal of the internal tetramethylsilane according to IUPAC recommendations. Data are reported as (br = broad, s = singlet, d = doublet, t = triplet, q = quartet, qn = quintet, sext = sextet, m = multiplet; coupling constant (*S*) in Hz; integration). High resolution mass spectra (HRMS) were recorded on MicromassAutoSpecUltima or VG (Micromass) 70-250-S Magnetic sector mass spectrometers in the University of Michigan mass spectrometry laboratory. Infrared (IR) spectra were recorded as thin films on NaCl plates on a Perkin Elmer Spectrum BX FT-IR spectrometer. Absorption peaks were reported in wavenumbers (cm^{-1}).

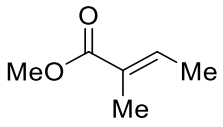

Methyl (*E*)-2-methylbut-2-enoate (3-3): A flame-dried round bottom flask was charged with K_2CO_3 (45.55 g, 329.60 mmol, 1.10 equiv.) and wetted with DMF (600 mL) and H_2O (60 mL). Compound **3-2** (30.00 g, 299.64 mmol, 1.00 equiv.) was added to the heterogeneous mixture and allowed to stir for 30 minutes at room temperature. The reaction flask was then cooled to 0 °C and

MeI (20.52 mL, 329.60 mmol, 1.10 equiv.) was slowly added to the reaction flask with vigorous stirring. The contents were left to slowly warm to room temperature and left to stir for 16 h. The reaction was then partitioned with Et_2O (50 mL) and aqueous layer was adjusted to pH 7 using 5% HCl and then extracted with Et_2O (3x 30 mL). The organic layer was washed with 1:1 $NaHCO_3$ (sat.): NaCl (sat.) (5x 20 mL), dried over Na_2SO_4, decanted, and then slowly concentrated *in vacuo*. The crude material was purified by column chromatography with 10% to 75% Et_2O/hexanes. (23.23 g, 203.49 mmol, 68%).

^{1}H NMR (600 MHz, $CDCl_3$) δ 6.82 (q, J = 7.0 Hz, 1H), 3.70 (s, 3H), 1.80 (s, 3H), 1.76 (d, J = 7.0 Hz, 3H).

HRMS (ESI-TOF) $[M+Na]^+$ m/z: calcd for $C_6H_{10}O_2$ 137.0578; Found 137.0585.

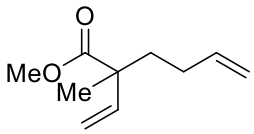

Methyl 2-methyl-2-vinylhex-5-enoate (3-4): A flame-dried round bottom flask was charged with prepared LDA (17.52 mmol, 1.0 equiv.), HMPA (4.0 mL), ans THF (40 mL) at –78 °C. Compound **3-3** (2.00 g, 17.52 mmol, 1.0 equiv.) was then added to the cooled solution of LDA dropwise over the course of 5 minutes. The reaction flask was warmed to 0 °C and allowed to stir for 30 minutes and then cooled again to –78 °C. Compound **2-123** (1.83 mL, 17.52 mmol, 1.0 equiv.) was added to the cooled solution dropwise. The contents were left to slowly warm to room temperature and left to stir for 16 h. The reaction was then quenched with NH_4Cl (sat.) and extracted with EtOAc (3x 20 mL). The organic layer was washed with NH_4Cl (sat.) (2x 20 mL), NaCl (sat.) (2x 20 mL),

dried over Na_2SO_4, decanted, and then concentrated *in vacuo*. The crude material was purified by column chromatography with 10% to 33% EtOAc/hexanes. (2.95 g, 14.79 mmol, 84%).

^{1}H NMR (500 MHz, $CDCl_3$) δ 6.02 (dd, J = 17.5, 10.8 Hz, 1H), 5.78 (ddt, J = 16.8, 10.1, 6.5 Hz, 1H), 5.12 (d, J = 8.8 Hz, 1H), 5.09 (d, J = 15.5 Hz, 1H), 5.01 (dq, J = 17.2, 1.7 Hz, 1H), 4.96 – 4.91 (m, 1H), 3.68 (s, 3H), 2.65 (d, J = 9.3 Hz, 2H), 2.07 – 1.91 (m, 2H), 1.86 – 1.77 (m, 1H), 1.69 (dd, J = 11.4, 5.3 Hz, 1H), 1.29 (s, 3H).

HRMS (ESI-TOF) $[M+H]^+$ m/z: calcd for $C_{10}H_{16}O_2$ 169.1223; Found 169.1227.

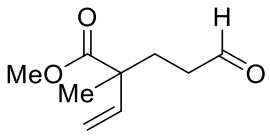

Methyl 2-methyl-5-oxo-2-vinylpentanoate (3-5): A flame-dried round bottom flask was charged with $K_2[OsO_2(OH)_4]$ (0.02 g, 0.06 mmol, 0.02 equiv.) under the inert atmosphere of a glove box. The flask was removed from the glove box and its solid material was dissolved in 4:1 1,4-dioxane/ H_2O (25 mL) and cooled to 0 °C. Compound **3-4** (0.50 g, 2.97 mmol, 1.0 equiv.) and 98% 2,6-lutidine (1.40 mL, 11.89 mmol, 4.0 equiv.) were added to the reaction flask followed by $NaIO_4$ (1.27 g, 5.94 mmol, 2.0 equiv.) at 0 °C. The reaction flask was allowed to slowly warm to room temperature and left to stir at room temperature for 6 h. DCM (20 mL) was used to partition the organic materials into an organic layer. The organic layer was isolated, washed by NaCl (sat.) (2x 5 mL), dried over Na_2SO_4, decanted, and then concentrated *in vacuo*. The crude material was purified by column chromatography with 10% to 33% EtOAc/hexanes. (0.13 g, 0.74 mmol, 25%).

^{1}H NMR (400 MHz, $CDCl_3$) δ 9.75 (s, 1H), 5.96 (dd, J = 17.5, 10.7 Hz, 1H), 5.16 (dd, J = 10.8, 0.7 Hz, 1H), 5.11 (dd, J = 17.5, 0.7 Hz, 1H), 3.68 (s, 3H), 2.47 – 2.39 (m, 2H), 2.00 (qdd, J = 14.0, 9.1, 6.4 Hz, 2H), 1.28 (s, 3H).

HRMS (ESI-TOF) $[M+H]^+$ m/z: calcd for $C_9H_{14}O_3$ 171.1016; Found 171.1028.

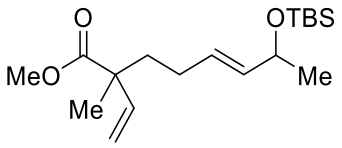

Methyl (*E*)-7-((*tert*-butyldimethylsilyl)oxy)-2-methyl-2-vinyloct-5-enoate (3-9): A flame-dried round bottom flask was charged with prepared LDA (10.22 mmol, 3.0 equiv.), HMPA (2.0 mL), and THF (30 mL) at –78 °C. Compound **3-3** (1.16 g, 10.22 mmol, 3.0 equiv.) was then added to the cooled solution of LDA dropwise. The reaction flask was warmed to 0 °C and allowed to stir for 30 minutes and then cooled again to –78 °C. Compound **2-125** (1.0 g, 3.41 mmol, 1.0 equiv.) was added to the cooled solution dropwise. The contents were left to slowly warm to room temperature and left to stir for 16 h. The reaction was then quenched with NH_4Cl (sat.) and extracted with EtOAc (3x 20 mL). The organic layer was washed with NH_4Cl (sat.) (2x 10 mL), NaCl (sat.) (2x 10 mL), dried over Na_2SO_4, decanted, and then concentrated *in vacuo*. The crude material was purified by column chromatography with 10% to 33% EtOAc/hexanes. (0.80 g, 2.42 mmol, 71%).

^{1}H NMR (500 MHz, $CDCl_3$) δ 6.33 (dt, J = 16.8, 10.3 Hz, 1H), 6.16 (dd, J = 15.3, 10.5 Hz, 1H), 5.72 (dd, J = 15.3, 5.6 Hz, 1H), 5.18 (d, J = 15.1 Hz, 2H), 5.05 (d, J = 9.2 Hz, 1H), 3.74 (s, 3H), 1.86 (m, 4H), 1.85 (m, 5H), 1.80 (dt, J = 7.1, 1.0 Hz, 2H), 1.29 (d, J = 7.2 Hz, 2H), 1.24 (d, J = 6.3 Hz, 3H), 0.91 (s, 9H), 0.07 (s, 6H).

^{13}C NMR (176 MHz, $CDCl_3$) δ 175.3, 143.3, 133.7, 130.8, 114.8, 70.2, 52.6, 42.5, 36.6, 31.2, 25.9, 24.8, 24.8, 24.8, 24.0, 17.8, -4.9, -4.9.

HRMS (ESI-TOF) $[M+H]^+$ m/z: calcd for $C_{18}H_{34}O_3Si$ 327.2355; Found 327.2353.

IR (film, cm^{-1}) 1260, 1720, 2860, 2910, 2930, 2960.

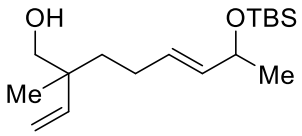

(*E*)-7-((*tert*-Butyldimethylsilyl)oxy)-2-methyl-2-vinyloct-5-en-1-ol (3-10): A flame-dried round bottom flask was charged with 95% LAH (0.18 g, 4.44 mmol, 2.0 equiv.) and Et_2O (15 mL) and cooled to 0 °C. Compound **3-9** (0.73 g, 2.22 mmol, 1.0 equiv.) was added dropwise to the cooled mixture over the course of 5 minutes. The reaction mixture was allowed to slowly warm to room temperature with vigorous stirring while being monitored for uncontrolled production of hydrogen gas byproduct. The contents were left to stir at room temperature for 4 h. The reaction was then cooled to 0 °C and DI H_2O was slowly added dropwise to the reaction mixture until bubbling slows. Then, NH_4Cl (sat.) was added to the reaction mixture slowly until bubbling stops and aluminum clumping is dispersed. The organic layer was washed by NaCl (sat.) (2x 10 mL), dried over Na_2SO_4, decanted, and then concentrated *in vacuo*. The crude material was purified by column chromatography with 10% to 33% EtOAc/hexanes. (0.62 g, 2.07 mmol, 93%).

^{1}H NMR (500 MHz, $CDCl_3$) δ 5.73 (dd, J = 17.6, 10.9 Hz, 1H), 5.54 (dt, J = 15.5, 6.5 Hz, 1H), 5.45 (dd, J = 15.3, 5.6 Hz, 1H), 5.19 (d, J = 10.9 Hz, 1H), 5.07 (d, J = 17.6 Hz, 1H), 4.25 (p, J = 5.9 Hz, 1H), 3.41 (d, J = 10.6 Hz, 1H), 3.36 (d, J = 10.6 Hz, 1H), 2.03 – 1.90 (m, 2H), 1.46 – 1.35 (m, 3H), 1.19 (d, J = 6.3 Hz, 3H), 1.04 (s, 3H), 0.90 (s, 9H), 0.06 (d, J = 3.9 Hz, 6H).

^{13}C NMR (176 MHz, $CDCl_3$) δ 143.7, 134.0, 131.1, 114.8, 72.7, 70.6, 42.5, 36.9, 31.2, 25.9, 24.9, 24.9, 24.9, 24.0, 22.6, 17.8, -4.9, -4.9.

HRMS (ESI-TOF) $[M+H]^+$ m/z: calcd for $C_{17}H_{34}O_2Si$ 299.2406; Found 299.2398.

IR (film, cm^{-1}) 2860, 2880, 2900, 2930, 2960.

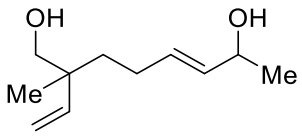

(*E*)-2-Methyl-2-vinyloct-5-ene-1,7-diol (3-8): A flame-dried round bottom flask was charged with compound **3-10** (0.98 mg, 3.27 mmol, 1.0 equiv.) in THF (5.0 mL) and cooled to 0 °C. 1M TBAF (11.46 mL, 11.46 mmol, 3.5 equiv.) was added to the cooled mixture. The reaction flask was allowed to slowly warm to room temperature and left to stir at room temperature for 16 h. NH_4Cl (sat.) was added to quench the reaction mixture. Et_2O (10 mL) was used to partition the organic materials into an organic layer. The organic layer was isolated, washed by NaCl (sat.) (2x 5 mL), dried over Na_2SO_4, decanted, and then concentrated *in vacuo*. The crude material was purified by column chromatography with 10% to 33% EtOAc/hexanes. (0.54 g, 2.95 mmol, 90%).

^{1}H NMR (500 MHz, $CDCl_3$) δ 5.70 (dd, J = 17.6, 10.9 Hz, 1H), 5.62 (dt, J = 15.3, 6.6 Hz, 1H), 5.51 (dd, J = 15.4, 6.6 Hz, 1H), 5.17 (d, J = 10.9 Hz, 1H), 5.05 (d, J = 17.7 Hz, 1H), 4.24 (p, J = 6.4 Hz, 1H), 3.39 (d, J = 10.6 Hz, 1H), 3.34 (d, J = 10.6 Hz, 1H), 1.97 (tt, J = 13.8, 7.0 Hz, 2H), 1.58 (s, 1H), 1.54 (s, 1H), 1.46 – 1.34 (m, 2H), 1.24 (d, J = 6.4 Hz, 3H), 1.01 (s, 3H).

^{13}C NMR (126 MHz, $CDCl_3$) δ 143.7, 134.0, 131.1, 114.8, 70.1, 68.9, 42.2, 36.5, 26.5, 23.4, 19.6.

HRMS (ESI-TOF) $[M+Na]^+$ m/z: calcd for $C_{11}H_{20}O_2$ 207.1361; Found 207.1367.

IR (film, cm^{-1}) 2920, 2940, 2970, 3260, 3330, 3350.

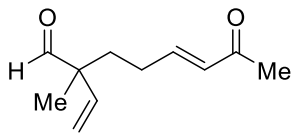

(*E*)-2-Methyl-7-oxo-2-vinyloct-5-enal (2-21): A flame-dried round bottom flask was charged with 95% DMP (3.08 g, 6.90 mmol, 2.6 equiv.) under the inert atmosphere of a glove box. The flask was removed from the glove box and its solid material was dissolved in DCM (25 mL) and cooled to 0 °C. Compound **3-8** (0.49 g, 2.65 mmol, 1.0 equiv.) was added to the cooled mixture followed by a dropwise addition of pyridine (0.86 mL, 10.61 mmol, 4.0 equiv.). The reaction flask was allowed to slowly warm to room temperature and left to stir at room temperature for 16 h. $NaHCO_3$ (sat.) (10 mL) and $Na_2S_2O_3$ (sat.) (10 mL) was added to quench the reaction mixture and left stirring for 30 minutes. The organic layer was washed by $NaHCO_3$ (sat.) (2x 10 mL), NaCl (sat.) (2x 10 mL), dried over Na_2SO_4, decanted, and then concentrated *in vacuo*. The crude material was purified by column chromatography with 10% to 33% EtOAc/hexanes. (0.39 g, 2.17 mmol, 82%).

^{1}H NMR (500 MHz, $CDCl_3$) δ 9.38 (s, 1H), 6.77 (dtd, J = 15.9, 6.8, 2.2 Hz, 1H), 6.08 (dd, J = 15.9, 2.0 Hz, 1H), 5.76 (ddd, J = 17.7, 10.9, 2.2 Hz, 1H), 5.33 (dd, J = 10.8, 2.1 Hz, 1H), 5.16 (dd, J = 17.6, 2.1 Hz, 1H), 2.24 (s, 3H), 2.22 – 2.13 (m, 2H), 1.75 (dt, J = 10.6, 5.7 Hz, 2H), 1.21 (s, 3H).

^{13}C NMR (151 MHz, $CDCl_3$) δ 202.1, 198.6, 147.3, 138.1, 131.6, 117.7, 52.6, 33.6, 27.2, 27.1, 18.0.

HRMS (ESI-TOF) $[M+H]^+$ m/z: calcd for $C_{11}H_{16}O_2$ 181.1229; Found 181.1238.

IR (film, cm^{-1}) 1670, 1720, 2920, 2940, 2950, 2970.

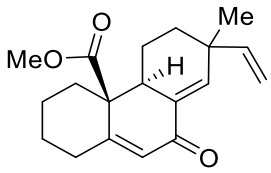

Methyl (4a*S*,4b*S*)-7-methyl-9-oxo-7-vinyl-1,3,4,4b,5,6,7,9-octahydrophenanthrene-4a(2*H*)-carboxylate (2-25): A flame-dried round-bottom flask was charged with 90% compound **2-22** (0.14 g, 0.89 mmol, 1.0 equiv.) and compound **2-21** (0.16 g, 0.89 mmol, 1.0 equiv.). The round-bottom flask was then transferred to a glovebox and 98% $Cu(OTf)_2$ (0.10 g, 0.28 mmol, 0.3 equiv.) was added to the mixture and the contents were removed from the glovebox and left to stir at room temperature under *neat* conditions for 16 h. The crude material was passed through a short silica plug using Et_2O as eluant. The resulting solution was evaporated into a round bottom flask and dissolved in PhMe (10.0 mL), and *p*-TSA (0.03 g, 0.28 mmol, 0.3 equiv.) was added. The reaction flask was equipped with a Dean-Stark trap for the azeotropic removal of water and a reflux condenser to be refluxed at 110 °C for 16 h. The crude material was concentrated *in vacuo* and purified by column chromatography with 10% to 33% EtOAc/hexanes. (0.11 g, 0.37 mmol, 42% yield of 50% purity, 4:1 dr).

^{1}H NMR (500 MHz, $CDCl_3$) δ 6.68 (s, 1H), 6.11 (s, 1H), 5.67 (dd, J = 17.5, 10.5 Hz, 1H), 5.01 (ddd, J = 7.0, 3.4, 1.4 Hz, 1H), 4.73 (dt, J = 17.5, 1.5 Hz, 1H), 3.58 (s, 3H), 2.81 – 2.72 (m, 2H), 2.60 (ddd, J = 13.9, 5.7, 2.8 Hz, 2H), 2.49 – 2.45 (m, 2H), 1.82 – 1.74 (m, 2H), 1.53 – 1.43 (m, 2H), 1.27 (t, J = 7.1 Hz, 2H), 1.15 (s, 3H).

HRMS (ESI-TOF) $[M+H]^+$ m/z: calcd for $C_{19}H_{24}O_3$ 301.1798; Found 301.1806.

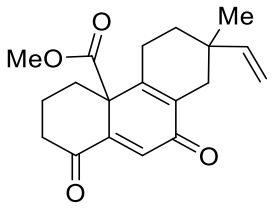

Methyl 7-methyl-1,9-dioxo-7-vinyl-1,3,4,5,6,7,8,9-octahydrophenanthrene-4a(2*H*)-carboxylate (2-178): A flame-dried round-bottom flask was transferred to a glovebox and 97% $Rh_2(cap)_4$ (1.10 mg, 0.002 mmol, 0.01 equiv.) was added, the flask was then removed from the glovebox. Compound **2-25** (50.0 mg, 0.17 mmol, 1.0 equiv.) and DCE (0.6 mL) were added to the reaction flask followed by T-HYDRO (0.18 mL, 1.33 mmol, 8.0 equiv.). The reaction mixture was stirred at room temperature for 48 h. The crude material was extracted using DCM and concentrated *in vacuo*, then purified by column chromatography with 10% to 33% EtOAc/hexanes. (19.1 mg, 0.06 mmol, 36%).

^{1}H NMR (500 MHz, $CDCl_3$) δ 6.38 (s, 1H), 5.95 (dd, J = 17.5, 10.8 Hz, 1H), 5.20 (d, J = 10.8 Hz, 1H), 5.07 (d, J = 17.7 Hz, 2H), 3.60 (s, 3H), 3.06 (dd, J = 20.8, 16.9 Hz, 2H), 2.84 (d, J = 16.4 Hz, 2H), 2.77 (d, J = 17.5 Hz, 2H), 2.58 – 2.48 (m, 2H), 2.47 – 2.39 (m, 2H), 1.90 – 1.75 (m, 2H), 1.70 – 1.63 (m, 2H), 1.34 (s, 3H).

HRMS (ESI-TOF) $[M+Na]^+$ m/z: calcd for $C_{19}H_{22}O_4$ 337.1416; Found 337.1417.

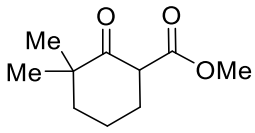

Methyl 3,3-dimethyl-2-oxocyclohexane-1-carboxylate (3-14): A flame-dried round-bottom flask was charged with 95% NaH (2.85 g, 118.86 mmol, 3.0 equiv.) under the inert atmosphere of

a glove box. The flask was removed from the glove box, and anhydrous THF (50 mL) was added to the dry material, and then compound **3-15** (5.00 g, 39.62 mmol, 1.0 equiv.) was slowly added to the reaction mixture followed by dimethyl carbonate (8.34 mL, 99.05 mmol, 2.5 equiv.). The reaction mixture was then refluxed at 75 °C for 8 h. The reaction was then allowed to come to room temperature before cooling to 0 °C. DI H_2O was used slowly added to the reaction vessel until the bubbling became to subside. Then, the mixture was partitioned with Et_2O (20 mL) and allowed to warm to room temperature. The aqueous layer was adjusted to pH 7 using 5% HCl and then extracted with Et_2O (3x 30 mL). The organic layer was washed with NH_4Cl (sat.) (5 mL), $NaHCO_3$ (sat.) (20 mL), NaCl (sat.) (20 mL), dried over Na_2SO_4, decanted, and then concentrated *in vacuo*. The crude material was purified by column chromatography with 10% to 33% EtOAc/hexanes. (4.27 g, 23.19 mmol, 58%).

^{1}H NMR (500 MHz, $CDCl_3$) δ 3.75 (d, J = 2.7 Hz, 3H), 2.23 (t, J = 6.2 Hz, 1H), 1.64 – 1.58 (m, 2H), 1.58 – 1.51 (m, 2H), 1.33 – 1.25 (m, 2H), 1.19 (s, 6H).

HRMS (ESI-TOF) $[M+Na]^+$ m/z: calcd for $C_{10}H_{16}O_3$ 207.0997; Found 207.1003.

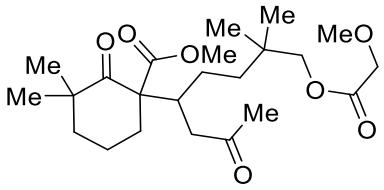

Methyl 1-(8-(2-methoxyacetoxy)-7,7-dimethyl-2-oxooctan-4-yl)-3,3-dimethyl-2-oxocyclohexane-1-carboxylate (3-16): A flame-dried round-bottom flask was charged with compound **3-15** (100 mg, 0.41 mmol, 1.0 equiv.) and compound **3-14** (109.4 mg, 0.49 mmol, 1.2 equiv. The flask was then transferred to a glovebox and 98% $Cu(OTf)_2$ (76.1 mg, 0.21 mmol, 0.3

equiv.) was added to the mixture and the contents were removed from the glovebox and left to stir at room temperature under *neat* conditions for 16 h. The crude material was purified by column chromatography with 10% to 33% EtOAc/hexanes. (54.8 mg, 0.13 mmol, 31%, 1:1 dr).

^{1}H NMR (500 MHz, $CDCl_3$) δ 4.34 (s, 2H), 4.98 (s, 2H), 3.67 (s, 3H), 3.35 (s, 3H), 2.59 – 2.51 (m, 2H), 2.12 – 2.04 (m, 2H), 2.02 – 1.90 (m, 2H), 1.74 – 1.62 (m, 2H), 1.39 – 1.28 (m, 2H), 1.25 – 1.18 (m, 3H), 1.18 – 1.11 (m, 2H), 1.10 (s, 6H), 1.08 – 1.05 (m, 1H), 0.91 (s, 6H).

^{13}C NMR (176 MHz, $CDCl_3$) δ 216.0, 207.9, 172.2, 170.6, 73.1, 70.3, 64.5, 58.8, 52.6, 44.3, 43.4, 39.2, 38.0, 37.7, 34.2, 32.6, 30.2, 27.7, 27.6, 27.6, 24.7, 24.7, 19.9.

HRMS (ESI-TOF) $[M+Na]^+$ m/z: calcd for $C_{23}H_{38}O_7$ 449.2515; Found 449.2539.

IR (film, cm^{-1}) 1230, 1250, 1720, 1740, 2840, 2950.

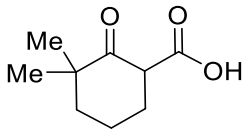

3,3-Dimethyl-2-oxocyclohexane-1-carboxylic acid (3-18): A flame-dried round-bottom flask was charged with NaOH (0.02 g, 0.60 mmol, 1.10 equiv.) and dissolved with H_2O (0.12 mL). Compound **3-14** (0.10 g, 0.54 mmol, 1.00 equiv.) was added to the mixture and the contents were left to stir at room temperature for 16 h. The reaction was quenched using 5% HCl (4 mL) and extracted with Et_2O (3x 5 mL). The organic layer was dried over Na_2SO_4, decanted, and then concentrated *in vacuo*. The resulting product was directly used in subsequent reactions. (0.04 g, 0.26 mmol, 48%).

^{1}H NMR (400 MHz, $CDCl_3$) δ 2.42 – 2.37 (m, 1H), 1.82 (q, J = 6.4, 5.9 Hz, 2H), 1.76 – 1.70 (m, 2H), 1.66 (q, J = 5.5, 4.8 Hz, 2H), 1.25 (q, J = 4.2, 3.7 Hz, 2H), 1.11 (s, 6H).

HRMS (ESI-TOF) $[M+H]^+$ m/z: calcd for $C_9H_{14}O_3$ 171.1016; Found 171.1128.

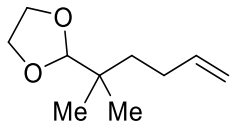

2-(2-Methylhex-5-en-2-yl)-1,3-dioxolane (3-35): A flame-dried round bottom flask was charged with 95% DMP (8.40 g, 18.81 mmol, 1.3 equiv.) under the inert atmosphere of a glove box. The flask was removed from the glove box and its solid material was dissolved in DCM (90 mL) and cooled to 0 °C. Compound **2-139** (1.85 g, 14.47 mmol, 1.0 equiv.) was added to the cooled mixture followed by a dropwise addition of pyridine (2.34 mL, 28.94 mmol, 2.0 equiv.). The reaction flask was allowed to slowly warm to room temperature and left to stir at room temperature for 6 h. $NaHCO_3$ (sat.) (20 mL) and $Na_2S_2O_3$ (sat.) (20 mL) was added to quench the reaction mixture and let stir 30 minutes. The mixture was partitioned using Et_2O (40 mL) and organic layer was washed by $NaHCO_3$ (sat.) (10 mL), NH_4Cl (sat.) (10 mL), NaCl (sat.) (10 mL), and then carefully concentrated *in vacuo*. The crude material was passed through a short silica plug using Et_2O as eluant. The resulting solution was evaporated into a round bottom flask and dissolved in ethylene glycol (5.5 mL) and methoxy dioxolane (23 mL) with *p*-TSA (0.37 g, 2.89 mmol, 0.2 equiv.). The reaction flask was stirred at 70 °C for 16 h. The reaction was then cooled to room temperature and quenched with DI H_2O (5 mL) and partitioned with Et_2O (10 mL). The organic layer was carefully concentrated *in vacuo* and purified by column chromatography with 10% to 75% Et_2O/hexanes. (1.60 g, 9.40 mmol, 65%).

^{1}H NMR (400 MHz, $CDCl_3$) δ 5.82 (ddt, J = 16.7, 10.1, 6.4 Hz, 1H), 5.01 (dd, J = 17.1, 1.8 Hz, 1H), 4.92 (dd, J = 10.1, 1.2 Hz, 1H), 4.56 (s, 1H), 3.98 – 3.90 (m, 2H), 3.90 – 3.82 (m, 2H), 2.06 (dd, J = 16.6, 7.2 Hz, 2H), 1.45 – 1.37 (m, 2H), 0.91 (s, 3H), 0.91 (s, 3H).

HRMS (ESI-TOF) $[M+H]^+$ m/z: calcd for $C_{10}H_{18}O_2$ 171.1380; Found 171.1388.

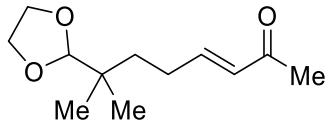

(*E*)-7-(1,3-Dioxolan-2-yl)-7-methyloct-3-en-2-one (3-36): A flame-dried round-bottom flask was charged with Grubbs 2nd generation catalyst (**1-141**) (0.09 g, 0.10 mmol, 0.01 equiv.) under the inert atmosphere of a glove box. The flask was removed from the glovebox, and anhydrous DCM (40 mL) was added. Then, compound **3-35** (1.74 g, 10.22 mmol, 1.0 equiv.) and ketone **2-141** (1.02 mL, 12.26 mmol, 1.2 equiv.) were added to the reaction mixture. The contents were left to stir under reflux conditions at 55 °C for 24 h. After this time, the heating was removed, and the reaction was left to cool to room temperature. The reaction was then directly dry loaded onto silica by concentration *in vacuo*. The crude material was purified by flash column chromatography with 10% to 33% EtOAc/hexanes. (1.40 g, 6.58 mmol, 64%).

^{1}H NMR (400 MHz, $CDCl_3$) δ 6.81 (dt, J = 15.9, 6.8 Hz, 1H), 6.08 (d, J = 16.0 Hz, 1H), 4.55 (s, 1H), 3.97 – 3.81 (m, 4H), 2.28 – 2.22 (m, 1H), 2.23 (s, 3H), 1.52 – 1.43 (m, 2H), 0.92 (s, 3H), 0.92 (s, 3H).

HRMS (ESI-TOF) $[M+H]^+$ m/z: calcd for $C_{12}H_{20}O_3$ 213.1485; Found 213.1492.

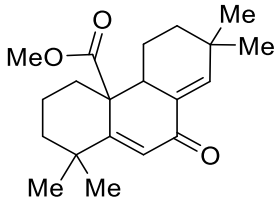

Methyl (4a*S*,4b*S*)-1,1,7,7-tetramethyl-9-oxo-1,3,4,4b,5,6,7,9-octahydrophenanthrene-4a(2*H*)-carboxylate (3-42): A flame-dried round-bottom flask was charged with compound **2-130** (31.7 mg, 1.88 mmol, 1.0 equiv.) and compound **3-14** (0.52 g, 2.82 mmol, 1.5 equiv.). The round-bottom flask was then transferred to a glovebox and 98% $Cu(OTf)_2$ (208.4 mg, 0.56 mmol, 0.3 equiv.) was added to the mixture, and the reaction vessel was removed from the glovebox and left to stir at room temperature under *neat* conditions for 16 h. Upon completion, the crude material was passed through a short silica plug using Et_2O as eluant. The resulting solution was evaporated into a round bottom flask and dissolved in toluene (4.0 mL) and *p*-TSA (72.1 mg, 0.56 mmol, 0.3 equiv.) was added. The reaction flask was equipped with a Dean-Stark trap for the azeotropic removal of water and a reflux condenser to be refluxed at 110 °C for 16 h. The crude material was concentrated *in vacuo* and purified by column chromatography with 10% to 33% EtOAc/hexanes. (94.5 mg, 0.30 mmol, 16% yield of 50% pure mass, 1:1 dr).

^{1}H NMR (400 MHz, $CDCl_3$) δ 6.68 (s, 1H), 6.07 (s, 1H), 3.60 (s, 3H), 2.75 (dd, J = 13.5, 1.9 Hz, 1H), 2.45 (d, J = 12.3 Hz, 2H), 2.14 – 2.02 (m, 2H), 1.93 – 1.72 (m, 2H), 1.68 – 1.45 (m, 2H), 1.35 (d, J = 9.9 Hz, 2H), 1.21 (td, J = 13.4, 4.2 Hz, 2H), 1.27 (br s, 3H), 1.24 (br s, 3H), 1.07 (s, 3H), 0.95 (s, 3H).

^{13}C NMR (126 MHz, $CDCl_3$) δ 187.9, 176.9, 169.8, 143.4, 133.9, 119.9, 52.6, 50.8, 42.1, 41.5, 38.3, 37.5, 35.0, 33.0, 30.3, 30.2, 29.6, 29.6, 20.5, 17.2.

HRMS (ESI-TOF) $[M+Na]^+$ m/z: calcd for $C_{20}H_{28}O_3$ 339.1936; Found 339.1939.

IR (film, cm^{-1}) 1230, 1670, 1730, 2870, 2920, 2940.

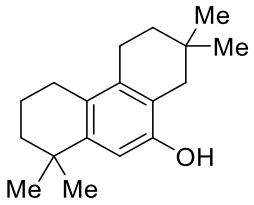

1,1,7,7-Tetramethyl-1,2,3,4,5,6,7,8-octahydrophenanthren-9-ol (3-47): A flame-dried round-bottom flask was charged with LiCl (24.7 mg, 0.58 mmol, 15.0 equiv.) under the inert atmosphere of a glove box. Compound **3-42** (12.3 mg, 0.03 mmol, 1.0 equiv.) and DMSO (1.0 mL) were added to the reaction flask. The reaction flask was equipped with a reflux condenser and heated at 180 °C for 24 h. The crude material was extracted using DCM and concentrated *in vacuo*, then purified by column chromatography with 10% to 33% EtOAc/hexanes. (3.5 mg, 0.01 mmol, 35%).

^{1}H NMR (500 MHz, $CDCl_3$) δ 12.47 (s, 1H), 6.84 (s, 1H), 2.76 (t, J = 6.4 Hz, 1H), 2.52 (t, J = 6.5 Hz, 1H), 1.94 (t, J = 6.4 Hz, 1H), 1.84 – 1.79 (m, 1H), 1.64 – 1.60 (m, 2H), 1.28 (s, 6H), 1.22 (s, 6H).

^{13}C NMR (126 MHz, CDCl3) δ 161.0, 155.9, 142.3, 134.5, 124.7, 113.4, 41.1, 38.4, 35.9, 35.0, 31.7, 31.7, 27.8, 26.9, 24.6, 23.4, 23.4, 19.4.

HRMS (ESI-TOF) $[M-H]^-$ m/z: calcd for $C_{18}H_{20}O_2$ 257.1905; Found 257.1909.

IR (film, cm^{-1}) 1360, 1470, 2840, 2930, 2990.

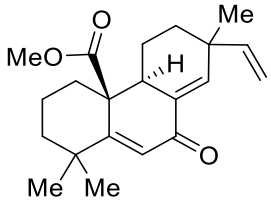

Methyl (4a*S*,4b*S*)-1,1,7-trimethyl-9-oxo-7-vinyl-1,3,4,4b,5,6,7,9-octahydrophenanthrene-4a(2*H*)-carboxylate (3-13): A flame-dried round-bottom flask was charged with compound **3-14** (0.88 g, 4.76 mmol, 1.2 equiv.) and compound **2-21** (0.72 g, 3.97 mmol, 1.0 equiv.). The round-bottom flask was then transferred to a glovebox and 98% $Cu(OTf)_2$ (0.44 g, 1.19 mmol, 0.3 equiv.) was added to the mixture and the contents were left to stir at room temperature under *neat* conditions for 16 h. The crude material was passed through a short silica plug using Et_2O as eluant. The resulting solution was evaporated into a round bottom flask and dissolved in PhMe (70 mL) and *p*-TSA (0.15 g, 1.19 mmol, 0.3 equiv.) was added. The reaction flask was equipped with a Dean-Stark trap for the azeotropic removal of water and a reflux condenser to be refluxed at 110 °C for 16 h. The crude organic material was purified by column chromatography with 10% to 33% EtOAc/hexanes. (0.11 g, 0.35 mmol, 9%, 1.4:1 dr).

^{1}H NMR (400 MHz, $CDCl_3$) δ 6.37 (s, 1H), 6.22 (s, 1H), 5.77 (dd, J = 17.5, 10.6 Hz, 1H), 5.07 – 4.98 (m, 2H), 3.60 (s, 3H), 2.22 – 2.15 (m, 2H), 2.09 (m, 2H), 1.98 – 1.91 (m, 2H), 1.17 (dd, J = 4.2, 1.5 Hz, 2H), 1.15 – 1.13 (m, 2H), 1.13 – 1.10 (m, 3H), 1.04 (s, 6H), 0.96 (s, 3H).

HRMS (ESI-TOF) $[M+H]^+$ m/z: calcd for $C_{21}H_{28}O_3$ 329.2111; Found 329.2102.

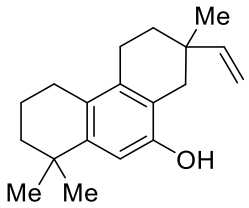

1,1,7-Trimethyl-7-vinyl-1,2,3,4,5,6,7,8-octahydrophenanthren-9-ol ((±)-aspewentin A ((±)-1-16)): To a flame-dried round bottom-flask was charged with compound **3-14** (112.7 mg, 0.61 mmol, 1.2 equiv.) and compound **3-21** (91.9 mg, 0.51 mmol, 1.0 equiv.). The flask was then transferred to a glovebox, and 98% $Cu(OTf)_2$ (55.3 mg, 0.15 mmol, 0.3 equiv.) was added to the

mixture, and the contents were left to stir at room temperature under *neat* conditions for 16 h. The crude material was then passed through a short silica plug using Et_2O as eluant. The resulting solution was evaporated into a round bottom flask and dissolved in PhMe (5 mL), and *p*-TSA (19.1 mg, 0.15 mmol, 0.3 equiv.) was added. The reaction flask was equipped with a Dean-Stark trap for the azeotropic removal of water and a reflux condenser to be refluxed at 110 °C for 16 h. The crude material was passed through a short silica plug using Et_2O as eluant. The collected solution was evaporated into a dry round-bottom flask and then transferred to a glovebox where LiCl (324 mg, 7.65 mmol, 15.0 equiv.) was added to the mixture. The contents of the flask were then dissolved in DMSO (5.0 mL) and heated to 180 °C for 24 h. The solution was diluted with DCM and washed by 1:1 DI H_2O: NaCl (sat.) (3x 10 mL). The crude organic material was concentrated *in vacuo* and purified by column chromatography with 10% to 33% EtOAc/hexanes. (2.9 mg, 0.01 mmol, 2% yield of 80% purity).

^{1}H NMR (500 MHz, $CDCl_3$) δ 6.66 (s, 1H), 5.89 (dd, J = 17.5, 10.8 Hz, 1H), 4.98 (d, J = 17.6 Hz, 1H), 4.95 (d, J = 10.6 Hz, 1H), 4.44 (s, 1H), 2.64 (d, J = 16.4 Hz, 1H), 2.55 (t, J = 6.7 Hz, 2H), 2.48 (t, J = 6.6 Hz, 2H), 2.44 (d, J = 16.5 Hz, 1H), 1.82 – 1.79 (m, 2H), 1.73 – 1.70 (m, 1H), 1.66 – 1.62 (m, 1H), 1.62 – 1.59 (m, 2H), 1.26 (s, 3H), 1.26 (s, 3H), 1.09 (s, 3H).

^{13}C NMR (126 MHz, $CDCl_3$) δ 151.2, 147.2, 143.8, 135.2, 126.4, 119.6, 111.1, 109.9, 38.7, 34.4, 34.0, 33.9, 32.0, 32.0, 26.7, 25.9, 24.3, 19.6.

HRMS (ESI-TOF) $[M-H]^-$ m/z: calcd for $C_{19}H_{26}O$ 269.1905; Found 269.1894.

IR (film, cm^{-1}) 1460, 2860, 2890, 2920, 2940, 2960.

Table III.3 ^{1}H NMR comparison of synthetic and natural aspewentin A.

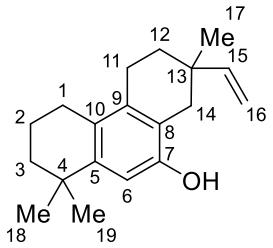

carbon assignment	Synthetic (±)-Aspewentin A	Natural (+)-Aspewentin A[35]	Δppm
---	^{1}H NMR (500 MHz, $CDCl_3$)	^{1}H NMR (500 MHz, $CDCl_3$)	--
6	6.66 (s, 1H)	6.66 (s, 1H)	0.00
15a	5.89 (dd, J = 17.5, 10.8 Hz, 1H)	5.89 (dd, J = 17.6, 10.8 Hz, 1H)	0.00
16a	4.98 (d, J = 17.6 Hz, 1H)	4.98 (br d, J = 17.6 Hz, 1H)	0.00
16b	4.95 (d, J = 10.6 Hz, 1H)	4.94 (br d, J = 10.8 Hz, 1H)	0.01
-OH	4.44 (s, 1H)	4.44 (br s, 1H)	0.00
14a	2.64 (d, J = 16.4 Hz, 1H)	2.64 (d, J = 16.4 Hz, 1H)	0.00
11	2.55 (t, J = 6.7 Hz, 2H)	2.55 (t, J = 6.6 Hz, 2H)	0.00
1	2.48 (t, J = 6.6 Hz, 2H)	2.48 (t, J = 6.5 Hz, 2H)	0.00
14b	2.44 (d, J = 16.5 Hz, 1H)	2.44 (d, J = 16.4 Hz, 1H)	0.00
2	1.82 – 1.79 (m, 2H)	1.80 (m, 2H)	0.00
12a	1.73 – 1.70 (m, 1H)	1.71 (m, 1H)	0.00
12b	1.66 – 1.62 (m, 1H)	1.64 (m, 1H)	0.00
3	1.62 – 1.59 (m, 2H)	1.60 (m, 2H)	0.00
18, 19	1.26 (s, 3H), 1.26 (s, 3H)	1.25 (s, 3H), 1.25 (s, 3H)	0.01
17	1.09 (s, 3H)	1.08 (s, 3H)	0.01

Table III.4 ^{13}C NMR comparison of synthetic and natural aspewentin A.

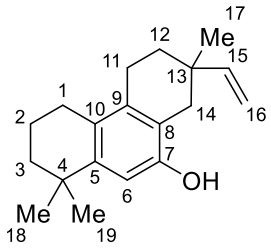

carbon assignment	Synthetic (±)-Aspewentin A	Natural (+)-Aspewentin A[35]	Δppm
--	^{13}C NMR (126 MHz, $CDCl_3$)	^{13}C NMR (125 MHz, $CDCl_3$)	--
7	151.2	151.2	0.0
15	147.2	147.1	0.1
5	143.8	143.8	0.0
9	135.2	135.1	0.1
10	126.4	126.4	0.0
8	119.6	119.6	0.0
16	111.1	111.1	0.0
6	109.9	109.9	0.0
3	38.7	38.7	0.0
14	34.4	34.4	0.0
13	34.4	34.4	0.0
12	34.0	34.0	0.0
4	33.9	33.8	0.1
19	32.0	32.0	0.0
18	32.0	31.9	0.1
1	26.7	26.7	0.0
17	25.9	25.8	0.1
11	24.3	24.2	0.1
2	19.6	19.6	0.0

III.7 NMR Spectra

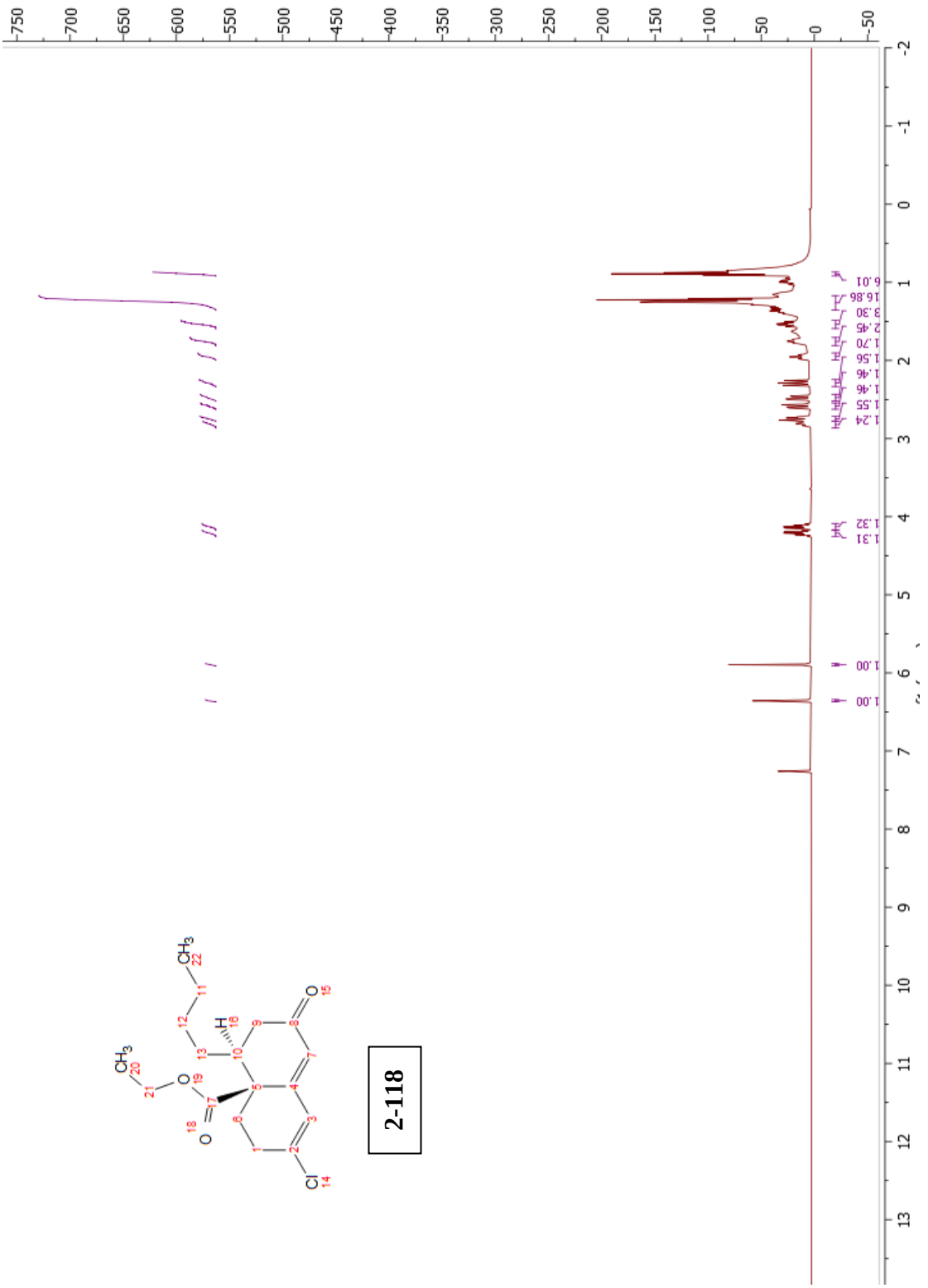

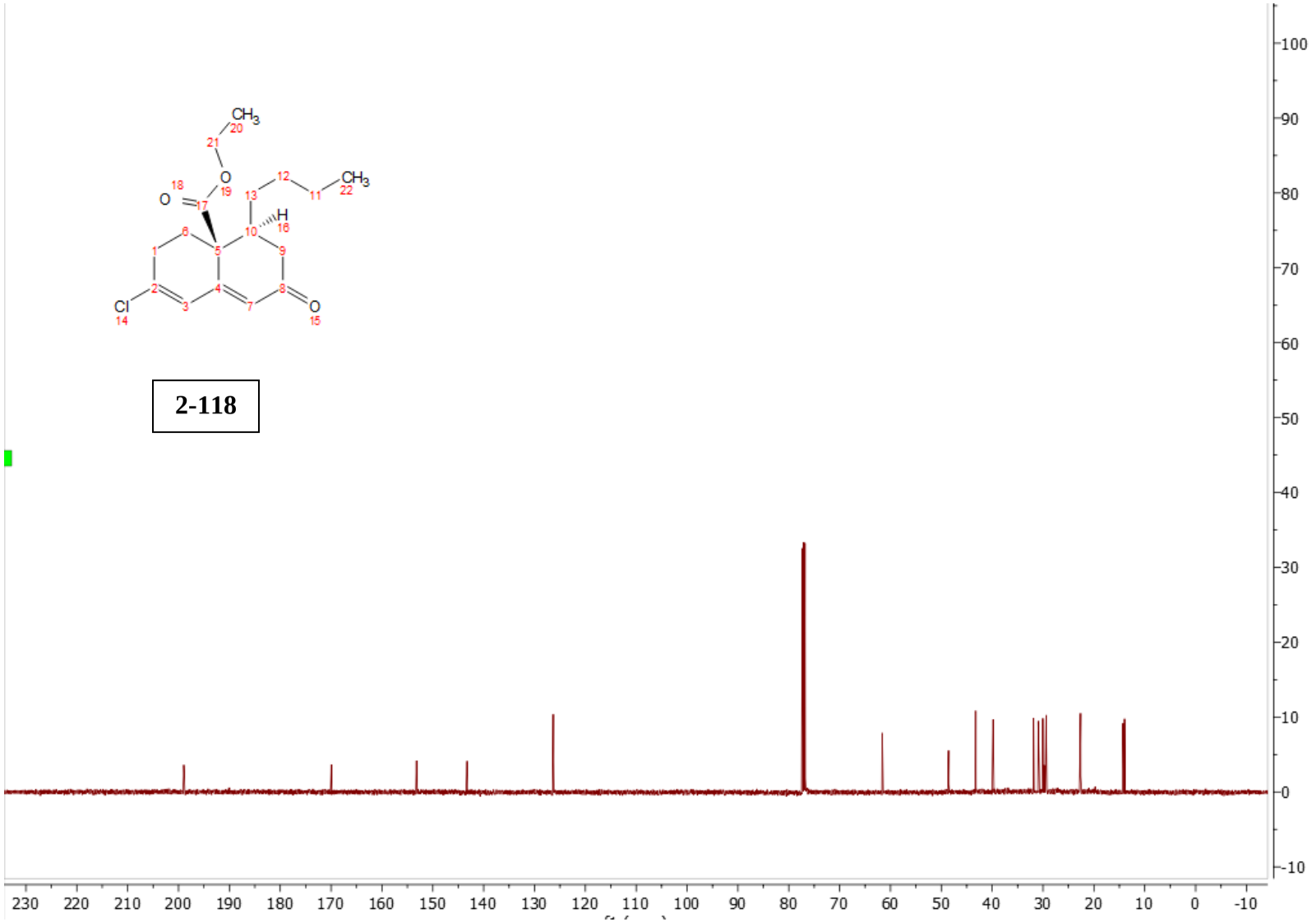
CH3
20
21
O
19
18
O
17
12
11
CH3
22
13
H
16
10
6
5
9
1
2
4
8
O
15
Cl
14
3
7
2-118
100
90
80
70
60
50
40
30
20
10
0
-10
230 220 210 200 190 180 170 160 150 140 130 120 110 100 90 80 70 60 50 40 30 20 10 0 -10

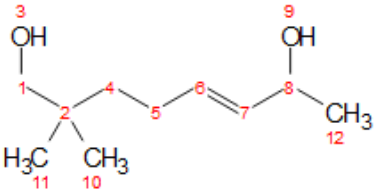
3
OH
9
OH
1
2
4
5
6
7
8
CH3
12
H3C
11
CH3
10

2-128

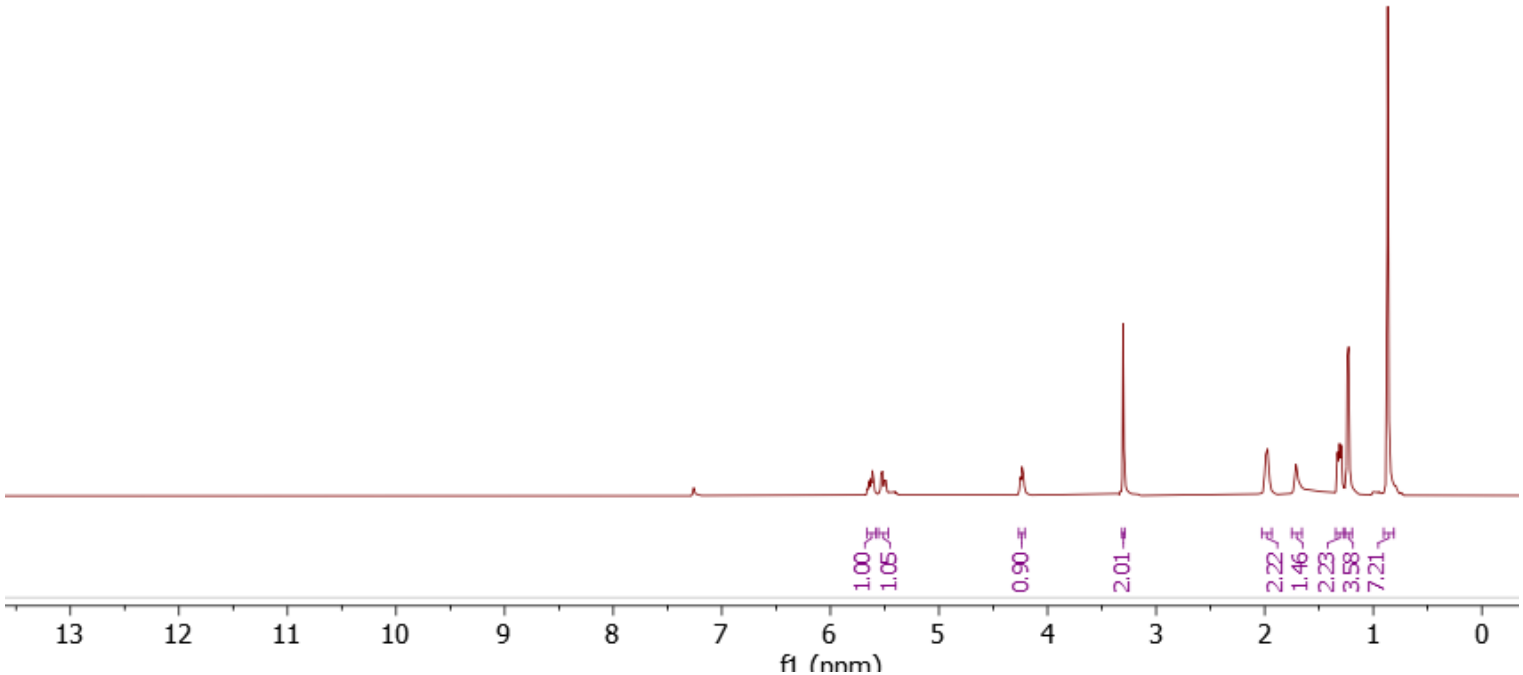
1.00
1.05
0.90
2.01
2.22
1.46
2.23
3.58
7.21
13
12
11
10
9
8
7
6
5
4
3
2
1
0
f1 (ppm)

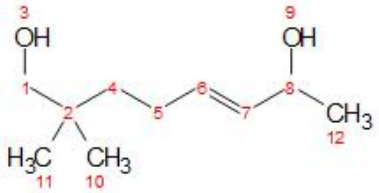
3
OH
1
2
4
5
6
7
8
9
OH
CH3
12
H3C
11
CH3
10

2-128

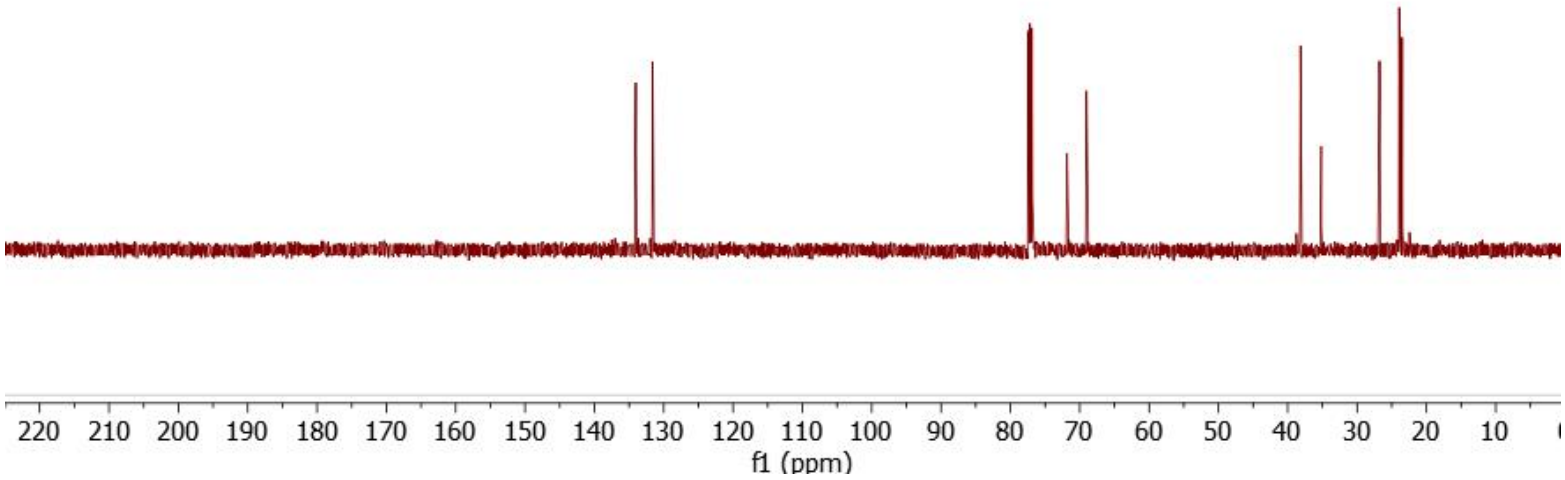
220 210 200 190 180 170 160 150 140 130 120 110 100 90 80 70 60 50 40 30 20 10
f1 (ppm)

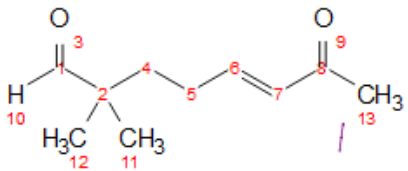
O
3
O
9
H
10
1
2
4
5
6
7
8
CH3
13
H3C
12
CH3
11

2-130

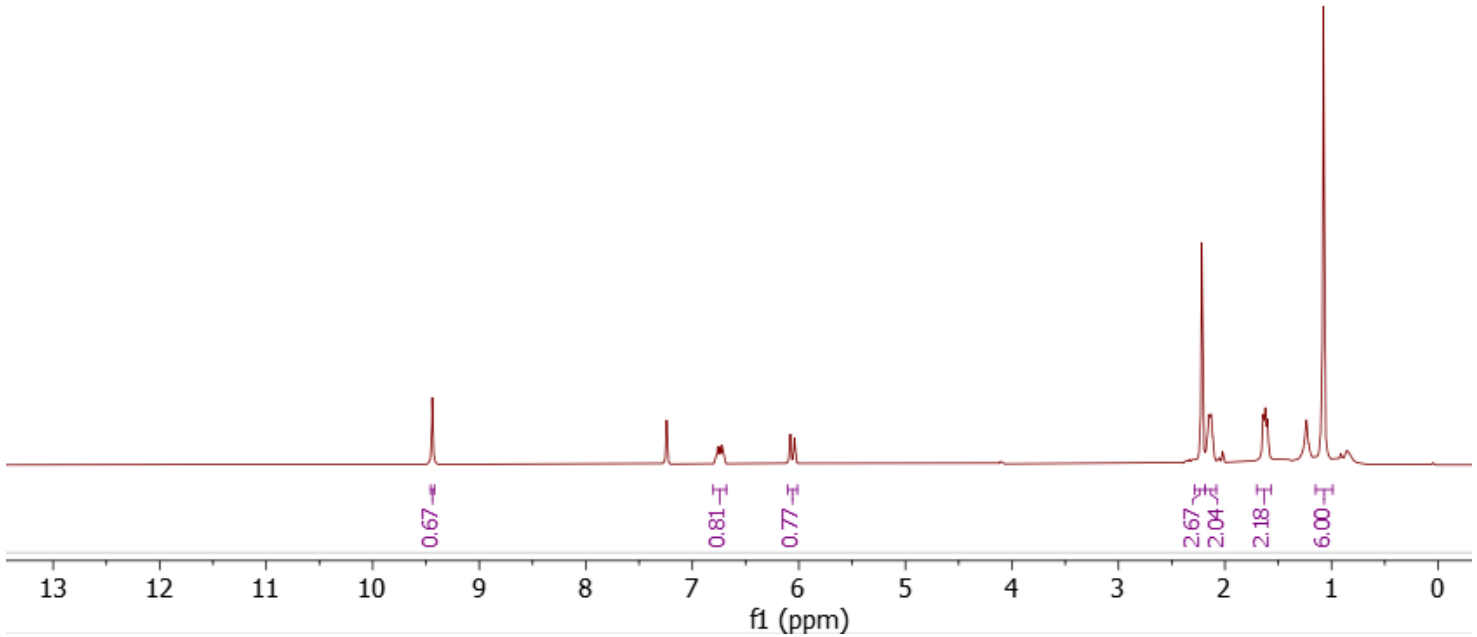
0.67
0.81
0.77
2.67
2.04
2.18
6.00
13
12
11
10
9
8
7
6
5
4
3
2
1
0
f1 (ppm)

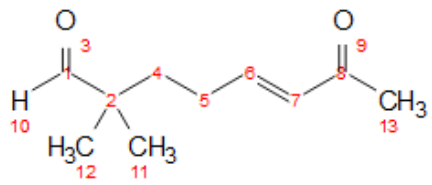
O
3
O
9
H
10
2
4
5
6
7
8
CH3
13
H3C
12
CH3
11

2-130

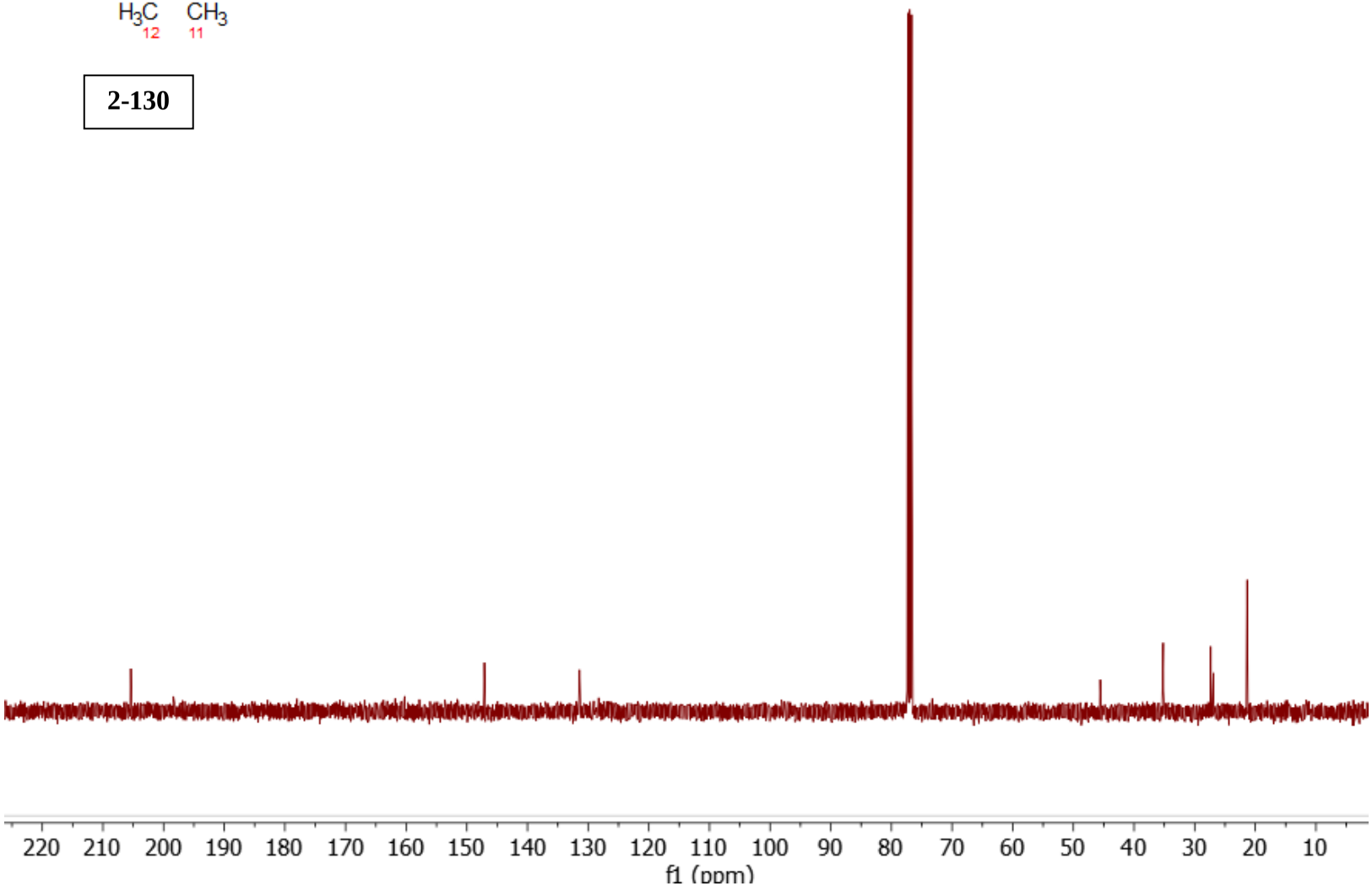
220 210 200 190 180 170 160 150 140 130 120 110 100 90 80 70 60 50 40 30 20 10
f1 (ppm)

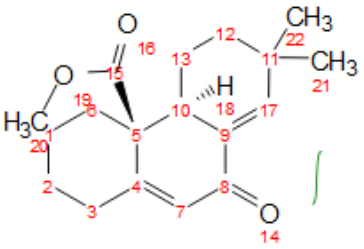
O
16
O
15
H3C
19
20
1
6
5
2
3
4
7
8
9
10
18
17
12
13
11
22
CH3
21
CH3
H
O
14

2-181

1.00
1.38
3.35
1.21
1.23
2.00
0.75
0.85
1.45
1.17
1.55
2.45
1.93
1.63
0.79
1.21
2.44
1.73
4.62
3.72
8.5
8.0
7.5
7.0
6.5
6.0
5.5
5.0
4.5
4.0
3.5
3.0
2.5
2.0
1.5
1.0
0.5
f1 (ppm)

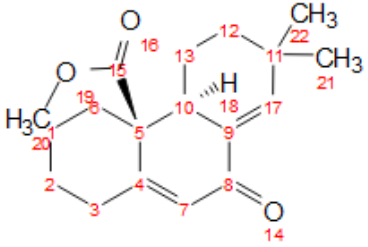
O
16
15
O
19
H3C
1
20
5
6
10
H
18
12
13
11
CH3
22
CH3
21
17
9
2
4
8
O
14
3
7

2-181

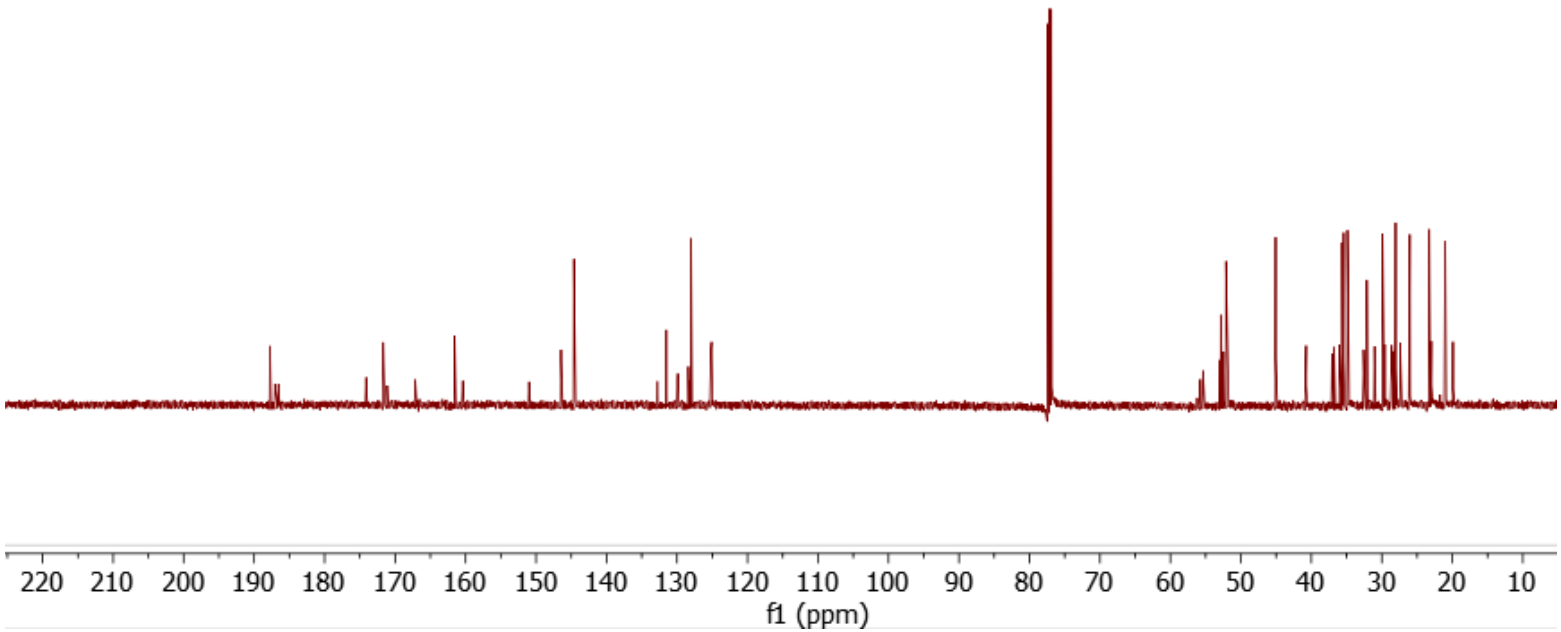
220 210 200 190 180 170 160 150 140 130 120 110 100 90 80 70 60 50 40 30 20 10
f1 (ppm)

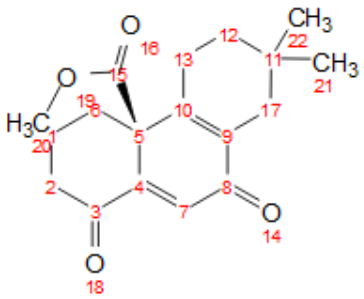
O
16
CH3
22
12
13
11
CH3
21
O
15
19
H3C
20
1
6
5
10
9
17
2
4
8
O
14
7
3
O
18

2-183

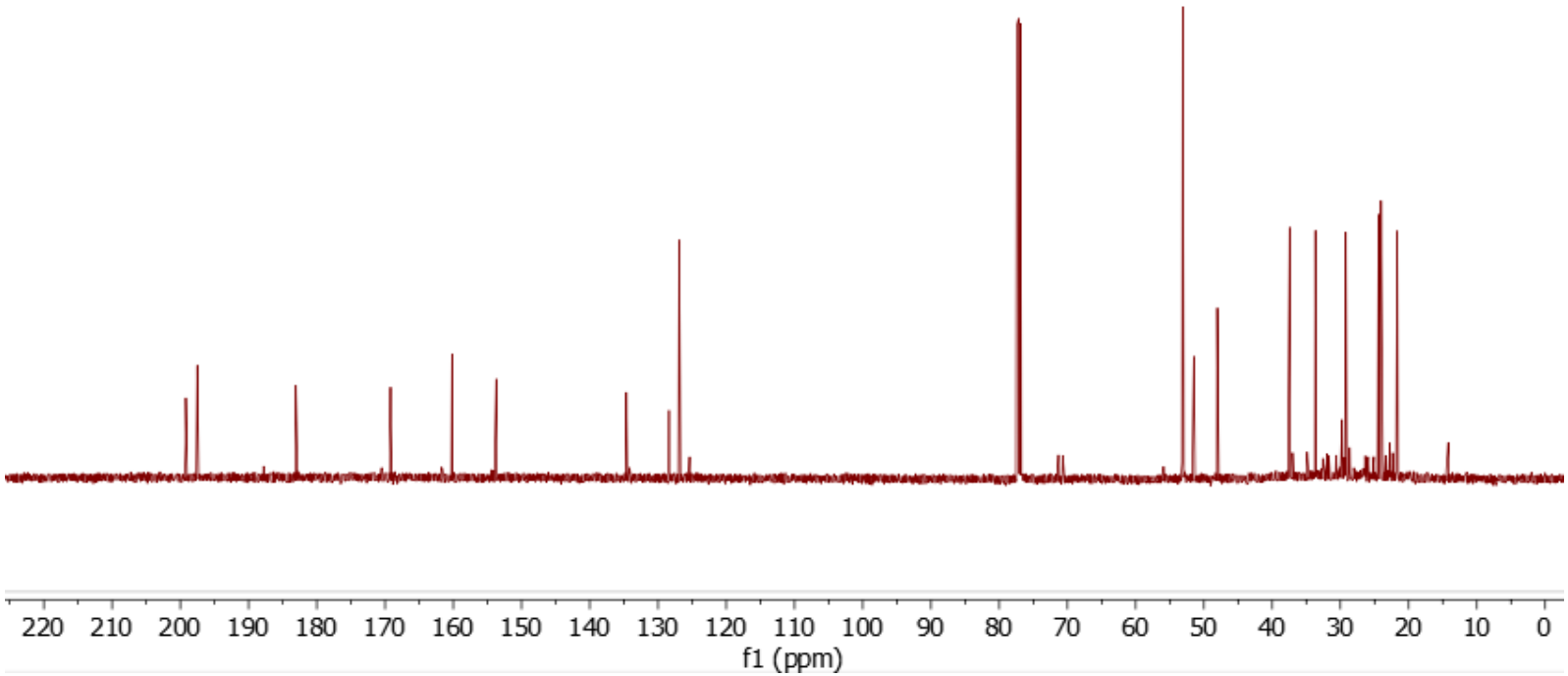
220 210 200 190 180 170 160 150 140 130 120 110 100 90 80 70 60 50 40 30 20 10 0
f1 (ppm)

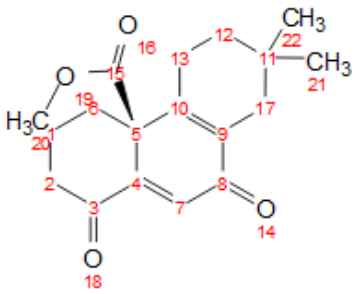
O
16
CH3
22
12
13
11
CH3
21
O
15
19
H3C
20
1
6
5
10
9
17
2
4
8
O
14
3
7
O
18

2-183

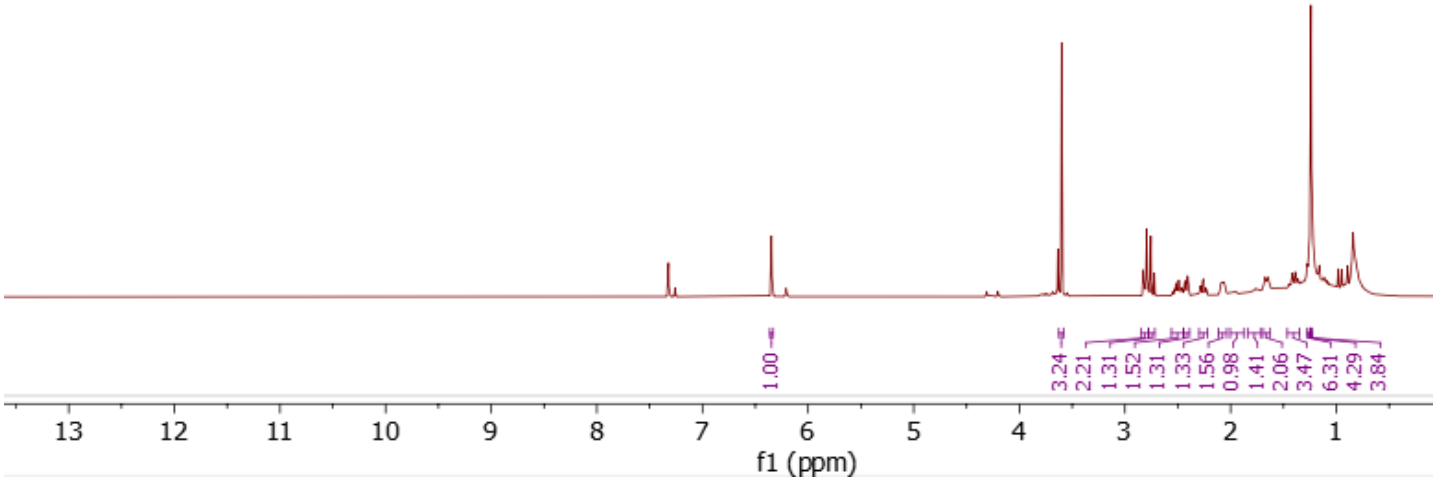
1.00
3.24
2.21
1.31
1.52
1.31
1.33
1.56
0.98
1.41
2.06
3.47
6.31
4.29
3.84
13
12
11
10
9
8
7
6
5
4
3
2
1
f1 (ppm)

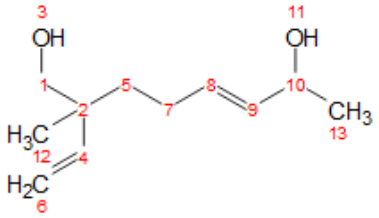
3
OH
1
2
5
7
8
9
10
11
OH
CH3
13
H3C
12
4
H2C
6

3-10

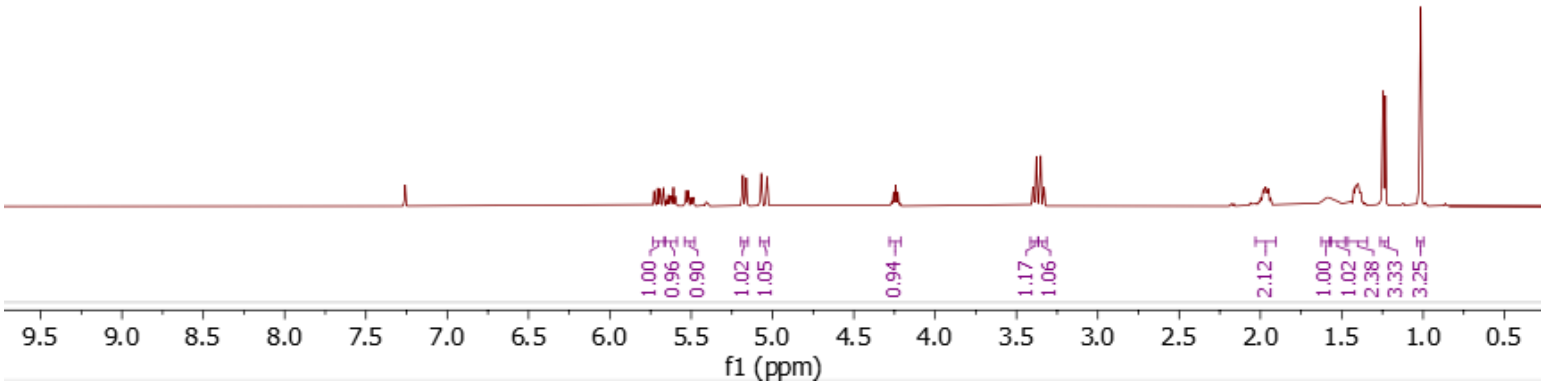
1.00
0.96
0.90
1.02
1.05
0.94
1.17
1.06
2.12
1.00
1.02
2.38
3.33
3.25
9.5
9.0
8.5
8.0
7.5
7.0
6.5
6.0
5.5
5.0
4.5
4.0
3.5
3.0
2.5
2.0
1.5
1.0
0.5
f1 (ppm)

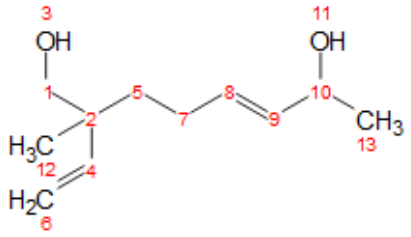
3
OH
1
2
5
7
8
9
11
OH
10
CH3
13
H3C
12
4
H2C
6

3-10

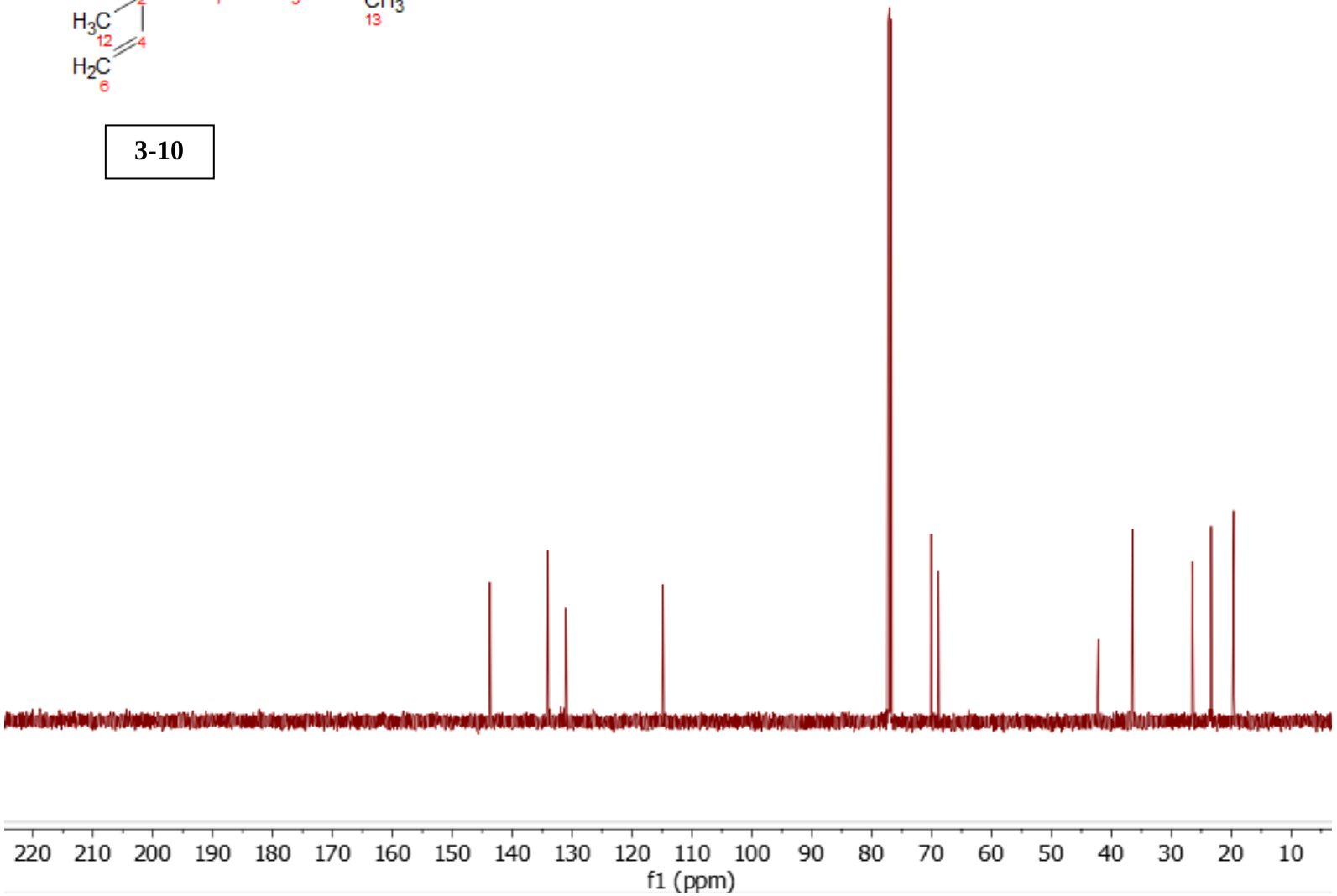
220 210 200 190 180 170 160 150 140 130 120 110 100 90 80 70 60 50 40 30 20 10
f1 (ppm)

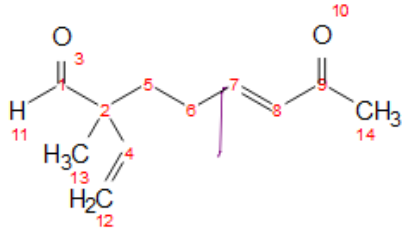
O
3
O
10
H
11
2
5
6
7
8
9
CH3
14
H3C
13
4
H2C
12

2-21

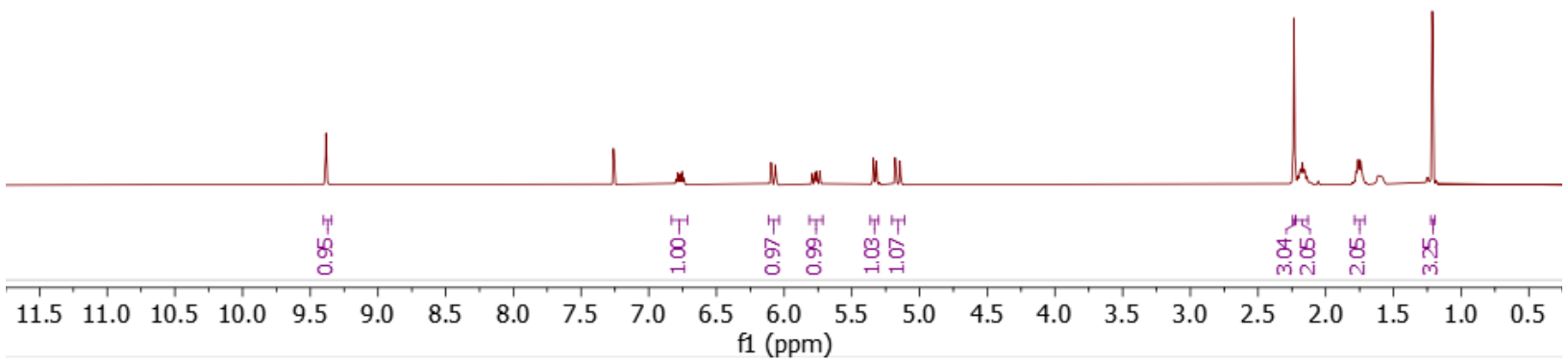
0.95
1.00
0.97
0.99
1.03
1.07
3.04
2.05
2.05
3.25
11.5 11.0 10.5 10.0 9.5 9.0 8.5 8.0 7.5 7.0 6.5 6.0 5.5 5.0 4.5 4.0 3.5 3.0 2.5 2.0 1.5 1.0 0.5
f1 (ppm)

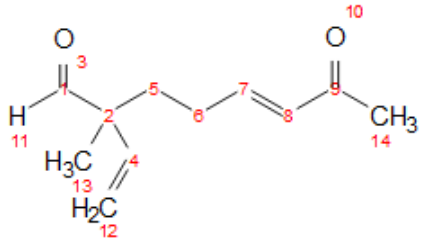
O
3
1
2
5
6
7
8
9
10
O
H
11
H3C
13
4
H2C
12
CH3
14

2-21

220 210 200 190 180 170 160 150 140 130 120 110 100 90 80 70 60 50 40 30 20 10
f1 (ppm)

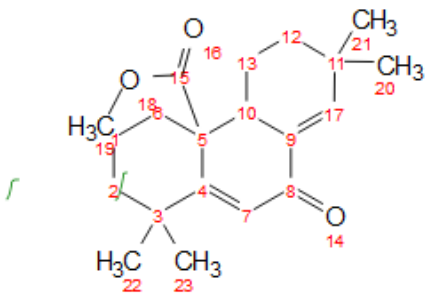
O
16
CH3
21
12
13
11
CH3
20
O
15
18
6
10
17
H3C
19
1
5
9
2
4
8
O
14
3
7
H3C
22
CH3
23

3-42

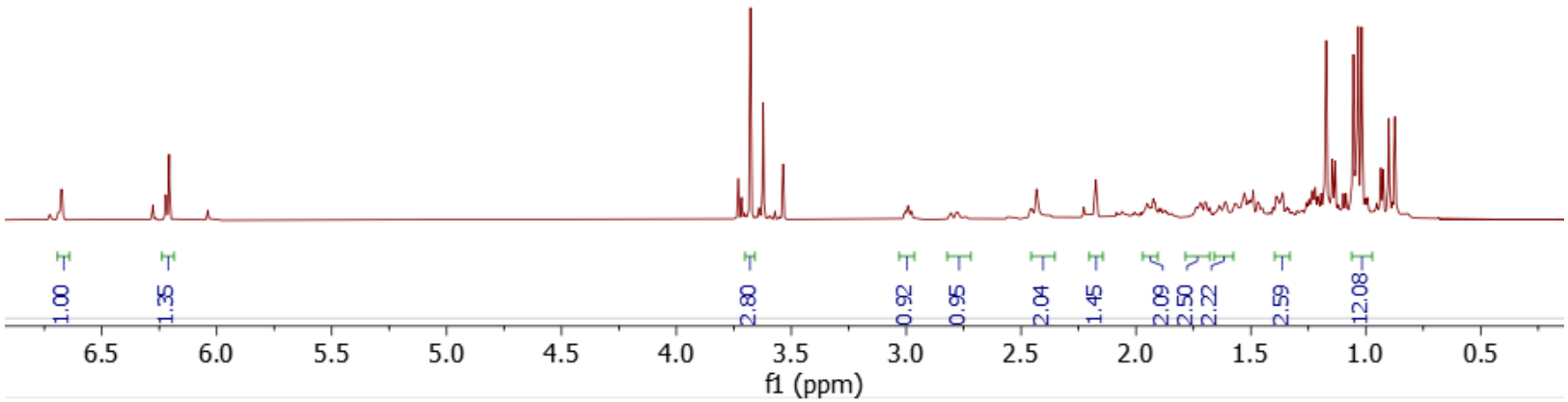
1.00
1.35
2.80
0.92
0.95
2.04
1.45
2.09
2.50
2.22
2.59
12.08
6.5
6.0
5.5
5.0
4.5
4.0
3.5
3.0
2.5
2.0
1.5
1.0
0.5
f1 (ppm)

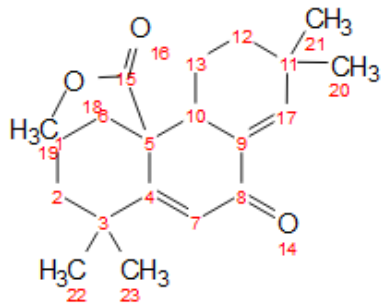
O
16
CH3
21
12
13
11
CH3
20
O
15
18
10
17
H3C
19
1
6
5
9
2
4
8
O
3
7
14
H3C
22
CH3
23

3-42

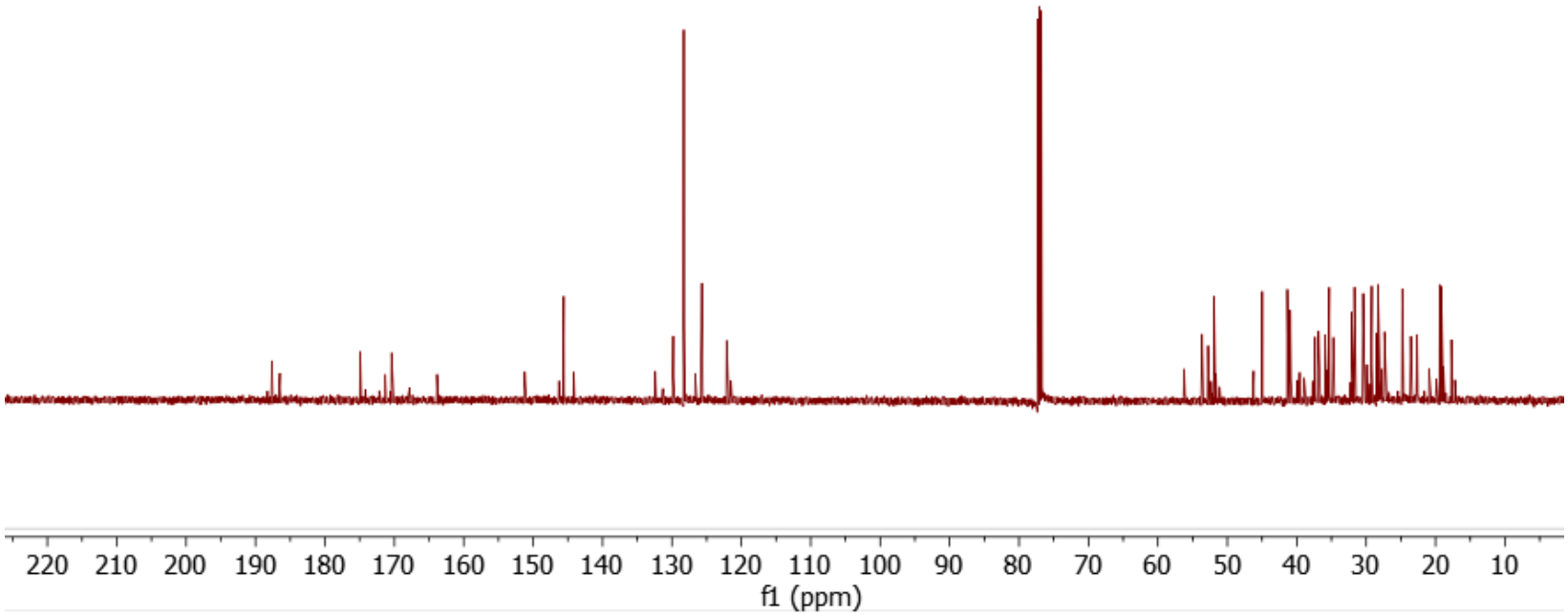
220 210 200 190 180 170 160 150 140 130 120 110 100 90 80 70 60 50 40 30 20 10
f1 (ppm)

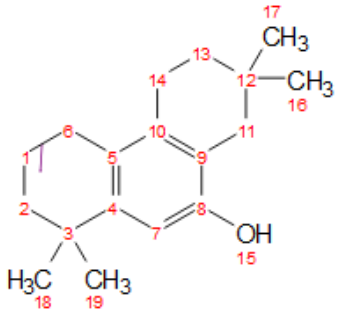
17
CH3
13
14
12
CH3
16
6
10
11
1
5
9
2
4
8
OH
3
7
15
H3C
CH3
18
19

3-47

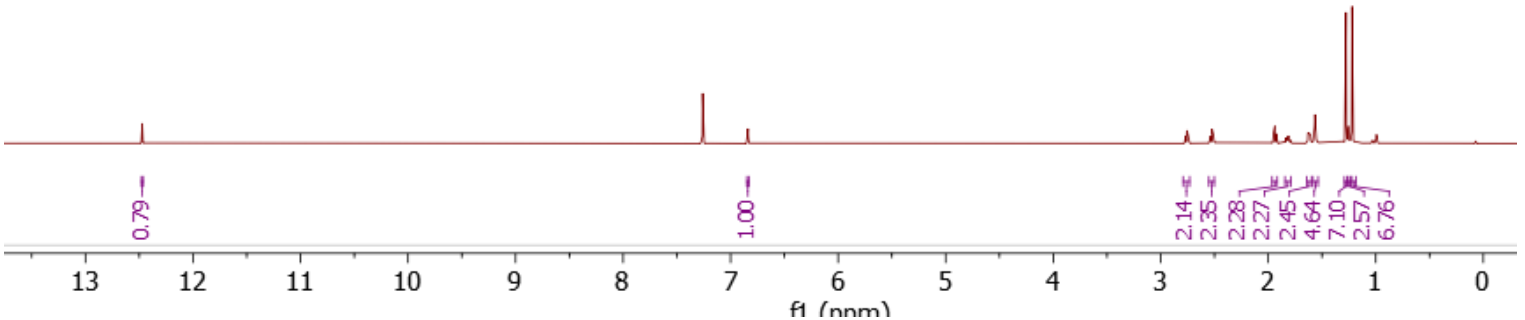
0.79
1.00
2.14
2.35
2.28
2.27
2.45
4.64
7.10
2.57
6.76
13
12
11
10
9
8
7
6
5
4
3
2
1
0
f1 (ppm)

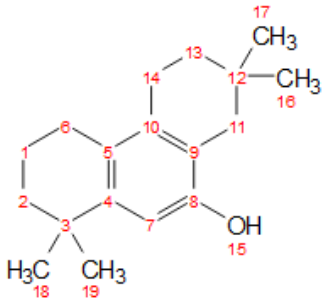
17
CH3
13
14
12
CH3
16
6
10
11
1
5
9
2
4
8
OH
3
7
15
H3C
CH3
18
19

3-47

230 220 210 200 190 180 170 160 150 140 130 120 110 100 90 80 70 60 50 40 30 20 10 0
f1 (ppm)

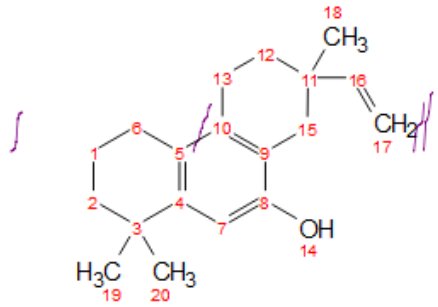
18
CH3
12
13
11
16
CH2
17
6
10
15
1
5
9
2
4
8
3
7
OH
14
H3C
CH3
19
20

1-16

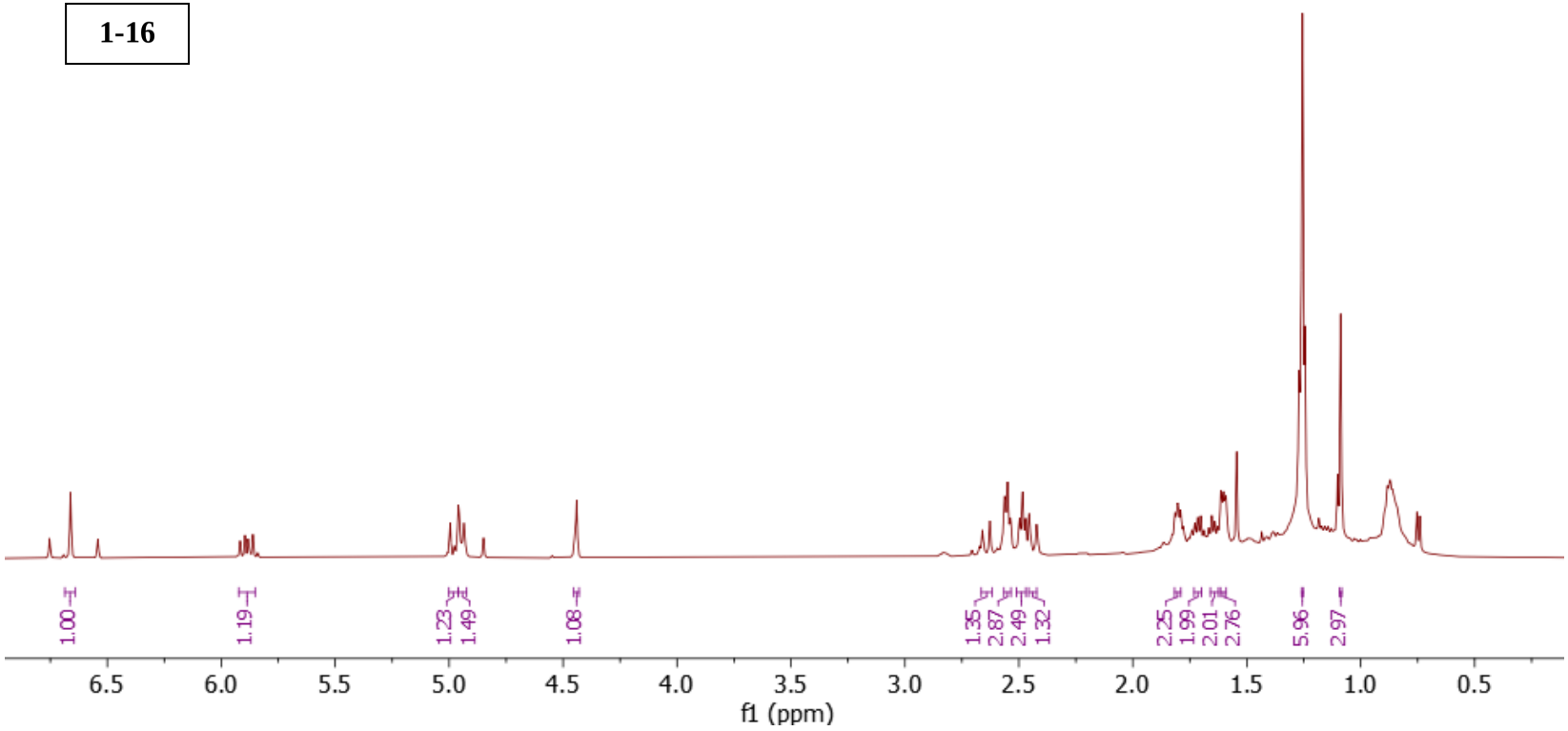
1.00
1.19
1.23
1.49
1.08
1.35
2.87
2.49
1.32
2.25
1.99
2.01
2.76
5.96
2.97
6.5
6.0
5.5
5.0
4.5
4.0
3.5
3.0
2.5
2.0
1.5
1.0
0.5
f1 (ppm)

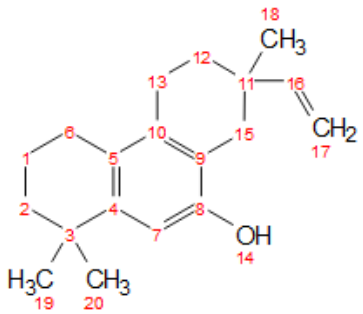
18
CH3
12
13
11
16
CH2
17
6
10
15
1
5
9
2
4
8
OH
14
3
7
H3C
CH3
19
20

1-16

150
140
130
120
110
100
90
80
70
60
50
40
30
20
f1 (ppm)

References

(1) Atanasov, A. G.; Zotchev, S. B.; Dirsch, V. M.; International Natural Product Sciences, T.; Supuran, C. T. Natural products in drug discovery: advances and opportunities. *Nat Rev Drug Discov* **2021**, *20*, 200-216.

(2) Pye, C. R.; Bertin, M. J.; Lokey, R. S.; Gerwick, W. H.; Linington, R. G. Retrospective analysis of natural products provides insights for future discovery trends. *Proc Natl Acad Sci U S A* **2017**, *114*, 5601-5606.

(3) Howes, M. J. R.; Quave, C. L.; Collemare, J.; Tatsis, E. C.; Twilley, D.; Lulekal, E.; Farlow, A.; Li, L.; Cazar, M. E.; Leaman, D. J.; Prescott, T. A. K.; Milliken, W.; Martin, C.; De Canha, M. N.; Lall, N.; Qin, H.; Walker, B. E.; Vasquez-Londono, C.; Allkin, B.; Rivers, M.; Simmonds, M. S. J.; Bell, E.; Battison, A.; Felix, J.; Forest, F.; Leon, C.; Williams, C.; Lughadha, E. N. Molecules from nature: Reconciling biodiversity conservation and global healthcare imperatives for sustainable use of medicinal plants and fungi. *Plants People Planet* **2020**, *2*, 463-481.

(4) Kingston, D. G. I. Modern Natural Products Drug Discovery and Its Relevance to Biodiversity Conservation. *J Nat Prod* **2011**, *74*, 496-511.

(5) Naman, C. B.; Leber, C. A.; Gerwick, W. H. Modern Natural Products Drug Discovery and Its Relevance to Biodiversity Conservation. *Microbial Resources: From Functional Existence in Nature to Applications* **2017**, 103-120.

(6) Firn, R. Nature's Chemicals: The Natural Products that Shaped Our World. *Nature's Chemicals: The Natural Products That Shaped Our World* **2010**, 1-250.

(7) Inaba, D.; Cohen, W. E.: *Uppers, downers, all arounders : physical and mental effects of psychoactive drugs*; 5th ed.; CNS Publications: Ashland, Or., 2004.

(8) Meyer, J. S.; Quenzer, L. F.: *Psychopharmacology : drugs, the brain, and behavior*; Sinauer Associates: Sunderland, Mass., 2005.

(9) Davis, E. M.; Croteau, R. Cyclization enzymes in the biosynthesis of monoterpenes, sesquiterpenes, and diterpenes. *Biosynthesis: Aromatic Polyketides, Isoprenoids, Alkaloids* **2000**, *209*, 53-95.

(10) Baran, P. S. Natural Product Total Synthesis: As Exciting as Ever and Here To Stay. *J Am Chem Soc* **2018**, *140*, 4751-4755.

(11) Corey, E. J. The Logic of Chemical Synthesis - Multistep Synthesis of Complex Carbogenic Molecules. *Angew Chem Int Edit* **1991**, *30*, 455-465.

(12) Nicolaou, K. C.; Chen, J. S.: *Classics in total synthesis III : further targets, strategies, methods*; Wiley-VCH: Weinheim, 2011.

(13) Nicolaou, K. C.; Edmonds, D. J.; Bulger, P. G. Cascade reactions in total synthesis. *Angew Chem Int Ed Engl* **2006**, *45*, 7134-7186.

(14) Nicolaou, K. C.; Snyder, S. A.: *Classics in total synthesis II : more targets, strategies, methods*; Wiley-VCH: Weinheim, 2003.

(15) Nicolaou, K. C.; Sorensen, E. J.: *Classics in total synthesis : targets, strategies, methods*; VCH: Weinheim ; New York, 1996.

(16) Ynigez-Gutierrez, A. E.; Bachmann, B. O. Fixing the Unfixable: The Art of Optimizing Natural Products for Human Medicine. *Journal of Medicinal Chemistry* **2019**, *62*, 8412-8428.
(17) Firn, R. D.; Jones, C. G. The evolution of secondary metabolism - a unifying model. *Mol Microbiol* **2000**, *37*, 989-994.
(18) Schwab, W. Metabolome diversity: too few genes, too many metabolites? *Phytochemistry* **2003**, *62*, 837-849.
(19) Croteau, R.; Karp, F.; Wagschal, K. C.; Satterwhite, D. M.; Hyatt, D. C.; Skotland, C. B. Biochemical-Characterization of a Spearmint Mutant That Resembles Peppermint in Monoterpene Content. *Plant Physiol* **1991**, *96*, 744-752.
(20) Ninkuu, V.; Zhang, L.; Yan, J. P.; Fu, Z. C.; Yang, T. F.; Zeng, H. M. Biochemistry of Terpenes and Recent Advances in Plant Protection. *Int J Mol Sci* **2021**, *22*.
(21) Buhaescu, I.; Izzedine, H. Mevalonate pathway: A review of clinical and therapeutical implications. *Clin Biochem* **2007**, *40*, 575-584.
(22) Pichersky, E.; Raguso, R. A. Why do plants produce so many terpenoid compounds? *New Phytol* **2018**, *220*, 692-702.
(23) Hadley, M. E.: *Endocrinology*; 4th ed.; Prentice Hall: Englewood Cliffs, NJ, 1996.
(24) Christianson, D. W. Structural and Chemical Biology of Terpenoid Cyclases. *Chem Rev* **2017**, *117*, 11570-11648.
(25) Rudolf, J. D.; Chang, C. Y. Terpene synthases in disguise: enzymology, structure, and opportunities of non-canonical terpene synthases. *Nat Prod Rep* **2020**, *37*, 425-463.
(26) Wu, Z. Y.; Zhang, Y. B.; Zhu, K. K.; Luo, C.; Zhang, J. X.; Cheng, C. R.; Feng, R. H.; Yang, W. Z.; Zeng, F.; Wang, Y.; Xu, P. P.; Guo, J. L.; Liu, X.; Guan, S. H.; Guo, D. A. Anti-inflammatory diterpenoids from the root bark of Acanthopanax gracilistylus. *J Nat Prod* **2014**, *77*, 2342-2351.
(27) Zhang, G. J.; Li, Y. H.; Jiang, J. D.; Yu, S. S.; Wang, X. J.; Zhuang, P. Y.; Zhang, Y.; Qu, J.; Ma, S. G.; Li, Y.; Liu, Y. B.; Yu, D. Q. Diterpenes and sesquiterpenes with anti-Coxsackie virus B3 activity from the stems of Illicium jiadifengpi. *Tetrahedron* **2014**, *70*, 4494-4499.
(28) Prawat, U.; Tuntiwachwuttikul, P.; Taylor, W. C.; Engelhardt, L. M.; Skelton, B. W.; White, A. H. Diterpenes from a Kaempferia Species. *Phytochemistry* **1993**, *32*, 991-997.
(29) Pinto, A. C.; Borges, C. 6 Diterpenes from Vellozia-Compacta. *Phytochemistry* **1983**, *22*, 2011-2015.
(30) Dettrakul, S.; Kittakoop, P.; Isaka, M.; Nopichai, S.; Suyarnsestakorn, C.; Tanticharoen, M.; Thebtaranonth, Y. Antimycobacterial pimarane diterpenes from the Fungus Diaporthe sp. *Bioorg Med Chem Lett* **2003**, *13*, 1253-1255.
(31) Evidente, A.; Venturi, V.; Masi, M.; Degrassi, G.; Cimmino, A.; Maddau, L.; Andolfi, A. In Vitro Antibacterial Activity of Sphaeropsidins and Chemical Derivatives toward Xanthomonas oryzae pv. oryzae, the Causal Agent of Rice Bacterial Blight. *J Nat Prod* **2011**, *74*, 2520-2525.
(32) Xia, X. K.; Qi, J.; Liu, Y. Y.; Jia, A. R.; Zhang, Y. G.; Liu, C. H.; Gao, C. L.; She, Z. G. Bioactive Isopimarane Diterpenes from the Fungus, Epicoccum sp. HS-1, Associated with Apostichopus japonicus. *Mar Drugs* **2015**, *13*, 1124-1132.
(33) Wang, X. N.; Bashyal, B. P.; Wijeratne, E. M. K.; U'Ren, J. M.; Liu, M. X.; Gunatilaka, M. K.; Arnold, A. E.; Gunatilaka, A. A. L. Smardaesidins A-G, Isopimarane and 20-

nor-Isopimarane Diterpenoids from Smardaea sp., a Fungal Endophyte of the Moss Ceratodon purpureus. *J Nat Prod* **2011**, *74*, 2052-2061.

(34) Gonzalez, A. G.; Ciccio, J. F.; Rivera, A. P.; Martin, J. D. New Halogenated Diterpenes from the Red Alga Laurencia-Perforata. *J Org Chem* **1985**, *50*, 1261-1264.

(35) Miao, F. P.; Liang, X. R.; Liu, X. H.; Ji, N. Y. Aspewentins A-C, Norditerpenes from a Cryptic Pathway in an Algicolous Strain of Aspergillus wentii. *J Nat Prod* **2014**, *77*, 429-432.

(36) Tounekti, T.; Munne-Bosch, S. Enhanced Phenolic Diterpenes Antioxidant Levels Through Non-transgenic Approaches. *Crit Rev Plant Sci* **2012**, *31*, 505-519.

(37) Abreu, M. E.; Muller, M.; Alegre, L.; Munne-Bosch, S. Phenolic diterpene and alpha-tocopherol contents in leaf extracts of 60 Salvia species. *J Sci Food Agr* **2008**, *88*, 2648-2653.

(38) Munne-Bosch, S.; Alegre, L.; Schwarz, K. The formation of phenolic diterpenes in Rosmarinus officinalis L-under Mediterranean climate. *Eur Food Res Technol* **2000**, *210*, 263-267.

(39) Eisenreich, W.; Bacher, A.; Arigoni, D.; Rohdich, F. Biosynthesis of isoprenoids via the non-mevalonate pathway. *Cell Mol Life Sci* **2004**, *61*, 1401-1426.

(40) Peters, R. J.; Ravn, M. M.; Coates, R. M.; Croteau, R. B. Bifunctional abietadiene synthase: free diffusive transfer of the (+)-copalyl diphosphate intermediate between two distinct active sites. *J Am Chem Soc* **2001**, *123*, 8974-8978.

(41) Li, X.; Li, X. M.; Li, X. D.; Xu, G. M.; Liu, Y.; Wang, B. G. 20-Nor-isopimarane cycloethers from the deep-sea sediment-derived fungus Aspergillus wentii SD-310. *Rsc Adv* **2016**, *6*, 75981-75987.

(42) Li, X.; Li, X. D.; Li, X. M.; Xu, G. M.; Liu, Y.; Wang, B. G. Wentinoids A-F, six new isopimarane diterpenoids from Aspergillus wentii SD-310, a deep-sea sediment derived fungus. *Rsc Adv* **2017**, *7*, 4387-4394.

(43) Vantamelen, E. E.; Marson, S. A. Biogenetic-Type Synthesis of Hydroxylated Tricyclic Diterpenes in the Pimarane Class. *Bioorg Chem* **1982**, *11*, 219-249.

(44) Nising, C. F.; Brase, S. Highlights in steroid chemistry: total synthesis versus semisynthesis. *Angew Chem Int Ed Engl* **2008**, *47*, 9389-9391.

(45) Zeelen, F. J. Steroid total synthesis. *Nat Prod Rep* **1994**, *11*, 607-612.

(46) Hanson, J. R. Steroids: partial synthesis in medicinal chemistry. *Nat Prod Rep* **2007**, *24*, 1342-1349.

(47) Yoder, R. A.; Johnston, J. N. A case study in biomimetic total synthesis: polyolefin carbocyclizations to terpenes and steroids. *Chem Rev* **2005**, *105*, 4730-4756.

(48) Vantamelen, E. E.; Zawacky, S. R.; Russell, R. K.; Carlson, J. G. Biogenetic-Type Total Synthesis of (+/-)-Aphidicolin. *J Am Chem Soc* **1983**, *105*, 142-143.

(49) Corey, E. J.; Lin, S. Z. A short enantioselective total synthesis of dammarenediol II. *J Am Chem Soc* **1996**, *118*, 8765-8766.

(50) Corey, E. J.; Liu, K. Enantioselective total synthesis of the potent anti-HIV agent neotripterifordin. Reassignment of stereochemistry at C(16). *J Am Chem Soc* **1997**, *119*, 9929-9930.

(51) Batsanov, A.; Chen, L. G.; Gill, G. B.; Pattenden, G. Acyl radical-mediated polyene cyclisations directed towards steroid ring synthesis. *J Chem Soc Perk T 1* **1996**, 45-55.

(52) Chen, L. G.; Gill, G. B.; Pattenden, G. New Radical-Mediated Polyolefin Cyclizations Directed Towards Steroid Ring Synthesis. *Tetrahedron Lett* **1994**, *35*, 2593-2596.

(53) Rendler, S.; Macmillan, D. W. Enantioselective polyene cyclization via organo-SOMO catalysis. *J Am Chem Soc* **2010**, *132*, 5027-5029.

(54) Meyer, W. L.; Manning, R. A.; Schindler, E.; Schroeder, R. S.; Shew, D. C. Diterpenoid Total Synthesis, an a-]B-]C Approach .8. Introduction of Oxygen at Carbon-11 - Total Synthesis of (+/-)-Carnosic Acid Dimethyl Ether and (+/-)-Carnosol Dimethyl Ether. *J Org Chem* **1976**, *41*, 1005-1015.

(55) Jiang, Y. Y.; Li, Q.; Lu, W.; Cai, J. C. Facile and efficient total synthesis of (+/-)-cryptotanshinone and tanshinone IIA. *Tetrahedron Lett* **2003**, *44*, 2073-2075.

(56) Overman, L. E.; Ricca, D. J.; Tran, V. D. Total synthesis of (+/-)-scopadulcic acid B. *J Am Chem Soc* **1997**, *119*, 12031-12040.

(57) Bie, P. Y.; Zhang, C. L.; Li, A. P.; Peng, X. J.; Wu, T. X.; Pan, X. F. First total synthesis of (+/-)-celaphanol A. *J Chin Chem Soc-Taip* **2002**, *49*, 581-583.

(58) Zhu, H.; Tu, P. F. A convenient strategy for the total synthesis of pisiferic acid type diterpenes. *Synthetic Commun* **2005**, *35*, 71-78.

(59) Li, C. M.; Geng, H. C.; Li, M. M.; Xu, G.; Ling, T. J.; Qin, H. B. Total synthesis of 1-oxomiltirone via Suzuki coupling. *Nat Product Bioprosp* **2013**, *3*, 117-120.

(60) Yadav, J. S.; Kondaji, G.; Reddy, M. S. R.; Srihari, P. Facile synthesis of alpha-iodo carbonyl compounds and alpha-iodo dimethyl ketals using molecular iodine and trimethylorthoformate. *Tetrahedron Lett* **2008**, *49*, 3810-3813.

(61) Fischer, M.; Harms, K.; Koert, U. Total Syntheses of 7,20-Oxa-Bridged Dinorditerpenes: Antihepatitis C Virus Active (+)-Elevenol from Flueggea virosa and (+)-Przewalskin. *Org Lett* **2016**, *18*, 5692-5695.

(62) Kiyooka, S.; Kaneko, Y.; Komura, M.; Matsuo, H.; Nakano, M. Enantioselective Chiral Borane-Mediated Aldol Reactions of Silyl Ketene Acetals with Aldehydes - Novel Effect of the Trialkylsilyl Group of the Silyl Ketene Acetal on the Reaction Course. *J Org Chem* **1991**, *56*, 2276-2278.

(63) Jorgensen, M.; Lee, S.; Liu, X. X.; Wolkowski, J. P.; Hartwig, J. F. Efficient synthesis of alpha-aryl esters by room-temperature palladium-catalyzed coupling of aryl halides with ester enolates. *J Am Chem Soc* **2002**, *124*, 12557-12565.

(64) Economou, C.; Tomanik, M.; Herzon, S. B. Synthesis of Myrocin G, the Putative Active Form of the Myrocin Antitumor Antibiotics. *J Am Chem Soc* **2018**, *140*, 16058-16061.

(65) Huang, Y.; Iwama, T.; Rawal, V. H. Highly enantioselective Diels-Alder reactions of 1-amino-3-siloxy-dienes catalyzed by Cr(III)-salen complexes. *J Am Chem Soc* **2000**, *122*, 7843-7844.

(66) Meng, Z.; Yu, H.; Li, L.; Tao, W.; Chen, H.; Wan, M.; Yang, P.; Edmonds, D. J.; Zhong, J.; Li, A. Total synthesis and antiviral activity of indolosesquiterpenoids from the xiamycin and oridamycin families. *Nat Commun* **2015**, *6*, 6096.

(67) Li, X.; Carter, R. G. Total Syntheses of Aromatic Abietane Diterpenoids Utilizing Advances in the Pummerer Rearrangement. *Org Lett* **2018**, *20*, 5546-5549.

(68) Zhao, Y. M.; Maimone, T. J. Short, enantioselective total synthesis of chatancin. *Angew Chem Int Ed Engl* **2015**, *54*, 1223-1226.

(69) Kondoh, A.; Arlt, A.; Gabor, B.; Furstner, A. Total synthesis of nominal gobienine A. *Chemistry* **2013**, *19*, 7731-7738.

(70) Xie, S.; Chen, G.; Yan, H.; Hou, J.; He, Y.; Zhao, T.; Xu, J. 13-Step Total Synthesis of Atropurpuran. *J Am Chem Soc* **2019**, *141*, 3435-3439.

(71) Gong, J.; Chen, H.; Liu, X. Y.; Wang, Z. X.; Nie, W.; Qin, Y. Total synthesis of atropurpuran. *Nat Commun* **2016**, *7*, 12183.

(72) Kong, L.; Su, F.; Yu, H.; Jiang, Z.; Lu, Y.; Luo, T. Total Synthesis of (-)-Oridonin: An Interrupted Nazarov Approach. *J Am Chem Soc* **2019**, *141*, 20048-20052.

(73) May, T. L.; Dabrowski, J. A.; Hoveyda, A. H. Formation of Vinyl-, Vinylhalide- or Acyl-Substituted Quaternary Carbon Stereogenic Centers through NHC-Cu-Catalyzed Enantioselective Conjugate Additions of Si-Containing Vinylaluminums to beta-Substituted Cyclic Enones. *J Am Chem Soc* **2011**, *133*, 736-739.

(74) Ao, J.; Sun, C.; Chen, B.; Yu, N.; Liang, G. Total Synthesis of Isorosthin L and Isoadenolin I. *Angew Chem Int Ed Engl* **2022**, *61*, e202114489.

(75) Arno, M.; Gonzalez, M. A.; Zaragoza, R. J. Diastereoselective synthesis of spongian diterpenes. Total synthesis of the furanoditerpene (-)-spongia-13(16),14-diene. *Tetrahedron* **1999**, *55*, 12419-12428.

(76) Toro, A.; Deslongchamps, P. Furanophane transannular Diels-Alder approach to (+)-chatancin: An asymmetric total synthesis of (+)-anhydrochatancin. *J Org Chem* **2003**, *68*, 6847-6852.

(77) Obrecht, D. Acid-Catalyzed Cyclization Reactions of Substituted Acetylenic Ketones - a New Approach for the Synthesis of 3-Halofurans, Flavones, and Styrylchromones. *Helv Chim Acta* **1989**, *72*, 447-456.

(78) Toyota, M.; Asano, T.; Ihara, M. Total synthesis of serofendic acids A and B employing tin-free homoallyl-homoallyl radical rearrangement. *Org Lett* **2005**, *7*, 3929-3932.

(79) Dolan, S. C.; Macmillan, J. A New Method for the Deoxygenation of Tertiary and Secondary Alcohols. *Journal of the Chemical Society-Chemical Communications* **1985**, 1588-1589.

(80) Phoenix, S.; Reddy, M. S.; Deslongchamps, P. Total synthesis of (+)-cassaine via transannular Diels-Alder reaction. *J Am Chem Soc* **2008**, *130*, 13989-13995.

(81) Magid, R. M.; Fruchey, O. S.; Johnson, W. L.; Allen, T. G. Hexachloroacetone-Triphenylphosphine - Mild Reagent for the Regioselective and Stereospecific Production of Allylic Chlorides from the Alcohols. *J Org Chem* **1979**, *44*, 359-363.

(82) Toro, A.; Nowak, P.; Deslongchamps, P. Transannular Diels-Alder entry into stemodanes: First asymmetric total synthesis of (+)-maritimol. *J Am Chem Soc* **2000**, *122*, 4526-4527.

(83) Nishiyama, Y.; Han-ya, Y.; Yokoshima, S.; Fukuyama, T. Total synthesis of (-)-lepenine. *J Am Chem Soc* **2014**, *136*, 6598-6601.

(84) Zhou, S.; Xia, K.; Leng, X.; Li, A. Asymmetric Total Synthesis of Arcutinidine, Arcutinine, and Arcutine. *J Am Chem Soc* **2019**, *141*, 13718-13723.

(85) Tomanik, M.; Economou, C.; Frischling, M. C.; Xue, M.; Marks, V. A.; Mercado, B. Q.; Herzon, S. B. Development of a Convergent Enantioselective Synthetic Route to (-)-Myrocin G. *J Org Chem* **2020**, *85*, 8952-8989.

(86) Vervoort, H. C.; Draskovic, M.; Crews, P. Histone Deacetylase Inhibitors as a Tool to Up-Regulate New Fungal Biosynthetic Products: Isolation of EGM-556, a Cyclodepsipeptide, from Microascus sp. *Organic Letters* **2011**, *13*, 410-413.

(87) Felsenfeld, G. The evolution of epigenetics. *Perspect Biol Med* **2014**, *57*, 132-148.

(88) Willbanks, A.; Leary, M.; Greenshields, M.; Tyminski, C.; Heerboth, S.; Lapinska, K.; Haskins, K.; Sarkar, S. The Evolution of Epigenetics: From Prokaryotes to Humans and Its Biological Consequences. *Genet Epigenet* **2016**, *8*, 25-36.

(89) Challis, G. L. Genome mining for novel natural product discovery. *J Med Chem* **2008**, *51*, 2618-2628.

(90) Pena, R. T.; Blasco, L.; Ambroa, A.; Gonzalez-Pedrajo, B.; Fernandez-Garcia, L.; Lopez, M.; Bleriot, I.; Bou, G.; Garcia-Contreras, R.; Wood, T. K.; Tomas, M. Relationship Between Quorum Sensing and Secretion Systems. *Front Microbiol* **2019**, *10*.

(91) Peng, X. Y.; Wu, J. T.; Shao, C. L.; Li, Z. Y.; Chen, M.; Wang, C. Y. Co-culture: stimulate the metabolic potential and explore the molecular diversity of natural products from microorganisms. *Mar Life Sci Tech* **2021**, *3*, 363-374.

(92) Cichewicz, R. H. Epigenome manipulation as a pathway to new natural product scaffolds and their congeners. *Natural Product Reports* **2010**, *27*, 11-22.

(93) Li, X. D.; Li, X. M.; Li, X.; Xu, G. M.; Liu, Y.; Wang, B. G. Aspewentins D-H, 20-Nor-isopimarane Derivatives from the Deep Sea Sediment-Derived Fungus Aspergillus wentii SD-310. *J Nat Prod* **2016**, *79*, 1347-1353.

(94) Li, X. D.; Li, X.; Li, X. M.; Xu, G. M.; Liu, Y.; Wang, B. G. 20-Nor-Isopimarane Epimers Produced by Aspergillus wentii SD-310, a Fungal Strain Obtained from Deep Sea Sediment. *Mar Drugs* **2018**, *16*.

(95) Liu, Y.; Virgil, S. C.; Grubbs, R. H.; Stoltz, B. M. Palladium-Catalyzed Decarbonylative Dehydration for the Synthesis of alpha-Vinyl Carbonyl Compounds and Total Synthesis of (-)-Aspewentins A, B, and C. *Angew Chem Int Ed Engl* **2015**, *54*, 11800-11803.

(96) Evans, D. A.; Rovis, T.; Johnson, J. S. Chiral copper(II) complexes as Lewis acids for catalyzed cycloaddition, carbonyl addition, and conjugate addition reactions. *Pure Appl Chem* **1999**, *71*, 1407-1415.

(97) Kaplan, W.; Khatri, H. R.; Nagorny, P. Concise Enantioselective Total Synthesis of Cardiotonic Steroids 19-Hydroxysarmentogenin and Trewianin Aglycone. *J Am Chem Soc* **2016**, *138*, 7194-7198.

(98) Desimoni, G.; Quadrelli, P.; Righetti, P. P. Copper(Ii) in Organic-Synthesis .8. Enantioselective Michael Reactions with Chiral Copper(Ii) Complexes as Catalysts. *Tetrahedron* **1990**, *46*, 2927-2934.

(99) Khatri, H. R.; Bhattarai, B.; Kaplan, W.; Li, Z.; Curtis Long, M. J.; Aye, Y.; Nagorny, P. Modular Total Synthesis and Cell-Based Anticancer Activity Evaluation of Ouabagenin and Other Cardiotonic Steroids with Varying Degrees of Oxygenation. *J Am Chem Soc* **2019**, *141*, 4849-4860.

(100) Cichowicz, N. R.; Kaplan, W.; Khomutnyk, Y.; Bhattarai, B.; Sun, Z.; Nagorny, P. Concise Enantioselective Synthesis of Oxygenated Steroids via Sequential Copper(II)-Catalyzed Michael Addition/Intramolecular Aldol Cyclization Reactions. *J Am Chem Soc* **2015**, *137*, 14341-14348.

(101) Bhattarai, B.; Nagorny, P. Enantioselective Total Synthesis of Cannogenol-3-O-alpha-l-rhamnoside via Sequential Cu(II)-Catalyzed Michael Addition/Intramolecular Aldol Cyclization Reactions. *Org Lett* **2018**, *20*, 154-157.

(102) Pulido, A.; Oliver-Tomas, B.; Renz, M.; Boronat, M.; Corma, A. Ketonic decarboxylation reaction mechanism: a combined experimental and DFT study. *ChemSusChem* **2013**, *6*, 141-151.

(103) Renz, M. Ketonization of carboxylic acids by decarboxylation: Mechanism and scope. *Eur J Org Chem* **2005**, *2005*, 979-988.

(104) Wang, Y. S.; Cui, H. Y.; Song, F.; Tan, H. Z.; Yi, W. M.; Zhang, Y. Upgrading Fast Pyrolysis Oil through Decarboxylation by Using Red Mud as Neutralizing Agent for Ketones Production and Iron Recovery. *Chemistryselect* **2022**, *7*.

(105) Poon, P. S.; Banerjee, A. K.; Laya, M. S. Advances in the Krapcho decarboxylation. *J Chem Res* **2011**, 67-73.

(106) Krapcho, A. P. Synthetic Applications of Dealkoxycarbonylations of Malonate Esters, Beta-Keto-Esters, Alpha-Cyano Esters and Related-Compounds in Dipolar Aprotic Media .2. *Synthesis-Stuttgart* **1982**, 893-914.

(107) Banerjee, A. K.; Correa, J. A.; Laya-Mimo, M. Total synthesis of sesquiterpenoids (+/-)-drim-8-en-7-one and (+/-)-albicanol. *J Chem Res-S* **1998**, 710-711.

(108) Logue, M. W.; Pollack, R. M.; Vitullo, V. P. Nature of Transition-State for Decarboxylation of Beta-Keto Acids. *J Am Chem Soc* **1975**, *97*, 6868-6869.

(109) Bigley, D. B.; May, R. W. Studies in Decarboxylation .4. Effect of Alkyl Substituents on Rate of Gas-Phase Decarboxylation of Some Betagamma-Unsaturated Acids. *J Chem Soc B* **1967**, 557-&.

(110) Bigley, D. B.; Weatherhead, R. H.; May, R. W. Studies in Decarboxylation .10. Effect of Beta-Substituents on Rate of Gas-Phase Decarboxylation of Beta-Gamma-Unsaturated Acids. *J Chem Soc Perk T 2* **1977**, 745-747.

(111) Alborno, A.; Bigley, D. B. Studies in Decarboxylation .15. The Effect of 3-Substitution on the Rate of Decarboxylation of Beta-Gamma-Unsaturated Acids. *J Chem Soc Perk T 2* **1982**, 15-17.

(112) Smith, L. I.; Rouault, G. F. Alkylation of 3-methyl-4-carbethoxy-2-cyclohexen-1-one (Hagemann's ester) related substances. *J Am Chem Soc* **1943**, *65*, 631-635.

(113) Oritani, T.; Yamashita, K.; Kabuto, C. Enantioselectivity of Microbial Hydrolysis of (+/-)-Decahydro-2-Naphthyl Acetates - Preparations and Absolute-Configurations of Chiral Decahydro-2-Naphthols. *J Org Chem* **1984**, *49*, 3689-3694.

(114) Johnson, R. G.; Ingham, R. K. The Degradation of Carboxylic Acid Salts by Means of Halogen - the Hunsdiecker Reaction. *Chem Rev* **1956**, *56*, 219-269.

(115) Barton, D. H. R.; Crich, D.; Motherwell, W. B. New and Improved Methods for the Radical Decarboxylation of Acids. *Journal of the Chemical Society-Chemical Communications* **1983**, 939-941.

(116) Kochi, J. K. A New Method for Halodecarboxylation of Acids Using Lead(4) Acetate. *J Am Chem Soc* **1965**, *87*, 2500-&.

(117) Walsh, C. T. Biologically generated carbon dioxide: nature's versatile chemical strategies for carboxy lyases. *Nat Prod Rep* **2020**, *37*, 100-135.

(118) Pareek, M.; Reddi, Y.; Sunoj, R. B. Tale of the Breslow intermediate, a central player in N-heterocyclic carbene organocatalysis: then and now. *Chem Sci* **2021**, *12*, 7973-7992.

(119) Lobell, M.; Crout, D. H. G. Pyruvate decarboxylase: A molecular modeling study of pyruvate decarboxylation and acyloin formation. *J Am Chem Soc* **1996**, *118*, 1867-1873.

(120) Patel, M. S.; Nemeria, N. S.; Furey, W.; Jordan, F. The Pyruvate Dehydrogenase Complexes: Structure-based Function and Regulation. *J Biol Chem* **2014**, *289*, 16615-16623.

(121) Bertoldi, M. Mammalian Dopa decarboxylase: structure, catalytic activity and inhibition. *Arch Biochem Biophys* **2014**, *546*, 1-7.

(122) Di Nardo, G.; Zhang, C.; Marcelli, A. G.; Gilardi, G. Molecular and Structural Evolution of Cytochrome P450 Aromatase. *Int J Mol Sci* **2021**, *22*.

(123) Davydov, R.; Razeghifard, R.; Im, S. C.; Waskell, L.; Hoffman, B. M. Characterization of the microsomal cytochrome P450 2B4 O2 activation intermediates by cryoreduction and electron paramagnetic resonance. *Biochemistry* **2008**, *47*, 9661-9666.

(124) Nam, W. High-valent iron(IV)-oxo complexes of heme and non-heme ligands in oxygenation reactions. *Acc Chem Res* **2007**, *40*, 522-531.

(125) Akhtar, M.; Wright, J. N.; Lee-Robichaud, P. A review of mechanistic studies on aromatase (CYP19) and 17alpha-hydroxylase-17,20-lyase (CYP17). *J Steroid Biochem Mol Biol* **2011**, *125*, 2-12.

(126) Gantt, S. L.; Denisov, I. G.; Grinkova, Y. V.; Sligar, S. G. The critical iron-oxygen intermediate in human aromatase. *Biochem Biophys Res Commun* **2009**, *387*, 169-173.

(127) Bathe, U.; Frolov, A.; Porzel, A.; Tissier, A. CYP76 Oxidation Network of Abietane Diterpenes in Lamiaceae Reconstituted in Yeast. *J Agric Food Chem* **2019**, *67*, 13437-13450.

(128) Bathe, U.; Tissier, A. Cytochrome P450 enzymes: A driving force of plant diterpene diversity. *Phytochemistry* **2019**, *161*, 149-162.

(129) Scheler, U.; Brandt, W.; Porzel, A.; Rothe, K.; Manzano, D.; Bozic, D.; Papaefthimiou, D.; Balcke, G. U.; Henning, A.; Lohse, S.; Marillonnet, S.; Kanellis, A. K.; Ferrer, A.; Tissier, A. Elucidation of the biosynthesis of carnosic acid and its reconstitution in yeast. *Nat Commun* **2016**, *7*, 12942.

(130) Greule, A.; Stok, J. E.; De Voss, J. J.; Cryle, M. J. Unrivalled diversity: the many roles and reactions of bacterial cytochromes P450 in secondary metabolism. *Nat Prod Rep* **2018**, *35*, 757-791.

(131) Gompper, R.; Wagner, H. U. Donor Acceptor-Substituted Cyclic Pi-Electron Systems - Probes for Theories and Building-Blocks for New Materials. *Angew Chem Int Edit* **1988**, *27*, 1437-1455.

(132) Thalji, R. K.; Roush, W. R. Remarkable phosphine-effect on the intramolecular aldol reactions of unsaturated 1,5-diketones: highly regioselective synthesis of cross-conjugated dienones. *J Am Chem Soc* **2005**, *127*, 16778-16779.

(133) Reese, C. B.; Stewart, J. C. M. Methoxyacetyl as a Protecting Group in Ribonucleoside Chemistry. *Tetrahedron Lett* **1968**, 4273-&.

(134) Catino, A. J.; Forslund, R. E.; Doyle, M. P. Dirhodium(II) caprolactamate: an exceptional catalyst for allylic oxidation. *J Am Chem Soc* **2004**, *126*, 13622-13623.

(135) Choi, H.; Doyle, M. P. Optimal TBHP allylic oxidation of Delta5-steroids catalyzed by dirhodium caprolactamate. *Org Lett* **2007**, *9*, 5349-5352.

(136) Donohoe, T. J.; Wheelhouse, K. M.; Lindsay-Scott, P. J.; Churchill, G. H.; Connolly, M. J.; Butterworth, S.; Glossop, P. A. Osmium-mediated oxidative cyclizations: a study into the range of initiators that facilitate cyclization. *Chem Asian J* **2009**, *4*, 1237-1247.

(137) Piccialli, V. RuO4-catalysed oxidative cyclisation of 1,6-dienes to trans-2,6-bis(hydroxymethyl)tetrahydropyranyldiols. A novel stereoselective process. *Tetrahedron Lett* **2000**, *41*, 3731-3733.

(138) McDonald, F. E.; Singhi, A. D. Syn-oxidative cyclizations of trishomoallylic alcohols: Stereoselective and stereospecific synthesis of trans-tetrahydropyranyl alcohols. *Tetrahedron Lett* **1997**, *38*, 7683-7686.

(139) Reetz, M. T.; Westermann, J.; Kyung, S. H. Direct Geminal Dimethylation of Ketones and Exhaustive Methylation of Carboxylic-Acid Chlorides Using Dichlorodimethyltitanium. *Chem Ber-Recl* **1985**, *118*, 1050-1057.

(140) Lee, J.; Wang, S.; Callahan, M.; Nagorny, P. Copper(II)-Catalyzed Tandem Decarboxylative Michael/Aldol Reactions Leading to the Formation of Functionalized Cyclohexenones. *Org Lett* **2018**, *20*, 2067-2070.

(141) Dauben, W. G.; Bunce, R. A. Organic-Reactions at High-Pressure - a Robinson Annulation Sequence Initiated by Michael Addition of Activated Cycloalkanones with Hindered Enones. *J Org Chem* **1983**, *48*, 4642-4648.

(142) Jurczak, J. Application of High-Pressure in Organic-Synthesis. *Physica B & C* **1986**, *139*, 709-716.

(143) Jurczak, J. Recent Advances in High-Pressure Organic-Synthesis. *High Pressure Research, Vol 7 and 8, Nos 1-3* **1991**, 23-29.

(144) Kwiatkowski, P.; Dudzinski, K.; Lyzwa, D. Effect of high pressure on the organocatalytic asymmetric Michael reaction: highly enantioselective synthesis of gamma-nitroketones with quaternary stereogenic centers. *Org Lett* **2011**, *13*, 3624-3627.

(145) Snider, B. B. Manganese(III)-Based Oxidative Free-Radical Cyclizations. *Chem Rev* **1996**, *96*, 339-364.

(146) Liu, X.; Chen, X.; Mohr, J. T. Regiocontrolled Oxidative C-C Coupling of Dienol Ethers and 1,3-Dicarbonyl Compounds. *Org Lett* **2016**, *18*, 3182-3185.

(147) Larsen, B. J. Development of Novel Anticancer Therapuetics: Total Synthesis of Lactimidomycin and its Analogs and Synthetic Strategies Towards Diterpene Natural Products. University of Michigan, 2015.